MOLECULAR REGULATION OF MORPHOGENESIS OF TASTE ORGANS IN THE EARLY STAGES OF MOUSE EMBRYOS

by

MOHAMED ISHAN

(Under the Direction of HONG-XIANG LIU)

ABSTRACT

Understanding the molecular regulation of taste organogenesis, which includes tongue, taste papillae and taste buds, is crucial considering that developmental defects in the tongue and taste papillae, such as aglossia, macroglossia, microglossia, ankyloglossia, ageusia, dysgeusia and hypogeusia can cause serious disease conditions such as muteness, taste-related disorders, and difficulties in food processing. Detailed information concerning molecular mechanisms governing tongue and taste papilla formation remains incomplete. Here, we demonstrate how neural crest (NC)-derived tongue mesenchyme regulates mesenchymal-epithelial interactions via Bone morphogenetic protein (BMP) and Neurofibromin 2 (Nf2) signaling pathways for the formation of tongue and taste papillae. To investigate the specific roles of BMP and Nf2 signaling pathways, we utilized NC and NC-derived specific *Wnt1-Cre* to constitutively activate ALK2 (*caAlk2*) and conditionally knock out *Alk3* (*Alk3 cKO*) and *Nf2* (*Nf2 cKO*) in a tongue mesenchyme-specific manner. We found that Type I BMP receptors ALK2 and ALK3 in the mesenchyme—the main determinants of the BMP signaling pathway—play distinct roles in tongue and taste papilla development. Dramatically smaller (microglossia) and misshapen tongues with progressively severe size reduction along the anteroposterior axis, absence of a pharyngeal region, and apparent changes in lingual tissues including the epithelium, muscle and nerve fibers were observed in *Wnt1-Cre/caAlk2* mutants, suggesting that ALK2-mediated BMP signaling in the mesenchyme is essential in orchestrating various

tissues for the proper development of the tongue and its appendages in a region-specific manner. In contrast, *Alk3 cKO* in the tongue mesenchyme resulted in the complete absence of taste papilla placodes. Further analyses using RNA-Sequencing, Mass spectrometry combined with functional analyses using tongue organ cultures revealed that ALK3-mediated BMP signaling in the mesenchyme suppresses the secretion of inhibitory secretory proteins and promotes taste papilla development in the tongue epithelium. In *Nf2 cKO* mutants, distinct alterations of cell proliferation in a region-specific manner were detected, i.e., cell proliferation decreased anteriorly and increased posteriorly, leading to a tip-pointed and posteriorly widened tongue in the early developmental stages. However, in the later stages, *Nf2 cKO* mutants had significantly decreased cell proliferation throughout the entire tongue organ, suggesting a stage-specific role of *Nf2* in regulating cell proliferation.

INDEX WORDS: Tongue, taste papillae, taste bud cells, neural crest cells, mesenchyme, organogenesis, *Wnt1-Cre*, BMP signaling, ALK2, ALK3, neurofibromin 2, hippo signaling, cell proliferation, apoptosis, secretory proteins

MOLECULAR REGULATION OF MORPHOGENESIS OF TASTE ORGANS IN THE EARLY STAGES OF MOUSE EMBRYOS

by

MOHAMED ISHAN

B.S., University of Peradeniya, Sri Lanka, 2014

A Dissertation Submitted to the Graduate Faculty of the University of Georgia in Partial Fulfillment of the Requirements for the Degree

DOCTOR OF PHILOSOPHY

ATHENS, GEORGIA

2021

MOLECULAR REGULATION OF MORPHOGENESIS OF TASTE ORGANS IN THE EARLY STAGES OF MOUSE EMBRYOS

by

MOHAMED ISHAN

Major Professor: Hong-Xiang Liu

Committee: Douglas B. Menke

Luke J. Mortensen

Steven L. Stice

Franklin D. West

Electronic Version Approved:

Ron Walcott

Dean of the Graduate School

The University of Georgia

August 2021

ACKNOWLEDGEMENTS

First, I want to express my sincerest thanks to my mentor Dr. Hong-Xiang Liu for her trust, guidance, encouragement, supervision, and motivation to achieve my dream. I have greatly enjoyed my time working with and learning from her. Dr. Liu trained me to be a better person both within and outside the lab and made time to support me whenever I needed it. Her excellent knowledge and work ethic have shaped me as an independent scientist. She has also been a mother figure to me, and I am honored and blessed to have a mentor like Dr. Liu.

I am very grateful to my advisory committee members, Drs. Douglas Menke, Luke Mortensen, Steven Stice, and Franklin West, for their time, support and feedback. Their input and suggestions have continually helped me to better shape my projects.

I thank my labmates in Dr. Liu's lab, Dr. Wenxin Yu, Zhonghou Wang, Naomi Kramer, and Dr. Guiqian Chen, for their great friendship, encouragement, and help whenever I needed it. I also offer my special thanks to Dr. Prasangi Rajapaksha for introducing me to Dr. Hong-Xiang Liu's lab. I am grateful to Liu lab undergraduates, Mckenzie Allen, Sunny Patel, and Ruchi Shah, for their help in my research.

I extend my special thanks to Dr. Suneth Sooriyapathirana at the University of Peradeniya, Sri Lanka, for all the help and guidance.

To my father, Mohamed Izzadeen Majeed; my mother, Aysha Yesmin; my wife, Shaima Nazaar; my sister, Haleemathul Zahadiya; my brother, Mohamed Jeleel Muhiyaddeen; and all my in-laws, I give my deepest love and thanks for their love, support and encouragement.

Finally, I would like to thank, Afaq Niyas, Suganthan Amirthagunanathan, Zahra Nawaz, Baviththira Suganthan, Natasha Perumal, Theekshana Jayalath and Samanthi Ranathunga for their invaluable friendship.

TABLE OF CONTENTS

LIST OF TABLES

Page

LIST OF FIGURES

Page

CHAPTER 1

INTRODUCTION AND LITERATURE REVIEW: MOLECULAR REGULATIONS INVOLVED IN THE DEVELOPMENT OF TONGUE AND TASTE PAPILLAE.

1.1 Introduction

The mammalian tongue is a specialized organ that comprises different tissue types and enables taste sensations, speaking and food processing. Its development is of vital importance because developmental defects in the tongue, such as aglossia, macroglossia, microglossia, and ankyloglossia, can cause serious disease conditions such as muteness, taste-related disorders, and difficulties in food processing (Chandrashekar et al., 2014). Furthermore, the tongue is one of the primary locations of taste buds, which are the sensory organs that transduce chemical stimuli from ingested foods to the central nervous system (Roper and Chaudhari, 2017). In mammals, taste buds are primarily located in the tongue, specifically in structures called gustatory papillae (Barlow, 2015). There are three types of gustatory papillae: multiple fungiform papillae, which are located in the anterior two-thirds of the oral tongue; two foliate papillae in the lateral edges of the posterior oral tongue; and a single circumvallate papilla (in mice), located in the midline of the border between the oral and pharyngeal tongue (Mbiene et al., 1997; Mistretta, 1972). In mice, fungiform papillae usually house 1-2 taste buds, whereas foliate and circumvallate papillae can house hundreds. Malformed taste buds can result in conditions such as ageusia, dysgeusia, and hypogeusia (Henkin et al., 1975).

Development of the tongue and taste papillae requires complex mesenchymal-epithelial interactions via multiple molecular signaling pathways, including transforming growth factor-β (TGF-β) (Parada and Chai, 2015; Parada et al., 2012), bone morphogenetic protein (BMP) (Beites et al., 2009; Ishan et al., 2020; Mistretta, 1991; Zhou et al., 2006), Sonic hedgehog (Shh) (Caplan et al., 2019; Liu et al., 2004; Millington et al., 2017; Mistretta et al., 2003), Wnt

(Liu et al., 2007; Thirumangalathu and Barlow, 2015), and fibroblast growth factor (FGF) (Petersen et al., 2011; Prochazkova et al., 2017). In particular, the tongue mesenchyme plays a crucial role in determining the migration, proliferation and differentiation of multiple cell types (Beites et al., 2009; Iwata et al., 2013; Parada and Chai, 2015; Parada et al., 2012; Petersen et al., 2011) and sends signals to the overlying epithelium for tongue and taste papilla formation (Beites et al., 2009; Petersen et al., 2011; Prochazkova et al., 2017). However, a detailed understanding of the mesenchymal contribution in taste organ formation is far from complete. Thus, studies examining the mechanisms underlying the development of the tongue and taste papillae are necessary and will provide knowledge and new insights to improve the treatment of disease conditions caused by developmental defects. In this review article, we will provide deeper insight into what is currently known about the molecular signaling pathways that regulate tongue and taste papilla formation.

1.2 Molecular regulation of tongue development

1.2.1 Tongue development

The tongue, a specialized organ composed of multiple tissue compartments, is the primary organ housing the taste papillae. The lingual tissues include a stratified epithelial sheet hosting taste buds, striated skeletal muscles in different orientations, and connective tissues, which serve to connect the epithelium and skeletal muscles, compartmentalize the various muscle orientations, and house nerve fibers and blood vessels traversing through the tongue (Cobourne et al., 2019). Tissue-tissue and cell-cell interactions are critical to the organization of these tissues (Ferguson et al., 1998; Thesleff et al., 1988; Thesleff et al., 1996), and impairment of these interactions during embryogenesis leads to developmental defects of the tongue that cause severe conditions (Hosokawa et al., 2010).

The lingual mesenchyme/connective tissue is primarily derived from the cranial neural crest (Liu et al., 2012a; Thirumangalathu et al., 2009). The neural crest (NC) is a multipotent stem cell population derived from the lateral ridges of the neural plate in early vertebrate embryos

(Leikola, 1976; Trainor, 2005). Through the fusion of the neural folds, NC cells delaminate from the dorsal part of the neural tube, migrate extensively and give rise to a wide variety of differentiated cell types, including neurons and glial cells of the peripheral nervous system and the connective tissue of the head (Barembaum and Bronner-Fraser, 2005).

In mice, cranial NC cells populate directly under the epithelium of the tongue primordium (branchial arches) as early as 3-5 somite stages [Embryonic day (E) 8.0-8.5]. NC-derived cells are extensively distributed in the tongue mesenchyme/connective tissue (Boggs et al., 2016; Liu et al., 2012a; Thirumangalathu et al., 2009) and are regarded as scaffolds of the tongue organ (Chai and Maxson, 2006; Cordero et al., 2011). These NC and NC-derived cells will eventually be replaced by myoblast cells, which begin to migrate into the developing tongue around E12.0 and differentiate to become intrinsic glossal muscles (Cobourne et al., 2019; Millington et al., 2017). Myogenic precursors, which will give rise to the tongue muscles, first enter the first branchial arch and begin to interact with cranial NC cells, thereby establishing a tissue-tissue interaction to determine the ultimate fate of their cells.

In mice, tongue formation starts with the emergence of three lingual swellings from the first branchial arch (BA1) at E10.5. Among these three swellings, the posterior swelling, i.e., the tuberculum impar, is the first to appear and is immediately followed by two lateral swellings. These swellings, originating from the BA1, will eventually fuse and form the anterior two-thirds of the tongue—the oral tongue—at E12.5. Parallel to the oral tongue formation, a small midline swelling, i.e., the copula, develops from BA2 and merges with another midline swelling originating from BAs 3–4 to form the posterior third of the tongue, i.e., the pharyngeal tongue (Cobourne et al., 2019). The most posterior boundary of the tongue is derived from the BA4, which also gives rise to the epiglottal swelling to form the epiglottis of the larynx (Jain and Rathee, 2021).

1.2.2 Molecular signaling pathways involved in the tongue development

During tongue development, the cranial NC and cranial mesodermal cells interact. Cranial NC cells give rise to connective tissues, which include tenocytes and fibroblasts in the tongue, while mesodermal cells will give rise to skeletal muscles in the tongue. Skeletal muscles in the tongue comprise intrinsic muscles, which originate within the tongue, and extrinsic muscles, which originate outside of the tongue (Hosokawa et al., 2010; Parada et al., 2012). Molecular regulation carried out by multiple signaling pathways primarily regulates either the cranial NC cells or the mesodermal cells during tongue development (Han et al., 2012; Iwata et al., 2013).

1.2.2.1 Transforming growth factor-β (TGF-β) signaling

Transforming growth factor-β **(**TGF-β) signaling plays a crucial role in cell proliferation, differentiation, migration and the synthesis of extracellular matrix (Bradley and Stern, 1967; Hosokawa et al., 2010; Massagué, 1998; Massagué and Gomis, 2006). In TGF-β signaling, TGF-β ligands bind to the TGF-β type II receptor (TGFβRII) receptor. Ligand-bound TGFβRII receptors then form a heterotetramer complex with TGF-β type I receptor to phosphorylate and activate downstream signaling components Smad 2/3. Phosphorylated Smad 2/3 then form a complex with co-mediator Smad (Smad 4) and translocate into the nucleus to transcribe downstream TGF-β target genes (Tzavlaki and Moustakas, 2020).

Mesenchymal-specific *Wnt1-Cre*-driven genetic deletion of the *TGFBR2* gene, which encodes TGFβRII receptors, results in severe defects in tongue development. It is important to note that TGFβRII expresses in the cranial NC-derived cells (Hosokawa et al., 2010; Parada et al., 2012). For example, microglossia, a phenomenon referring to a smaller tongue with decreased muscle cells, has been documented in *Wnt1-Cre;TGFBR2*$^{flox/flox}$ knockout mice. The loss of muscle cells results from the failed proliferation of myogenic cells despite the ability of an indistinguishable number of myogenic precursor cells to migrate into the tongue primordia of *Wnt1-Cre;TGFBR2*$^{flox/flox}$ mutants compared to littermate controls. In addition, the myogenic cell differentiation of *Wnt1-Cre;TGFBR2*$^{flox/flox}$ mutants has been shown to be affected, leading to

compromised skeletal muscle organization. Type I collagen, the main component of the connective tissue that predominantly resides in the lamina propria region of the tongue, and Scleraxis (Scx), a basic helix–loop–helix (bHLH) transcription factor present in mature tendons, were also expressed in the perimysium, epimysium, and septum surrounding tongue muscle fibers but were diminished in *Wnt1-Cre;TGFBR2*$^{flox/flox}$ mutants. Scx-expressing cells are mainly derived from cranial NC cells. Treatment of the control tongue primordium with TGF-β-soaked beads resulted in enhanced Scx expression, suggesting that TGF-β signaling induces Scx expression and regulates cranial NC differentiation during tongue organogenesis (Hosokawa et al., 2010).

Interestingly, the absence of *TGFBR2* from the mesenchyme resulted in a significant reduction in Fibroblast growth factor 10 (FGF10) expression in the tongue primordium, suggesting that TGF-β signaling induces FGF10 in the cranial NC cells during tongue formation. Treatment of *Wnt1-Cre;TGFBR2*$^{flox/flox}$ tongue cell cultures or explants with exogenous FGF10 increased the number of muscle cells. In contrast, in the presence of TGF-β2 ligands, FGF10 expression was enhanced in the primary tongue cell cultures (Hosokawa et al., 2010).

When myogenic cells from control mouse tongue primordium and cranial NC cells from *Wnt1-Cre;TGFBR2*$^{flox/flox}$ mouse tongue primordium were mixed and seeded in a collagen scaffold and transplanted into host mice, disorganized muscle cell formation was detected. However, no changes in muscle cell organization were detected in myogenic cells isolated from the control or in *Wnt1-Cre;TGFBR2*$^{flox/flox}$ mutants cultured with cranial NC cells isolated from control tongue primordium, thereby indicating that cranial NC cells are necessary for the proper organization of muscle cells (Hosokawa et al., 2010).

Interestingly, it has been reported that the absence of *TGFBR2* from tongue mesenchyme-specific cells activates the noncanonical TGF-β2-mediated TGF-β type I and III receptors TGFβRI/TGFβRIII signaling pathway through the activation of p38 mitogen-activated protein kinase (MAPK) and Tyrosine-protein kinase ABL1 (ABL1) instead of Smad 2/3 (Iwata et

al., 2012) in *Wnt1-Cre;TGFBR2*$^{flox/flox}$ mutants (Iwata et al., 2013). When noncanonical TGF-β2-mediated TGFβRI/TGFβRIII signaling activity was inhibited by blocking the formation of the TGFβRI/TGFβRIII complex through the deletion of the TGFβRI receptor, the microglossia phenotype was rescued. Cell proliferation increased in the *TGFBR2*$^{fl/fl}$*;Wnt1-Cre;TGFBR1*$^{fl/+}$ mice, which indicates that noncanonical TGF-β signaling regulates cell proliferation. Although the number of myofibers were almost restored in the *TGFBR2*$^{fl/fl}$*;Wnt1-Cre;TGFBR1*$^{fl/+}$ mice compared to *Wnt1-Cre;TGFBR2*$^{flox/flox}$ mutants, myofiber disorganization was detected similar to that in the latter, thereby suggesting that noncanonical TGF-β signaling regulates the proliferation and differentiation of myoblasts, while canonical TGF-β signaling regulates muscle organization in the developing tongue. Expression levels of key TGF-β signaling regulators, bone morphogenetic protein 5 (*BMP5)*, *FGF4*, and Follistatin (Fst)—but not *FGF5*, *FGF6*, and *Wnt10a*—were restored in *TGFBR2*$^{fl/fl}$*;Wnt1-Cre;TGFBR1*$^{fl/+}$ mice compared to *Wnt1-Cre;TGFBR2*$^{flox/flox}$ mice, which suggests that *BMP5*, *FGF4*, and *Fst* are regulated by noncanonical TGF-β signaling through ABL1, whereas *FGF5*, *FGF6*, and *Wnt10a* are regulated by canonical TGF-β signaling. Furthermore, when ABL1 activity was blocked through the addition of nilotinib (Jabbour et al., 2008), gene expression of *FGF4* and tenascin C (*Tnc*) a large hexametric glycoprotein present in the ECM, and cell proliferation were restored in the *TGFBR2*$^{fl/fl}$*;Wnt1-Cre* mutants, suggesting that the TGF-β/ABL1 signaling pathway mediates tongue organogenesis through the regulation of cell proliferation in the absence of *TGFBR2*-derived canonical TGF-β signaling (Iwata et al., 2013).

Elastic fibers, collagen fibers and glycoproteins are major components of the extracellular matrix that constitutes the tongue's cranial NC-derived connective tissue. Disorganized, immature elastic fibers, collagen fibers and compromised gene expression of *Tnc*, were detected in *Wnt1-Cre;TGFBR2*$^{flox/flox}$ mutants, indicating that a loss of *TGFBR2* in the cranial NC affects the organization of extracellular matrix components. In *Wnt1-Cre;TGFBR2*$^{flox/flox}$ mutants, tongue *Fst* and *Wnt10a* transcription levels were significantly upregulated, and *BMP5*, *FGF4*,

FGF5, and *FGF6* transcript levels were significantly downregulated. In addition, exogenous FGF4, FGF5, FGF6, and a neutralizing antibody for follistatin partially rescued the muscle defects seen in *Wnt1-Cre;TGFBR2*$^{flox/flox}$ mutants, indicating that not only FGF signaling but also BMP signaling is regulated by the TGF-β signaling in the developing tongue (Iwata et al., 2013).

Smad 4 is a common regulator in both TGF-β and BMP signaling. Smad 4 is expressed in both myogenic progenitors and cranial NC-derived cells in the developing tongue primordium (Han et al., 2012). The genetic deletion of *Smad 4* through myogenic progenitor-specific *Myf5-Cre* resulted in observable microglossia with disorganized muscle fibers. In *Myf5-Cre;Smad4*$^{flox/flox}$ mice, muscle fibers positive for MHC (myosin heavy chain), a marker for fully differentiated myoblasts, were significantly reduced, indicating decreased myogenic differentiation. In *Myf5-Cre;Smad4*$^{flox/flox}$ mice, myogenin, a myogenic differentiation determinant that labels the terminal differentiation of myogenic cells, was significantly reduced, but not the myoblast determination protein (Myod1), which labels the undifferentiated proliferating myoblasts (Berkes and Tapscott, 2005), indicating that the absence of *Smad 4* particularly affects the terminal differentiation of myoblasts. Similar to *Wnt1-Cre;TGFBR2*$^{flox/flox}$ mice, the migration of myogenic progenitors was not affected in *Myf5-Cre;Smad4*$^{flox/flox}$ mice. No changes in cell proliferation or apoptosis were detected in *Myf5-Cre;Smad4*$^{flox/flox}$ mice, which indicates that the microglossia phenotype is likely due to failed muscle fiber organization. In addition, the length of muscle fibers and myotybe fusion were significantly reduced in these mice, leading to a defective muscle cell differentiation as a result of the genetic deletion of *Smad 4* in myogenic cells (Han et al., 2012).

In *Myf5-Cre;Smad4*$^{flox/flox}$ mice, FGF ligand *FGF6* and FGF receptor *FGFR4* expression were significantly downregulated. The addition of exogenous FGF6 to the tongue cell cultures resulted in an increase of myoblast fusion and myotube length in the *Myf5-Cre;Smad4*$^{flox/flox}$ cell cultures, along with increased expression of FGFR4, myogenin, and myoblast fusion-related genes Caveolin 3, β1-integrin and Prostacyclin. Taken together, it is evident that Smad 4-

mediated TGF-β signaling in tongue myogenic cells regulates FGF6 and FGFR4 expression during tongue organogenesis through regulating the differentiation of myogenic cells (Han et al., 2012).

1.2.2.2 Bone Morphogenetic Protein (BMP) signaling

Bone Morphogenetic Protein (BMP) ligands, receptors and downstream signaling components are present in both the tongue epithelium and the mesenchyme (Beites et al., 2009; Jung et al., 1999; Kawasaki et al., 2012; Suga et al., 2007; Zhou et al., 2006). Specifically, mesenchymal BMP signaling is important in tongue organogenesis, as constitutive activation of type I BMP receptor *Alk2* in neural crest derived tongue mesenchyme using *Wnt1-Cre* resulted in a bifid or misshapen tongue (Ishan et al., 2020). Mesenchymal ALK2-BMP signaling is BA-specific in its regulation of target genes *Id1*, *Snail1*, *Snai2*, and *Runx2*, differentially affecting cell proliferation and apoptosis for appropriate tongue organogenesis (Ishan et al., 2020).

1.2.2.3 Wnt signaling

Wnt5a is a ligand that is primarily involved in noncanonical Wnt signaling and has been demonstrated to play important roles in cell migration and polarity (He et al., 2008; Schlessinger et al., 2007; Witze et al., 2008) and to affect the elongation of organ structures (Cervantes et al., 2009; Qian et al., 2007; Yamaguchi et al., 1999). In the embryonic tongue, at E12.5, Wnt5a has stronger expression in the anterior tongue and weak or no expression in the posterior tongue as well as in the intermolar eminence region (Liu et al., 2012b). In the anterior tongue, Wnt5a has stronger expression in the mesenchyme compared to the epithelium. In the later stages (E16.5, E18.5), Wnt5a shows an intense expression in the subepithelial band of the mesenchyme, with weaker signals at E18.5 tongue compared to E16.5. Interestingly, no Wnt5a expression was detected in postnatal tongues (Liu et al., 2009), which demonstrates its crucial role in the embryonic stages of tongue organogenesis. Considerably shorter tongues were detected in *Wnt5a*$^{-/-}$ mutants (Liu et al., 2009; Liu et al., 2012b), demonstrating the role of Wnt5a in regulating anterior tongue growth. *Wnt5a*$^{-/-}$ mutants have also been shown to demonstrate

ankyloglossia, a phenomenon in which the tongue tip is attached to the mandible, thereby restricting free tongue movement (Lalakea and Messner, 2003; Morita et al., 2004). When *Wnt5a*$^{-/-}$ tongues were dissected and cultured without the mandible, a shorter tongue still developed, thereby indicating that a shorter tongue is not a result of mechanical restraints exerted through the mandible (Liu et al., 2012b).

E15.5 *Wnt5a*$^{-/-}$ mutants have demonstrated compromised integrity of the mesenchyme, with reduced intermediate filaments, which suggests that Wnt5a$^{-/-}$ affects cytoskeletal organization. Furthermore, muscle organization has also been shown to be affected in *Wnt5a*$^{-/-}$ mutants. Interestingly, cell proliferation decreased in the mesenchyme of E15.5 *Wnt5a*$^{-/-}$ mutants compared to the increased proliferation in E13.5 *Wnt5a*$^{-/-}$ mutant mesenchyme (Liu et al., 2012b).

When exogenous Wnt5a was added in higher concentration to tongue cultures, wild-type tongue increased in length but decreased in width, thereby demonstrating that Wnt5a can increase tongue length. Furthermore, the addition of exogenous Wnt5a decreased cell proliferation, which indicates that Wnt5a regulates cell proliferation by balancing proliferation during tongue organogenesis. Moreover, Vimentin, a marker for mesenchymal cells expression was increased in *Wnt5a*$^{-/-}$ mutants with the addition of exogenous Wnt5a (Liu et al., 2012b).

1.2.2.4 Sonic hedgehog (Shh) signaling

The primary cilia in mammals play a central role in signal transduction and have been shown to be associated with multiple signaling pathways, including Sonic hedgehog (Shh) (Briscoe and Thérond, 2013). Shh signaling has two major pathways: canonical and noncanonical signaling. In canonical signaling, glycoprotein Shh ligands bind to the Patched (Ptc) receptor and deactivate it. When Shh ligands are absent, the Ptc receptor inhibits the Smoothened (Smo) receptor, thus preventing downstream Shh signaling activity. In the presence of the Shh ligand, Ptc inhibition of Smo is abolished, and Ptc will eventually degrade. Smo then activates a downstream signaling cascade through the Gli family proteins, which will

translocate into the nucleus and transcribe downstream target genes. There are three Gli proteins (Gli1, 2, 3). These proteins are Shh-dependent. Among the Gli proteins, only Gli1 functions as a full-length transcriptional activator, whereas Gli2 and Gli3 have both activator (Gli2A, Gli3A) and repressor (Gli2R, Gli3R) forms. Although Gli2 and Gli3 have both forms, Gli2 behaves mainly as an activator and Gli3 as a repressor. Activated Smo converts Gli3R into Gli3A during the functional Shh signaling cascade. Both Gli1 and Ptc are direct targets of Shh signaling, thereby enabling the identification of Shh-responsive cells. Because Ptc is degraded upon Shh ligand binding, the transcription of Ptc is necessary as a negative regulator for the Shh signaling pathway (Carballo et al., 2018).

The primary cilia regulate posttranslational modification and are involved in transforming full-length Shh signaling transcription factors Gli2/3 proteins to GliA or GliR isoforms (Sasai and Briscoe, 2012). Gli2 is considered the predominant activator of the hedgehog (Hh) signaling pathway (Matise et al., 1998). In contrast, Gli3 is a weak activator and, in some cases, compensates for the loss of Gli2 activity (McDermott et al., 2005; Mo et al., 1997; Sasaki et al., 1997).

Kif3a is an intraflagellar protein, a key regulator in the Shh signaling pathway (Millington et al., 2017). When *Kif3a*$^{f/f}$ was knocked out in cranial NC-specific *Wnt1-Cre*, aglossia, a phenomenon referring to the complete absence of the tongue, developed in *Kif3a*$^{f/f}$*;Wnt1-Cre* mutants (Millington et al., 2017). In these mutants, only extrinsic muscle with a disorganized pattern was observed, thereby demonstrating the importance of the primary cilia in NC cells to tongue organogenesis. When *Kif3a* was knocked out using myoblast-specific *MyoDi-Cre*, normal tongue development was detected, confirming that it is not Kif3a in myoblasts but cranial NC that is needed for proper tongue organogenesis. Loss of cilia in the cranial NC also affected the mesodermally derived muscle precursors in the developing tongue and resulted in increased cell death in both cranial NC and mesoderm-derived muscle cells, indicating two likely factors that inhibit tongue development. Loss of *Kif3a* cranial NC-specific mesenchymal cells also

affected Shh signaling activity, significantly downregulating the Shh downstream signaling component Gli1. When Hh pathway downstream transcriptional mediators Gli2 and Gli3 were genetically deleted using *Wnt1-Cre*, the aglossia phenotype developed in the *Gli2$^{f/f}$;Gli3$^{f/f}$;Wnt1-Cre* embryos. Interestingly, overexpression of the Gli3 repressor form using *ROSAGli3TFlag;Wnt1-Cre* led to the complete loss of the distal portion of the tongue with bifid or cleft proximal tongue, thereby suggesting that Hh signaling—likely through Gli activators—regulates tongue development (Millington et al., 2017).

In *Kif3a$^{f/f}$;Wnt1-Cre* mutants, GliA forms were significantly downregulated, indicated by the downregulation of the Fox genes (Foxf1, Foxf2, Foxd1 and Foxd2), which are target genes of Gli proteins (Jeong et al., 2004). When GliA forms were genetically deleted in NC cells by impairing Gli2A and Gli3A, aglossia developed in *Gli2$^{f/f}$;Gli3d699$^{/+}$;Wnt1-Cre* mutants. In these mutants, Gli2A was replaced by the Gli3 allele, which only expresses as truncated Gli3R (Gli3 Repressor form) (Böse et al., 2002). Overexpression of Gli2 using ΔNGli2 mice (Mill et al., 2003) partially rescued tongue growth. It is evident that the Shh signaling pathway in the cilia plays a crucial role in tongue organogenesis through GliA regulation (Millington et al., 2017).

Similar to *Kif3a* knockouts, when Shh signaling receptor Smoothened (*Smo*) was genetically deleted in the cranial NC-derived mesenchyme using *Wnt1-Cre*, the tongue failed to develop. Moreover, in *Wnt1-Cre;Smon/c* mutants, Myf5- and MyoD-expressing muscle precursors were not detected. In *Wnt1-Cre;Smon/c* mice, Gli2FL (Gli2 full length) isoform significantly diminished, and Gli2 truncate isoform significantly increased. The full-length form usually gives rise to the active form, while the truncated form gives rise to the repressor form. It is evident that the Shh signaling pathway as a whole utilizes the Gli activator form for tongue organogenesis (Jeong et al., 2004; Millington et al., 2017).

1.2.2.5 Dlx5 and Dlx6

Genetic deletion of *Hand*, a basic helix-loop-helix transcription (bHLH) factor (Charité et al., 2001), in NC cells leads to aglossia. *Hand2* is a direct transcriptional target of Dlx5 and Dlx6.

Interestingly, the loss of *Hand2* in NC cells has been shown to lead to aberrant expression of Dlx5 and Dlx6 in the mandible arch, suggesting that Hand2 restricts Dlx5 and Dlx6 during tongue organogenesis. The expression of Dlx5 and Dlx6 promotes *Runx2* expression (Holleville et al., 2007), which plays a crucial role in osteogenesis (Ducy et al., 1997; Komori et al., 1997; Otto et al., 1997), thereby suggesting that the loss of *Hand2* likely initiates an osteogenic pathway in the mandibular arch (Barron et al., 2011).

1.3. Molecular regulation of taste papilla development

1.3.1 Formation of taste papillae

At E12.5, the tongue attains its spatulated shape, and taste papilla placodes start to appear in the developing tongue. When the rudimentary tongue appears at E11.5, the tongue epithelium is composed of a homogenous epithelial bilayer (Barlow, 2015; Kramer et al., 2019). At around E12-E12.5, taste papilla placodes begin to appear as columnar epithelial cells in locations where fungiform and circumvallate taste papillae develop (Farbman and Mbiene, 1991; Fujimoto et al., 1993; Mistretta, 1991; Poulsen et al., 2017). At E14.5, the epithelium in the taste papillae will invaginate to create a distinct mesenchymal core (Farbman and Mbiene, 1991; Whitehead and Kachele, 1994). During this time, nerve fibers will reach and penetrate the epithelium and become taste nerve fibers (Krimm et al., 2015). These nerve fibers densely innervate the papillary epithelium around E16 (Hall et al., 1999). In contrast to fungiform and circumvallate taste papillae, foliate taste papillae develop later, at E14.5. In rodents, taste bud cells will start to develop around E18.5 but do not differentiate fully until after the first postnatal week. However, taste bud cells in the soft palate differentiate before birth (El-Sharaby et al., 2001a; El-Sharaby et al., 2001b; El Shahawy et al., 2017; Harada et al., 2000).

Taste papilla development displays a distinctive pattern (Mbiene et al., 1997; Mistretta, 1972; Mistretta, 1998) in which multiple fungiform papillae develop in the anterior tongue, two foliate papillae in the posterior lateral region, and one circumvallate papilla cluster in the border

between the anterior and posterior tongue. In mice, each fungiform taste papilla houses one taste bud, whereas foliate and circumvallate papillae house hundreds of taste buds.

1.3.2 Molecular regulation of fungiform papilla development

In mice, there are approximately 100 fungiform taste papillae in the anterior two-thirds of the oral tongue as a patterned array (Mistretta et al., 1999). Multiple molecular signaling pathways are involved in the development of fungiform taste papillae.

1.3.2.1 Wnt signaling

1.3.2.1.1 Canonical Wnt signaling

Wnt is a main signaling pathway among those involved in fungiform taste papilla development. Wnt signaling has three main signaling pathways: (a) canonical Wnt, (b) the noncanonical planer cell polarity pathway, and (c) the noncanonical Wnt/Ca^{+2} pathway. Among these pathways, it has been shown that canonical Wnt signaling pathways primarily regulate taste papilla development, whereas the noncanonical planer cell polarity pathway mainly regulates tongue development. In the canonical Wnt signaling pathway (Fig. 1.1), the binding of the Wnt ligands to the receptor complex—composed of the Frizzled (Fz) and the lipoprotein receptor-related protein (LRP)5/6—triggers the disruption of the destruction complex comprising Axin, adenomatosis polyposis coli (APC), protein phosphatase 2A (PP2A), glycogen synthase kinase 3 (GSK3) and casein kinase 1α (CK1α) and induces the membrane translocation of Axin to the cytoplasmic tail of LRP5/6, thereby allowing cytoplasmic β-catenin to translocate into the nucleus and form complexes with transition factors Lef or Tcf to transcribe Wnt signaling target genes (Fig. 1.1). In the absence of Wnt ligands, cytoplasmic β-catenin is degraded by the destruction complex. GSK3 and the casein kinase in the destruction complex phosphorylate cytoplasmic β-catenin and promote ubiquitination-mediated proteolytic destruction, making it unavailable for nuclear translocation (Komiya and Habas, 2008).

Several genes encoding Wnt ligands, including *Wnt3*, *Wnt3a*, *Wnt6*, *Wnt10a*, *Wnt10b*, are expressed in the embryonic tongue epithelium (Liu et al., 2012b). Among these ligands, *Wnt10b*

is restricted to fungiform and circumvallate taste papillae (Iwatsuki et al., 2007). Analysis of Wnt/β-catenin signaling activity through examination of the β-galactosidase activity in TOPGAL mice in the developing embryonic mouse tongue revealed that Wnt/β-catenin signaling begins to appear at E12.5, when the taste papilla placodes begin to initiate, and intensifies in the fungiform papillae at E14.5 but begins to decline thereafter

Functional analyses to test the importance of Wnt/β-catenin signaling to fungiform taste papilla development have revealed that the addition of LiCl promotes Shh^{+} placode initiation in the cultured tongue primordia (Liu et al., 2007). LiCl inhibits GSK3 activity on the destruction complex and prevents the phosphorylation of cytoplasmic β-catenin. In studies, when cytoplasmic β-catenin was stabilized through the mutation of endogenous β-catenin, where the coding region for the serine and threonine residues would be removed through epithelial-specific K14-derived Cre recombination, ectopic taste papilla placodes developed into fungiform taste papillae. These serine and threonine residues are the targets of phosphorylation for the subsequent β-catenin degradation. However, such β-catenin stabilization is stage dependent. If the β-catenin stabilization occurs before the specification of taste papilla placodes, it results in the diversion of the lingual epithelium from the developing taste papillae (Thirumangalathu and Barlow, 2015). However, similar to K14-mediated stabilization of β-catenin, when tamoxifen-induced stabilization was performed at E12.5 in *Shh-CreERT2;Ctnnb1*$^{(ex3)fl}$ mice, enlarged taste papillae were seen in these mutants compared to the controls (Thirumangalathu and Barlow, 2015).

Another study demonstrated that epithelial-specific K5-induced ectopic *Dkk1* expression resulted in the absence of taste papilla placodes. Dkk1 is a secreted antagonist that blocks canonical Wnt signaling by binding to the Lrp 5/6 coreceptors and preventing the formation of active Wnt–Frizzled–LRP5/6 receptor complexes (Zorn, 2001). Epithelial Dkk1 expression in that study also led to the downregulation of Shh receptor Ptch1 in placodal and underlying

mesenchymal cells, thereby indicating the cross-talk between Wnt and Shh signaling in taste papilla development.

Analysis of the canonical Wnt signaling transcription factors, including Tcf1, Tcf3, Tcf4, and Lef1, revealed that only Lef1 had an expression pattern similar to Wnt/β-catenin signaling activity (Iwatsuki et al., 2007). Lef1 showed high expression in the developing tongue epithelium at E12.5 and remained high until E14.5. Genetic deletion of Lef1 in the developing embryos resulted in smaller, less distinct fungiform taste papillae at E14.5 compared to the wild-type control or heterozygous *Lef1*$^{+/-}$ embryos. However, a complete absence of fungiform taste papillae was observed in postnatal day 0 *Lef1-null* mice.

Furthermore, *Wnt10b-null* mice also demonstrated reduced size and number of fungiform taste papillae. However, fungiform papillae loss in *Wnt10b-null* mice was milder compared to the complete loss of fungiform papillae in *Lef1-null* mice (Iwatsuki et al., 2007). This effect could be rescued, as evidenced by increases in the number of fungiform taste papilla on E12.5 tongues cultured with LiCl (Iwatsuki et al., 2007).

Although fungiform taste papillae are reduced or absent from neonatal *Lef1-* or *Wnt10b-null* mice, the initiation of fungiform taste papilla development in the early stages of embryonic development raises concern over the presence of multiple Wnt signaling components other than Wnt10b in the epithelium that play a crucial role in patterning fungiform taste papilla placodes (Iwatsuki et al., 2007). For example, the deletion of Gpr177, a sorting regulator for the secretion of Wnt ligands, in the tongue epithelium resulted in the disruption of fungiform taste papilla placode initiation (Zhu et al., 2014). The expression of early taste placode markers such as Shh, BMP2, BMP4 and BMP7 were all inhibited in the tongue epithelium of both E12.5 and E14.5 Gpr177 knockout mice. Gpr177 predominantly expressed in the tongue epithelium and weakly in the tongue mesenchyme at E11.5 (Zhu et al., 2014). Studies of TOPGAL mice, which have a β-galactosidase gene driven by the T cell factor/TCF promoter to mark Wnt/β-catenin signaling activity, have demonstrated that Wnt/β-catenin signaling activity is present in the entire tongue

epithelium at E14.5, especially in the fungiform taste papillae (Iwatsuki et al., 2007; Liu et al., 2007). In Shh-Cre-driven epithelial-specific Gpr177 knockout mice, no TOPGAL staining was present in tongues that lacked fungiform taste papilla placodes, demonstrating that Wnt/β-catenin signaling activity is essential for taste papilla placode initiation.

Axin2 is a direct target of Wnt/β-catenin signaling and expresses in the fungiform taste papillae and mesenchyme underneath the tongue epithelium at E14.5. Interestingly, in *Gpr177* knockout mice, Axin2 failed to express (Zhu et al., 2014). Furthermore, in *Gpr177Shh-Cre/ Ctnnb1*$^{(ex3)fx/+}$ mice, in which the epithelial β-catenin was stabilized in the epithelial *Gpr177* knockout mice, enlarged, high-density taste papillae were detected in the *Gpr177Shh-Cre* mutants (Liu et al., 2007; Zhu et al., 2014), thereby demonstrating the intraepithelial role of the Wnt/β-catenin signaling pathway during fungiform taste papilla formation. Interestingly, when only one allele of Gpr177 was deleted, as in *Gpr177*$^{(fx/+)}$*Shh-Cre/ Ctnnb1*$^{(ex3)fx/+}$ mice, much smaller fungiform taste papillae were detected compared to those mice with loss of both *Gpr177* alleles, indicating the dose-dependent role of canonical Wnt signaling in fungiform taste papilla development. The addition of LiCl to activate Wnt/β-catenin signaling resulted in a dramatic increase in Shh+ taste papilla placodes in E11.5 tongue explants of epithelial *Gpr177* knockout mice. However, the addition of LiCl at E12.5 epithelial *Gpr177* knockout mice tongue explants did not result in taste papillae restoration, which suggests the stage-specific roles of canonical Wnt signaling activity.

1.3.2.1.2 Noncanonical Wnt signaling

Although the tongue is small in *Wnt5a*$^{-/-}$ mutants (Jorissen et al., 2003; Liu et al., 2009; Liu et al., 2012b), no changes in fungiform or circumvallate papillae pattern, number or development have been detected to date. Nonetheless, as a result of truncated tongue, fungiform papillae density in fact increases in *Wnt5a*$^{-/-}$ mutants (Jorissen et al., 2003; Liu et al., 2009; Liu et al., 2012b). However, in the presence of exogenous Wnt5a, fungiform papillae were significantly reduced or absent in both wild-type and *Wnt5a*$^{-/-}$ knockout mice. The addition of

LiCl to activate canonical Wnt signaling in *Wnt5a*$^{-/-}$ mice resulted in increased fungiform papillae compared to the effect observed with LiCl alone. Exaggerated fungiform papilla development in *Wnt5a*$^{-/-}$ mice implies that in the normal tongue, Wnt5a exerts a balancing influence to maintain the appropriate number of papillae. Reduced X-gal staining of the tongue epithelium after TOPGAL reporter mouse tongues were cultured with exogenous Wnt5a revealed that endogenous Wnt/β-catenin signaling was decreased, thereby demonstrating that Wnt5a eliminates canonical Wnt signaling and suppresses fungiform papilla development in the tongue epithelium. In the tongue epithelium, Wnt5a in the mesenchyme exerts its function through binding to the Ror2 coreceptor in the epithelium (Liu et al., 2012b) and mediates fungiform papilla development through the β-catenin independent pathway (Gao et al., 2011; Nishita et al., 2006; Yamamoto et al., 2007).

1.3.2.2 Shh signaling

Among the signaling molecules that are present during the early stages of fungiform taste papilla development, Shh plays a crucial role (D'Agostino et al., 2013; Liu et al., 2004; Mistretta et al., 2003). In mice, Shh is present in the fungiform taste papilla placodes (Bitgood and McMahon, 1995; Hall et al., 1999; Jung et al., 1999), whereas the receptors for the Shh signaling pathway, Ptc, and transcription factors regulated by the Shh signaling pathways such as Gli1 are expressed in similar patterns as Shh but not in identical cell populations (Goodrich et al., 1996; Hall et al., 1999; Hui et al., 1994; Marigo et al., 1996a; Marigo et al., 1996b). These expression patterns of Shh, Ptc and Gli signaling components indicate that the Shh signaling pathway is active during fungiform taste papilla morphogenesis (Hall et al., 2003).

In the embryonic tongue, Shh begins to express in a diffused fashion but is later progressively restricted by the developing taste papillae. Before the tongue attains its spatulated shape, diffused Shh immunosignals are evident in the mandible swellings of E12 rats (E10.5 mice). These Shh signals become more intense in the lateral tongue swellings of E13 rats (E11.5 mice), which will eventually merge and develop into the tongue. By E14.0 (E12.5 in

mice), large, intense but irregular patches of Shh immunosignals can be detected on either side of the median furrow and in front of the intermolar eminence region where the fungiform taste papillae develop. These Shh signals in E14 rat tongues are restricted to the lingual epithelium corresponding the taste papilla placodes, which will eventually give rise to the fungiform or circumvallate taste papillae. From E15-E18 (E13.5-E15.5 in mice), these Shh signals are restricted to well-formed taste papillae. At the same time, on the posterior tongue, intense Shh signals are observed in the region in which the circumvallate taste papilla will develop. Although Shh expresses in the anterior oral tongue, it is absent from the medium furrow and very low in the intermolar eminence regions of the oral tongue. Moreover, the pharyngeal tongue has no Shh expression at any stage of tongue development (Liu et al., 2004; Mistretta et al., 2003).

Shh is primarily restricted to the apical epithelium of the developing fungiform taste papillae, although Shh signals are also present in the mesenchyme subjacent to the fungiform epithelium in a more diffuse pattern at E15-E16 (rats). In the posterior tongue, initial patches of Shh immunoproducts will develop into a distinctive Shh line in the basement region of the epithelium by E14 and become weaker compared to the anterior tongue epithelium by E15-E16 (rats) (Liu et al., 2004; Mistretta et al., 2003).

In contrast, the Shh signaling receptor Ptc coincides with Shh expression in the developing tongue. Similar to Shh, Ptc also begins to express in a diffuse pattern and is progressively restricted to developing taste papilla placodes and to taste papillae from E13-E18 (rats). However, these Ptc immunoproducts are more diffused compared to Shh immunoproducts and encircle the more intense Shh signals in the fungiform taste papillae at E15 and E16 (rats).

In E13 rat tongues cultured for 2 days with cyclopamine, a steroidal alkaloid inhibitor of the Shh signaling pathway that binds directly to the Smo receptor and thus prevents the activation of the downstream signaling cascade (Chen et al., 2002), numerous and crowded fungiform taste papillae developed in the anterior tongue. These fungiform taste papillae were

distributed in the medium furrow and the posterior oral tongue anterior to the circumvallate papilla (intermolar eminence), regions in which fungiform taste papillae will never form in vivo. In E14 rat tongues cultured with cyclopamine, an increased number of fungiform taste papillae were observed in the entire oral tongue except in the medium furrow and pharyngeal tongue. The effect of Shh disruption is also stage-dependent. No difference in fungiform taste papilla development was noticed in E16 or E18 rat tongues cultured with cyclopamine, thereby suggesting that once the papillae attain their morphology and placement, Shh signaling does not impact the maintenance of fungiform taste papillae. Similar to cyclopamine, Shh-blocking antibody also demonstrated a similar phenotype when added to the E12 or E14 rat tongue cultures, thereby demonstrating that the Shh pathway regulates taste papilla development and is crucial in preventing the formation of fungiform taste papillae in the interpapillary space and medium furrow on the anterior tongue and the intermolar eminence on the posterior oral tongue. Furthermore, it is important to note that once taste papilla development has been initiated (e.g., by cyclopamine), the molecular program for fungiform papilla formation continues to progress even after the source of the Shh signal disturbance is removed (Liu et al., 2004). However, the cyclopamine exposure time is critical for the onset of ectopic fungiform taste papilla development between the anterior vs posterior oral tongue; the anterior tongue requires relatively low exposure time to initiate ectopic fungiform taste papilla development.

Shh is a morphogen, which is a signaling molecule that emanates from a distinct region of a tissue and spreads outward in a concentration gradient (Tabata and Takei, 2004) to induce cellular responses for cell patterning during embryonic development. It has been proposed that intense expression of Shh in taste papilla placodes activates putative fungiform papillae genes or gene complexes and directs fungiform papilla formation (Liu et al., 2004). Cells surrounding the taste papilla placodes respond to lower Shh levels and activate nonfungiform genes or gene complexes, thereby preventing the formation of fungiform papillae in the interpapillary space. Once Shh activity has been disrupted (e.g., by a blocking antibody or cyclopamine), the

interpapillary activation of nonfungiform papillae pathways by low Shh activity will be lost, and, as a result, new fungiform taste papillae emerge in the interpapillary spaces or the regions where fungiform taste papilla do not develop in vivo, which supports the concentration-dependent effects of Shh in the patterning and initiation of fungiform taste papilla development. Interestingly, Ptc expression has been detected in these newly formed fungiform taste papillae corresponding to the pattern of Shh in E14 rat tongues cultured with cyclopamine. Similar to cyclopamine, another steroidal alkaloid inhibitor, jervine, has also been shown to result in an increased number of fungiform taste papillae, thereby further confirming the inhibitory role of Shh signaling in fungiform taste papilla development.

In *ShhGFPCRE/Smo$^{f/f}$* mice whose Smo receptor was knocked out, robust Shh immunosignals were detected in the E12.5 lingual epithelium. In contrast, weak Shh immunosignals were detected in the lingual mesenchyme of E12.5 *ShhGFPCRE/Smo$^{f/f}$* mice (El Shahawy et al., 2017). These immunosignals detected in the interpapillary space and the lingual mesenchyme were a result of protein diffusion from the taste papilla placodes. Interestingly, at E14.5, when Shh immunosignals were restricted to the fungiform taste papillae (Barlow and Klein, 2015), these immunosignals expanded in the tongue epithelium of the *ShhGFPCRE/Smo$^{f/f}$* mice. Instead of remaining confined to the fungiform taste papillae, enlarged and overproduced Shh-expressing spots were detected in the tongues of both E14.5 and E15.5 *ShhGFPCRE/Smo$^{f/f}$* mice (El Shahawy et al., 2017). Interestingly, *ShhGFPCRE/Smo$^{f/f}$* mutants display Shh expressing placode-like structures and with underlying Ptc^{+} mesenchyme, suggesting the de novo formation of fungiform taste papillae. Importantly, fungiform taste papilla induction begins at E12.5 and ceases by E14.5.

E11.5 Shh knockout using epithelial-specific ShhCreERT2/Shhf, resulted in overproduction of fungiform taste papillae (El Shahawy et al., 2017), further confirming the inhibitory roles of Shh signaling in fungiform taste papilla development.

Analysis of *ShhGFPCRE/Smo*$^{f/f}$ embryos as well as E10.5 and E11.5 tamoxifen-induced *ShhCreERT2/Shh*^{f} tongues for Wnt10b, a taste papilla placode marker, revealed abnormal expression of Wnt10b in the E15.5-E17.5 tongues, whereas Wnt10b transcripts stopped expressing in the controls after E14.5 (El Shahawy et al., 2017). These data suggest that the loss of Shh signaling activity promotes and sustains the induction of fungiform taste papilla placodes even after the active phase (E12.5-E14.5) of taste papilla formation. It is also evident that Shh inhibits fungiform papilla formation during the active phase of fungiform papilla development. Furthermore, Shh also contributes to the patterned distribution of fungiform papillae in the anterior tongue by expressing within the lingual epithelium but not in the mesenchyme (Hall et al., 2003; Iwatsuki et al., 2007; Liu et al., 2004; Mistretta et al., 2003).

Overall, Shh signaling pathways regulate mesenchymal-epithelial interaction in the development of fungiform taste papillae, specifying cell fate in developing fungiform papillae, promoting fungiform papilla growth and patterning the fungiform papilla development in the tongue.

1.3.2.3 BMP signaling

The BMP signaling pathway is another necessary pathway for the development of taste papillae. BMPs are a large group of secretory factors belonging the TGF-β superfamily and are important regulators of numerous developmental roles, including cell proliferation, apoptosis, differentiation and cell migration (Balemans and Van Hul, 2002; Botchkarev and Kishimoto, 2003; Botchkarev and Sharov, 2004; Zhang and Li, 2005). BMP signaling also has canonical and noncanonical pathways, although the canonical pathway plays the crucial role in taste papilla development. The role of the noncanonical BMP signaling pathway in taste papilla development remains to be understood. In the BMP signaling pathway (Fig. 1.2), BMP ligands bind to the heteromeric receptor complex formed from Type I and Type II receptors. BMP ligands will bind to Type II receptors (BMP receptor type 2/Bmpr-2, Activin receptor type 2A/Actr-2A and Actr-2B). Ligand-bound type II BMP receptors will then activate Type I BMP

receptors (Actr-1A or Alk2, Bmpr1-A or Alk3, and Bmpr-1B or Alk6) through phosphorylating their glycine-serine-rich motif, also known as the GS domain. Type I BMP receptors are the main determinant of downstream signaling specificity. Activated Type I BMP receptors then phosphorylate downstream signaling components known as regulatory Smads (R-Smads/Smad 1/5/8). Phosphorylated Smad 1/5/8 will form a complex with co-mediator Smad (co-Smad 4) and translocate to the nucleus to transcribe downstream target genes (Fig. 1.2). Inhibitory Smads (I-Smads, Smad 6/7) are involved in the negative feedback inhibition of the BMP signaling pathway (Bragdon et al., 2011; Wang et al., 2014).

Among the BMP ligands, the crucial roles of BMP2 and BMP4 in taste papilla development have been revealed through in situ expression analyses (Bitgood and McMahon, 1995; Hall et al., 2003; Jung et al., 1999). BMP7 also plays an important role in the development of epithelial tissues (Bitgood and McMahon, 1995; Chen et al., 2004; Hall et al., 2003; Jung et al., 1999). Analysis of BMP ligand distribution in rat tongues revealed that BMP2 and BMP4 begin to express in diffuse patterns in E13 rat tongues, gradually becoming confined to regions where fungiform taste papillae will develop at E14 and continuing to express within the fungiform taste papillae by E15. In the E14 epithelium, BMP4 is intense within the thin line along the basement membrane of taste papilla placodes and between placode regions. At E15, BMP4 becomes denser in the fungiform papillae epithelium compared to the epithelium between papillae. BMP4 is also expressed in the tongue mesenchyme at E13 and becomes less intense at the E14 mesenchyme (Zhou et al., 2006).

In contrast, Noggin, a BMP antagonist, has been shown to have similar distribution to that of BMP ligands, beginning with a diffuse distribution in the E13 tongue epithelium and becoming progressively restricted to fungiform taste papilla placodes by E14. The Noggin immunoproduct is dense in the fungiform taste papilla placode epithelium at E14 compared to the between-placode epithelium. At E15, Noggin becomes denser and more restricted in the apical region of

fungiform papillae. In contrast to the epithelium, weaker Noggin immunosignals have been detected in the tongue mesenchyme at E14 (Zhou et al., 2006).

The addition of BMP2, 4, and 7 ligands to E13+3D rat tongue cultures resulted in the concentration-dependent formation of numerous and distinct fungiform taste papillae in the anterior tongue region. Similar to BMP ligands, the addition of Noggin to E13+3D cultures resulted in a noticeable increase in fungiform taste papillae. Interestingly, large fungiform taste papillae developed in the anterior tongues of the E13 Noggin cultures with higher Noggin concentrations, supporting the effect of BMP signaling on regulating papillae size. Furthermore, the separate addition of BMP2, 4, 7 ligands to E14+2D rat tongue cultures resulted in a significantly lower total number of fungiform taste papillae compared to the controls. However, the addition of the combination of all three BMP ligands (BMP2, 4, 7) to E14 rat tongue cultures did not result in further reduction of fungiform taste papillae, suggesting that BMP ligands (BMP2, 4, 7) utilize the same signaling pathway to regulate taste papilla development. In contrast to BMP ligands, the addition of Noggin to E14 rat tongue cultures resulted in the concentration-dependent development of a significantly high number of fungiform taste papillae. Despite this increase, the effect of Noggin is restricted to the fungiform taste papillary region. Extra papillae did not develop in the typical nonpapillary regions, including the intermolar eminence region. This difference indicates that exogenous BMP can oppose the BMP action that otherwise inhibits the formation of fungiform taste papillae. Higher Noggin concentration in E14+2D cultures also forces the fungiform taste papillae to merge in a linear fashion, which suggests that the normal BMP function of maintaining the interpapillary space is opposed by the excess Noggin in these situations (Zhou et al., 2006).

The placement of beads soaked with BMP2, 4, and 7 in tongue cultures resulted in the inhibition of fungiform papilla formation in the lingual epithelium surrounding the beads. In contrast, the placement of Noggin-soaked beads in this region resulted in a higher density of fungiform taste papilla formation in the surrounding area. Furthermore, in E14 tongue cultures

implanted with beads soaked in BMP2, 4, or 7, even after the Shh inhibitor cyclopamine was added to the cultures and left to continue to culture for 2 days, fungiform taste papillae did not develop in the regions surrounding the regions with the beads, demonstrating that BMPs can inhibit fungiform taste papilla formation even in the absence of the Shh signaling pathway (Zhou et al., 2006).

Follistatin, a secreted polypeptide and a BMP signaling pathway antagonist, is another crucial molecule involved in the development of fungiform taste papillae (Beites et al., 2009). The expression of follistatin in tongue development coincides with the active timeframe in which fungiform taste papillae begin to develop. Follistatin first expresses in the developing tongue at E11.5 and continues to express throughout the tongue mesenchyme subjacent to the tongue epithelium at E12.5. At E13.5, folistatin has a relatively higher expression in the posterior tongue mesenchyme, where the intermolar eminence develops. After E14.5, follistatin expression begins to decline, and by E16.5, follistatin is barely detectable in the tongue mesenchyme. In the absence of follistatin, ectopic papillae begin to express in the intermolar eminence region, which normally does not host taste papillae. In studies using *Fst*$^{-/-}$ mice, the keratinized barrier in the posterior tongue epithelium became compromised compared to the control tongue (Beites et al., 2009). Furthermore, the lack of filiform papillae was seen corresponded to the region in which the keratinized barrier in the posterior tongue epithelium became compromised. Despite the presence of fungiform taste papillae in *Fst*$^{-/-}$ mice, changes in their size and spacing were noticed in the anterior tongue region of these mice, in which the fungiform papillae were organized as tight clusters (Beites et al., 2009).

Sox2 is taste bud stem/progenitor cell marker (Okubo et al., 2006) and expresses in the taste papilla placodes of the tongue epithelium at E12.5. Analysis of Sox2 in *Fst*$^{-/-}$ mice at E14.5 detected relatively lower expression in the anterior tongue. Interestingly, Sox2 expression expanded in the intermolar eminence region of *Fst*$^{-/-}$ mice, a region that is usually devoid of

Sox2-expressing taste papillae. The expression of Sox2 in this case indicates that follistatin is crucial for Sox2 expression (Beites et al., 2009).

The absence of follistatin also reduces Shh expression and Wnt-β-catenin activity. In *Fst*$^{-/-}$ mice, Shh expression was shown to be significantly reduced in both E12.5 and E14.5 tongues compared to littermate controls. Moreover, the evaluation of Wnt-β-catenin in *Fst*$^{-/-}$ mice with the BAT-Gal reporter allele, where LacZ expression is controlled by β-catenin/TCF-response element, demonstrated decreased Wnt-β-catenin activity. X-Gal-stained cell clusters in *Fst*$^{-/-}$ mice were smaller compared to littermate controls. Shh expression and Wnt-β-catenin were noticed in the epithelium of the intermolar eminence region (Beites et al., 2009).

Follistatin binds and inhibits the BMP7 ligand, which is present in the lingual epithelium during the early stages of tongue development (E11.5) but becomes progressively restricted to the anterior tongue and then to the fungiform papillae taste buds. BMP7 is also present in low levels in the tongue mesenchyme and muscles. In *Fst*$^{-/-}$ mice, elevated levels of p-Smad 1/5/8 and BMP7 were detected in the ectopic taste papillae, demonstrating that follistatin suppresses BMP7 and BMP7-mediated signaling activity during tongue development and controls the size and patterning of the fungiform taste papillae in the anterior tongue while inhibiting the formation of ectopic taste papillae in the posterior oral tongue, especially in the intermolar eminence region. Tongues cultured with BMP7 showed depressed Shh and Wnt-β-catenin activity, which was attributed to the reduced number and size of Shh-positive taste papillae in the anterior tongue (Beites et al., 2009).

The absence of both BMP7 and follistatin was shown to rescue the absence of filiform taste papillae in the posterior tongue and the loss of Shh expression in the developing fungiform papillae in the anterior tongue, thereby confirming the inhibitory role of BMP7 in the development of taste papillae and the regulatory role of follistatin on BMP7 activity through antagonizing BMP7 (Beites et al., 2009).

1.3.2.4 Fibroblast growth factor (FGF) signaling

The Fibroblast growth factor (FGF) signaling pathway is another signaling pathway that regulates mainly fungiform progenitor field size (Prochazkova et al., 2017). In the FGF signaling pathway, the FGF10 ligand is mainly expressed in the tongue mesenchyme, where taste papillae develop. In *FGF10* knockout mice, larger fungiform taste papillae were observed in E14.5 knockout mice compared to controls, which indicates that FGF10 negatively regulates the size of fungiform taste papillae. Furthermore, when Sprouty 2 (*Spry2*), an Receptor tyrosine kinases (RTK) signaling antagonist, was knocked out, smaller fungiform taste papillae were detected in E14.5 tongues compared to littermate controls, thereby demonstrating the role of FGF signaling in controlling the size of the papillary field of fungiform taste papillae. Interestingly, the pattern of fungiform taste papillae was not altered in either the *FGF10* or *Spry2* knockout mice (Prochazkova et al., 2017).

When *Spry2* knockout and *FGF10-null* mice were crossed with BAT-gal mice to elucidate the interaction between FGF and the Wnt/β-catenin signaling pathway, *Spry2*$^{-/-}$ tongues at E14.5 showed strong X-gal signals in the fungiform papillary areas, but such signals were largely absent in the interpapillary epithelium compared to wild-type tongues. In contrast to the *Spry2*$^{-/-}$ and wild types, *FGF10*$^{-/-}$ mice had more diffuse X-gal signals, suggesting that FGF signaling regulates fungiform papillae size by inhibiting the expansion of the Wnt signaling field (Prochazkova et al., 2017).

Wnt10a and Wnt10b both express in the tongue epithelium. Of these two Wnt ligands, Wnt10b is considered the principal activating ligand (Iwatsuki et al., 2007; Liu et al., 2007; Orriols et al., 2017) and is mainly restricted to the within taste papilla placodes. Wnt10a, by contrast, expresses throughout the taste papilla placodes (Prochazkova et al., 2017). The addition of LiCl to E12.5 tongue cultures resulted in faster Wnt10b response, thereby demonstrating its role as the principal autoregulatory activator for fungiform taste papilla development. LiCl treatment also upregulated Dkk1 expression, indicating that upregulated Wnt

signaling activates negative regulation of its activity. Dkk1 is an antagonist of the Wnt signaling pathway (Prochazkova et al., 2017). In contrast, the addition of Wnt signaling inhibitor PNU74654, to cultures resulted in the downregulation of both Wnt10a and Wnt10b. PNU74654 arrests Wnt signaling target gene transcription through disrupting the β-catenin/Tcf complex (Leal et al., 2015; Prochazkova et al., 2017), The alteration of FGF signaling activity by using recombinant FGF protein as an FGF signaling activator or SU5402, a FGF signaling inhibitor, resulted in no change to Wnt10a or Wnt10b expression levels. In the presence of SU5402 in cultures, Sostdc1 expression was significantly reduced, whereas it significantly increased in the presence of recombinant FGF10 protein. However, Sostdc1, which is an inhibitor of the Wnt signaling pathway, was upregulated in *Spry2*$^{-/-}$ mutants and downregulated in *FGF10*$^{-/-}$ mutants, which suggests that FGF signaling inhibits Wnt signaling through Sostdc1. Sostdc1 is a known inhibitor of fungiform taste papillae (Ahn et al., 2010; Prochazkova et al., 2017) and expresses uniformly in the papillary field during fungiform taste papilla development, corresponding to the regions in which FGF10 is expressing. Sostdc1 expression is localized mainly to the border between the epithelium and mesenchyme. At E13.5 and E14.5, within the multilayered tongue epithelium, cells closer to the mesenchyme are Sostdc1+, while superficial layers are Sostdc1-.

Other FGF ligands, such as FGF1 and FGF2 along with FGF receptor FGFr2b, have been detected in the lingual epithelium at E11.5 (Du et al., 2016; Jung et al., 1999; Nie, 2005) but their functions in taste papilla development has yet to be discovered.

1.3.2.5 Epidermal growth factor (EGF) signaling

Epidermal growth factor (EGF) is a secreted factor known to regulate the spacing of other epithelial appendages, including hair (Mak and Chan, 2003) and denticles (Urban et al., 2004). The EGF signaling pathway also plays an important role in determining interpapillary space in developing embryonic rat tongues (Liu et al., 2008).

EGF begins to express in the tongue epithelium at E14 in rats and, by E15, is present in all epithelial layers including the papillary placode and interplacode regions. EGF immunosignals

are also present in the mesenchyme. From E16-E18, EGF immunosignals become more intense in the tongue epithelium as well as the fungiform papillae. In contrast, EGF receptor EGFR has a patchy distribution in the E13 tongue epithelium. Importantly, at E13, EGF ligands are absent. At E13-E14, EGFR is localized throughout the tongue epithelium, with intense EGFR immunosignals in E14 tongues compared to E13. However, from E15-E18, EGFR becomes progressively restricted to the interpapillary epithelium and is absent from the fungiform papilla epithelium. In contrast to EGF, EGFR immunosignals are not obvious in the mesenchyme subjacent to the epithelium (Liu et al., 2008).

In E13+2D rat tongue cultures in which the development of fungiform papilla had not yet begun in the merged tongue swellings or in E14+2D cultures in which fungiform taste papilla placodes had just begun to develop, the administration of exogenous EGF resulted in concentration-dependent decreases of fungiform taste papillae regardless of the stage at which it was administered. Higher concentrations of exogenous EGF had more profound effects on the development of the fungiform taste papillae, thereby demonstrating the role of EGF in promoting the interpapillary space (Liu et al., 2008).

The addition of EGF inhibitor compound 56 (Bridges et al.,1996), which blocks endogenous EGFR action, resulted in an increased number of fungiform taste papillae in E14+2D cultures. In the absence of endogenous EGF signaling activity, the fungiform taste papillae fuse and cluster, further confirming the role of EGFR in maintaining the interpapillary space. The addition of both exogenous EGF and compound 56 to tongue cultures rescued the EGF-mediated fungiform taste papillae inhibition, thereby demonstrating that EGF exerts its function through EGFR and that, in the blockade of EGFR, fungiform taste papillae can develop even in the presence of endogenous or exogenous EGF ligands. Interestingly, the effect of EGF is so potent that Shh signaling inhibition through cyclopamine cannot rescue the fungiform taste papillae loss caused by exogenous EGF, which demonstrates that EGF can override Shh disruption. Shh disruption

in the developing tongue in the early stages of taste papilla development causes excess development of fungiform papillae (Liu et al., 2004; Mistretta et al., 2003).

The EGF signaling pathway utilizes PI3K/Akt, MEK/ERK and p38 MAPK as downstream signaling components (Irmer et al., 2007; Jorissen et al., 2003). Akt, ERK1/2 and -p38 MAPK are present in both the taste papilla epithelium as well as in the interpapillary epithelium. When EGF signaling is activated in the presence of exogenous EGF, phosphorylation of Akt and ERK1/2 but not of -p38 MAPK occurs, indicating that EGF utilizes the PI3K/Akt and MEK/ERK pathways in taste papilla development. In the presence of PI3K activation inhibitor LY294002 or MEK/ERK activation inhibitor U0126, EGF-dependent fungiform papillae loss is fully recovered (Liu et al., 2008).

1.3.2.6 Retinoic acid signaling pathway

Signaling components of the retinoic acid signaling pathway are known to express in the developing tongue (Dollé et al., 1994; Dollé et al., 1990; Niederreither et al., 2002; Niederreither et al., 1997; Ruberte et al., 1992). In *ShhGFPCRE/Smo*$^{f/f}$ or tamoxifen-induced *ShhCreERT2/Shh*^{f} mice in which Shh signaling activity was knocked out, expression levels of Retinoic acid (RA) signaling pathway transcriptional targets RARb and RARg were significantly upregulated. Furthermore, the immunosignals of retinoic acid receptors RARβ and RARγ, which are encoded by RARb and RARg, were significantly increased in the *ShhGFPCRE/Smo*$^{f/f}$ and tamoxifen-induced *ShhCreERT2/Shh*^{f} mouse tongue epithelia, indicating that the absence of the Shh signaling pathway enhances the RA signaling pathway in the epithelium (El Shahawy et al., 2017).

The Cyp26a family is known to play a crucial role in the regulating retinoic acid signaling pathway (Pennimpede et al., 2010; White and Schilling, 2008). Among the members in the Cyp26 family, Cyp26a1 and Cyp26c1, which are present in the tongue epithelium (Abu-Abed et al., 2002; de Roos et al., 1999), have been shown to be significantly decreased in *ShhGFPCRE/Smo*$^{f/f}$ mutant tongue epithelia and in tamoxifen-induced *ShhCreERT2/Shh*^{f}

tongues, indicating that the absence of Shh signaling activity affects the expression of Cyp26a1/c1. It has been shown that Cyp26a1/c1 is present in the lingual epithelium during the active phase of fungiform papilla development but that after E14.5, Cyp26a1/c1 begins to deteriorate and stops expressing after E16.5 in normal tongues. Despite its presence in the lingual epithelium, Cyp26a1/c1 is absent from the region in which fungiform and circumvallate papillae develop and from the pharyngeal tongue region. It is evident that Shh signaling controls RA signaling through Cyp26a1/c1 during the active phase of fungiform taste papilla development (El Shahawy et al., 2017).

Interestingly, changes in Cyp26a1/c1 levels only occurred when Shh activity was inhibited before E12.5. In contrast to the *ShhGFPCRE/Smo*$^{f/f}$ or E10.5 and E11.5 tamoxifen-induced *ShhCreERT2/Shh*^{f} tongues, no changes in Cyp26a1/c1 levels were detected in E12.5 *ShhCreERT2/Shh*^{f} mutant tongues. It is also important to note that Cyp26a1/c1 may not be the direct target of the Shh signaling pathway as the tongue explants with SAG, an antagonist to Shh signaling pathway receptor Smo, resulting in enhanced Cyp26a1 expression in the lingual epithelium but not in the pharyngeal tongue epithelium (El Shahawy et al., 2017).

In control tongues treated with retinoids, oversized Shh+ placodes developed. In addition, ectopic Shh signals developed in a concentration-dependent manner in tongues treated with RARβ agonist CD2314 and RARγ agonist CD1530, with higher concentrations causing the development of ectopic Shh+ taste papilla placodes flanking the intermolar eminence region. Interestingly, when the RA pathway was inhibited in control and *ShhGFPCRE/Smo*$^{f/f}$ mutants using pan-RAR inverse agonist BMS493, weak or no Shh signals were detected. It is evident that the RA signaling pathway promotes fungiform papilla placode formation (El Shahawy et al., 2017).

1.3.2.7 Six1 and Six4 in fungiform papilla development

A family of six genes referred to as Six1-6 encodes transcription factors. Among the members of this group, Six1 and Six4 demonstrate regulatory roles in taste papilla development

(Suzuki et al., 2010a, b; Suzuki et al., 2011). At E11.5, Six1 expresses in the lingual mesenchyme under the epithelium and intensifies in the lingual muscle by E17.5. Six1 also expresses in the apical region of the fungiform papillae at E15.5, becoming limited to the papillary epithelium by E16.5 and absent altogether from E18.5 fungiform papillae. Six1 does not express in the mesenchymal core of fungiform papillae (Suzuki et al., 2010a, b; Suzuki et al., 2011).

By contrast, Six4 begins to express in the tongue epithelium at E11.5 and, by E12.5, it also expresses in the dorsal tongue epithelium and lingual muscles. Six4 expresses on the surface of the fungiform papillae, weakening and becoming limited to the papillary epithelium by E16.5. At E18.5, Six4 stops expressing in the fungiform papillae (Suzuki et al., 2010a; Suzuki et al., 2011).

In *Six1*$^{-/-}$ mice, a higher number of fungiform papillae developed at E14.5 compared to wild-type mice. These fungiform papillae were larger in diameter and arranged in more irregular patterns, with more papillae located close to the medium furrow compared to wild-type mice. In wild-type mice, fungiform papillae demonstrate a patterned distribution. Some fungiform papillae in *Six1*$^{-/-}$ mice fused to form clusters. Although fungiform papillae developed in large numbers in the midembryonic stages (E14.5), further development was halted, and no new fungiform papilla development occurred. As a result, compared to wild-type mice at E19, *Six1*$^{-/-}$ mice had smaller and fewer fungiform papillae, whereas wild-type mice developed more fungiform papillae from E14.5–E19. Taste papilla placode markers Wnt10b and Shh expression were elevated in E13 *Six1*$^{-/-}$ mutants' taste papilla primordial epithelium compared to wild-type mice, likely describing the enlarged papillae at E14.5 (Suzuki et al., 2010a, b; Suzuki et al., 2011).

In contrast to *Six1*$^{-/-}$ mutants, *Six4*$^{-/-}$ mutants showed no significant morphological changes in the fungiform papillae compared to wild-type mice. However, *Six1*$^{-/-}$ and *Six4*$^{-/-}$ double knockouts had more severe defects compared to *Six1*$^{-/-}$ mutants in the later stages of fungiform papilla development (E19). The fungiform papillae of *Six1*$^{-/-}$ and *Six4*$^{-/-}$ double knockouts were much

smaller, shorter and often had a filiform-like appearance compared to wild-type and *Six1*$^{-/-}$ mice. Although E14.5 *Six1*$^{-/-}$ and *Six4*$^{-/-}$ double knockout mice demonstrated enlarged and fused fungiform papillae with reduced interpapillary space, similar to *Six1*$^{-/-}$ mice, the number of fungiform papillae did not increase compared to wild-type mice, which indicates that the cumulative absence of Six1 and Six4 determines fungiform papilla development differently compared to the absence of only one transcription factor. It is possible that Six1 has more regulatory effects than Six4 on fungiform papilla development (Suzuki et al., 2010a, b; Suzuki et al., 2011).

1.3.3 Molecular regulation involved in circumvallate and foliate papilla development

In contrast to the molecular regulation of fungiform taste papilla development, studies to dissect the molecular mechanism behind the development of circumvallate taste papilla are far from complete. One main reason for this research gap is that the main signaling pathways that control fungiform taste papilla development, including Shh, Wnt, BMP and EGF, play little to no role in the development of circumvallate papilla. For example, Shh signaling inhibition has no effects on circumvallate papilla development (Liu et al., 2004; Mistretta et al., 2003), nor does the activation or inhibition of Wnt/β-catenin signaling (Iwatsuki et al., 2007). Moreover, the BMP signaling antagonist Follistatin or Noggin affect ectopic taste papilla development and increase fungiform taste papilla development but have no effect on circumvallate papilla development (Beites et al., 2009; Zhou et al., 2006). Another reason for the differences in molecular regulation between the fungiform and circumvallate taste papillae could be the differences in the embryonic origins of the anterior and posterior tongue (Zhang and Oakley, 1996). The fungiform papillae located in the anterior tongue are derived from the ectoderm, while the circumvallate papilla, located in the posterior tongue, are likely derived from the endoderm (Kist et al., 2014; Zhang and Oakley, 1996), hence the discrepancies in molecular signaling pathways in regulating taste papilla development.

The circumvallate taste papilla placode develop from a compact collection of epithelial cells and epithelial thickening of the dorsal epithelium in the middle of the border between the oral and pharyngeal tongue at E11.5. At E12.5, placodal condensation is more apparent, and undergo major morphological changes around E13-E13.5 to attain the domed structure with an apex and two epithelial trenches characteristic of the circumvallate papilla. At E14.5, these epithelial trenches will grow into the mesenchyme and complete the initial morphogenesis of the circumvallate papilla (Petersen et al., 2011).

1.3.3.1 FGF signaling pathway

Among the signaling components of the FGF signaling pathway, FGF antagonists Sprouty 1 (Spry1) and Spry2 are expressed in the tongue epithelium at E12.5 (Petersen et al., 2011). In mice with Spry2, an antagonist of the FGF signaling pathway, knocked out, a relatively larger circumvallate papilla placode was observed in E11.5 *Spry2*$^{-/-}$ mutants compared to wild-type mice. The enlarged circumvallate papilla placode then continued to grow larger, both laterally and along the anterior-posterior axis, becoming two distinct papillae by E14.5, thereby demonstrating the role of FGF signaling in regulating the development of circumvallate papilla (Petersen et al., 2011). Furthermore, in *Spry2*$^{-/-}$ mice, the expression of taste papilla placode and taste bud progenitor marker Sox2 (Okubo et al., 2006) was shown to expand both laterally and along the anterior-posterior axis corresponding to the region in which an enlarged circumvallate placode domain developed in tongues at E11.5 and E12.5. In addition to Sox2, the expression domains of Shh, BMP7 and Wnt10b (Beites et al., 2009; Liu et al., 2007) that are important regulators of taste papilla placode development and were also shown to have expanded in the circumvallate placode of *Spry2*$^{-/-}$ mutants compared to wild-type mice, suggesting that the inactivation of Spry2 thus leads to a larger taste papilla progenitor field. In the absence of *Spry2*, FGF signaling target gene *Etv5* (Roehl and Nüsslein-Volhard, 2001) is upregulated compared to wild types. *Spry1*$^{-/-}$ and *Spry2*$^{-/-}$ double knockout mice had much wider Sox2 and Etv5 expression domains compared to the circumvallate papilla placode of *Spry2*$^{-/-}$

mice. Interestingly, *Spry1*$^{-/-}$ and *Spry2*$^{-/-}$ double knockouts had multiple circumvallate papillae (Petersen et al., 2011).

The FGF10 ligand is expressed in the tongue mesenchyme subjacent to the epithelium along the midline of the E11.5 and E12.5 posterior tongue. FGF receptors FGFR2 and FGFR3 express in the circumvallate placode, which demonstrates that epithelium and mesenchyme interaction is mediated by FGF signaling in the circumvallate papilla development. The inhibition of FGF signaling through the addition of FGF signaling inhibitor SU5402 (Mohammadi et al., 1997) to E11.5 wild-type cultures has been shown to result in the absence of circumvallate papillae. The addition of SU5402 to E12.5 cultures resulted in the development of absent or malformed circumvallate papillae, indicating that FGF signaling plays a crucial role in circumvallate papilla development at 11.5 but a lesser one at E12.5. Interestingly, the deletion of *FGF10* resulted in the complete absence of circumvallate papilla, which demonstrates the inductive role of mesenchymal FGF10 in circumvallate papilla development. In the absence of both Spry2 and FGF10, a single circumvallate papilla developed, which demonstrates that the deletion of both Spry2 and FGF10 counterbalances their effects, thereby rescuing circumvallate papilla development (Petersen et al., 2011).

Overall, it is evident that the role of FGF10-mediated FGF signaling is to promote the circumvallate papilla progenitor field. Under normal conditions, the presence of Spry1 and Spry2 inhibits FGF10 activity, thus allowing for the formation of one circumvallate papilla. In the absence of Spry1 and Spry2, FGF10 ligands have no antagonist to regulate their effects and, consequently, bind to the FGFR 2/3 receptors in the circumvallate placode epithelium and promote the circumvallate papilla progenitor field, thus leading to multiple circumvallate papillae. In the absence of Spry2, Spry1 continues Fgf10 inhibition, leading to circumvallate papilla duplication.

1.3.3.2 Role of Pax9 and Pax1 in circumvallate and foliate papilla development

Pax9 is a transcription factor and also plays an important role in the development of circumvallate and foliate papillae (Kist et al., 2014). Pax9 is expressed in the epithelium of the placodes and trenches of both circumvallate and foliate taste papillae. Pax9 is also present in the mesenchyme beneath the foliate papilla epithelium. In the absence of Pax9, shortened epithelial tranches were observed despite the formation of circumvallate papilla. The mesenchyme-specific genetic deletion of Pax9 using *Wnt1-Cre* transgenic mice resulted in no obvious changes to foliate papilla development, indicating that epithelial Pax9 plays a crucial role in the development of circumvallate and foliate papillae. Moreover, the absence of Pax9 also affected Shh signaling activity in both the circumvallate and foliate papillae of E14.5 mice. In *Pax9*$^{-/-}$ mice, Shh, Gli1 and Ptch1 transcripts were downregulated in the circumvallate and foliate papillae but not in the fungiform papillae (Kist et al., 2014).

Pax1 is a transcriptional regulator and an early target of Pax9 in the developing circumvallate papilla. It is expressed at the tips of the invigilating circumvallate papilla trenches of wild-type mice but is absent from *Pax9*$^{-/-}$ mutants. Furthermore, the absence of *Pax1* has been shown to result in shorter circumvallate papilla trenches. The promotion of cell proliferation and shorter circumvallate papilla trenches by Pax1 is likely attributable to reduced cell proliferation as a result of *Pax1*$^{-/-}$ (Kist et al., 2014).

In addition, it has been reported that a lack of dystonin (Ichikawa et al., 2006) also resulted in malformed circumvallate papilla. Dystonin is a plakin family member (Bernier et al., 1995) and is expressed in the neural tissues and cross-link F-actin, intermediate filaments and microtubules during axonogenesis (Dalpé et al., 1998; Leung et al., 1999).

1.3.3.3 Role of Wilms' tumor 1 (WT1) in circumvallate papilla development

Wilms' tumor 1 (WT1) is a tumor suppressor gene of a pediatric embryonal tumor called Wilms' tumor (nephroblastoma), which develops due to an abnormal cellular differentiation during organogenesis (Sangkhathat et al., 2010). WT1 begins to express in E12.5 mice in a

diffused pattern but by E14.5 is restricted to the epithelium of the developing circumvallate taste papilla and surrounding tissues. In *WT1*$^{-/-}$ mice, when taste papilla placodes emerge at E12.5, the development of the circumvallate papilla placode is severely impaired, and they lose the characteristic epithelial thickenings that usually indicate the initiation of circumvallate papilla development. Furthermore, Sox2 expression was lost and nonspecific Shh signals reportedly developed in *WT1*$^{-/-}$ mice. It has been reported that BMP4, Shh, and Lef1 are target genes of WT1 (Hartwig et al., 2010) and are coexpressed with WT1 in the developing circumvallate papilla. In *WT1*$^{-/-}$ mice, reduced or largely absent mRNA transcripts and/or immunoproducts of Lef1, Ptch1 and BMP4 were detected in the circumvallate papilla at E14.5, thereby demonstrating that the loss of WT1 significantly affected Lef1, Ptch1 and BMP4 expression compared to wild-type tongues. Overall, WT1 is an important regulator of circumvallate papilla development and regulates BMP4, Shh, and Wnt β-catenin pathways during circumvallate papilla development (Gao et al., 2014).

1.3.3.4 Six1 and Six4 in circumvallate and foliate papilla development

In the circumvallate papilla, Six1 begins to weakly express in the basal side of the epithelium and mesenchyme at E13.5 and intensifies in the trench epithelium of the circumvallate papilla by E16.5. By E17.5, Six1 expression is restricted to the bottom trenches of the circumvallate papilla. In the foliate papillae, Six1 expresses in the trench epithelia at E15.5 and is limited to the bottom trenches by E17.5 (Suzuki et al., 2010b).

In the circumvallate papilla, at E13.5, Six4 expresses in the entire oral epithelium but not in the invaginated area. At E15.5, strong Six4 expression has been observed in the trench epithelium similar to that of Six1, as it is also restricted to the bottom of the trenches of the circumvallate papilla. In the foliate papillae, Six4 expresses in the trench epithelium at E15.5 and is restricted to the bottom of the trenches by E18.5 (Suzuki et al., 2010a, b; Suzuki et al., 2011).

In the absence of Six1, E13.5 *Six1*$^{-/-}$ mice developed an extensive invagination in the circumvallate papilla field that later developed into shallower trenches at E14.5. Despite the similarity of the size of this field between *Six1*$^{-/-}$ and wild-type mice, the circumvallate surface was hollowed out in the *Six1*$^{-/-}$ mutants at E14.5. By E19, *Six1*$^{-/-}$ mutants developed shallower trenches with smaller and underdeveloped circumvallate papilla compared to wild-type mice. Analysis of Shh expression, a necessary marker for the formation of circumvallate papilla (Kim et al., 2009), in the developing circumvallate papilla placode at E13.5 revealed intense expression in *Six1*$^{-/-}$ mutants compared to wild-type mice. However, Shh expression weakened in E14.5 *Six1*$^{-/-}$ mutants' circumvallate papilla and was barely detectable in the papilla epithelium and absent entirely from the trenches of E16.5 *Six1*$^{-/-}$ mutants. In wild-type mice, Shh expresses in both the papilla epithelium and in trenches, becoming limited to the trenches and von Ebner glands at E18.5. By contrast, in *Six1*$^{-/-}$ mice, Shh expression is restricted to the bottom of the trenches of the circumvallate papilla, indicating that the absence of Six1 affects Shh expression (Suzuki et al., 2010a, b; Suzuki et al., 2011).

Similarly, at E14.5, *Six1*$^{-/-}$ mutants were reported to have elevated foliate papillae compared to wild-type mice, but later in their development (E19), the mutants had comparatively malformed and shorter foliate papillae. Both the circumvallate and foliate papillae connected to the von Ebner glands in wild-type mice but failed to do so in *Six1*$^{-/-}$ mutants. Compared to *Six1*$^{-/-}$ mutants, *Six1*$^{-/-}$ and *Six4*$^{-/-}$ double knockout mice had more extensive epithelial invagination into the mesenchyme, which later developed into smaller, malformed circumvallate papilla by E19. In contrast to wild-type and *Six1*$^{-/-}$ mutant mice, *Six1*$^{-/-}$ and *Six4*$^{-/-}$ double knockout mice had irregular trench length, with one trench being much deeper than the other. Interestingly, in these E19 mice, Shh only expressed at the bottom of the longer trench of the circumvallate papilla, not the shorter trench (Suzuki et al., 2010a, b; Suzuki et al., 2011).

Moreover, in *Six1*$^{-/-}$ and *Six4*$^{-/-}$ double knockout mice, an absence of epithelial elevations usually present in the margin of the posterior tongue was observed in E14.5 tongues compared

to those of wild-type mice. From E14.5-E15.5, the initial epithelial elevation begins to occur in the foliate papillary field. Similar to *Six1*$^{-/-}$ mutant mice, *Six1*$^{-/-}$ and *Six4*$^{-/-}$ double knockout mice were also reported to develop smaller, malformed foliate papillae by E19 (Suzuki et al., 2011).

1.3.3.5 Role of Yap signaling in the development of circumvallate papillae

Yes-associated proteins (YAP) are a key transcriptional regulator in the Hippo signaling pathway, which plays an important role in organogenesis and in tumorigenesis (Wang et al., 2017). The nuclear translocation of Yap regulates the specification, proliferation and differentiation of progenitor cells (Camargo et al., 2007b; Pan, 2010; Panciera et al., 2016). Yap is also considered a common deactivator of Hippo signaling. Phosphorylated (p) Yap, in contrast, induces cell growth arrest during tissue development (Davis and Tapon, 2019; Yu et al., 2015a; Yu and Guan, 2013; Yu et al., 2015b) and considered as an indicator of Hippo signaling. In E16 tongues, nuclear localized Yap expression was detected in the trench and the invaginating epithelium of the circumvallate papilla. In the apex region of circumvallate papilla, Yap is mainly present in cell cytoplasm. In contrast to Yap, cytoplasmic localization of p-Yap has been detected in the trench and the invaginating epithelium of the circumvallate papilla at E16. In addition, Ki67, a marker for the proliferating cells, has been observed in the lateral trench wall and invaginating epithelium but not in the epithelium of the apex region of the circumvallate papilla, indicating that Yap promotes cell proliferation and, consequently, circumvallate papilla development (Kim et al., 2021).

It has been reported that p-Yap inhibits the Wnt signaling pathway by sequestering cytoplasmic β-catenin or by interacting with Wnt receptor Disheveled (Hansen et al., 2015; Heallen et al., 2011; Imajo et al., 2015; Kim and Jho, 2016). In contrast, Yap activates β-catenin, thereby promoting the transcription of the Wnt signaling target gene through the β-catenin/TCF transcription factor complex (Hansen et al., 2015; Kim and Jho, 2014). At E16, β-catenin is detectable in the boundary epithelium and the epithelium forming the circumvallate papilla trench, and unphosphorylated β-catenin is present throughout the circumvallate papilla

epithelium with strong nuclear and cytoplasmic localization in the cells of the circumvallate papilla apex and in the invaginating epithelium of the developing circumvallate papilla. Unphosphorylated β-catenin is considered the active form of β-catenin that will eventually translocate to the nucleus. The presence of nuclear unphosphorylated β-catenin and Yap in the apical and lateral portion of the developing circumvallate papilla epithelium suggests that the interaction between Yap and active β-catenin may be involved in the organization of epithelial cells during circumvallate papilla development (Kim et al., 2021).

1.3.3.6 Noncanonical Wnt and Shh signaling

In noncanonical Wnt signaling, the Disheveled receptor activates small GTPase, namely, RhoA, CDC42 and Rac, which then activate Rho-associated kinase (ROCK) and c-Jun N-terminal kinase (JNK) to promote cell adhesion, cytoskeletal rearrangement, etc. (Choi and Han, 2002; Habas et al., 2003; Winklbauer et al., 2001). Rho effector molecules ROCKs are protein serine/threonine kinases (Keller et al., 2002) and play crucial roles in circumvallate papilla development.

Wnt11, a ligand in the noncanonical Wnt signaling pathway, is mainly expressed in the tongue epithelium at E13.5 and in the apex epithelium of the E15.5 circumvallate papilla (Kim et al., 2009). In contrast, Shh is expressed in the apical epithelium of the E13.5 tongue and at E15.5 in the lateral epithelium of the circumvallate papilla, where taste buds and von Ebner glands will develop later. At E13.5, ROCK1 is expressed mainly in the apex epithelium of circumvallate papilla, and weak ROCK1 expression has also been detected in the epithelium of the E15.5 circumvallate papilla field, similar to the location of Wnt11 expression, indicating that Wnt11 and ROCK1 interact during the circumvallate papilla formation. Unlike the pattern of Shh expression, phalloidin, which labels actin filaments, has been detected in the apex epithelium at both E13.5 and E15.5. Interestingly, at E15.5, phalloidin expression was opposite to the pattern of Shh expression, indicating that Shh plays a role in circumvallate papilla development through interacting with the cytoskeleton. The addition of Y27632, a pharmacological inhibitor of

ROCK1, to E13.5 tongue cultures resulted in striking changes in circumvallate papilla development that decreased the apical epithelium but significantly increased the lateral epithelium, which eventually gives rise to the von Ebner glands. Cell proliferation was also increased in the von Ebner glands forming the lateral epithelium. Interestingly, in the Y27632-fed cultures, the intensity of Shh expression was elevated in both the apical and lateral circumvallate papilla epithelium, but the expression of phalloidin was dramatically reduced, indicating that ROCK1 plays an important role in regulating cytoskeletal formation during the morphogenesis of circumvallate papilla (Kim et al., 2009). Further, it is possible that Shh and ROCK1 form an antagonistic regulation of circumvallate papilla formation.

When Shh is overexpressed through Shh electroporation, the invagination of circumvallate papilla epithelium decreases, but apex epithelium continues to enlarge, which is accompanied by reduced cell proliferation in the basal region of the circumvallate papilla forming the epithelium. Phalloidin staining showed increased actin filament formation in the epithelia of the dorsal and apex tongue regions but not in the lateral epithelium of the developing circumvallate papilla in the presence of excess Shh activity. Furthermore, Shh overexpression resulted in increased ROCK1 and Wnt11 expression in the developing circumvallate papilla epithelium. When Shh activity was blocked using Shh neutralizing antibody 5E1, the invagination of the epithelium to form the von Ebner glands decreased. Furthermore, the expression patterns of ROCK1 changed in this case, with stronger localization of ROCK1 detected in the apex region of the circumvallate papilla epithelium and tongue dorsal region. Wnt11 was detected in the lateral wall of the developing circumvallate papilla. Pholloidin staining demonstrated that actin filaments formed in both the apical and lateral regions of circumvallate papilla epithelium. It is possible that Shh regulates the formation of actin filaments through Wnt11 and ROCK1 for the proper development of circumvallate papilla. Shh exerts its function through a negative feedback mechanism during circumvallate papilla development. Overall, it is possible that noncanonical Wnt signaling downstream component ROCK1 regulates the shape of the apex

region of the circumvallate papilla through the formation of actin filaments, and Shh likely plays a crucial role in the development of the von Ebner glands (Kim et al., 2009).

1.4 Summary

The development of the tongue and taste papillae requires mesenchymal-epithelial interactions governed by the complex network of multiple molecular signaling pathways. Understanding these molecular networks is crucial in creating therapies to treat developmental defects associated with the tongue and taste papilla development. In this review article, we have provided an extensive report on the molecular regulation carried out by major signaling pathways, including transforming growth factor-β (TGF-β), bone morphogenetic protein (BMP), Wnt, and Sonic hedgehog (Shh) in the cranial neural crest (NC)-derived tongue mesenchyme and epithelium in regulating NC cells, myogenic precursor cells and myoblast differentiation in tongue organogenesis. Furthermore, we have provided detailed analyses of how Shh and Wnt signaling initiate taste papilla development and other signaling pathways including fibroblast growth factor (FGF) and epidermal growth factor (EGF) signaling patterns the progenitor field during taste papilla development.

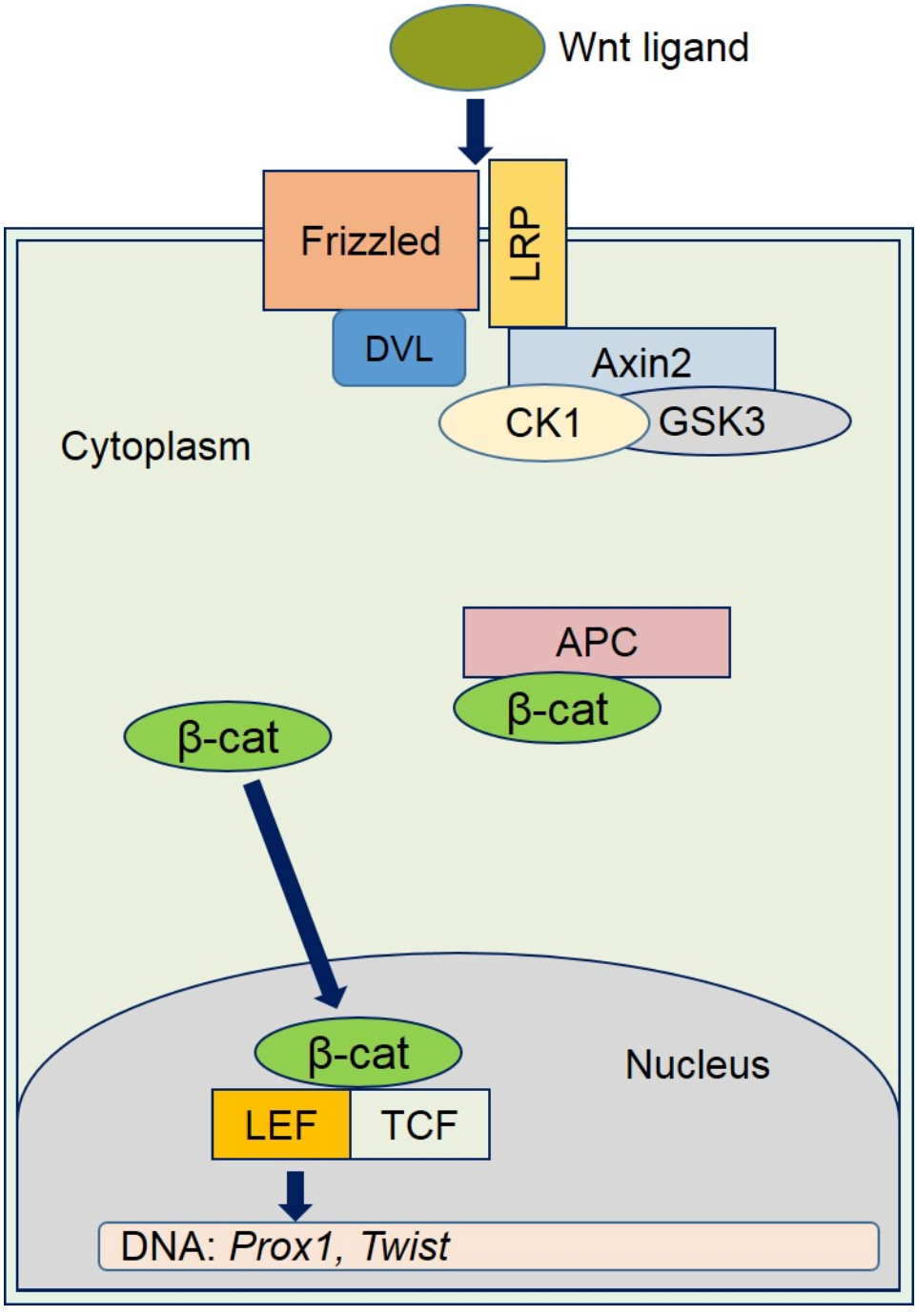
Wnt ligand
Frizzled
LRP
DVL
Axin2
CK1
GSK3
Cytoplasm
APC
β-cat
β-cat
β-cat
Nucleus
LEF
TCF
DNA: Prox1, Twist

Figure 1.1. Schematic diagram to represent the canonical Wnt/β-catenin signaling pathway. LRP: lipoprotein receptor-related protein; Dvl: Dishevelled; APC: adenomatosis polyposis coli; GSK3: glycogen synthase kinase 3, CK1: casein kinase 1α.

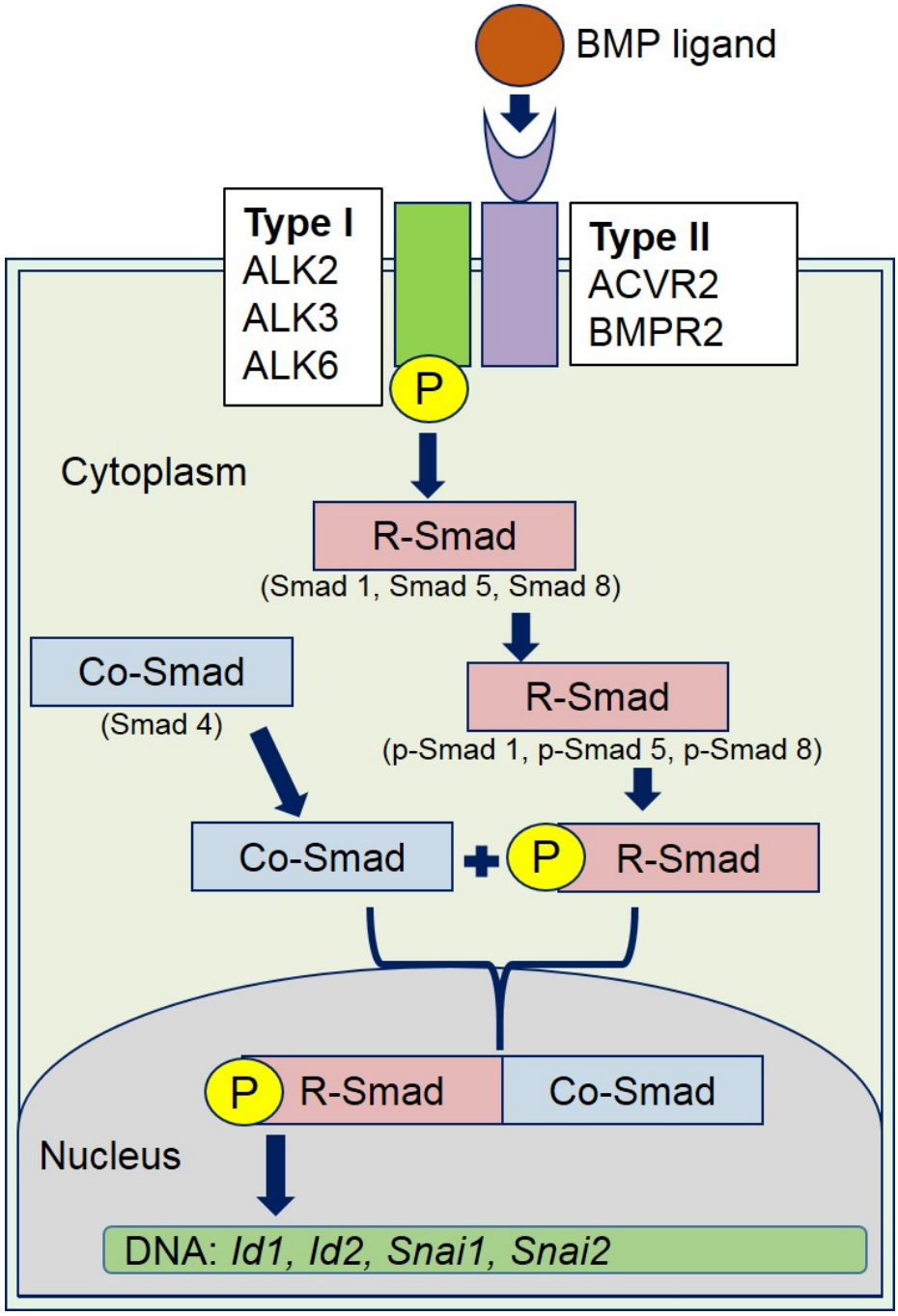
BMP ligand
Type I
ALK2
ALK3
ALK6
Type II
ACVR2
BMPR2
P
Cytoplasm
R-Smad
(Smad 1, Smad 5, Smad 8)
Co-Smad
(Smad 4)
R-Smad
(p-Smad 1, p-Smad 5, p-Smad 8)
Co-Smad
P
R-Smad
P
R-Smad
Co-Smad
Nucleus
DNA: Id1, Id2, Snai1, Snai2

Figure 1.2. Schematic diagram to represent the canonical BMP signaling pathway. ALK: activin like kinase; BMPR: Bone morphogenetic protein receptor; R-Smad: regulatory Smad; Co-Smad: co-mediator Smad, P: Phosphorylated

CHAPTER 2

INCREASED ACTIVITY OF MESENCHYMAL ALK2-BMP SIGNALING CAUSES POSTERIORLY TRUNCATED MICROGLOSSIA AND DISORGANIZATION OF LINGUAL TISSUES[1]

[1]Mohamed Ishan, Guiqian Chen, Chenming Sun, Shi-You Chen, Yoshihiro Komatsu, Yuji Mishina, Hong-Xiang Liu. 2020. *Genesis*. 58 (1), e23337. Reprinted here with the permission of publisher.

2.1 Abstract

Proper development of taste organs including the tongue and taste papillae require interactions with the underlying mesenchyme through multiple molecular signaling pathways. The effects of bone morphogenetic proteins (BMPs) and antagonists are profound, however, the tissue-specific roles of distinct receptors are largely unknown. Here we report that constitutive activation (ca) of ALK2-BMP signaling in the tongue mesenchyme (marked by *Wnt1-Cre*) caused microglossia - a dramatically smaller and misshapen tongue with a progressively severe reduction in size along the anteroposterior axis and absence of a pharyngeal region. At E10.5 the tongue primordia (branchial arches 1-4) formed in *Wnt1-Cre/caAlk2* mutants while each branchial arch responded to elevated BMP signaling distinctly in gene expression of BMP targets (*Id1*, *Snai1*, *Snai2*, *Runx2*), proliferation (*Cyclin-D1*) and apoptosis (*p53*). Moreover, elevated ALK2-BMP signaling in the mesenchyme resulted in apparent defects of lingual epithelium, muscles, and nerves. In *Wnt1-Cre/caAlk2* mutants, a circumvallate papilla was missing and further development of formed fungiform papillae were arrested in late embryos. Our data collectively demonstrate that ALK2-BMP signaling in the mesenchyme plays essential roles in orchestrating various tissues for proper development of the tongue and its appendages in a region-specific manner.

Keywords: Bone morphogenetic protein (BMP) signaling, tongue mesenchyme, microglossia**,** branchial arch, proliferation, apoptosis.

2.2 Introduction

The mammalian tongue is an organ comprised of multiple highly organized tissues that enable its critical functions, including speaking, food processing, and taste sensation. Developmental defects in the tongue such as aglossia, macroglossia, microglossia, and ankyloglossia (Chandrashekar et al., 2014) can cause serious disease conditions like dysphasia, dysphagia, and dysgeusia. The development of the tongue requires tissue-tissue interactions governed by multiple signaling pathways (Iwata et al., 2013; Liu et al., 2009; Liu et al., 2012a; Liu et al., 2012b; Millington et al., 2017). Thus, studies on the organogenesis and molecular regulation of the tongue and its appendages will help to understand the mechanisms underlying the tongue anomalies.

In mice, emergence of the tongue starts with the appearance of three lingual swellings from the first branchial arch (BA 1) at gestational day (E) 11.5. These swellings fuse and form the anterior two thirds of the tongue – the oral tongue at E12.5. Concurrently with the formation of the oral tongue, a small midline swelling (the copula) develops from BA 2 and fuses with another midline swelling originating from BAs 3-4 to form the posterior third of the tongue – the pharyngeal tongue (Cobourne et al., 2019). At this stage, myoblast cells migrate into the developing tongue and differentiate to become intrinsic glossal muscles (Cobourne et al., 2019; Millington et al., 2017). Meanwhile taste papilla placodes emerge on the dorsal surface (Mbiene et al., 1997; Mistretta, 1972) and will develop into taste papillae that host taste buds. The proper formation of the tongue and its appendages is an integrated process that requires a tight coordination among BAs 1-4 and various types of tissues/cells.

Bone morphogenetic proteins (BMP) are secreted proteins that may act in a paracrine manner to activate intracellular signaling in the surrounding cells and play crucial roles in cell growth, differentiation and apoptosis during the development of many organs (Bragdon et al., 2011; Wang et al., 2014). BMPs bind to the type II BMP receptors (BMPR2, ACVRII), activate type I BMP receptors (ALK2, ALK3, ALK6) and phosphorylate downstream signaling component

Smad1, 5, and 8 to promote the expression of BMP target genes (e.g., *Id1*, *Snai1*, *Snai2*, *Runx2*). Type I BMP receptors are known to be the main determinants of the downstream signaling activity (Wang et al., 2014). It has been reported that BMP ligands (BMP 2, 3, 4, 6, 7), antagonists (noggin and follistatin) and receptors (ALK2, ALK3 and ALK6) are present in both epithelium and mesenchyme of the developing tongue (Beites et al., 2009; Jung et al., 1999; Kawasaki et al., 2012; Suga et al., 2007; Zhou et al., 2006). The effects of BMP ligands and their antagonists in the tongue and taste papilla development are profound (Beites et al., 2009; Zhou et al., 2006). However, the specific roles of mediating receptors and involved tissue compartments of BMP signaling in tongue organogenesis are largely unknown.

Constitutive activation of *ALK3* in the neural crest and derived mesenchyme causes a slightly defected tongue in a previous study focusing on cleft palate formation and delayed tooth differentiation (Liu et al., 2013) . In the present study, we report that a proper level of ALK2-mediated BMP (hereafter ALK2-BMP) signaling in neural crest and derived mesenchymal cells (marked by *Wnt1-Cre*) is essential in regulating proliferation and apoptosis of these cells at an early embryonic stage for the proper tongue shape and size. Also, ALK2-BMP signaling plays important regulatory roles in mesenchymal interactions with other lingual tissues for their organization, and the development of taste papillae and taste buds.

2.3 Materials and Methods

2.3.1 Mouse lines and tissue collection

The animal use was approved by the institutional animal care and use protocols of the University of Georgia and in accordance with National Institute of Health guidelines for proper care and use of animals for research. Mice carrying constitutively activated form of type I BMP receptor *Alk2* (CAG-Z-EGFP-caAlk2) transgene (hereafter *caAlk2*) were provided by Yuji Mishina, University of Michigan, USA (Fukuda et al., 2006). Heterozygous *Wnt1-Cre* mice [B6.Cg-Tg (Wnt1-Cre) 11Rth Tg(Wnt1-GAL4) 11Rth/J, Jackson Laboratory, Stock# 009107] were bred with homozygous *caAlk2* breeders to generate the *Wnt1-Cre/caAlk2* mice.

Homozygous RFP mice [B6.Cg-Gt (ROSA)26 Sortm14(CAG-tdTomato)Hze/J, The Jackson Laboratory, Stock# 007914] were used as the reporter to bred with *Wnt1-Cre* breeders to generate *Wnt1-Cre/RFP* mice. Wild type (C57BL/6J, Jackson Laboratory, Stock# 000664) mice were used to cross with homozygous *caAlk2* breeders to generate the *C57BL/6J WT/caAlk2* mice.

Littermates that were negative for *Wnt1-Cre* were used as controls (*Cre*$^{-}$*/caAlk2*). Genotype of mice were confirmed using specific primers. PCR product of Cre (200 bp) were identified using primers CreF (5'-CTC GTG ATC TGC AAC TCC AGTC-3') and CreR (5'-GAG ACT AGT GAG ACG TGC TACT-3'). PCR products of *caAlk2* (580 bp) were identified using primers TF41 (5'-GTG CTG GTT ATT GTG CTG TCTC-3') and TF61 (5'-TGT GAG CGA GTA GTA ACA ACC-3'). PCR product of RFP (200 bp) were identified using primers oIMR9103 (5'- GGC ATT AAA GCA GCG TAT CC-3') and oIMR9105 (5'- CTG TTC CTG TAC GGC ATG G-3').

Timed pregnant mice were euthanized using CO_2 followed by cervical dislocation for embryonic tissue collection. Embryos were harvested at E10.5, E12.5, E14.5, E16.5 and E18.5. Noon of the day of vaginal plug detection was designated as embryonic day 0.5 (E0.5). All embryo dissections were performed between 12.00 PM and 3.00 PM for consistency across litters. The uterus with embryos was removed and embryos were retrieved under a microscope. Stages of the embryos were confirmed by the number of somite pairs and development of multiple organs. Dissected tissues were further processed for different analyses as described below.

2.3.2 Whole mount immunohistochemistry

Immunohistochemistry against Sonic Hedgehog (Shh), a developing papilla marker, was performed on whole tongue on the mandible (E12.5, E14.5) using goat polyclonal, affinity-purified antibody against mouse Shh N-terminal peptide [amino acids 25-198] (AF464, R&D Systems, Minneapolis, MN) as previously described (Liu et al., 2004; Mistretta et al., 2003; Zhou et al., 2006). E12.5 and E14.5 tongues with mandibles were fixed in 4% paraformaldehyde

(PFA) in 0.1 M PBS, at 4ºC for 2 hr, then transferred to 100% methanol for storage at -20ºC until use.

Tongues were treated with 6% H_2O_2 in 100% methanol at room temperature for 5 hr to block endogenous peroxidase activity followed by rehydration through a descending methanol series (50%, 25%, and 0% in 0.1 M PBS) at room temperature for 30 min each. Antigen retrieval was performed by heating the tissues at 92- 95ºC for 5 min in Universal Antigen Retrieval Agent (CTS015; R&D Systems, Minneapolis, MN). PBS/MT (0.1 M PBS with 2% skim milk powder and 0.1% Triton X-100) was used to block nonspecific staining. Tongues were then incubated with primary antibody at a 1:300 dilution in 10% normal donkey serum (NDS) (D9663; Sigma Aldrich, St Louis, MO) in PBS/MT at 4ºC for 48 hr. After rinses with PBS/MT (five times, 1 hr each on ice) tissues were incubated at 4ºC for 24 hr with biotin-conjugated rabbit anti-goat secondary antibody (1:500, BA-5000; Vector Laboratories, Burlingame, CA) in 1% NDS in PBS/MT. Following the rinses with PBS/MT (five times, 1 hr each on ice), tongues were incubated at 4ºC for 24 hr with peroxidase-conjugated streptavidin in blocking solution (1:500, PK6200; Vector Laboratories, Burlingame, CA). After five rinses in PBS/MT and two rinses in PBT (0.1 M PBS with 0.1% Triton X-100 and 0.2% bovine serum albumin) for 1 hr each on ice, tongues were pre-incubated in nickel-intensified DAB solution (SK4100; Vector Laboratories, Burlingame, CA) without H_2O_2 at room temperature for 30 min followed by incubation with DAB solution containing 0.0003% H_2O_2. The reaction was stopped by PBS rinses twice for 1 hr each. Tongues were then transferred into 4% PFA in 0.1 M PBS at 4ºC for further fixation and photographed in PBS.

2.3.3 Immunohistochemistry on sections

Embryos were fixed with 4% PFA in 0.1 M PBS at 4ºC for 2 hr, cryoprotected in 30% sucrose at 4ºC for 48 hr, then embedded in OCT (#23730571; Fisher Scientific, Waltham, MA) and rapidly frozen. Serial sections were cut at 10 μm in thickness. Sections were air dried, rehydrated, and blocked with 10% NDS in PBS-X (0.1 M PBS, 0.3% Triton X-100) at room

temperature for 1 hr. Primary antibodies listed in Table 2.1 were diluted in PBS-X containing 1% NDS (carrier solution). Sections incubated with carrier solution without primary antibody were used as negative controls.

After incubation with primary antibodies at 4ºC for 24 hr, sections were washed three times with 0.1 M PBS, and then incubated with secondary antibodies conjugated with Alexa Fluor 488, or 647 (1:500, Jackson immune research, West Grove, PA) in carrier solution at room temperature for 1 hr. After rinsing in PBS, sections were counterstained with DAPI solution (200 ng/ml in PBS, D1306; Life Technologies, Carlsbad, CA) at room temperature for 10 min. After thorough rinsing in PBS the sections were air dried and mounted with ProLong® Diamond antifade medium (P36970; Fisher Scientific, Waltham, MA).

2.3.4 Early taste bud labeling with Keratin 8 (K8) immunosignals on epithelial sheets

Peeling of epithelial sheets from E18.5 tongues of *Wnt1-Cre/caAlk2* mutants and *Cre*$^{-}$*/caAlk2* littermate controls was performed as previously described (Venkatesan et al., 2016). A mixture of collagenase A (1 mg/mL, #10103578001; Roche Diagnostics, Basal, Switzerland) and dispase II (2.5 mg/mL; # 10374300; Roche Diagnostics, Basal, Switzerland) in 0.1 M PBS was injected into the sub-epithelial space of E18.5 *Wnt1-Cre/caAlk2* mutant and littermate control tongues. After the injection, tongues were incubated at 37ºC for 30 min followed by fixation in 4% PFA in 0.1 M PBS at room temperature for 1 hr. The epithelial sheet of the tongue was separated from the lamina propria and then rinsed three times in 0.1 M PBS at room temperature for 30 min each.

Following the incubation with 10% NDS in PBS-X at room temperature for 1 hr to block nonspecific staining, the epithelial sheets were incubated with primary antibody against K8 in carrier solution at 4ºC for 48 hr. After three rinses in 0.1 M PBS at room temperature for 30 min each, epithelial sheets were incubated at 4ºC for 24 hr with Alexa Fluor 647-conjugated donkey anti-rat secondary antibody (1:500, #712-605-150; Jackson Immune research, West Grove, PA)

in carrier solution. The epithelial sheets were rinsed with 0.1 M PBS and transformed into 4% PFA in 0.1 M PBS at 4ºC for further fixation and photographed in PBS.

2.3.5 RNA extraction and quantitative reverse transcriptase PCR

Individual branchial arches (BA) (1-4) from *Wnt1-Cre/caAlk2* mutants and *Cre⁻/caAlk2* littermate controls were dissected at E10.5 and immersed in Trizol (#15596018; Life technologies, Carlsbad, CA) solution for RNA extraction. A total of 9 tissues (pooled 3 tissues x 3 replicates) were used from each BA for RNA extraction. Tissues were homogenized with a PorGen 700D tissue homogenizer (Fisher Scientific, Waltham, MA) and RNA was extracted using the RNeasy Plus kit (#74136; Qiagen, Hilden, Germany). RNA concentrations were determined using Nanodrop 8000 spectrophotometer (Nanodrop, Thermo Scientific, Waltham, MA). Complementary DNA were synthesized from the RNA extracts using SuperScript™ First-Strand Synthesis System (#11902018; Fisher scientific, Waltham, MA). The cDNA products were used to analyze the expression of selected genes using the primers in Table 2.2.

2.3.6 Western blotting

Proteins were extracted from the mesenchyme using Radioimmunoprecipitation assay buffer/ RIPA buffer (1% NP-40, 150 mmol/L NaCl, 50 mmol/L Tris-HCl, 0.5% Sodium deoxycholate, 0.1% SDS, 1 mmol/L EDTA, pH 7.4). The epithelium was removed from E10.5 BAs of *Wnt1-Cre/caAlk2* mutant (n=3) and *Cre⁻/caAlk2* littermate control (n=3) mouse embryos as previously described (Liu et al., 2008). Protein concentrations were determined using Pierce™ BCA protein assay kit (#23225; Thermo Fisher Scientific, Waltham, MA) and Synergy™ 4 microplate reader (#7161000; BioTek Instruments, Winooski, VT). Protein extracts were then resolved using SDS-PAGE and transferred to nitrocellulose membranes. Membranes were blocked with 3% Bovine Serum Albumin (A-420-100; Gold Biotechnology, St Louis, MO) in Tris-buffered saline with Tween 20 buffer/TBST buffer (20 mM Tris pH 7.5, 150 mM NaCl, 0.1% Tween 20) at room temperature for 1 hr. The membranes were incubated with primary antibodies (Rabbit anti p-Smad1/5/8, rabbit p-Smad2/3, and GAPDH; Table 2.1) in blocking

buffer (3% BSA in TBST) at 4ºC for 24 hr. After three rinses in TBST (10 min each), membranes were incubated with Alexa Fluor 647-conjugated goat anti-rabbit (1:10,000, #711-605-152, Jackson Immunoresearch, West Grove, PA) and Alexa Fluor 647-conjugated donkey anti-mouse (1:10,000, #715-605-150, Jackson Immunoresearch, West Grove, PA) secondary antibodies in blocking buffer at room temperature for 2 hr. Band detection was performed using chemiluminescence (ChemiDoc^{MP} Imaging System, Bio-Rad ChemiDoc, Hercules, CA).

2.3.7 Scanning electron microscopy

E10.5 BAs and E12.5-E18.5 tongues from *Wnt1-Cre/caAlk2* mutants and *Cre^{-}/caAlk2* littermate controls were fixed in 2.5% glutaraldehyde (#75520; Electron Microscopy Science, Hatfield, PA) and 4% PFA in 0.1 M PBS at room temperature for 24 hr. Tongues were then rinsed in 0.1 M PBS and subsequently post-fixed in a sequence of aqueous 1% OsO_4 (#19150; Electron Microscopy Science, Hatfield, PA), 1% tannic acid (#16201; Sigma Aldrich, St Louis, MO), 1% OsO_4, at 4ºC for 1 hr each. Tissues were then dehydrated through an ascending series of ethanol (35%, 50%, 70%, 90% and 100%, three changes at each concentration); and ethanol was displaced by three changes of hexamethyldisilazane (HMDS, #440191; Sigma Aldrich, St Louis, MO) for 45 min each. Residual HMDS was evaporated slowly in a fume hood until the tissues were completely dry. Tissues were mounted onto specimen stubs, lightly sputter-coated with gold/palladium (Leica Gold/Carbon coater; Georgia Electron Microscope Core Facility, University of Georgia) and imaged using a scanning electron microscope (FEI Teneo FE-SEM; Georgia Electron Microscope Core Facility, University of Georgia).

2.3.8 Photomicroscopy and data analyses

Immunostained whole mount tissues were imaged under a stereomicroscope (Olympus SZX16). Sections were examined thoroughly under a fluorescent light microscope (EVOS FL, Life Technologies). Co-localization of immunosignals were confirmed and photographed using a laser-scanning confocal microscope (Zeiss LSM 710, Biomedical Microscopy Core at the

University of Georgia). Adobe Photoshop (2015) was used for figure assembling and image editing was minimal to improve clarity.

Quantitative analyses were made to obtain the number of p-Smad1/5/8^{+}, cleaved (c) Caspase-3^{+}, Ki67^{+} and DAPI^{+} total mesenchymal cells per unit area (mm^{2}) on BA sections. Immunoreacted serial transverse sections of *Cre^{-}/caAlk2* littermate control (n=3) and *Wnt1-Cre/caAlk2* (n=3) BAs were thoroughly examined under a fluorescent light microscope (EVOS FL, Life Technologies). Single-plane laser-scanning confocal photomicrographs were obtained from every other section to include the representative and corresponding regions of BAs of littermate control and *Wnt1-Cre/caAlk2* mutants. Ki67^{+} and DAPI^{+} mesenchymal cells were counted in a selected area of BAs, while p-Smad1/5/8^{+} and cCaspase-3^{+} cells were quantified in the entire BAs 1-4 on every other sections.

Measurements of the length and width of the tongues were performed using the images of Shh immunostained E12.5 littermate control (n=3) and *Wnt1-Cre/caAlk2* mutant (n=3) tongues. The distance between the anterior most point and posterior end of Shh^{+} circumvallate papillae placode was considered as the length. The widest region in the anterior 2/3 of the oral tongue was taken as the width. NIH-ImageJ software was used to measure the length and width of E12.5 tongues, Western blot band intensities and the area of individual BAs. For the quantitative RT-PCR, changes of gene expression levels in individual BAs of *Wnt1-Cre/caAlk2* and littermate control groups were presented as means ± standard deviation ($\bar{X}$ ± SD; n = 3) of $2^{-\Delta CT}$ values.

Student's *t*-test was used for the statistical analysis of the tongue length and width, and intensities of Western blot bands of p-Smads between E12.5 *Wnt1-Cre/caAlk2* mutants and littermate controls. One-way analysis of variance (ANOVA) followed by Fisher's least significant difference (LSD) analyses was performed to test the statistical significance of gene expression levels among individual BAs of E10.5 C57BL/6J wild type (WT) and *C57BL/6J WT/caAlk2* embryos. Two-way ANOVA followed by Fisher's least significant difference (LSD) analyses was

used to compare the gene expression levels in individual BAs between *Wnt1-Cre/caAlk2* and *Cre⁻/caAlk2* littermate controls. A *P* value <0.05 was taken as a statistically significant difference.

2.4 Results

2.4.1 Constitutive activation of ALK2-BMP signaling in neural crest and derived mesenchymal cells results in posteriorly truncated microglossia

To elevate the activity of type I BMP receptor ALK2-mediated BMP (hereafter ALK2-BMP) signaling in the tongue mesenchyme, transgenic mouse model with a constitutively activated (ca) form of *Alk2* (*caAlk2*) was used to cross with *Wnt1-Cre* that mark neural crest-derived mesenchymal cells in the tongue (Liu, Komatsu, Mishina, & Mistretta, 2012; Thirumangalathu, Harlow, Driskell, Krimm, & Barlow, 2009). Compared to *Cre⁻/caAlk2* littermate controls (Fig. 2.1A), deficiencies were evident in multiple craniofacial regions of E12.5 *Wnt1-Cre/caAlk2* mouse embryos including brain (Fig. 2.1B, arrow), eyes (Fig. 2.1B, arrowhead) and orofacial region (Fig. 2.1B, open arrowhead). Mutant mice had microglossia (Fig. 2.1D, F), with a significantly smaller tongue in mutants than that in littermate controls (526.51±14.18 μm versus 1163.09±13.78 μm in length of oral tongue, $P<0.01$ in Fig. 2.1G; 352.43±6.5 μm versus 749.23±4.25 μm in width, $P<0.01$ in Fig. 2.1H). In the majority of *Wnt1-Cre/caAlk2* mouse embryos, tongue swellings fused at the midline for a unitary tongue tip (24 mutants out of 32, Fig. 2.1D, F) while some had a bifid anterior tongue (8 mutants out of 32, image not shown). A progressive decrease in tongue size was consistently observed along the anteroposterior axis in all of the mutants (tongues with a unitary or bifid tip). Although the *Wnt1-Cre/caAlk2* mutant tongue was smaller, fungiform taste papilla placodes were observed on the anterior tongue region (Fig. 2.1D and F, arrowheads) similarly to those in the littermate control (Fig. 2.1C, E, arrowheads). On the smaller anterior tongues, fewer rows of fungiform taste papillae were seen and there was not an apparent change of density of papilla placodes. In the position where a distinct circumvallate papilla placode was observed in the littermate control tongues (Fig. 2.1E,

arrow), an enlarged Shh$^+$ patch of tissue, presumably circumvallate papilla placode, was observed in the tongues of *Wnt1-Cre/caAlk2* mutants (Fig. 2.1F, arrow). A pharyngeal part of the tongue posterior to the presumable Shh$^+$ circumvallate was missing in *Wnt1-Cre/caAlk2* mutants (Fig. 2.1F).

2.4.2 Fungiform papillae were well developed in the smaller E14.5 *Wnt1-Cre/caAlk2* mutant tongue

At E14.5 when tongue and taste papillae attain their stereotypical shape and spatial distribution (Fig. 2.2A), *Wnt1-Cre/caAlk2* mutants continued to exhibit microglossia (Fig. 2.2B) compared to the *Cre$^-$/caAlk2* littermate control (Fig. 2.2A). Developing fungiform taste papillae were observed in the tongue of E14.5 *Wnt1-Cre/caAlk2* mutants (Fig. 2.2B, D, arrowheads, inset in 2D) in similar structure to those of littermate controls (Fig. 2.2A, C, arrowheads, inset in 2.2C). Similarly to E12.5, there was not an apparent change of papilla density on the smaller anterior tongues. Further, the pharyngeal tongue region was missing and a Shh$^+$ circumvallate papilla seen in littermate controls (Fig. 2.2C, arrow) was absent in E14.5 *Wnt1-Cre/caAlk2* mutants (Fig. 2.2D). Similar to E12.5, both unitary (14 out of 18, Fig. 2.2F) and bifid (4 out of 18, Fig. 2.2B, D) anterior tips was observed in the smaller tongues of E14.5 *Wnt1-Cre/caAlk2* mutants.

Next, we examined outgrowth and branching of nerve fibers that traverse through the tongue mesenchyme and innervate the developing taste papillae. At E14.5, in contrast to extensive βIII-tubulin$^+$ nerve fibers approaching taste papillae in the littermate control (Fig. 2.2E, open arrowhead), nerve fibers were absent in the vicinity of *Wnt1-Cre/caAlk2* mutant fungiform taste papillae (Fig. 2.2F). Obviously, βIII-tubulin$^+$ nerve fibers were present in *Wnt1-Cre/caAlk2* mutant mandible (Fig. 2.2F, open arrowheads). On sections, compared to the extensively branched nerve fibers in littermate control tongues (Fig. 2.2G, arrowhead), βIII-tubulin$^+$ nerve fibers were loosely distributed in the *Wnt1-Cre/caAlk2* mutant tongue mesenchyme (Fig. 2I, arrowhead). Moreover, these fibers did not branch out into taste papillae nor penetrate the

epithelium (Fig. 2.2J) in contrast to the dense distribution of nerve fibers in the papilla core in littermate controls (Fig. 2.2H, arrowhead).

To evaluate the further development of fungiform papillae, E16.5 littermate control (Fig. 2.2K, L) and *Wnt1-Cre/caAlk2* mutant (Fig. 2.2M, N) tongues were examined using scanning electron microscopy. Similar to E14.5, developing fungiform papillae were observed in the E16.5 *Wnt1-Cre/caAlk2* mutants (Fig. 2.2M-N, arrowheads) similarly in structure to those of littermate controls (Fig. 2.2K-L, arrowheads).

2.4.3 Development and organization of multiple lingual tissues were deficient in the E18.5 *Wnt1-Cre/caAlk2* mutant tongue

Wnt1-Cre/caAlk2 mutant mice die shortly after birth, thus E18.5 embryos were harvested as the last stage for phenotypic analyses (Fukuda et al., 2006). Compared to the *Cre^{-}/caAlk2* littermate controls (Fig. 2.3A), microglossia in E18.5 *Wnt1-Cre/caAlk2* mutants was evident (Fig. 3B). Neither pharyngeal tongue nor circumvallate papilla (Fig. 2.3A, arrow) was seen in the E18.5 *Wnt1-Cre/caAlk2* mutants (Fig. 2.3B). In the littermate control tongues spine-like filiform papillae and flaking of the superficial epithelial cells were profound (Fig. 2.3A, C and D, open arrowheads). In contrast, filiform papillae were less profound and epithelial cell flaking was not noticed on the surface of *Wnt1-Cre/caAlk2* mutant tongue (Fig. 2.3B, E and F).

Fungiform papillae were observed in the oral tongue of E18.5 *Wnt1-Cre/caAlk2* mutants (Fig. 2.3B, E-F), however these fungiform papillae (Fig. 2.3E-F, arrowheads) were underdeveloped compared to those of E18.5 littermate controls (Fig. 2.3C-D, arrowheads) as they were similar in appearance to those in E16.5 littermate control (Fig. 2.2K-L, arrowheads) and *Wnt1-Cre/caAlk2* (Fig. 2.2M-N) mutant tongues. Further, early taste buds were detected in the tongue epithelial sheets (Fig. 2.3I, arrowheads) and sagittal tongue sections (Fig. 2.3J) of *Wnt1-Cre/caAlk2* mutants with a pan taste cell marker Keratin 8 (K8^{+}) as those in littermate control epithelial sheets (Fig. 2.3G, arrowheads) and sagittal sections (Fig. 2.3H). Among the taste buds detected in the E18.5 *Wnt1-Cre/caAlk2* mutants, 41% had a typical morphology as

those in littermate controls (Fig. 2.3H), while the majority (59% as in Fig. 2.3J) appeared to have an increased height from base to apex with most K8+ cells located apically. Such shape of taste buds were also observed in E17.5 littermate control and *Wnt1-Cre/caAlk2* tongues (data not shown). In contrast to the dense innervation of taste buds in the littermate controls (Fig. 2.3H, open arrowhead), βIII-tubulin^{+} nerve fibers were absent in taste buds and dramatically reduced in the mesenchymal core of fungiform papillae in *Wnt1-Cre/caAlk2* mutants (Fig. 2.3J, open arrowhead).

Neural crest-derived mesenchyme/connective tissue serves as a scaffold that is important for tissue differentiation and organization (Rinon et al., 2007) . To identify the effects of altered ALK2-BMP signaling in the connective tissue, main lingual tissues were examined. Vimentin^{+} stromal cells were extensively distributed in the E18.5 tongue mesenchyme of both littermate controls (Fig. 2.4A) and *Wnt1-Cre/caAlk2* mutants (Fig. 2.4B). A dense layer was obvious in the lamina propria – a zone of loose connective tissue under the epithelium, in both littermate controls (Fig. 2.4A and inset, arrowheads) and *Wnt1-Cre/caAlk2* mutants (Fig. 2.4B and inset, arrowheads). E-Cadherin^{+} epithelium was progressively thinner along the anteroposterior axis in the dorsal surface of oral tongue of E18.5 *Wnt1-Cre/caAlk2* mutants (Fig. 2.4D and inset, arrowhead) compared to that of littermate controls (Fig. 2.4C and inset, arrowhead). Fungiform taste papillae were not as well developed in the E18.5 *Wnt1-Cre/caAlk2* mutant tongues (arrow in inset of Fig. 2.4D) as those in the littermate controls (arrow in inset of Fig. 2.4C). Further, Spine-like filiform papillae were not evident in the *Wnt1-Cre/caAlk2* mutant tongues (open arrowhead in inset of Fig. 2.4D) as that of littermate control tongues (open arrowhead in inset of Fig. 2.4C). Defects in muscle differentiation and organization were examined using muscle specific marker Desmin. All four intrinsic glossal muscles were disorganized in the E18.5 *Wnt1-Cre/caAlk2* mutants (Fig. 2.4F, F_1) compared to littermate controls (Fig. 2.4E, E_1). Superior and inferior longitudinal muscles that are close to the dorsal and ventral tongue surface (Fig. 2.4E_1, sLG, iLG) were not apparent in the *Wnt1-Cre/caAlk2* mutants (Fig. 2.4F_1). Transverse muscles

(Fig. 2.4E_1, Tr) were sparse and largely empty in the space for their distribution in *Wnt1-Cre/ caAlk2* mutants (Fig. 2.4F_1, Tr). In contrast, vertical muscles (Fig. 2.4E_1, Ve) were increased in bundle size in the middle region of the tongue in *Wnt1-Cre/ caAlk2* mutants (Fig. 2.4F, Ve).

2.4.4 Tongue primordia (i.e., branchial arches) developed deficiently in E10.5 *Wnt1-Cre/caAlk2* mutants

To understand the cause of microglossia in *Wnt1-Cre/caAlk2* mutants, the development of tongue primordia (i.e., BAs 1-4) was examined. *Wnt1-Cre* marked *RFP* signals were distributed in BAs 1-4 (Fig. 2.5A_1, arrowheads) at E10.5. RFP^+ cells were under E-$cadherin^+$ epithelium and exclusively present in the mesenchyme (Fig. 2.5A_2-A_6).

An elevated activation of ALK2-BMP signaling was validated by detecting the phosphorylation of Smads. Phosphorylated (p)-Smad1/5/8 known to mediate BMP signaling was detected at a higher level in E10.5 BAs of *Wnt1-Cre/caAlk2* mutants compared to *Cre^- /caAlk2* littermate controls (595.02±17.56 versus 155.29±6.26 in mean grey scale intensity, $P<0.05$ in Fig. 2.5B). In contrast, the level of p-Smad2/3 that is known to mediate TGF-β signaling (Grönroos et al., 2012) was not apparently altered in *Wnt1-Cre/caAlk2* mutants (82.56±11.65 versus 71.98±4.49 in mean grey scale intensity, $P>0.05$ in Fig. 2.5B). On sections, mesenchymal cells that were positive for p-Smad1/5/8 immunosignals were significantly increased ($P<0.05$, Fig. 2.5D) in each of BAs 1-4 of E10.5 *Wnt1-Cre/caAlk2* mutants (Fig. 2.5C_4-C_6, 5D) compared to littermate controls (Fig. 2.5C_1- C_3, 5D). Further, an alteration of mesenchymal cell density in BA 1 (increase) and BA 4 (decrease) was observed in the E10.5 *Wnt1-Cre/caAlk2* mutants ($P<0.05$, Fig. 2.5D).

All four BAs (n=18) were developed, and from the side view of BAs 1-4 there were no obvious differences between *Wnt1-Cre/caAlk2* mutants (Fig. 2.5E_2) and littermate controls (Fig. 2.5E_1). However, dorsal view showed that BA 1 had a flat dorsal surface in E10.5 *Wnt1-Cre/caAlk2* mutants (Fig. 2.5F_2, arrowhead) in contrast to the profound swelling in littermate controls (Fig. 2.5F_1, arrowhead). An enlarged copula was observed in *Wnt1-Cre/caAlk2* mutant

BA 2 (Fig. 2.5F$_2$, arrow) compared to that of the *Cre$^-$/caAlk2* littermate control (Fig. 2.5F$_1$, arrow).

2.4.5 BAs 1-4 exhibited distinct gene expression and changes in *Wnt1-Cre/caAlk2* mutants

To understand the downstream factors that are mediating the tongue region-specific effects of elevated ALK2-BMP signaling, individual BAs were separated under a microscope at the clear boundaries between BAs, and transcripts of BMP target genes for cell growth (*Id1*, *Snai1*, *Snai2* and *Runx2*) were analyzed in E10.5 C57BL/6J wild type (WT), *Wnt1-Cre/caAlk2* mutants and *Cre$^-$/caAlk2* littermate controls. Overall, individual BAs showed different gene expression levels and alterations (Fig. 2.6A). Out of the four tested BMP target genes, levels of *Snai2* and *Runx2* were significantly different (P<0.05) among BAs 1-4 in E10.5 C57BL/6J WT embryos (Fig. 2.6A). No significant changes in *Id1* and *Snai1* expression levels were observed within any of the E10.5 WT BAs. In contrast to those in littermate controls, gene expression levels were altered in *Wnt1-Cre/caAlk2* mutant BAs (Fig. 2.6B). Specifically, compared to *Cre$^-$/caAlk2* littermate controls, *Wnt1-Cre/caAlk2* mutants had: (1) no detected level of *Snai1* and *Snai2* expression in BA 1 of *Wnt1-Cre/caAlk2* mutants; (2) increased *Snai1 and Snai2,* and decreased *Runx2* in BA 2 (P<0.05*,* Fig. 2.6B); (3) significantly higher mRNA levels of all the BMP target genes tested in BA 4 (P<0.05); (4) no alterations of gene expression in BA 3 (Fig. 2.6B, P>0.05).

Of note, differences of BMP target gene expression in E10.5 BAs were detected between C57BL/6J WT and *Cre$^-$/caAlk2* littermate controls. To understand whether the discrepancies were caused by the transgene insertion, C57BL/6J WT were bred with *caAlk2* to generate *caAlk2* heterozygotes (*C57BL/6J WT/caAlk2*) for analyses of the gene expression in BAs. Of all the BMP target genes tested, the expression patterns in *C57BL/6J WT/caAlk2* BAs (Fig. 2.6B) resembled those in *Cre$^-$/caAlk2* littermates (Fig. 2.6B) and were different from those in C57BL/6J WT controls (Fig. 2.6A).

To understand the relevance of cell proliferation and apoptosis with the posteriorly truncated microglossia in *Wnt1-Cre/caAlk2* mutants, transcripts of proliferation relevant gene *Cyclin-D1* and key apoptosis gene *p53* in individual BAs were analyzed in E10.5 *Wnt1-Cre/caAlk2* mutants and *Cre*$^{-}$*/caAlk2* littermate controls (Fig. 2.7A). Increased gene expression of *Cyclin-D1* was detected in BAs 1 (P<0.05, Fig. 2.7A) and 2 (P<0.05, Fig. 2.7A), whereas *p53* expression levels were higher in BAs 1 and 4 of *Wnt1-Cre/caAlk2* mutants compared to the corresponding *Cre*$^{-}$*/caAlk2* littermate control BAs (P<0.05, Fig. 2.7A). No significant changes in *Cyclin-D1* expression were observed in BA 3-4 in E10.5 *Wnt1-Cre/caAlk2* mutants (P>0.05, Fig. 2.7A) compared to *Cre*$^{-}$*/caAlk2* littermate controls (Fig. 2.7A). Similarly, no significant changes in *p53* expression were observed in BA 2-3 in E10.5 *Wnt1-Cre/caAlk2* mutants (P>0.05, Fig. 2.7A) compared to *Cre*$^{-}$*/caAlk2* littermate controls (Fig. 2.7A). Ki67^{+} proliferating cells were more densely distributed per unit area (mm^2) in BA 1 and 2 of E10.5 *Wnt1-Cre/caAlk2* mutants (Fig. 2.7B$_2$, B$_4$, P<0.05 in 2.7D) than that of *Cre*$^{-}$*/caAlk2* littermate controls (Fig. 2.7B$_1$, B$_3$ and 2.7D). In contrast, the density of Ki67^{+} proliferating cells was decreased in BA 4 of *Wnt1-Cre/caAlk2* mutants (Fig. 2.7B$_6$, P<0.05 in 2.7D) compared to the *Cre*$^{-}$*/caAlk2* littermate control BA 4 (Fig. 2.7B$_5$ and 2.7D). No obvious changes in Ki67^{+} cells were detected in the BA 3 of *Wnt1-Cre/caAlk2* mutants (Fig. 2.7B$_6$, P>0.05 in 2.7D) compared to those of *Cre*$^{-}$*/caAlk2* littermate controls (Fig. 2.7B$_5$ and 2.7D). Further, mesenchymal cells marked by immunosignals of apoptotic cell marker cleaved (c) Caspase-3 were significantly higher in E10.5 BA 1, 3 and 4 of *Wnt1-Cre/caAlk2* mutants (Fig. 2.7C$_2$, C$_6$, P<0.05 in 2.7E) than corresponding BAs of *Cre*$^{-}$*/caAlk2* littermate controls (Fig. 2.7C$_1$, C$_5$ and 2.7E). However, no significant changes in cCaspase-3^{+} cells was observed in *Wnt1-Cre/caAlk2* mutant BA 2 (Fig. 2.7C$_4$, P>0.05 in 2.7E) compared to the *Cre*$^{-}$*/caAlk2* littermate control BA 2 (Fig. 2.7C$_3$ and 2.7E).

2.5 Discussion

Our present study demonstrated that elevated ALK2-BMP signaling in neural crest and derived mesenchyme leads to posteriorly truncated microglossia and disorganized lingual

tissues. The more severe tongue deformity along the anteroposterior axis and distinct alterations of gene expression and cell behavior in BAs 1-4 of *Wnt1-Cre/caAlk2* mutants indicate that neural crest-derived mesenchymal cells in BAs 1-4 respond to elevated ALK2-BMP signaling in a region-specific manner. Overall, our results indicated that appropriate levels of ALK2-BMP signaling activity in neural crest-derived mesenchyme plays essential roles in coordinating various tissue and cell types for the proper formation of the tongue organ and its epithelial appendages (taste papillae and taste buds). The phenotype is severe and different from the mild defect resulted from the elevated ALK3-BMP signaling activity (Li et al., 2013) , which indicates distinct roles of specific receptor-mediated BMP signaling in the tongue organogenesis.

2.5.1 Appropriate levels of ALK2-BMP signaling activity in neural crest and the derived lingual mesenchyme is required for proper tongue organogenesis

The neural crest is a multipotent cell population derived from the lateral ridges of the neural plate in early vertebrate embryos (Leikola, 1976; Trainor, 2015). In mice, cranial neural crest cells populate directly under the epithelium of the tongue primordium (branchial arch 1) as early as 1-2 somite stages (E8.0-8.5) (Serbedzija et al., 1992). Neural crest-derived cells are extensively distributed in the mesenchyme/connective tissue of the tongue (Boggs et al., 2016; Liu et al., 2012a; Thirumangalathu et al., 2009) and are regarded as scaffolds of the tongue organ (Chai and Maxson, 2006; Cordero et al., 2011). Structural and molecular disruption of neural crest and neural crest-derived cells causes severe defects in tongue formation. For instance, lacking primary cilia in neural crest cells causes aglossia (Millington et al., 2017). Deficient molecular signaling of Wnt (Liu et al., 2009; Liu et al., 2012b; Zhong et al., 2015; Zhu et al., 2017) and TGF-β (Iwata et al., 2013) result in microglossia due to defects in cells migrating into and surviving in the tongue anlage. Our study in demonstration of the importance of ALK2-BMP signaling in neural crest and derived mesenchymal cells in the tongue formation suggest that organogenesis of the tongue involves a complex network of molecular signaling

pathways. Detection of an increased p-Smad1/5/8 and unchanged p-Smad2/3 level in the E10.5 *Wnt1-Cre/caAlk2* mutant BAs confirmed that the intracellular cascades of ALK2-BMP signaling were through p-Smad1/5/8 that is separate from TGF-β signaling that utilizes p-Smad2/3 (Grönroos et al., 2012). Moreover, our observations of an uneven severity of tongue development in *Wnt1-Cre/caAlk2* mutants suggest that tongue formation is finely tuned in a region-specific manner.

To understand the progressively increased severity of tongue deformity along the anteroposterior axis, we detected expression levels of genes in individual BAs including BMP target genes associated with cell growth (*Id1*, *Snai1*, *Snai2* and *Runx2*), cell proliferation regulating gene (*Cyclin-D1*) and apoptosis control gene (*p53*) in *Wnt1-Cre/caAlk2* mutant, *Cre*$^{-}$*/caAlk2* littermate control and C57BL/6J wild type (WT) mice. Individual BAs had significantly different expression levels of BMP target genes *Snai2* and *Runx2* in E10.5 C57BL/6J WT embryos suggesting distinct levels of BMP signaling activity. Moreover, alterations of gene expression levels in each BA of *Wnt1-Cre/caAlk2* mutants were different suggesting that individual BAs respond to elevated ALK2-BMP signaling distinctly. BA 4 was most responsive such that all tested BMP target genes were altered. Ultimately a significantly lower cell proliferation in BA 4 and higher apoptosis in BA 3 and 4 (Pietsch et al., 2008) might be the cause of the decreased cell number in BA 4 mesenchyme and absence of pharyngeal tongue since BAs 3-4 are the main contributor to the formation of pharyngeal tongue (Cobourne et al., 2019; Parada et al., 2012). Differences of BMP target gene expression pattern in E10.5 BAs were detected between C57BL/6J WT and *Cre*$^{-}$*/caAlk2* littermate controls. This was confirmed by the data from an independent experiment in *caAlk2* hemizygous embryos through crossing with C57BL/6J WT breeders. Although we do not have evidence-based explanations, this discrepancy of gene expressions might be caused by (1) the genetic background difference-since *caAlk2* mice are maintained mixture of 129S6 and C57BL/6J, and (2) alterations in gene expressions by transgene insertion, which is not uncommon. However, these *Cre*$^{-}$*/caAlk2*

littermate controls did not exhibit phenotypic alterations demonstrating that the phenotypes we observed in *Wnt1-Cre/caAlk2* mutants were due to the activation of *caAlk2*.

We observed a significantly higher level of *p53* transcripts and more apoptotic cells in BA 1 of *Wnt1-Cre/caAlk2* mutants, however, the cell proliferation regulating gene *Cyclin-D1* (Yang et al., 2006) as well as cell proliferation were increased in BA 1-2. A promoted cell proliferation in the mutant BA 1 and 2 may overwrite the cell death and be responsible for the formation of the small oral tongue to which BA 1 and a portion of BA 2 contribute (Cobourne et al., 2019; Parada et al., 2012). This is supported by the increased cell count in the mesenchyme of mutant BA1.

Interestingly, we noticed that even though *Wnt1-Cre* labeled most, if not all, of the cells in the mesenchyme of BAs 1-4, only a population of mesenchymal cells had promoted cell proliferation or apoptosis. The data indicate that the mesenchymal cells in BAs responded to elevated ALK2-BMP signaling activity distinctly.

In summary, our data showed that expression levels of BMP target genes are distinct among individual BAs and that neural crest and the derived mesenchymal cells in individual BAs respond differentially in gene expression and cell behaviors to the constitutive activation of ALK2-BMP signaling. The results suggest that distinct levels of ALK2-BMP signaling activity in individual BAs are required for the cell behavior and functions during normal tongue development.

2.5.2 ALK2-BMP signaling regulates the interactions of neural crest-derived mesenchyme with other lingual tissues for their proper development and organization

As aforementioned, the tongue is comprised of multiple tissues that are connected by the mesenchyme/connective tissue arising primarily from neural crest and serving as a scaffold of the organ (Rinon et al., 2007). The neural crest-derived tongue mesenchyme compartmentalizes lingual muscles and allows nerves and blood vessels to traverse through. In the present study, we provide evidence for an important role of mesenchymal ALK2-BMP signaling in regulating the development of multiple tissues in the tongue. Constitutive activation

of ALK2-BMP signaling in tongue mesenchyme led to altered orientation of muscle fibers, reduced branching and growth of nerves, thinner epithelium and arrest of further development of fungiform papillae and taste buds at late embryonic stages.

During the initial formation of the tongue organ, neural crest and neural crest-derived cells migrate into the tongue primordium before myogenic progenitors (Parada et al., 2012), and it has been speculated that neural crest-derived cells in the tongue mesenchyme acts as a niche that release molecular instructions to direct survival, proliferation and differentiation of myogenic progenitors as well as the patterning of the muscle (Parada and Chai, 2015; Parada et al., 2012). In the present study, we observed missing of muscle fibers at certain orientations (e.g., longitudinal and transverse muscle fibers) in *Wnt1-Cre/caAlk2* mutant mice suggesting that ALK2-BMP signaling regulate how mesenchymal cells interact and guide myogenic processes and patterning.

In addition to the defects of muscle cells in *Wnt1-Cre/caAlk2* mutants, there were also changes in the nerve outgrowth and branching. Although nerve fibers were not tracked to distinguish the gustatory (chorda tympani) from somatosensory (trigeminal) innervating fibers, we observed that *Wnt1-Cre/caAlk2* mutant tongues lack βIII-tubulin^{+} nerve fibers in the vicinity of taste papillae and surrounding epithelium at E14.5, within early fungiform taste buds and surrounding epithelium at E18.5. The results indicate that both nerves were affected by the elevated ALK2-BMP signaling in tongue mesenchyme. Glial cells including the myelinating Schwann cells are derived from neural crest (Mayor and Theveneau, 2013). Our results support the idea that ALK2-BMP signaling is involved in regulating the interactions of neural crest-derived stromal and/or Schwann cells with axons for proper nerve outgrowth, pathfinding and/or branching.

The development of epithelial appendages requires the interactions with the underlying mesenchyme (Thesleff, 2003). Both direct (Ribatti and Santoiemma, 2014) and indirect (Jussila and Thesleff, 2012) cell-cell interactions between mesenchymal and epithelial cells have been

reported. Multiple signaling pathways are involved in the mesenchymal-epithelial interactions (Puthiyaveetil et al., 2016), among which BMP signaling plays important roles (Merrill et al., 2008). Profound effects of BMPs (2, 4 and 7) and antagonists (noggin and follistatin) in taste papilla formation and patterning have been reported (Beites et al., 2009; Zhou et al., 2006). Here we provide evidence that ALK2 is a mediating receptor of BMP signaling in lingual mesenchyme for its interactions with other tissues.

Moreover, our results showed that *Wnt1-Cre/caAlk2* mutants had well-formed fungiform papillae on the small tongue, however at E18.5 tongue epithelium became thinner and further development of fungiform papillae and taste buds were arrested. The data indicate that appropriate level of ALK2-BMP signaling is critical in mesenchymal interactions with the overlying epithelium for epithelial cell proliferation and differentiation, thus advancing fungiform papilla development. It is noteworthy that early taste buds were formed in the less advanced fungiform papillae without innervation, indicating that taste bud formation and cell differentiation are nerve-independent which is also supported by other reports (Castillo et al., 2014; Farbman and Mbiene, 1991; Fritzsch et al., 1997; Ito et al., 2010; Mbiene et al., 1997; Ren et al., 2017). However, lack of innervation might be one of causes for the arrest of further development of fungiform taste buds observed in E18.5 mutant tongues. Further, our observation that the *Wnt1-Cre/caAlk2* mutants had an enlarged Shh^{+} patch of tissue that was presumably a circumvallate papilla placode at E12.5 but lacked a circumvallate taste papilla at E14.5 indicates that the circumvallate is initially specified but eventually is not sustained. It is possible that the pharyngeal tongue region is important for sustaining the development of the circumvallate papilla.

Collectively, our data provide evidence that ALK2-BMP signaling in neural crest-derived mesenchyme regulates mesenchymal interactions with other lingual tissues including epithelium, muscles, and nerves for their development and organization. Since type I BMP receptors are present in both tongue epithelium and mesenchyme (Beites et al., 2009; Jung et

al., 1999; Kawasaki et al., 2012; Li et al., 2013; Suga et al., 2007; Zhou et al., 2006), further studies are needed to understand the specific roles of each receptor in distinct tissue compartments.

2.6 Acknowledgements

We give thanks to: Dr. Steven Stice, Dr. Franklin West, Dr. Luke Mortensen, and Dr. Douglas Menke at The University of Georgia, Athens, Georgia, for the discussion and feedbacks; Dr. Charlotte Mistretta for offering her lab space for the preliminary studies. This study was supported by the National Institutes of Health, grant number R01DC012308 to HXL, R01DE025897 to YK, and R01DE020843 to YM

Table 2.1. Primary antibodies used for immunohistochemistry.

Primary antibody	Source (catalog number, company)	Dilution
Goat anti Shh	AF464, R&D systems, Minneapolis, MN	1:300
Rabbit anti p-Smad1/5/9	#13820, Cell signaling, Danvers, MA	1:1000
Rabbit anti p-Smad2/3	#3101, Cell signaling, Danvers, MA	1:1000
Mouse anti GAPDH	G8795, Sigma Aldrich, St Louis, MO	1:10,000
Rabbit anti βIII-tubulin	ab18207, Abcam, Cambridge, United Kingdom	1:1000
Chicken anti Vimentin	AB5733, EMD millipore, Burlington, MA	1:1000
Rabbit anti Desmin	ab15200, Abcam, Cambridge, United Kingdom	1:1000
Goat anti E-Cadherin	AF748, R&D systems, Minneapolis, MN	1:1000
Rat anti Keratin 8	TROMA-I, Developmental Studies Hybrydoma Bank, Iowa city, IA	1:1000
Sheep anti Ki67	AF7649, R&D systems, Minneapolis, MN	1:500
Rabbit anti cCaspase-3	#9661, Cell signaling, Danvers, MA	1:500

Table 2.2. Primer sequences used in the quantitative reverse transcriptase PCR.

Gene	Primer sequence
Id1	Forward 5' GAG TCT GAA GTC GGG ACC AC 3' Reverse 5' CCT CAG CGA CAC AAG ATGC 3'
Snai1	Forward 5' CTT GTG TCT GCA CGA CCT GT 3' Reverse 5' CTT CAC ATC CGA GTG GGT TT 3'
Snai2	Forward 5' GGC TGC TTC AAG GAC ACA TT 3' Reverse 5' TTG GAG CAG TTT TTG CAC TG 3'
Runx2	Forward 5' AAG AAG AGC CAG GCA GGT GC 3' Reverse 5' CAT ACC GAG GGA CAT GCC TGAG 3'
Cyclin D1	Forward 5' GAC GGC GTC AAA TAT GTC CT 3' Reverse 5' CTG GAG AGT GAC AGC ATG GA 3'
p53	Forward 5' CGG GTG GAA GGA AAT TTG TA 3' Reverse 5' TAG CAC TCA GGA GGG TGA GG 3'

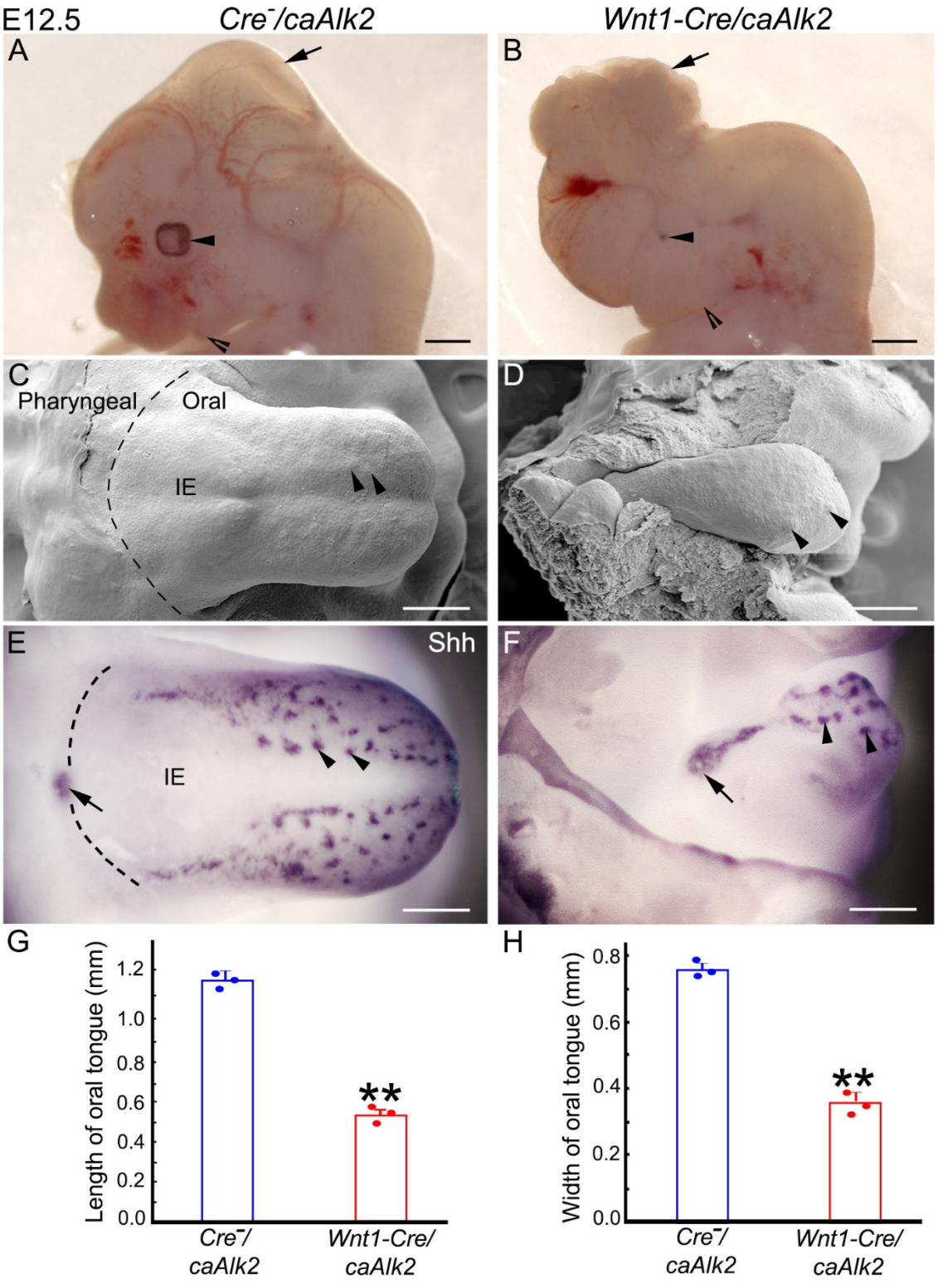
E12.5
Cre-/caAlk2
Wnt1-Cre/caAlk2
A
B
C
Pharyngeal
Oral
IE
D
E
Shh
IE
F
G
Length of oral tongue (mm)
1.2
1.0
0.8
0.6
0.4
0.2
0.0
**
Cre-/ caAlk2
Wnt1-Cre/ caAlk2
H
Width of oral tongue (mm)
0.8
0.6
0.4
0.2
0.0
**
Cre-/ caAlk2
Wnt1-Cre/ caAlk2

Figure 2.1. Representative images (A-F) and measurement of tongue size (G-H) to illustrate the deficiencies of craniofacial region and tongue in E12.5 *Wnt1-Cre/caAlk2* mutants compared to *Cre*$^{-}$*/caAlk2* littermate controls. A, B: Light microscopy images of a littermate control (A) and *Wnt1-Cre/caAlk2* mutant (B). Arrows point to the brain; arrowheads point to the eye; open arrowheads point to the orofacial region. Scale bars: 1 mm. **C, D:** Scanning electron microscopy (SEM) images of littermate control (C) and *Wnt1-Cre/caAlk2* mutant (D) tongues. Scale bars: 200 μm. **E, F:** Light microscopy images of whole mount immunoreaction for Shh (blue), a developing taste papilla marker, in littermate control (E) and *Wnt1-Cre/caAlk2* mutant (F) tongues. Arrowheads in C-F point to fungiform taste papilla placodes. The arrow in E and F points to the Shh^{+} circumvallate papilla placode in the posterior oral tongue. Dashed lines in C and E separate the oral tongue from the pharyngeal tongue. IE: intermolar eminence. Scale bars: 200 μm. **G, H:** Histograms ($\bar{X}$±SD; n=3) represent the length (G) and width (H) of the oral tongue in *Wnt1-Cre/caAlk2* and littermate controls. ***P*≤0.01 Students *t*-test compared to littermate control tongue.

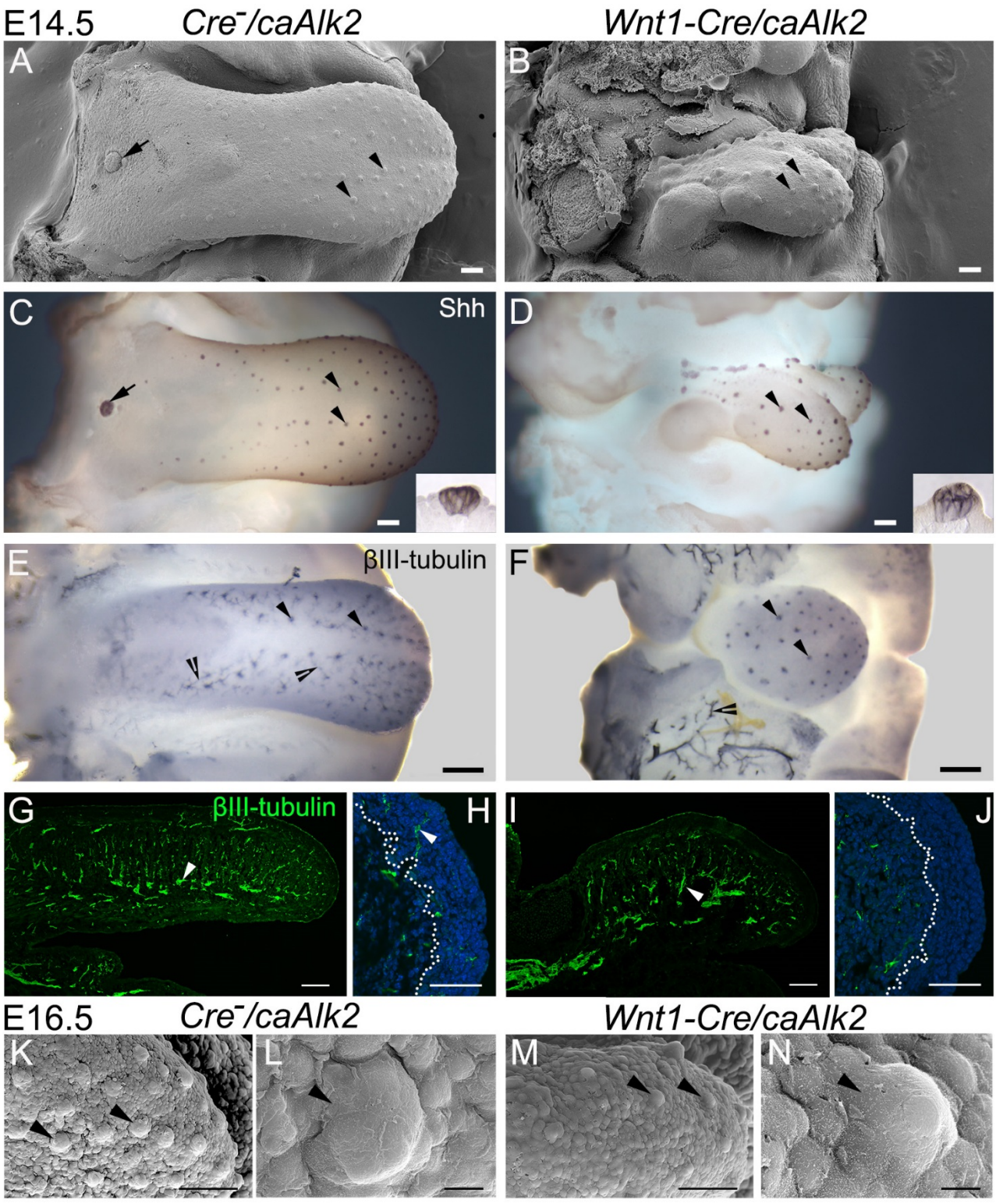
E14.5
Cre-/caAlk2
Wnt1-Cre/caAlk2
A
B
C
Shh
D
E
βIII-tubulin
F
G
βIII-tubulin
H
I
J
E16.5
Cre-/caAlk2
Wnt1-Cre/caAlk2
K
L
M
N

Figure 2.2. **Development of tongue and taste papillae in E14.5 and E16.5 *Wnt1-Cre/caAlk2* mutant and *Cre⁻/caAlk2* littermate control mice. A-F:** Whole mount images (SEM in A-B, light microscopy in C-F) of littermate control (A, C, E) and *Wnt1-Cre/caAlk2* (B, D, F) tongues. Whole mount immunoreactions were performed against Shh (C, D) or βIII-tubulin (E, F). Insets in C and D show the restriction of Shh immunoproducts to fungiform taste papilla epithelium on tongue sections. Arrowheads in A-F point to developing fungiform taste papillae. Arrows in A and C point to the circumvallate papilla. Open arrowheads in E and F point to βIII-tubulin$^+$ nerve fibers in littermate control (E) and *Wnt1-Cre/caAlk2* mutant (F) tongues. Scale bars: 100 μm. **G-J:** Single-plane laser scanning confocal images of sagittal sections of littermate control (G) and *Wnt1-Cre/caAlk2* mutant (I) tongues immunostained for βIII-tubulin (green). H and J are high magnification images of the anterior tip of littermate control (H) and *Wnt1-Cre/caAlk2* mutant tongues (J). Arrowheads in G-I point to βIII-tubulin$^+$ nerve fibers. Dotted lines in H and J separate the epithelium from the underlying mesenchyme. Scale bars: 100 μm G, I; 50 μm in H, J. **K-N:** SEM images of E16.5 littermate control (K, L) and *Wnt1-Cre/caAlk2* mutant (M, N) tongues to illustrate the left anterior tongue tip (K, M) and a fungiform papilla (L, N) in a littermate control (K, L) and *Wnt1-Cre/caAlk2* mutant (M, N) tongue. Arrowheads point to fungiform papillae. Scale bars: 100 μm K, M; 10 μm in L, N.

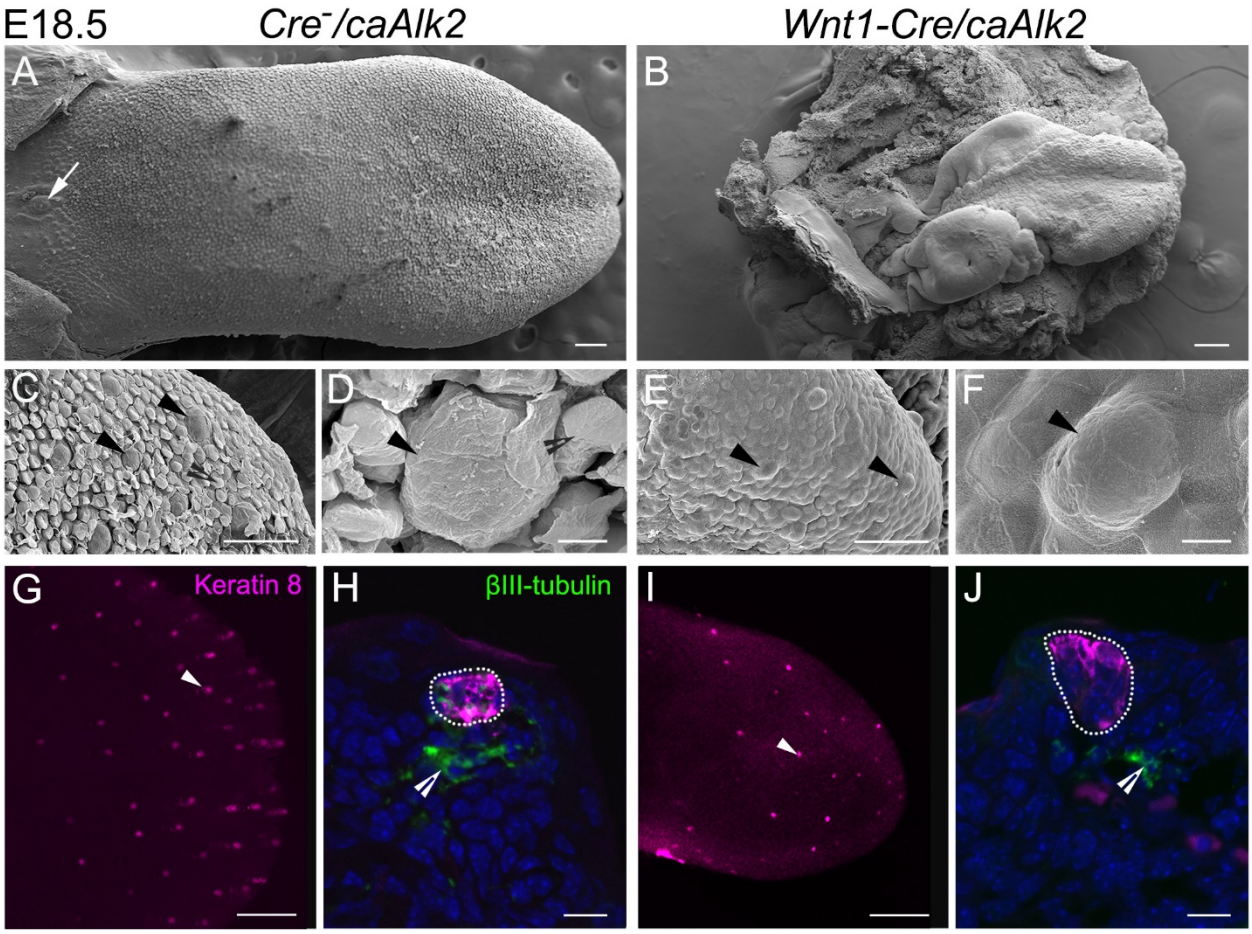
E18.5
Cre-/caAlk2
Wnt1-Cre/caAlk2
A
B
C
D
E
F
G
Keratin 8
H
βIII-tubulin
I
J

Figure 2.3. Further advancement of taste papilla development and formation of early taste buds in E18.5 *Wnt1-Cre/caAlk2* mutant and *Cre⁻/caAlk2* littermate control tongues. **A-F:** SEM images of E18.5 littermate control (A, C, D) and *Wnt1-Cre/caAlk2* mutant (B, E, F) tongues. The arrow in A points to the circumvallate papilla. In C-F, arrowheads point to fungiform papillae, open arrowheads in C, D point to filiform papillae. High magnification images of the left anterior tongue tip (C, E) and a fungiform papilla (D, F) in a littermate control (A, C, D) and *Wnt1-Cre/caAlk2* mutant (B, E, F) tongue. Scale bars: 500 μm in A, B; 100 μm in C, E; 10 μm in D, F. **G, I:** Littermate control (G) and *Wnt1-Cre/caAlk2* mutant (I) tongue epithelial sheets immunostained with pan-taste cell marker K8 (magenta). Arrowheads point to $K8^+$ fungiform taste buds. Scale bars: 200 μm. **H, J:** Single-plane laser scanning confocal images of sagittal sections of littermate control (H) and *Wnt1-Cre/caAlk2* mutant (J) tongues immunostained with K8 (magenta) and βIII-tubulin (green). Dotted lines in H and J encircle $K8^+$ taste buds; open arrowheads point to βIII-tubulin$^+$ nerve fibers. Scale bars: 20 μm.

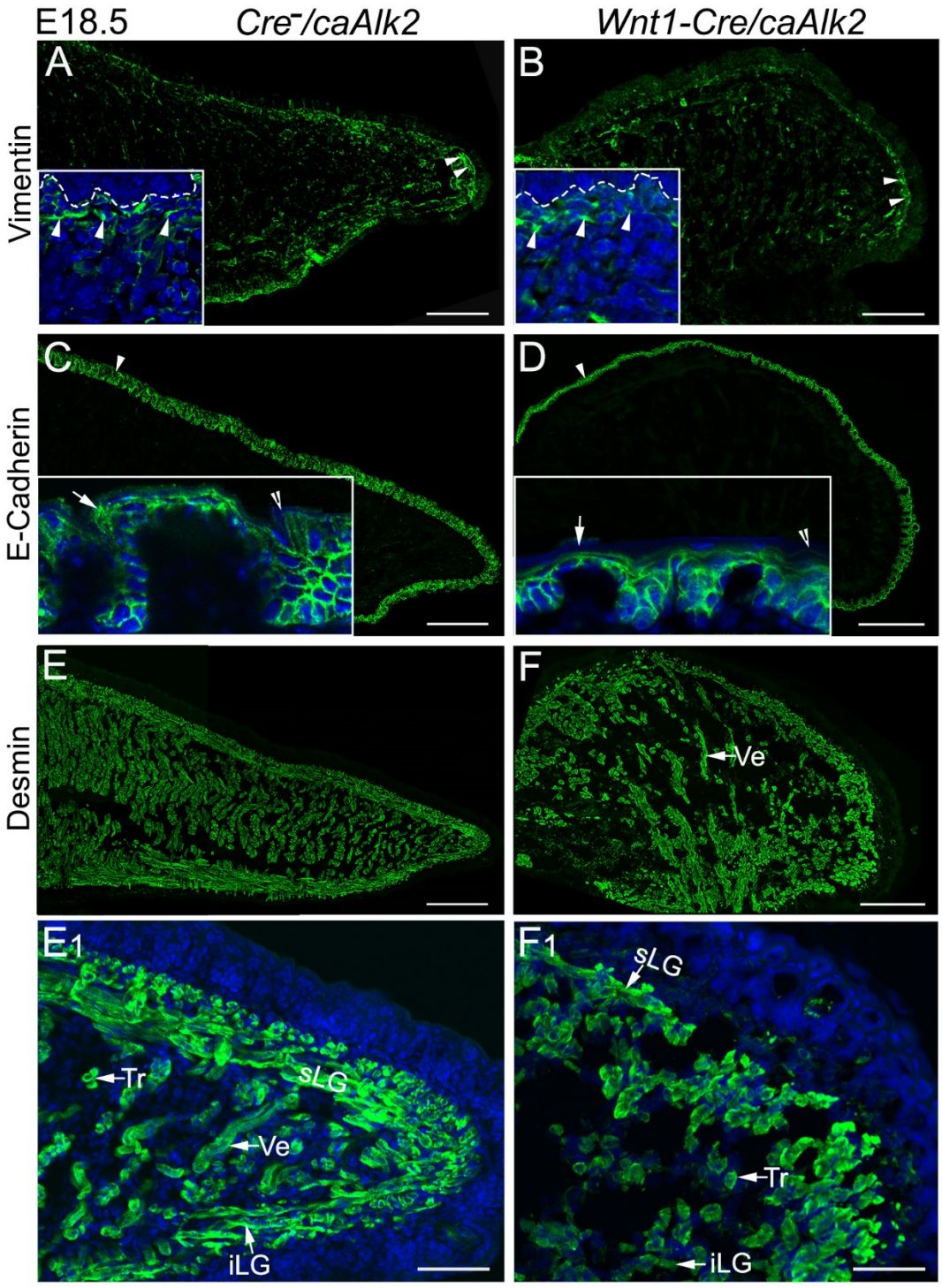
E18.5
Cre-/caAlk2
Wnt1-Cre/caAlk2
A
B
Vimentin
C
D
E-Cadherin
E
F
Desmin
Ve
E1
F1
Tr
sLG
Ve
iLG
sLG
Tr
iLG

Figure 2.4. Representative photomicrographs of sagittal sections of E18.5 *Wnt1-Cre/caAlk2* mutant and *Cre^{-}/caAlk2* littermate control tongues. **A-F:** Single-plane laser scanning confocal images of littermate control (A, C, E) and *Wnt1-Cre/caAlk2* mutant (B, D, F) tongues immunostained with mesenchymal cell marker Vimentin (A-B, green), epithelial cell marker E-Cadherin (C-D, green), or muscle cell marker Desmin (E-F, green). Insets in A-D show representative high magnification images. Arrowheads in A and B point to the dense stromal cell layer under the epithelium. Dashed lines in insets of A and B separate the epithelium from the underlying mesenchyme. Arrows in insets of C and D point to fungiform papillae. Arrowheads in C and D point to the epithelium. Open arrowheads in insets of C and D point to filiform papillae. E_1 and F_1 are high magnification images of E and F. sLG: superior longitudinal muscle, iLG: inferior longitudinal muscle, Ve: vertical muscle, Tr: transverse muscle. Scale bars: 100 μm in A-F; 50 μm in E1, F1.

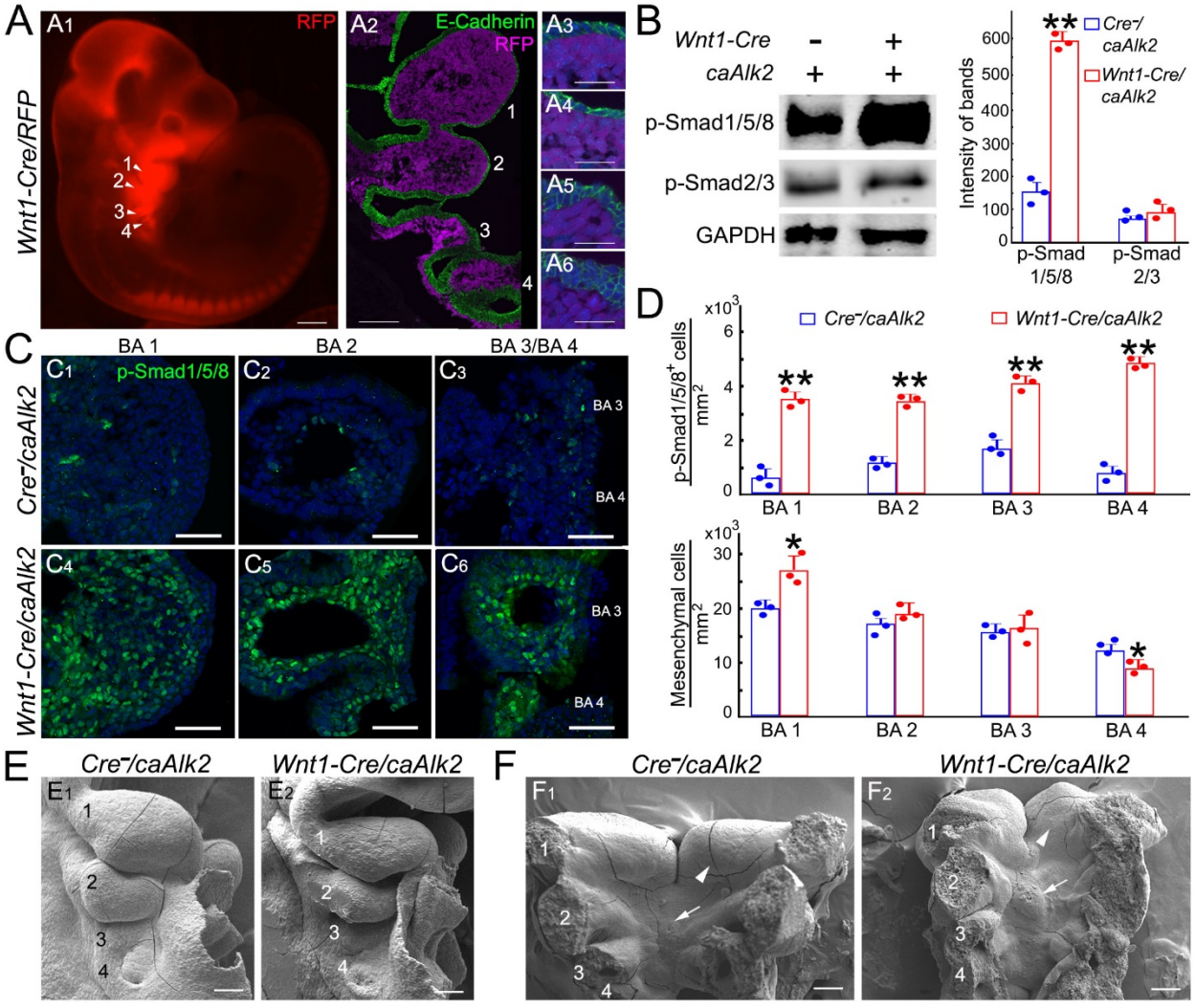
A
A1
RFP
Wnt1-Cre/RFP
A2
E-Cadherin
RFP
A3
A4
A5
A6
B
Wnt1-Cre
caAlk2
p-Smad1/5/8
p-Smad2/3
GAPDH
Intensity of bands
Cre-/caAlk2
Wnt1-Cre/caAlk2
p-Smad 1/5/8
p-Smad 2/3
C
BA 1
BA 2
BA 3/BA 4
C1
p-Smad1/5/8
C2
C3
BA 3
BA 4
Cre-/caAlk2
C4
C5
C6
Wnt1-Cre/caAlk2
D
p-Smad1/5/8+ cells mm2
Mesenchymal cells mm2
BA 1
BA 2
BA 3
BA 4
E
Cre-/caAlk2
Wnt1-Cre/caAlk2
E1
E2
F
F1
F2

Figure 2.5. Representative photomicrographs of E10.5 branchial arches (BAs) of Wnt1-Cre/RFP, *Wnt1-Cre/caAlk2,* and *Cre^{-}/caAlk2* littermate controls. **A:** Whole mount image of E10.5 *Wnt1-Cre/RFP* embryo. Numerals 1-4 in A show individual BAs. A_2-A_6 are single-plane laser scanning confocal images of *Wnt1-Cre/RFP* BAs immunostained with E-Cadherin (green). A_3-A_6 are high magnification images of individual BAs in A_2. Scale bars: 400 μm in A_1; 100 μm in A_2; 50 μm in A_3-A_6. **B:** Western blot bands (left) of p-Smad1/5/8, p-Smad2/3, and GAPDH in the mesenchyme of BAs 1-4 of littermate controls and *Wnt1-Cre/caAlk2* mutants. Histogram (right) represents the intensities of Western blot bands of p-Smad1/5/8, p-Smad2/3 as means ± standard deviation ($\bar{X}$±SD; n=3). **P*≤0.05 Students *t*-Test compared to littermate control group. **C:** Single-plane laser scanning confocal images of littermate control (C_1-C_3) and *Wnt1-Cre/caAlk2* (C_4-C_6) BA transverse sections immunostained with p-Smad1/5/8 (green). Scale bars: 50 μm. **D:** Histograms ($\bar{X}$±SD; n=3) represent the total number of p-Smad1/5/8^{+} cells per mm^2 (top) and total number of mesenchymal cells per mm^2 (bottom) in individual BAs of *Wnt1-Cre/caAlk2* and littermate controls. **P*≤0.05, ***P*≤0.01 compared to littermate control BAs using two-way ANOVA followed by Fisher's least significant difference (LSD) analyses. **E, F:** SEM images to illustrate the side (E) and dorsal (F) view of BAs of littermate control (E_1, F_1) and *Wnt1-Cre/caAlk2* mutant (E_2, F_2). Numerals 1-4 in E and F mark individual BAs 1-4. Arrowheads in F point to the dorsal swelling of BA 1. Arrows in F point to the copula in BA 2. Scale bars: 100 μm.

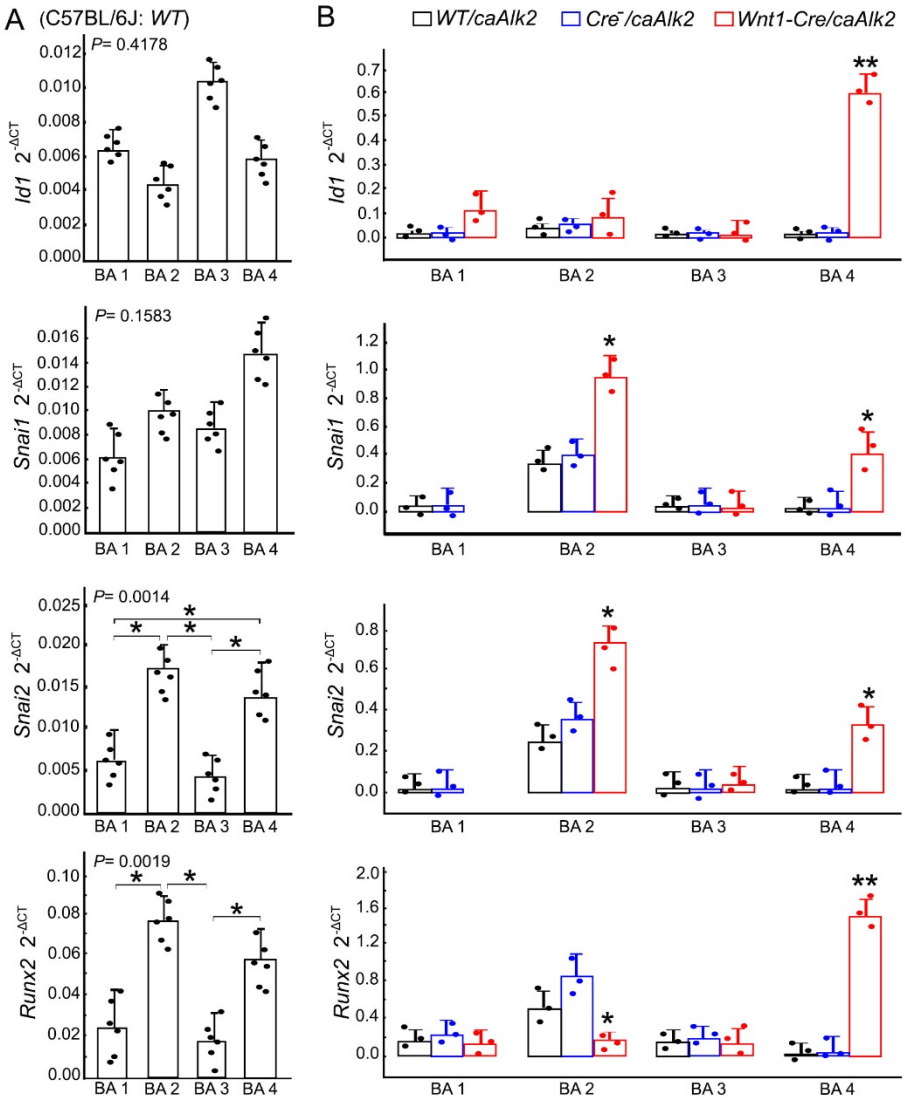
A
(C57BL/6J: WT)
B
WT/caAlk2
Cre-/caAlk2
Wnt1-Cre/caAlk2
Id1 2-ΔCT
Snai1 2-ΔCT
Snai2 2-ΔCT
Runx2 2-ΔCT
P= 0.4178
P= 0.1583
P= 0.0014
P= 0.0019
BA 1
BA 2
BA 3
BA 4

Figure 2.6. Quantitative RT-PCR of BMP target genes in E10.5 branchial arches of C57BL/6J wild type (WT) (A); *Wnt1-Cre/caAlk2* mutant, *Cre⁻/caAlk2* littermate control and *C57BL/6J WT/caAlk2* (B) embryos. Histograms represent means ± standard deviation ($\bar{X}$±SD) of $2^{-\Delta CT}$ values of examined BMP target genes (*Id1*, *Snai1*, *Snai2*, *Runx2*) in individual BAs of C57BL/6J wild type (WT) (A; n=6), *C57BL/6J WT/caAlk2* (Black bars in B; n=3), *Cre⁻/caAlk2* littermate control (Blue bars in B; n=3) and *Wnt1-Cre/caAlk2* (Red bars in B; n=3) mice. **P*≤0.05 (A) one-way ANOVA followed by Fisher's LSD analyses. **P*≤0.05, ***P*≤0.01 (B) compared to corresponding BAs of *Cre⁻/caAlk2* littermate control using two-way ANOVA followed by Fisher's LSD analyses.

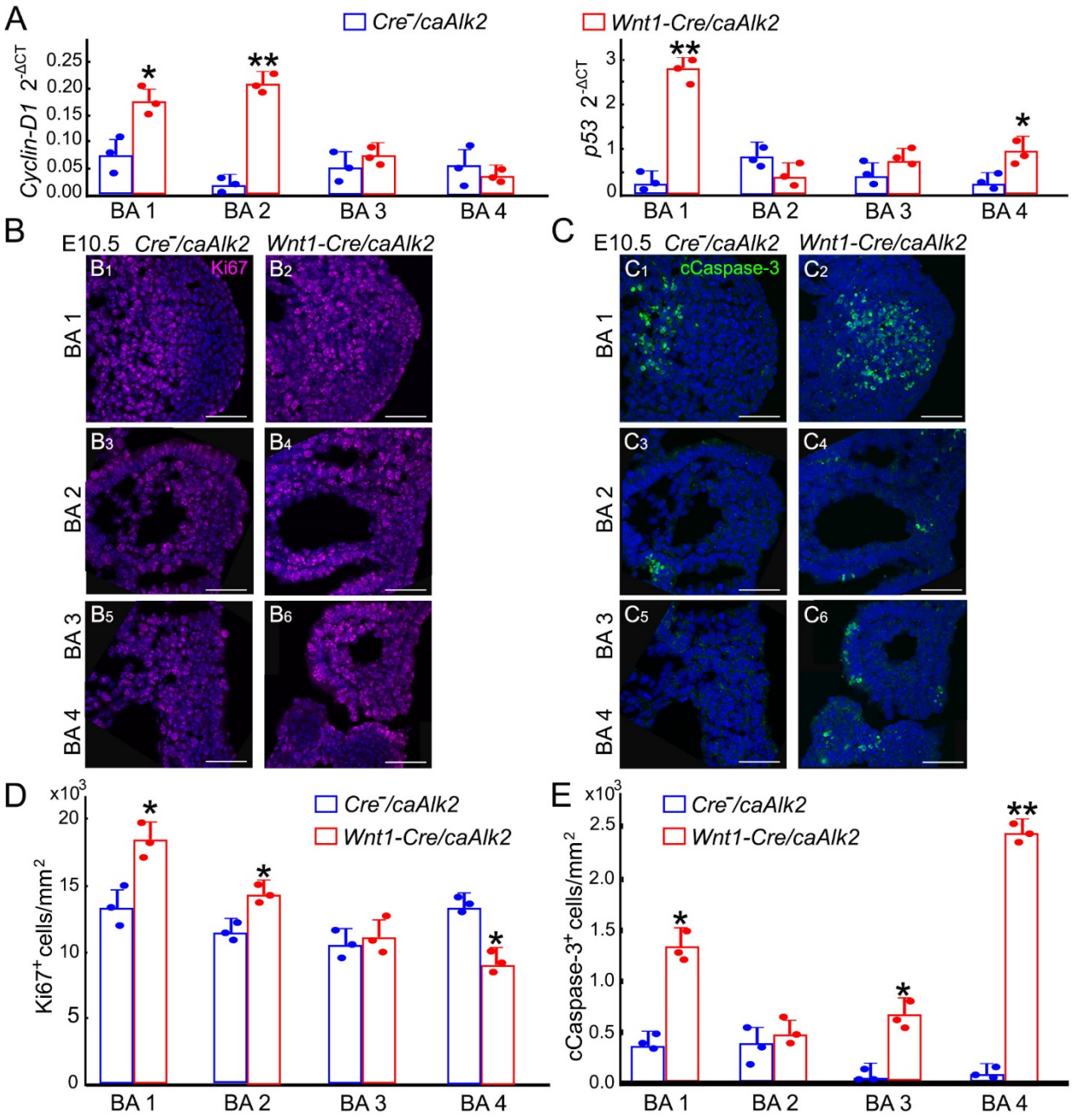
A
Cre⁻/caAlk2
Wnt1-Cre/caAlk2
Cyclin-D1 2-ΔCT
p53 2-ΔCT
BA 1
BA 2
BA 3
BA 4
B
E10.5 Cre⁻/caAlk2 Wnt1-Cre/caAlk2
Ki67
C
cCaspase-3
D
Ki67+ cells/mm2
E
cCaspase-3+ cells/mm2

Figure 2.7. Effect of elevated ALK2-BMP signaling on cell proliferation and apoptosis in E10.5 BAs. A: Histograms ($\bar{X}$±SD; n=3) of $2^{-\Delta CT}$ values of cell proliferation associated gene *Cyclin-D1* and apoptosis associated gene *p53* in individual BAs of *Wnt1-Cre/caAlk2* and *Cre*$^{-}$*/caAlk2* littermate control. **P*≤0.05, ***P*≤0.01 compared to the corresponding BA of littermate control using two-way ANOVA followed by Fisher's LSD analyses. **B, C:** Single-plane laser scanning confocal images of transverse BA sections immunostained with cell proliferation marker Ki67 (B, magenta) or apoptosis marker cleaved (c) Caspase-3 (C, green) in littermate control (B_1, B_3, B_5/C_1, C_3, C_5) and *Wnt1-Cre/caAlk2* (B_2, B_4, B_6/C_2, C_4, C_6) mice. Scale bars: 50 µm. **D, E:** Histograms ($\bar{X}$±SD; n=3) of the total number of Ki67^{+} cells per mm^2 (D) or cCaspase-3^{+} cells per mm^2 (E) in individual BAs of littermate controls and *Wnt1-Cre/caAlk2* mutants. **P*≤0.05, ***P*≤0.01 compared to the corresponding BA of littermate control using two-way ANOVA followed by Fisher's LSD analyses.

CHPATER 3

ALK3-MEDIATED BMP SIGNALING IN THE NEURAL CREST-DERIVED TONGUE MESENCHYME PROMOTE TASTE PAPILLA DEVELOPMENT THROUGH SUPPRESSING THE SECRETION OF INHIBITORY SECRETORY PROTEINS[1]

[1]Mohamed Ishan, Zhonghou Wang, Yuji Mishina, Hong-Xiang Liu. To be submitted to *Development*.

3.1 Abstract

Development of epithelial appendages including taste papilla requires mesenchymal-epithelial interactions governed by multiple molecular signaling pathways including bone morphogenetic protein (BMP) signaling pathway. In the present study, we report the important roles of type I BMP receptor ALK3-mediated BMP signaling pathway (ALK3-BMP signaling hereafter) in the neural crest-derived (NC) tongue mesenchyme in regulating the development of taste papillae. We used *Wnt1-Cre* to conditionally knock out (*cKO*) *Alk3* in a mesenchyme-specific manner. At E12.0, *Wnt1-Cre/Alk3*^{cKO} mutants had a truncated tongue as compared to *Cre*$^{-}$*/Alk3*$^{fx/fx}$ littermate controls. At E12.0 when Shh^{+} taste papilla placodes emerge, they were completely absent in the *Wnt1-Cre/Alk3*^{cKO} tongues. Bulk RNA-Seq analysis demonstrated that many more differentially expressed genes (DEGs) in the *Wnt1-Cre/Alk3*^{cKO} mutant epithelium compared to those in the mesenchyme of E12.0 tongue suggesting the specific roles of mesenchymal ALK3-BMP signaling in epithelial-mesenchymal interactions. DEGs related to secretory proteins (*Nbl1*, *Pkm2*) were up-regulated in the *Wnt1-Cre/Alk3*^{cKO} mutant mesenchyme. Inhibition of Shh^{+} taste papilla when E12.0 wild type tongues were cultured with the proteins isolated from the *Wnt1-Cre/Alk3*^{cKO} mutant mesenchyme-derived conditioned media indicates an enhanced secretion of inhibitory proteins. To identify the potential secretory protein(s), liquid chromatography-mass spectrometry and western blot analyses were performed on the mesenchyme-derived conditioned media isolated from the *Wnt1-Cre/Alk3*^{cKO} mutant and *Cre*$^{-}$*/Alk3*$^{fx/fx}$ littermate controls and detected Nbl1 and Pkm2, known secretory proteins, at a significantly higher level in *Wnt1-Cre/Alk3*^{cKO} mutant tongue mesenchyme-derived conditioned media. Together, our data suggest that ALK3-BMP signaling in the tongue mesenchyme suppress the secretion of inhibitory secretory proteins and promote taste papilla development.

Keywords: ALK3-BMP signaling, taste papillae, mesenchyme, neural crest, tongue, secretory proteins

3.2 Introduction

The sense of taste is one of the five basic senses and carried out by taste buds located in the epithelial appendages called taste papillae (Barlow, 2015; Chaudhari and Roper, 2010; Liu et al., 2004; Mistretta et al., 2003). In rodents, these taste papillae develop on the tongue in a stereotypical pattern with abundant fungiform in the anterior oral tongue, bilateral foliate, and a single circumvallate on the midline of the border between the oral and pharyngeal tongue (Mistretta et al., 2005). Despite of the papilla type, each taste papilla is structurally composed of an epithelium, in which taste buds reside, and a mesenchymal core (Barlow, 2015). Taste papillae form well before histologically recognizable taste buds emerge (Barlow, 2015; Krimm et al., 2015). Studies to address the development of taste papilla are of vital importance as cells in the taste papilla provide progenitor cell populations to replenish and maintain taste buds (Miura and Barlow, 2010; Okubo et al., 2009; Stone et al., 1995).

The development of taste papillae requires mesenchymal-epithelial interactions governed by multiple molecular signaling pathways including bone morphogenetic protein (BMP) signaling pathway (Beites et al., 2009; Ishan et al., 2020; Zhou et al., 2006). BMPs are secreted proteins that are pivotal for cell growth, differentiation, and apoptosis during the development of many organs (Bragdon et al., 2011; Wang et al., 2014). BMPs belong to TGF-β superfamily. Upon ligand binding, the type II BMP receptors (ACVR2, BMPR2) activate type I BMP receptors (ALK2, ALK3, ALK6) via phosphorylation, activating the downstream signaling cascade. Type I BMP receptors are the main determinants of downstream BMP signaling specificity (Bragdon et al., 2011; Wang et al., 2014). The roles of type I BMP receptor ALK2, BMP ligands and their antagonists in the development of tongue and taste papilla are profound (Beites et al., 2009; Ishan et al., 2020; Zhou et al., 2006). Here, we report type I receptor ALK3-mediated BMP signaling pathway (ALK3-BMP hereafter) in the mesenchyme regulate mesenchymal factors for the formation of taste papillae.

In this study, we used *Wnt1-Cre* to conditionally knockout *Alk3* (*Alk3 cKO*) in neural crest (NC) and NC-derived cells. We found that *Alk3 cKO* in NC-derived tongue mesenchyme exhibited an absolute loss of taste papillae. In combination with RNA sequencing, liquid chromatography-mass spectrometry and functional analyses using tongue organ culture system, our results indicate that ALK3-BMP signaling in the NC-derived lingual mesenchyme suppresses the secretion of inhibitory secretory proteins and promotes taste papilla development.

3.3 Materials and Methods

3.3.1 Animal use and tissue collection.

The use of animals was approved by the Institutional Animal Care and Use Committee at the University of Georgia. The studies were performed in compliance with the National Institutes of Health Guidelines for the care and use of animals in research. The animals were maintained in the animal facilities in the Department of Animal and Dairy Science at the University of Georgia.

Alk3 floxed (*Alk3*$^{fx/fx}$) mice with type I BMP receptor Alk3 flanked with loxP sites (fx/fx) were provided by Dr. Yuji Mishina, University of Michigan (Mishina et al., 1995). Heterozygous *Wnt1-Cre* mice [B6.Cg-Tg (Wnt1-Cre) 11Rth Tg(Wnt1-GAL4) 11Rth/J, Jackson Laboratory, Stock# 003829], *Sox10-Cre* (B6; CBA-Tg (Sox10-cre) 1Wdr/J, Stock#025807) were bred with homozygous *Alk3*$^{fx/fx}$ breeders to generate the *Wnt1-Cre/Alk3*$^{fx/-}$ and *Sox10-Cre/Alk3*$^{fx/-}$ mice. *Wnt1-Cre/Alk3*$^{fx/-}$ and *Sox10-Cre/Alk3*$^{fx/-}$ mice were backcrossed with *Alk3*$^{fx/fx}$ breeders to generate the *Wnt1-Cre/Alk3*^{cKO} and *Sox10-Cre/Alk3*^{cKO} embryos. Wild type (WT, C57BL/6J) and nuclear tdTomato nuclear EGFP double reporter [(nTnG) (B6; 129S6-Gt-GT(ROSA)26Sortm1(CAG-tdTomato*,EGFP*)Ees/J, #023035] mice were purchased from the Jackson Laboratory (Stock No: 000664). *Cre*- littermates with two LoxP sites were used as controls (*Cre*$^{-}$*/Alk3*$^{fx/fx}$). Timed pregnant mice were euthanized with CO_2 followed by cervical dislocation. Embryos (E10.5-E12.0) were dissected from the uterus under a dissection

microscope. Noon of the day on which the dam was positive for the vaginal plug was designated as embryonic (E) E0.5. The stages of embryos were confirmed by the number of somite pairs and the development of multiple organs. The following primers were used for genotyping: 5'-GCAGCTGCTGCTGCAGCCTCC -3' and 5'- TGGCTACAATTTGTCTCATGC -3' for *Alk3 foxed* (230 bp) and WT (150 bp) fragments; 5'- GGTTTGGATCTTAACCTTAGG -3' and 5'-TGGCTACAATTTGTCTCATGC -3' for the recombined allele (180 bp) driven by *Wnt1-Cre*; 5′-ATTGCTGTCACTTGGTCGTGGC -3′ and 5'- GGAAAATGCTTCTGTCCGTTTGC -3' for the *Cre* gene product (200 bp).

3.3.2 Whole mount Immunohistochemistry

E10.5 branchial arches (BAs) or E12.0 $Cre^{-}/Alk3^{fx/fx}$ and $Wnt1\text{-}Cre/Alk3^{cKO}$ tongues or E12.0+2 day WT tongue organ cultures were processed for sonic hedgehog (Shh) immunohistochemistry as previously described in (Liu et al., 2004). Briefly, tongue organs or cultures were fixed in 4% paraformaldehyde (PFA) at 4°C for 2 hr and then washed in 0.1 M phosphate-buffered saline (PBS). Blocking of endogenous hydrogen peroxidase was performed using 6% H_2O_2 in 100% methanol followed by a heated antigen retrieval process (at 95°C for 5 min). After blocking non-specific binding in 2% non-fat milk in 0.1 M PBS containing 0.1% Triton X-100 (PBS/MT) the organs were incubated in goat anti Shh primary antibody (Table 3.1) in 10% normal donkey serum (NDS; D9663; Sigma Aldrich, St Louis, MO) in PBS/M at 4°C for 48 hr. After thorough washing in PBS/MT on ice (1 hr each x 5), the organs were incubated in biotin-conjugated secondary antibody (1:500, BA-5000, Vector laboratories, Burlingame, CA) in 1% NDS in PBS/MT at 4°C for 24 hr and subjected to peroxidase conjugated streptavidin in blocking solution (1:500, PK6200; Vector
Laboratories, Burlingame, CA) at 4°C for 24 hr after rinsing in PBS/MT on ice (1 hr each ×5). After PBS/MT (1 hr each × 5) and PBT (0.1 M PBS, 0.1% Triton X-100 and 0.2% bovine serum albumin; 1 hr each ×2) rinses on ice, tongue organs were processed for DAB reaction (SK4100:

Vector laboratories, Burlingame, CA). The stained tongues were imaged using a SZX16 Olympus Stereomicroscope.

3.3.3 Immunohistochemistry on sections

E12.0 *Cre^{-}/Alk3$^{fx/fx}$* and *Wnt1-Cre/Alk3^{cKO}* tongue tongue tissues were dissected from the mandible and fixed in 4% PFA in 0.1 M PBS at 4°C for 2 hr. PFA-fixed tongue tissues were cryoprotected in 30% sucrose in 0.1 M PBS at 4°C for at least 24 hr, embedded in O.C.T. compound (#23730571; Fisher Scientific, Waltham, MA), and rapidly frozen. Cryostat sectioning was done at 10 µm in thickness for immunohistochemistry.

Tongue sections were air-dried at room temperature for 1 hr and rehydrated in 0.1 M PBS. Blocking of nonspecific binding was carried out by incubation with 10% NDS in 0.1 M PBS containing 0.3% Triton X-100 (X100, Sigma, St. Louis, MO) at room temperature for 30 min. Then the sections were incubated with primary antibodies listed in table 3.1 in the carrier solution (1% normal donkey serum, 0.3% Triton X-100 in 0.1 M PBS) at 4°C for 24 hr. Sections treated with carrier solution without a primary antibody were used as the negative control. After rinsing in 0.1 M PBS (10 min x 3 at room temperature), sections were incubated with Alexa Fluor® 488 or 647-conjugated secondary antibody (1:500, Invitrogen, Eugene, OR) in carrier solution at room temperature for 1 hr. Sections were rinsed with 0.1 M PBS (10 min X 3 at room temperature) and counterstained with DAPI (200 ng/ml in PBS, D1306; Life Technologies, Carlsbad, CA) at room temperature for 10 min. After thorough rinsing in 0.1 M PBS, sections were air-dried and mounted with Prolong® Diamond antifade mounting medium (P36970; Fisher Scientific, Waltham, MA). Immunostained sections were examined under a fluorescent light microscope (EVOS FL, Life Technologies, Carlsbad, CA). Laser scanning confocal microscope (Zeiss LSM 710, Biomedical Microscopy Core at the University of Georgia) was used to photograph single-plane images.

3.3.4 Scanning electron microscopy (SEM)

E10.5-E12.0 *Cre^{-}/Alk3$^{fx/fx}$* littermate control and *Wnt1-Cre/Alk3^{cKO}* mutant BAs and/or tongues were fixed in 2.5% glutaraldehyde (#75520; Electron Microscopy Science, Hatfield, PA) and 4% PFA in 0.1 M PBS (pH 7.3) at 4°C for 24 hr. After rinsing in 0.1 M PBS at room temperature (10 min each x 3) and post-fixed in a sequence of aqueous 1% O_SO_4 (#19150, Electron Microscopy Science, Hatfield, PA) in 0.1 M PBS, 1% tannic acid (#16201, Sigma Aldrich, St. Louis, MO) in MQ-H_2O, 1% O_SO_4 in MQ-H_2O, on ice for 1 hr each, tissues were dehydrated in an ascending series of ethanol (35, 50, 70, 90, 100%), and hexamethyldisilazane (HMDS, #440191; Sigma Aldrich, St. Louis, MO) at room temperature (1 hr each x 3). After a slow air dry in a fume hood, tongue tissues were mounted on specimen stubs and sputter-coated with gold/palladium (Leica Gold/Carbon coater; Georgia Electron Microscope Core Facility, University of Georgia). Tissues were then imaged using a scanning electron microscope (FEI Teneo FE-SEM; Georgia Electron Microscope Core Facility, University of Georgia).

3.3.5 Mesenchymal cell cultures

E11.5 *Cre^{-}/Alk3$^{fx/fx}$* littermate control and *Wnt1-Cre/Alk3^{cKO}* mutant tongue mesenchyme were separated from the epithelium as described (Liu et al., 2008). Briefly, dissected *Cre^{-}/Alk3$^{fx/fx}$* littermate control and *Wnt1-Cre/Alk3^{cKO}* mutant tongue swellings were incubated in a mixture of 1 mg/ml Collagenase A (#10103578001; Roche Diagnostics, Basal, Switzerland) and 2.5 mg/ml Dispase II (# 10374300; Roche Diagnostics, Basal, Switzerland) enzymes at 37°C for 30 min. After thorough rinse in 0.1 M PBS, epithelia were removed from the mesenchyme. Separated mesenchyme were then transferred to a culture dish and broken down in to small pieces. Cultures were fed with a 1:1 mixture of Dulbecco's modified Eagle's medium and Ham's nutrient F12 (#11320033, DMEM/F12, GIBCO, Gaithersburg, MD), containing 1% fetal bovine serum (SH30396.03, Cytiva, Marlborough, MA), 2% B27 culture supplement (#17504044, GIBCO, Gaithersburg, MD) and 50 µg/ml gentamicin sulfate(#15750060, GIBCO, Gaithersburg,

MD) and kept in a humidified incubator at 37°C. Every 3 days, old media (conditioned media) were removed from the culture dishes and cells were fed with fresh media. Harvested conditioned media were stored in -80 until ready to use.

3.3.6 Extracellular vesicles (EVs) and protein isolation from the conditioned media

E11.5+3, +6 and +9 conditioned media isolated from *Cre^{-}/Alk3$^{fx/fx}$* littermate control and *Wnt1-Cre/Alk3^{cKO}* mutant mesenchymal cell cultures were pooled together to extract extracellular vesicles (EVs) as described (Whittaker et al., 2020). Briefly, mesenchyme-derived conditioned media were transferred to Amicon® filters (UFC910024, Millipore Sigma, Burlington, MA). EVs were isolated by centrifugation at 4000g for 10 min and washed with ice cold PBS++ (SH30264.02, Cytiva, Marlborough, MA) before centrifuged again at 4000g for 10 min. Isolated EVs were resuspended in DMEM/F12 to get EV-enriched media. Filtered media through the Amicon® filters before the PBS++ wash, was collected to isolate proteins. Proteins from the filtered media were extracted using the protein precipitation kit (#2100, Millipore Sigma, Burlington, MA) following the manufacturer's specifications. Proteins were mixed with DMEM/F12 to get protein-enriched media. Media without EVs and proteins were considered as EVs and protein depleted media.

3.3.7 Tongue organ cultures

E12.0+2 day tongue organ cultures were performed as described (Mbiene et al., 1997; Mistretta et al., 2003). Briefly, E12.0 whole tongues were dissected from the mandible of WT embryos and placed on sterile Millipore HA filters on stainless steel grids in culture dishes. Cultures were fed with standard culture medium [DMEM/F12, containing 1% fetal bovine serum, 2% B27 culture supplement and 50 µg/ml gentamicin sulfate] and kept in a humidified incubator at 37°C.

For experiments with co-cultures, mesenchyme of the E12.0 *Cre^{-}/Alk3$^{fx/fx}$* littermate control and *Wnt1-Cre/Alk3^{cKO}* mutant tongues were placed closer to E12.0 WT tongues and continued to grow for 2 days in standard culture media.

For experiments with mesenchyme-derived conditioned media, E12.0 WT tongues were cultured for 2 days with the media isolated from E12.0+1 day *Cre^{-}/Alk3$^{fx/fx}$* littermate control or *Wnt1-Cre/Alk3^{cKO}* mutant tongue mesenchyme cultures. For experiments with exogenous agents, EV-enriched or protein-enriched or EV-protein-depleted media isolated from the E11.5 *Cre^{-}/Alk3$^{fx/fx}$* littermate control and *Wnt1-Cre/Alk3^{cKO}* mutant mesenchymal cells derived conditioned media were added to the standard culture medium and continued to grow for 2 days. WT tongues cultured with EVs, proteins or EV-protein depleted media isolated from the standard culture media were used as controls. After 2 days, cultures were collected and processed for whole mount Sonic hedgehog (Shh) immunoreactions.

3.3.8 Liquid chromatography-mass spectrometry (LC–MS)

Proteins isolated from the E11.5+3, +6 and +9 *Cre^{-}/Alk3$^{fx/fx}$* littermate control and *Wnt1-Cre/Alk3^{cKO}* mutant mesenchymal cells derived conditioned media were resolved in a 9% sodium dodecyl sulphate (SDS)-polyacrylamide gel. When the gel front reached 1 Cm into SDS-polyacrylamide gel, electroporation was stopped and the SDS gel piece between the well and the gel front was cut and submitted to the Proteomics and Mass Spectrometry Facility, University of Georgia to perform LC-MS analyses using Thermo-Fisher LTQ Orbitrap Elite Mass Spectrometer coupled with a Proxeon Easy NanoLC system (Waltham, MA). The MS data were acquired using Xcalibur software (version 2.2, Thermo Fisher Scientific, Waltham, MA). Thermo Proteome Discoverer (version 1.4) with Mascot (Matrix Science) and Uniprot databases were used to for the proteins identification, modification and characterization. Protein score was used to match the combined scores detected from all observed MS to the amino acid sequence within a protein with a mass precision value of 2 ppm.

3.3.9 *In situ* hybridization

Tongue tissue of *Cre^{-}/Alk3$^{fx/fx}$* littermate control and *Wnt1-Cre/Alk3^{cKO}* mutant were dissected in 0.1 M PBS, fixed with 4% PFA at 4°C for 24 hr. PFA-fixed tissues were washed with 0.1 M PBS (10 min each x 3) and dehydrated through ascending series of methanol (35, 50, 70, 90,

100%) and stored in 100% methanol at -20°C until ready to use. Whole-mount *in situ* hybridization for *Alk3* was performed as previously described (Lauter et al., 2011) using digoxigenin-labeled riboprobes. Plasmids carrying *Alk3* was provided by Dr. Yuji Mishina (University of Michigan). Digoxigenin-labeled antisense *Alk3* RNA probe was prepared by linearizing with EcoR1 (New England Biolabs, Ipswich, MA), followed by transcription with T7 RNA polymerase (Promega, Madison, WI).

3.3.10 RNA extraction and quantitative reverse transcriptase polymerase chain reaction (qRT-PCR)

Separated mesenchymal and epithelial tissues from the E12.0 *Cre^{-}/Alk3$^{fx/fx}$* littermate control and *Wnt1-Cre/Alk3^{cKO}* mutant tongues were immersed in Trizol solution (#15596018, Life technologies, Carlsbad, CA) for RNA extraction. RNA extraction was performed using RNeasy Plus kit (#74136; Qiagen, Hilden, Germany) following the manufacturer's specifications. A total of nine mesenchymal tissues and/or epithelial tissues (pooled three tissues x three replicates) were used for RNA extraction. RNA concentrations were measured using Nanodrop 8000 spectrophotometer (Nanodrop, Thermo Scientific, Waltham, MA). Complementary DNA (cDNA) synthesized from the extracted RNA using SuperScript™ First-Strand Synthesis System (#11902018; Fisher scientific, Waltham, MA). Synthesized cDNA were used to analyze the expression of selected genes listed in Table 3.2.

3.3.11 Data analyses

Quantitative analyses were made to obtain the number of p-Smad 1/5/8+ cells per unit area (mm^2) on E12.0 *Cre^{-}/Alk3$^{fx/fx}$* littermate control and *Wnt1-Cre/Alk3^{cKO}* mutant tongues. Serial tongue sections of *Cre^{-}/Alk3$^{fx/fx}$* littermate controls (n=3) and *Wnt1-Cre/Alk3^{cKO}* mutants (n=3) immunostained with p-Smad 1/5/8 were thoroughly analyzed under a fluorescent light microscope (EVOS FL, Life Technologies). Single-plane laser scanning confocal photomicrographs were taken from every other section for quantification using a scanning confocal microscope (Zeiss LSM 710, Biomedical Microscopy Core at the University of

Georgia). p-Smad 1/5/8^{+} cells were quantified in a selected area of E12.0 tongues. For qRT-PCR, changes of gene expression levels in *Cre^{-}/Alk3$^{fx/fx}$* littermate control and *Wnt1-Cre/Alk3^{cKO}* mutant epithelium and mesenchyme were presented as means ± standard deviation (X ± SD; n = 3) of $2^{-\Delta CT}$ values. Two-way analyses of variance (ANOVA) followed by Fisher's LSD analyses were used to compare p-Smad 1/5/8^{+} cells per unit area (mm^2) in tongues between *Cre^{-}/Alk3$^{fx/fx}$* littermate control and *Wnt1-Cre/Alk3^{cKO}* mutants. A *p*-value less than 0.05 was taken as statistically significant.

3.4 Results

3.4.1 Bone morphogenetic protein (BMP) signaling components expressed in the developing tongue

To understand the expression of BMP signaling components in developing tongues, RNA sequencing analysis was performed in E12.5 wild type (WT) tongue epithelium and mesenchyme. We found the majority of the BMP signaling components including ligands (*BMP2*, *BMP4* and *BMP7*), type I receptors (*Alk2*, *Alk3*, *Alk6*), type II receptors (B*mpr2*, *Acvr2a*, *Acvr2b*), transcription factors (*Smad1*, *Smad4*, *Smad5* and, *Smad8*) and antagonists (*Nog*/Noggin, *Fst*/follistatin) were expressed in both the tongue epithelium and mesenchyme (Fig. 3.1A). However, among the signaling components analyzed, *Alk6* and *Fst* expression were significantly high in the E12.5 WT the tongue mesenchyme compared to the epithelium ($p<0.05$ in Fig. 3.1A). In contrast, *BMP7*, *Bmpr2* and *Acvr2b* expressions were significantly reduced in the tongue mesenchyme compared to the E12.5 tongue epithelium ($p<0.05$ in Fig. 3.1A).

Type I BMP receptors are the main determinant of the BMP signaling pathway (Bragdon et al., 2011; Wang et al., 2014). To understand the role of type I BMP receptor ALK3-mediated BMP (hereafter ALK3-BMP) signaling in the tongue mesenchyme for tongue and taste papilla development, the *Alk3* receptor was knocked out using *Wnt1-Cre*, which labels the neural crest (NC)-derived mesenchymal cells in the developing tongue (Liu et al., 2012a; Thirumangalathu et al., 2009). To analyze the distribution of *Alk3* mRNA transcripts in the early stages of tongue

development, *Alk3* in-situ hybridization was performed on E12.0 *Cre^{-}/Alk3$^{fx/fx}$* littermate controls and *Wnt1-Cre/Alk3^{cKO}* mutant mice. Similar to the RNA-Seq data, *Alk3* mRNA transcripts were detected in epithelium (Epi in Fig. 3.1B), mesenchymal region subjacent to the epithelium (Mes1 in Fig. 3.1B) and deeper layers of the mesenchyme (Mes2 in Fig. 3.1B) of the E12.0 *Cre^{-}/Alk3$^{fx/fx}$* littermate control tongue. However, in *Wnt1-Cre/Alk3^{cKO}* mutants, Alk3 transcripts were only detected in the epithelial layer (Epi in Fig. 3.1B) and the deeper layers of the mesenchyme (Mes2 in Fig. 3.1B). No Alk3 mRNA transcripts were detected in the mesenchymal layer subjacent to the epithelium of *Wnt1-Cre/Alk3^{cKO}* mutant tongues (Mes1 in Fig. 3.1B).

Next, we validated the *Alk3* expression in the E12.0 *Cre^{-}/Alk3$^{fx/fx}$* littermate control and *Wnt1-Cre/Alk3^{cKO}* mutant tongue using quantitative reverse transcriptase PCR (qRT-PCR) analyses and found that *Alk3* expression was significantly reduced in the *Wnt1-Cre/Alk3^{cKO}* mutant tongue mesenchyme (p<0.01 in Fig. 3.1C) compared to *Cre^{-}/Alk3$^{fx/fx}$* littermate control tongue mesenchyme. However, no significant changes in *Alk3* expression were detected in the *Wnt1-Cre/Alk3^{cKO}* mutant tongue epithelium compared to the *Cre^{-}/Alk3$^{fx/fx}$* littermate control tongue epithelium (p>0.05 in Fig. 3.1C).

The absence of ALK3-BMP signaling activity in the mesenchyme was validated by detecting the phosphorylation (p) of Smad 1/5/8, a known mediator of the downstream BMP signaling activity. As expected, a significantly low number of p-Smad 1/5/8^{+} mesenchymal cells were detected in the E12.0 *Wnt1-Cre/Alk3^{cKO}* mutant tongue (Fig. 3.1E, p<0.01 in Fig. 3.1F) compared to that of *Cre^{-}/Alk3$^{fx/fx}$* littermate controls (Fig. 3.1D, F). Interestingly, a significantly low number of p-Smad 1/5/8^{+} cells were observed in the E12.0 *Wnt1-Cre/Alk3^{cKO}* mutant tongue epithelium (Fig. 3.1E, p<0.05 in Fig. 3.1F) as compared to the *Cre^{-}/Alk3$^{fx/fx}$* littermate control tongue epithelium (Fig. 3.1D, F).

3.4.2 Mesenchyme specific *Wnt1-Cre* mediated *Alk3 cKO* in neural crest and neural crest-derived tongue mesenchyme leads to altered tongue development and the absolute loss of taste papilla.

To understand the effect of ALK3-BMP signaling in the mesenchyme for the tongue and taste papilla development, *Wnt1-Cre/Alk3*^{cKO} mutant and *Cre*$^{-}$*/Alk3*$^{fx/fx}$ littermate control branchial arches (BAs, tongue primordium) and tongues were analyzed from E10.5-E12.0, the time frame where the tongue and taste papilla placodes start to develop. Similar to the *Cre*$^{-}$*/Alk3*$^{fx/fx}$ littermate controls (Fig. 3.2A, C), no obvious changes in the BAs were noticed in the E10.5 *Wnt1-Cre/Alk3*^{cKO} mutants (Fig. 3.2B, D). All four BAs were detected in the *Wnt1-Cre/Alk3*^{cKO} mutants (roman numerals in Fig. 2B) similar to the *Cre*$^{-}$*/Alk3*$^{fx/fx}$ littermate controls (roman numerals in Fig. 3.2A). Next, the developing taste papilla marker, sonic hedgehog (Shh), was analyzed in the *Cre*$^{-}$*/Alk3*$^{fx/fx}$ littermate control and *Wnt1-Cre/Alk3*^{cKO} mutant BAs. Diffused Shh immunosignals were detected in both *Cre*$^{-}$*/Alk3*$^{fx/fx}$ littermate control (Fig. 3.2C) and *Wnt1-Cre/Alk3*^{cKO} mutant (Fig. 3.2D) BAs. At E11.5, when initial tongue swellings emerge from the BAs, stereotypical lateral swellings were observed in the *Cre*$^{-}$*/Alk3*$^{fx/fx}$ littermate controls (solid arrowheads in Fig. 3.2E, G). In contrast, a more advanced tongue with pointed tongue tip was observed in the E11.5 *Wnt1-Cre/Alk3*^{cKO} mutants (solid arrowhead in Fig. 3.2F). Compared to the diffused Shh immunosignals (solid arrowheads in Fig. 3.2G) in the lateral tongue swellings of *Cre*$^{-}$*/Alk3*$^{fx/fx}$ littermate control anterior tongue, Shh immunosignals in the *Wnt1-Cre/Alk3*^{cKO} mutant tongue were restricted to the tip region (solid arrowheads in Fig. 3.2H).

At E12.0, when *Cre*$^{-}$*/Alk3*$^{fx/fx}$ littermate control tongue attains its spatulated shape (Fig. 3.3A) and Shh^{+} taste papilla placodes emerge (Fig. 3.3C), *Wnt1-Cre/Alk3*^{cKO} mutants had an underdeveloped tongue (Fig. 3.3B) resembling the E11.5 *Wnt1-Cre/Alk3*^{cKO} tongue (Fig. 3.2F). Compared to the well-developed and stereotypically located fungiform (arrowheads in Fig. 3C, the arrowhead in Fig. 3.3E) and circumvallate (CV, the arrow in Fig. 3.3C) papilla placodes in *Cre*$^{-}$*/Alk3*$^{fx/fx}$ littermate control tongue, the *Wnt1-Cre/Alk3*^{cKO} mutants exhibited an absolute loss

of Shh^{+} fungiform (Fig. 3.3D, F) and CV (Fig. 3.3D) taste papilla placodes. To confirm the absence of taste papilla placodes in *Wnt1-Cre/Alk3^{cKO}* mutants, we used another taste papilla placode marker Prox1. We observed that Prox1^{+} taste papilla placodes were also absent in the *Wnt1-Cre/Alk3^{cKO}* mutants (Fig. 3.3H) compared to the *Cre^{-}/Alk3$^{fx/fx}$* littermate controls (Fig. 3.3G).

Deletion of *Alk3* gene in the NC lineage using *Wnt1-Cre* mouse model results in cardiac defects and embryonic lethality at E12.5 (Stottmann et al., 2004). To determine if the cells in the *Wnt1-Cre/Alk3^{cKO}* mutant tongues were proliferating and not affected due to the early embryonic lethality at E12.5, a number of Ki67+ proliferating and cleaved (c)-Caspase 3+ (c-Cas 3) apoptotic cells were analyzed. No apparent changes in Ki67^{+} and/ or c-Cas+ cells were detected between E12.0 *Cre^{-}/Alk3$^{fx/fx}$* littermate control (Fig. 3.3I, K) and *Wnt1-Cre/Alk3^{cKO}* mutant tongue (Fig. 3.3J, L) epithelium and mesenchyme. However, qRT-PCR analyses on the cell proliferation specific gene, *Cyclin-D1* (CycD1 in Fig. 3M), revealed that, E12.0 *Wnt1-Cre/Alk3^{cKO}* mutant tongue epitheliums had significantly high *Cyclin-D1* expression (p<0.05 in Fig. 3.3M) compared to the *Cre^{-}/Alk3$^{fx/fx}$* littermate control tongue epithelium (Fig. 3.3M). No significant differences in *Cyclin-D1* expression were detected between *Cre^{-}/Alk3$^{fx/fx}$* littermate control and *Wnt1-Cre/Alk3^{cKO}* mutant tongue mesenchyme (p>0.05 in Fig. 3.3M). A significantly high amount of the apoptosis specific gene, *p53,* was detected in the E12.0 *Wnt1-Cre/Alk3^{cKO}* mutant tongue mesenchyme (p<0.05 in Fig. 3.3M) compared to the *Cre^{-}/Alk3$^{fx/fx}$* littermate control tongue mesenchyme (Fig. 3.3M). Expression levels of *p53* were not affected in the E12.0 *Wnt1-Cre/Alk3^{cKO}* mutant tongue epithelium compared to those of *Cre^{-}/Alk3$^{fx/fx}$* littermate controls (p>0.05 in Fig. 3.3M).

3.4.3 Tongue mesenchyme specific *Sox10* derived conditional knockout of *Alk3* resulted in a similar phenotype as *Wnt1-Cre/Alk3^{cKO}* mutants

It has been reported that *Wnt1-Cre* can cause non-specific labeling (Chen et al., 2017) and raises concerns over the specificity of the phenotype resulting from the *Wnt1-Cre/Alk3^{cKO}*

mutants. To confirm the specificity of the phenotype, we used *Sox10-Cre* mouse model. *Sox10* is specifically expressed in the NC cells (Southard-Smith et al., 1998) and provide an ideal model system to validate the phenotype caused by the NC-derived tongue mesenchyme specific genetic deletion of *Alk3*.

First, a double Cre reporter, nTnG, was utilized to cross with *Sox10-Cre* to examine the specificity and efficiency of the *Sox10-Cre* model. We were only able to detect *Sox10-Cre* driven nuclear GFP signals (nGFP in Fig. 3.4A) in the tongue mesenchyme - no nGFP+ cells were detected in the tongue epithelium (Fig. 3.4A). Then, we used *Sox10-Cre* to conditionally knockout *Alk3* in tongue mesenchyme. Consistent with the E12.0 *Wnt1-Cre/Alk3*^{cKO} mutant phenotype, E12.0 *Sox10-Cre/Alk3*^{cKO} mutants also had an underdeveloped tongue (Fig. 3.4C, E) with the complete absence of fungiform and CV papilla placodes (Fig. 3.4E). On the other hand, E12.0 *Cre*$^{-}$*/Alk3*$^{fx/fx}$ littermate control mice had a stereotypical tongue (Fig. 3.4B, D) with well-developed fungiform (arrowheads in Fig. 3.4D) and CV papilla placodes (the arrow in Fig. 3.4D). We further analyzed Ki67^{+} cell proliferation and c-Cas 3^{+} apoptosis to understand their relevance to the stunted tongue growth and absence of taste papilla placodes in E12.0 *Sox10-Cre/Alk3*^{cKO} mutants (Fig. 3.4G, I). These analyses revealed no apparent changes in Ki67^{+} and c-Cas 3^{+} cells in the *Sox10-Cre/Alk3*^{cKO} mutants (Fig. 3.4G, I) with respect to the *Cre*$^{-}$*/Alk3*$^{fx/fx}$ littermate control mice (Fig. 3.4F, H).

3.4.4 RNA-seq analyses reveled that many more Differentially expressed genes (DEGs) in the *Wnt1-Cre/Alk3*^{cKO} mutant tongue epithelium

Mesenchymal-epithelial interactions are essential for the development of epithelial appendages, including taste papilla (Beites et al., 2009; Petersen et al., 2011; Prochazkova et al., 2017). To identify the changes in the genetic profile that lead to the absence of taste papilla in the epithelium as a result of *Alk3 cKO* in the mesenchyme, RNA-Sequencing analysis was performed on E12.0 *Wnt1-Cre/Alk3*^{cKO} mutants and *Cre*$^{-}$*/Alk3*$^{fx/fx}$ littermate controls. A total of 350 differentially expressed genes (DEGs) were detected by Cuffdiff in the *Wnt1-Cre/Alk3*^{cKO}

mutants vs *Cre⁻/Alk3$^{fx/fx}$* littermate control (|FC|>1, p<0.05, FDR q<0.05), which are displayed in the Venn diagram (Fig. 3.5A). Among the 350 DEGs, 287 genes were detected in the *Wnt1-Cre/Alk3^{cKO}* mutant epithelium, 57 genes were detected in the *Wnt1-Cre/Alk3^{cKO}* mutant mesenchyme, and six genes were detected in both *Wnt1-Cre/Alk3^{cKO}* mutant epithelium and mesenchyme (Fig. 3.5A). Among the DEGs detected in the *Wnt1-Cre/Alk3^{cKO}* mutant epithelium, 183 genes were significantly upregulated, and 104 genes were significantly downregulated in *Wnt1-Cre/Alk3^{cKO}* mutants (Fig. 3.5A). Moreover, in the *Wnt1-Cre/Alk3^{cKO}* mutant mesenchyme, 29 genes were significantly upregulated, and 28 genes were significantly downregulated compared to the *Cre⁻/Alk3$^{fx/fx}$* littermate control mesenchyme (Fig. 3.5A). Five genes were significantly upregulated in both epithelium and mesenchyme of the *Wnt1-Cre/Alk3^{cKO}* mutants compared to the *Cre⁻/Alk3$^{fx/fx}$* littermate controls. Interestingly, one gene was significantly upregulated in the mesenchyme but downregulated in the epithelium of *Wnt1-Cre/Alk3^{cKO}* mutants compared to the *Cre⁻/Alk3$^{fx/fx}$* littermate controls.

DEGs in E12.0 tongue tissues in *Wnt1-Cre/Alk3^{cKO}* mutant and *Cre⁻/Alk3$^{fx/fx}$* littermate control groups were enriched in multiple gene ontology (GO) terms and Kyoto Encyclopedia of Genes and Genomes (KEGG) pathways, including multiple tissues and biological processes. Based on DEG function, some genes were selected and are shown in Fig. 3.5B volcano plots. In the *Wnt1-Cre/Alk3^{cKO}* mutant tongue epithelium, we found DEGs related to multiple molecular signaling pathways, e.g. Wnt (*Lrp4*, *Fzd10*, *Lgr5*, *Dkk3*, *Prox1*, *Wnt2*, *Wnt11*), Shh (*Hhip*) and FGF (*Dusp6*, *Etv5*). In contrast to the epithelium, a majority of the DEGs identified in the *Wnt1-Cre/Alk3^{cKO}* mutant tongue mesenchyme were related to structural proteins (*Col22a1*, *Col9a3*, *Myh7*, *Myo6*), exocytosis (*Myo5b*, *Trim72*, *Cplx2*), intracellular trafficking (*Actn2*, *Hrc*, *Myo6*) and secretory proteins (*Nbl1*, *Pkm2*, *Cryab*) (Fig. 3.5B, C, D). Interestingly, a majority of the DEGs related to structural proteins, intracellular trafficking, exocytosis were down-regulated in the *Wnt1-Cre/Alk3^{cKO}* mutant mesenchyme compared to the *Cre⁻/Alk3$^{fx/fx}$* littermate control group (Fig. 3.5C, D).

Mesenchymal factors (proteins, extracellular vesicles etc.) play a crucial role in communicating with the overlying epithelial cells during cell, tissue and organ development. We analyzed the *Wnt1-Cre/Alk3*^{cKO} mutant mesenchyme DEG list to identify any mesenchymal factors. Remarkably, in the *Wnt1-Cre/Alk3*^{cKO} mutant mesenchyme, DEGs related to inhibitory secretory proteins (*Nbl1*, *Pkm2*) were up-regulated compared to the *Cre*$^{-}$*/Alk3*$^{fx/fx}$ littermate control group (Fig. 3.5B). In contrast, stimulatory proteins (*Cryab*) were down regulated in the *Wnt1-Cre/Alk3*^{cKO} mutant tongue mesenchyme as compared to the *Cre*$^{-}$*/Alk3*$^{fx/fx}$ littermate control tongue mesenchyme (Fig. 3.5B, D).

Since the genes related to the intracellular trafficking and exocytosis had been downregulated in the *Wnt1-Cre/Alk3*^{cKO} mutant tongue mesenchyme, we next examined the number of extracellular vesicles (EVs) extracted from the E11.5 *Cre*$^{-}$*/Alk3*$^{fx/fx}$ littermate control and *Wnt1-Cre/Alk3*^{cKO} mutant tongue mesenchyme-derived conditioned media (Fig. 3.5D). Compared to the EVs isolated from the *Cre*$^{-}$*/Alk3*$^{fx/fx}$ littermate control mesenchyme-derived conditioned media, *Wnt1-Cre/Alk3*^{cKO} mutant mesenchyme-derived conditioned media had a relatively low amount of EVs (Fig. 3.5D).

3.4.5 ALK3-BMP signaling in the mesenchyme interacts with the epithelium through secretory factors

To learn what factors mediate ALK3-BMP-mesenchymal-epithelial interactions, co-cultures of E12+2 day WT tongues with *Wnt1-Cre/Alk3*^{cKO} or *Cre*$^{-}$*/Alk3*$^{fx/fx}$ littermate control tongue mesenchyme by the side (Fig. 3.6A) were performed. We found that taste papillae were fewer and less profound in the WT tongues co-cultured with *Wnt1-Cre/Alk3*^{cKO} tongue mesenchyme than the WT tongues co-cultured with *Cre*$^{-}$*/Alk3*$^{fx/fx}$ littermate tongue mesenchyme (Fig. 3.6A). In the WT tongues, co-cultured with *Cre*$^{-}$*/Alk3*$^{fx/fx}$ littermate tongue mesenchyme, both fungiform (arrowheads in Fig. 3.6A) and CV (the arrow in Fig. 3.6A) papillae were detected compared to the WT tongues co-cultured with *Wnt1-Cre/Alk3*^{cKO} tongue mesenchyme. This suggests that it is likely through secreted factors, not direct contact, *Alk3 cKO* tongue mesenchyme alters

epithelial cell differentiation. To confirm this idea, we collected tongue mesenchyme-derived conditioned medium from *Wnt1-Cre/Alk3^{cKO}* mutant and *Cre^{-}/Alk3$^{fx/fx}$* littermate controls. As expected, taste papilla formation was suppressed in WT tongue cultures fed with *Wnt1-Cre/Alk3^{cKO}* tongue mesenchyme-derived conditioned media (Fig. 3.6B) in contrast to the WT tongue cultures fed with *Cre^{-}/Alk3$^{fx/fx}$* littermate control tongue mesenchyme-derived conditioned media (Fig. 3.6B). Well-formed fungiform (arrowheads in Fig. 3.6B left panel) and CV papilla (the arrow in Fig. 3.6B left panel) were detected in the WT tongues cultured with *Cre^{-}/Alk3$^{fx/fx}$* littermate control tongue mesenchyme-derived conditioned media. Whereas, in the WT tongues cultured with *Wnt1-Cre/Alk3^{cKO}* tongue mesenchyme-derived conditioned media, only CV papilla was detected (the arrow in Fig. 3.6B right panel).

3.4.6 Secretory proteins from the *Wnt1-Cre/Alk3^{cKO}* mesenchyme act as inhibitors for the development of taste papillae

Next, we attempted to determine what constitutes the *Wnt1-Cre/Alk3^{cKO}* secretory factors that inhibit epithelial cell differentiation to form taste papillae. No changes in fungiform and/or CV taste papilla development were noticed in E12+2 day WT tongue cultured with EVs isolated from the culture media (Fig. 3.7A), *Cre^{-}/Alk3$^{fx/fx}$* littermate controls (Fig. 3.7B) or *Wnt1-Cre/Alk3^{cKO}* mutant (Fig. 3.7C) mesenchyme-derived conditioned media. However, the development of taste papillae (both fungiform and CV) was inhibited in the WT tongues cultured with proteins isolated from the *Wnt1-Cre/Alk3^{cKO}* mutant tongue mesenchyme-derived conditioned media (Fig. 3.7F). In contrast to the *Wnt1-Cre/Alk3^{cKO}* mutants, well-developed taste papillae were seen in WT tongues cultured with proteins isolated from the culture media (Fig. 3.7D) and or *Cre^{-}/Alk3$^{fx/fx}$* littermate controls (Fig. 3.7E) mesenchyme-derived conditioned media. Similarly to the EV-enriched tongue cultures, taste papilla (fungiform and CV) development, was not affected in the WT tongues cultured with EV and protein deleted media isolated from the media (Fig. 3.7G) or *Cre^{-}/Alk3$^{fx/fx}$* littermate controls (Fig. 3.7H) or *Wnt1-Cre/Alk3^{cKO}* mutant (Fig. 3.7I) mesenchyme-derived conditioned media.

To identify the inhibitory secretory proteins that suppress the taste papilla development in the *Wnt1-Cre/Alk3*^{cKO} mutants, proteomics analyses were performed using the E11.5 mesenchyme-derived conditioned media isolated from the *Cre*$^{-}$*/Alk3*$^{fx/fx}$ littermate control and *Wnt1-Cre/Alk3*^{cKO} mesenchymal cell cultures. First, sodium dodecyl sulphate–polyacrylamide gel electrophoresis (SDS-PAGE) was performed on mesenchyme-derived conditioned media isolated from the *Cre*$^{-}$*/Alk3*$^{fx/fx}$ littermate controls and *Wnt1-Cre/Alk3*^{cKO} mutants to recognize the abundance of secretory proteins. We found many more proteins bands from both *Cre*$^{-}$*/Alk3*$^{fx/fx}$ littermate control and *Wnt1-Cre/Alk3*^{cKO} mutant conditioned media representing multiple secretory protein candidates (Fig. 3.8A). Interestingly, in the *Wnt1-Cre/Alk3*^{cKO} mutant mesenchyme-derived conditioned media, we found several protein bands that were either only present (A_1 bracket in Fig. 3.8A) or highly expressed (A_2 bracket in Fig. 3.8A) compared to the protein bands detected in the *Cre/Alk3*^{cKO} mutant mesenchyme-derived conditioned media (Fig. 3.8A).

Next, we performed liquid chromatography-mass spectrometry (LC-MS) to identify the secretory proteins in mesenchyme-derived conditioned media isolated from the *Cre*$^{-}$*/Alk3*$^{fx/fx}$ littermate controls and *Wnt1-Cre/Alk3*^{cKO} mutant mesenchymal cell cultures. LC-MS analyses identified 41 proteins from the *Wnt1-Cre/Alk3*^{cKO} mesenchyme-derived conditioned media and 13 proteins from the *Cre*$^{-}$*/Alk3*$^{fx/fx}$ littermate control mesenchyme-derived conditioned media (Fig. 3.8B, table 3.3). All 13 proteins identified from the *Cre*$^{-}$*/Alk3*$^{fx/fx}$ littermate control mesenchyme-derived conditioned media were also detected in the *Wnt1-Cre/Alk3*^{cKO} mesenchyme-derived conditioned media (Fig. 3.8B, table 3.3). Strikingly, we found additional 28 proteins, including a known inhibitory secretory protein Pkm2, which were only detected in the *Wnt1-Cre/Alk3*^{cKO} mesenchyme-derived conditioned media (Fig. 3.8B, table 3.3).

Proteins identified in E11.5 *Cre*$^{-}$*/Alk3*$^{fx/fx}$ littermate control and *Wnt1-Cre/Alk3*^{cKO} mutant mesenchyme-derived conditioned media were enriched in multiple GO terms related to many biological processes (Fig. 3.8C). E.g. Integrin-β catenin signaling pathway (Pkm2, Alpha-Actin2,

Fibronectin), regulators of epithelial cell proliferation and autophagy (14-3-3 protein zeta/delta, 14-3-3 protein epsilon), regulators of protein stability (Nucleophosmin 1, Eaf2), structural proteins (Alpha-Actin2, Keratin 17, Keratin 76) etc.

RNA-Seq and LC-MS analyses on *Wnt1-Cre/Alk3*^{cKO} mutants and *Cre*$^{-}$*/Alk3*$^{fx/fx}$ littermate controls revealed Nbl1 and Pkm2 as potential candidate proteins that can act as inhibitory factors for the development of taste papillae. Moreover, RNA-Seq analysis also detected significantly high amount of *Nbl1* and *Pkm2 mRNA* transcripts in the E12.0 *Wnt1-Cre/Alk3*^{cKO} mutant tongue mesenchyme compared to the *Cre*$^{-}$*/Alk3*$^{fx/fx}$ tongue mesenchyme (p<0.05 in Fig. 3.9A). No changes in *Nbl1* expression levels were detected in the E12.0 *Wnt1-Cre/Alk3*^{cKO} mutant tongue epithelium compared to the *Cre*$^{-}$*/Alk3*$^{fx/fx}$ tongue mesenchyme (p>0.05 in Fig. 3.9A). In contrast to the *Nbl1* and *Cre*$^{-}$*/Alk3*$^{fx/fx}$ tongue epithelium, E12.0 *Wnt1-Cre/Alk3*^{cKO} mutant tongue epithelium had significantly high *Pkm2* expression (p<0.05 in Fig. 3.9A). qRT-PCR analyses using *Nbl1*, *Pkm2* primers further validated the significantly high expression of *Nbl1*, *Pkm2* in the E12.0 *Wnt1-Cre/Alk3*^{cKO} mutant tongue mesenchyme. Contrary to the RNA-Seq result, qRT-PCR analysis demonstrated that no significant differences in *Pkm2* expression levels between the *Cre*$^{-}$*/Alk3*$^{fx/fx}$ and *Wnt1-Cre/Alk3*^{cKO} mutant tongue epithelium. Finally, western blot analyses demonstrated that, increased level of Nbl1 in the *Wnt1-Cre/Alk3*^{cKO} mutant mesenchyme-derived conditioned media (Fig. 3.9B) compared to the *Cre*$^{-}$*/Alk3*$^{fx/fx}$ littermate controls mesenchyme-derived conditioned media (Fig. 3.9B).

3.5 Discussion

In the present study to discern roles for type I receptor ALK3-mediated BMP signaling in the tongue mesenchyme for tongue and taste papilla development, we show that *Alk3 cKO* in neural crest (NC) lineage resulted in the absolute loss of taste papilla and defects in tongue organogenesis. The presence of many more DEGs in the *Wnt1-Cre/Alk3*^{cKO} mutant epithelium because of *Alk3 cKO* in the mesenchyme indicates that ALK3-BMP signaling in the mesenchyme regulates mesenchymal-epithelial interactions. The absence of taste papillae

when co-cultured with *Wnt1-Cre/Alk3*^{cKO} mutant mesenchyme or proteins isolated from the *Wnt1-Cre/Alk3*^{cKO} mutant mesenchyme-derived conditioned media, along with liquid chromatography-mass spectrometry, (LC-MS) analyses suggest that mesenchymal ALK3-BMP signaling control the secretion of inhibitory proteins. Overall, our results indicate that ALK3-BMP signaling activity in NC-derived mesenchyme plays essential roles in regulating inhibitory proteins and promote the development of taste papillae.

3.5.1 ALK3-BMP signaling in the tongue mesenchyme is essential for the development of taste papillae

Taste papillae are distinct and protrude from the tongue dorsum by E13.5 (Kaufman, 1992); they remain in stereotypic locations thereafter (Farbman and Mbiene, 1991; Paulson et al., 1985) . The formation of taste papillae require mesenchymal-epithelial interactions controlled by a complex network of molecular signaling (Krimm, 2007; Krimm et al., 2015). This includes multiple morphogens/growth factors such as Shh, Wnt/β-catenin, BMP, FGF, etc (Beites et al., 2009; Castillo-Azofeifa et al., 2017; Castillo et al., 2014; Gaillard and Barlow, 2011; Gaillard et al., 2017; Gaillard et al., 2015; Iwatsuki et al., 2007; Liu et al., 2007; Liu et al., 2008; Thirumangalathu and Barlow, 2015; Zhou et al., 2006). Our present study provides evidence for multiple facets of function of the ALK3-BMP signaling in the tongue mesenchyme in regulation of taste papilla development and tongue organogenesis. Most importantly, the deletions of *Alk3* in NC lineage driven by *Wnt1-Cre* lead complete absence of taste papillae and developmentally retarded tongue at E12.0 compared to the littermate control group.

As mentioned before, the BMP signaling pathway is one of the main signaling pathways controlling taste papilla development. BMP ligands (BMP 2, 4, 7) have been shown to inhibit taste papilla development (Beites et al., 2009; Zhou et al., 2006) while BMP antagonists Noggin and folistatin promote taste papilla development (Beites et al., 2009; Zhou et al., 2006). Based on previous reports, it can be speculated that inhibition of BMP signaling promotes taste papilla development. However, our findings are contrary to these published reports and suggest that

inhibiting the taste papilla development is not the sole function of the BMP signaling pathway. Our findings suggest that different components of the BMP signaling pathway (i.e. ligands, antagonists, and receptors) have their specific roles. It is, in fact, possible that ALK3-BMP may counter the inhibitory roles carried out by BMP ligands. However, it is worth noticing that BMP ligands involved in the taste papilla development are mainly located in the tongue epithelium and that our findings, by way of the *Alk3 cKO* in the mesenchyme, indicating BMP signaling have tissue specific effects on taste papilla development.

3.5.2 ALK3-BMP signaling in the tongue mesenchyme inhibit the secretion of inhibitory secretory protein

RNA-Seq analyses showed that *Alk3 cKO* in the tongue mesenchyme led to many more differentially expressed genes (DEGs) in the *Wnt1-Cre/Alk3*^{cKO} mutant epithelium compared to the mesenchyme indicating the important roles between the NC-derived mesenchyme with the overlying epithelium through the ALK3-BMP signaling pathway. Given that many genes related to intracellular trafficking and exocytosis have been downregulated and genes related to secretory proteins (Neuroblastoma suppressor of tumorigenicity 1/Nbl1, pyruvate kinase muscle isozyme 2/Pkm2) have been upregulated, our data indicates that ALK3-BMP signaling in the mesenchyme regulates the intracellular transport of mesenchymal factors, mainly secretory proteins. Inhibition of the taste papilla development in the 12.0+2 day wild type tongue cultures with the proteins isolated from the *Wnt1-Cre/Alk3*^{cKO} mesenchyme-derived conditioned media confirms the possible role of mesenchymal ALK3-BMP signaling in taste papilla development through secretory proteins. Furthermore, the identification of many more proteins, including Pkm2 from the LC-MS analyses using mesenchyme-derived conditioned media isolated from *Wnt1-Cre/Alk3*^{cKO} mesenchymal cell cultures clearly indicates that ALK3-BMP signaling is likely inhibiting the secretion of these proteins in-vivo. Based on our own gene expression, LC-MS and functional analyses, we propose that ALK3-BMP in NC-derived tongue mesenchyme promotes taste papilla formation by suppressing the secretion of inhibitory secretory proteins.

Wnt/β-catenin signaling pathway is a major signaling pathway involved in the differentiation of tongue epithelial cells and formation of taste papillae (Iwatsuki et al., 2007; Liu et al., 2007; Thirumangalathu and Barlow, 2015). We believe that Nbl1 and Pkm2, known inhibitors of the β-catenin mediated signaling pathway, are promising mesenchymal secretory protein candidates (Clausen et al., 2011; Nolan et al., 2015; Nolan and Thompson, 2014). We hypothesize that under normal conditions, mesenchymal ALK3-BMP signaling suppresses the secretion of these proteins, allowing epithelial Wnt/β-catenin signaling to promote taste papilla development. However, in the absence of mesenchymal ALK3-BMP signaling, Nbl1 and Pkm2 inhibit epithelial Wnt/β-catenin signaling, thereby resulting in the absence of taste papillae observed in *Wnt1-Cre/Alk3*^{cKO} mutants.

During embryonic development of taste papillae, roles of other molecular or genetic programs in the tongue mesenchyme, such as FGF signaling, (Petersen et al., 2011; Prochazkova et al., 2017) and Wt1 (Gao et al., 2014) have been reported. It is also possible that these inhibitory proteins do not directly regulate taste papilla development in the epithelium through Wnt/β-catenin signaling; rather, they interact with other factors (i.e. FGF, WT) in the tongue mesenchyme to regulate taste papilla formation. Further studies are needed to delineate the requirement of signaling networks for the proper development of different types of taste papillae.

Overall, we report that ALK3-BMP signaling in NC-derived tongue mesenchyme plays an important role in the regulation of multiple facets of tongue organ development, including the formation of tongue and taste papillae. We identify that mesenchymal ALK3-BMP signaling regulate the secretion of inhibitory secretory proteins and thereby control the formation of taste papillae. Moreover, we provide evidence that ALK3-BMP singling in the mesenchyme is a major regulator in the mesenchymal-epithelial interactions for the formation of taste papillae.

3.6 Acknowledgments

We give thanks to: Dr. Steven Stice, Dr. Franklin West, Dr. Luke Mortensen, and Dr. Douglas Menke at The University of Georgia, Athens, Georgia, for the discussion and feedbacks. This study was supported by the National Institutes of Health, grant number R01DC012308 and R21DC018089 to HXL, and R01DE020843 to YM

Table 3.1. Primary antibodies used for immunohistochemistry.

Primary antibody	Source (catalog number, company)	Dilution
Goat Shh	AF464, R&D systems, Minneapolis, MN	1:300
Rabbit anti p-Smad 1/5/8	#13820, Cell signaling, Danvers, MA	1:500
Goat anti E-cadherin	AF748, R&D systems, Minneapolis, MN	1:1000
Rabbit anti Prox1	PA5-85552, Invitrogen, Waltham, MA	1:100
Sheep anti-Ki67	AF7649, R&D systems, Minneapolis, MN	1:500
Rabbit anti c-Cas 3	#9661, Cell signaling, Danvers, MA	1:500

Table 3.2. Primer sequences used for the quantitative reverse transcriptase PCR (qRT-PCR)

Gene	Primer sequence
Cyclin D1	Forward 5' GAC GGC GTC AAA TAT GTC CT 3' Reverse 5' CTG GAG AGT GAC AGC ATG GA 3'
p53	Forward 5' CGG GTG GAA GGA AAT TTG TA 3' Reverse 5' TAG CAC TCA GGA GGG TGA GG 3'
Nbl1	Forward 5' GGACAAGAGTGCCTGGTGTGAA 3' Reverse 5' GACGCTGTAACTGAAGCATTGTC 3'
Pkm2	Forward 5' CAGAGAAGGTCTTCCTGGCTCA 3' Reverse 5' GCCACATCACTGCCTTCAGCAC 3'
Alk3	Forward 5' GCAGCTGCTGCTGCAGCCTCC 3' Reverse 5' TGGCTACAATTTGTCTCATGC 3'

Table 3.3. Proteins identified from the Liquid chromatography-mass spectrometry analyses

Number	Gene	Protein score	
		Ctrl	*Alk3 cKO*
1	H1.3	184.71	365.13
2	PTMA	168.00	201.43
3	Actb	132.60	202.84
4	H1.5	105.01	160.44
5	HSP90ab1	99.42	495.76
6	H4C1	97.44	260.57
7	HSPA5	95.13	101.50
8	H2BC14	91.27	285.93
9	Tubb5	88.98	130.46
10	MARCKSL1	73.54	67.45
11	H3-5	57.00	51.51
12	Hbb-y	48.29	183.49
13	TUBA1C	46.81	84.35
14	Hsp90aa1	—	455.24
15	Krt76	—	220.77
16	Fn1	—	165.99
17	Ywhaz	—	151.40
18	Krt17	—	132.75
19	Eef1a1	—	124.81
20	Prdx1	—	109.41
21	Hspd1	—	106.81

22	Ywhae	—	106.03
23	Hsp90b1	—	101.12
24	Ldha	—	96.87
25	Ppib	—	95.69
26	Atp5f1a	—	90.74
27	Hbz	—	89.44
28	H1-1	—	89.01
29	Npm1	—	85.75
30	Hspa8	—	76.66
31	Gapdh	—	68.16
32	Hbb-bh1	—	63.87
33	Atp5f1b	—	62.57
34	Eef2	—	57.99
35	Flna	—	51.20
36	Serpinh1	—	49.67
37	Arhgdia	—	49.57
38	Ncl	—	48.54
39	Marcks	—	47.05
40	Pkm2	—	41.44
41	Basp1	—	40.41

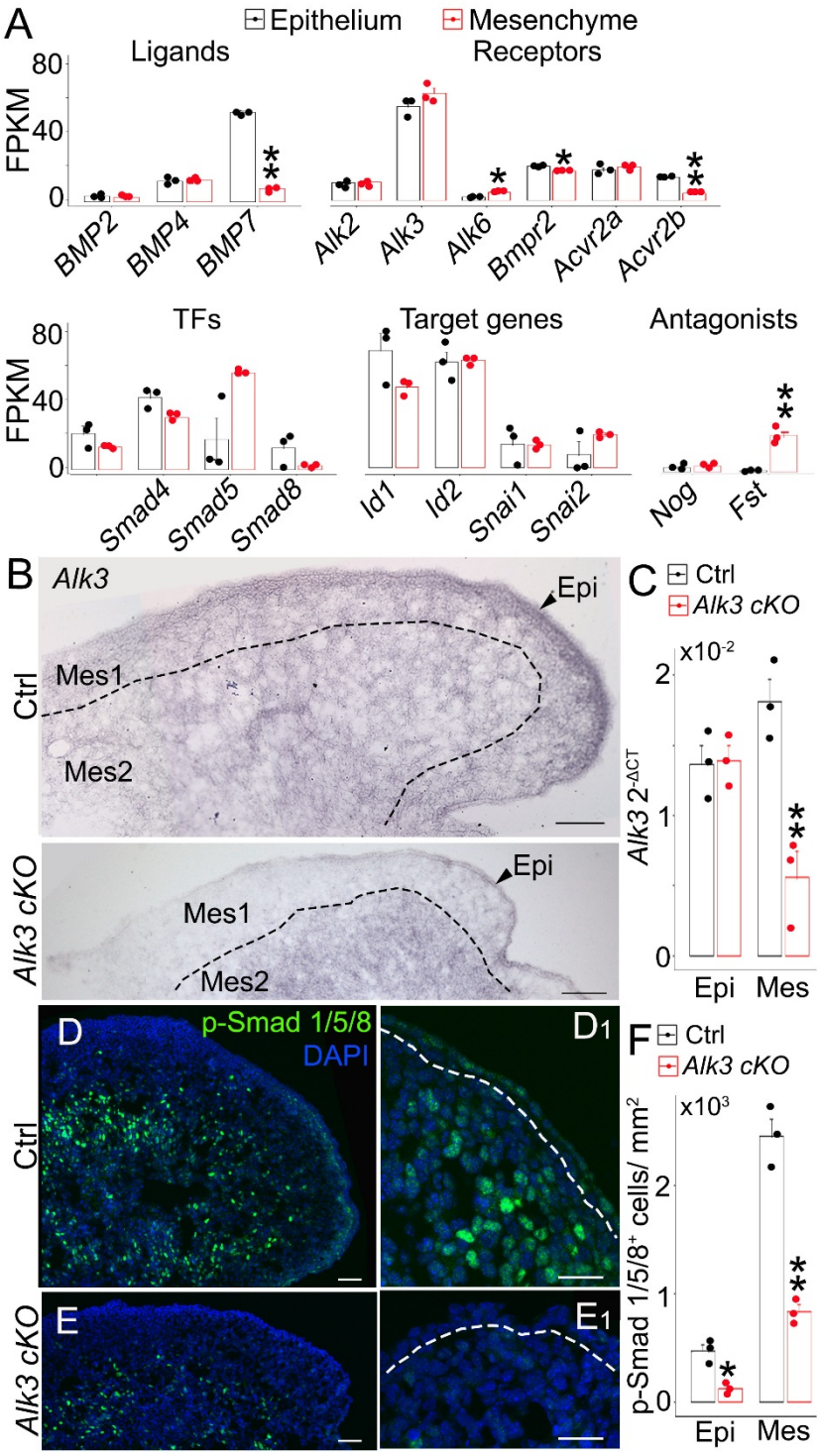
A
Epithelium
Mesenchyme
Ligands
Receptors
FPKM
80
40
0
BMP2
BMP4
BMP7
Alk2
Alk3
Alk6
Bmpr2
Acvr2a
Acvr2b
TFs
Target genes
Antagonists
Smad4
Smad5
Smad8
Id1
Id2
Snai1
Snai2
Nog
Fst
B
Alk3
Epi
Mes1
Mes2
Ctrl
Alk3 cKO
C
Ctrl
Alk3 cKO
x10-2
Alk3 2-ΔCT
2
1
0
Epi
Mes
D
p-Smad 1/5/8
DAPI
D1
E
E1
F
x10³
p-Smad 1/5/8⁺ cells/ mm²

Figure 3.1. BMP signaling activity in the developing tongue. A: Histograms (X±SD; n=3) to represent the FPKM (Fragments Per Kilobase Million) values of BMP ligands, receptors, transcription factors (TFs), target genes and antagonists in the E12.5 wild type tongue epithelium and mesenchyme. **B:** Light microscopy images of whole tongue sections from E12.0 *Cre⁻/Alk3$^{fx/fx}$* littermate control and *Wnt1-Cre/Alk3^{cKO}* mutant mice. In situ hybridization was performed using an antisense probe for *Alk3*. Arrowheads in B point to the epithelium (Epi). Dashed lines in B separate the mesenchymal layers subjacent to the epithelium (Mes1) from the deeper mesenchymal layers (Mes2). Scale bars: 100 μm. **C:** A Histogram (X±SD; n=3) to represent the $2^{-\Delta CT}$ values of *Alk3* gene transcripts in *Cre⁻/Alk3$^{fx/fx}$* littermate control (Ctrl) and *Wnt1-Cre/Alk3^{cKO}* mutant (*Alk3 cKO*) tongue epithelium (Epi) and mesenchyme (Mes). *$p \leq 0.05$, **$p \leq 0.01$ compared to the *Cre⁻/Alk3$^{fx/fx}$* littermate control using two-way ANOVA followed by Fisher's least significant difference (LSD) analyses. **D-E:** Single-plane laser scanning confocal images of sagittal tongue sections, immunostained with BMP signaling downstream signaling activity marker p-Smad 1/5/8 (green) in *Cre⁻/Alk3$^{fx/fx}$* littermate control (Ctrl, D) and *Wnt1-Cre/Alk3^{cKO}* mutant mice (*Alk3 cKO*, E). D_1 and E_1 are high magnification images of the anterior tongue tip of *Cre⁻/Alk3$^{fx/fx}$* littermate control (D) and *Wnt1-Cre/Alk3^{cKO}* mutant mice (E). Scale bars: 50 μm in D, E; 25 μm in D_1, E_1. **F:** A histogram (X±SD; n=3) to represent the number of p-Smad 1/5/8$^+$ cells per mm^2 in *Cre⁻/Alk3$^{fx/fx}$* littermate control (Ctrl) and *Wnt1-Cre/Alk3^{cKO}* mutant (*Alk3 cKO*) tongue epithelium (Epi) and mesenchyme (Mes). *$p \leq 0.05$, **$p \leq 0.01$ compared to the *Cre⁻/Alk3$^{fx/fx}$* littermate control using two-way ANOVA followed by Fisher's LSD analyses.

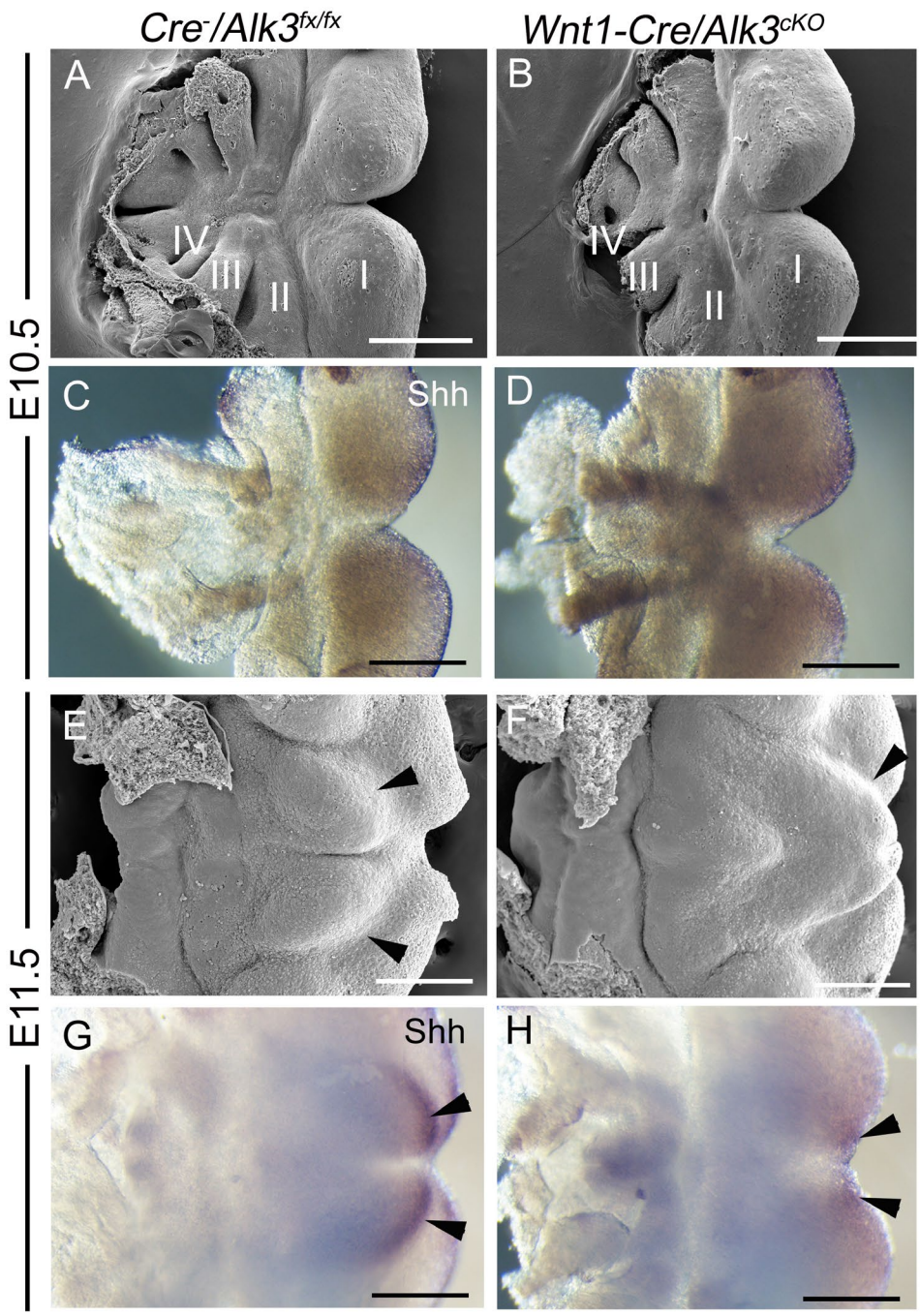
Cre-/Alk3fx/fx
Wnt1-Cre/Alk3cKO
A
B
IV
III
II
I
IV
III
II
I
E10.5
C
Shh
D
E11.5
E
F
G
Shh
H

Figure 3.2. Tongue primordium (branchial arches) and early tongue development in *Cre^{-}/Alk3$^{fx/fx}$* littermate control and *Wnt1-Cre/Alk3^{cKO}* mice. **A-H:** Whole mount images (scanning electron microscopy images A-B, E-F and light microscopy images C-D, G-H) of *Cre^{-}/Alk3$^{fx/fx}$* littermate control (A, C, E, G) and *Wnt1-Cre/Alk3^{cKO}* (B, D, F, H) E10.5 branchial arches (A-D) and E11.5 tongues (E-H). Roman numerals I-IV in A and B represent BAs 1-4. Whole mount immunoreaction were performed against developing taste papilla marker sonic hedgehog (Shh-blue,). Arrowheads in E point to lateral tongue swellings in *Cre^{-}/Alk3$^{fx/fx}$* littermate control tongue. The arrowhead in F points to fused and pointed tip of *Wnt1-Cre/Alk3^{cKO}* mutant tongue. Arrowheads in G and H point to diffuse Shh immunosignals in *Cre^{-}/Alk3$^{fx/fx}$* littermate control (G) and *Wnt1-Cre/Alk3^{cKO}* mutants (H). Scale bars: 200 μm.

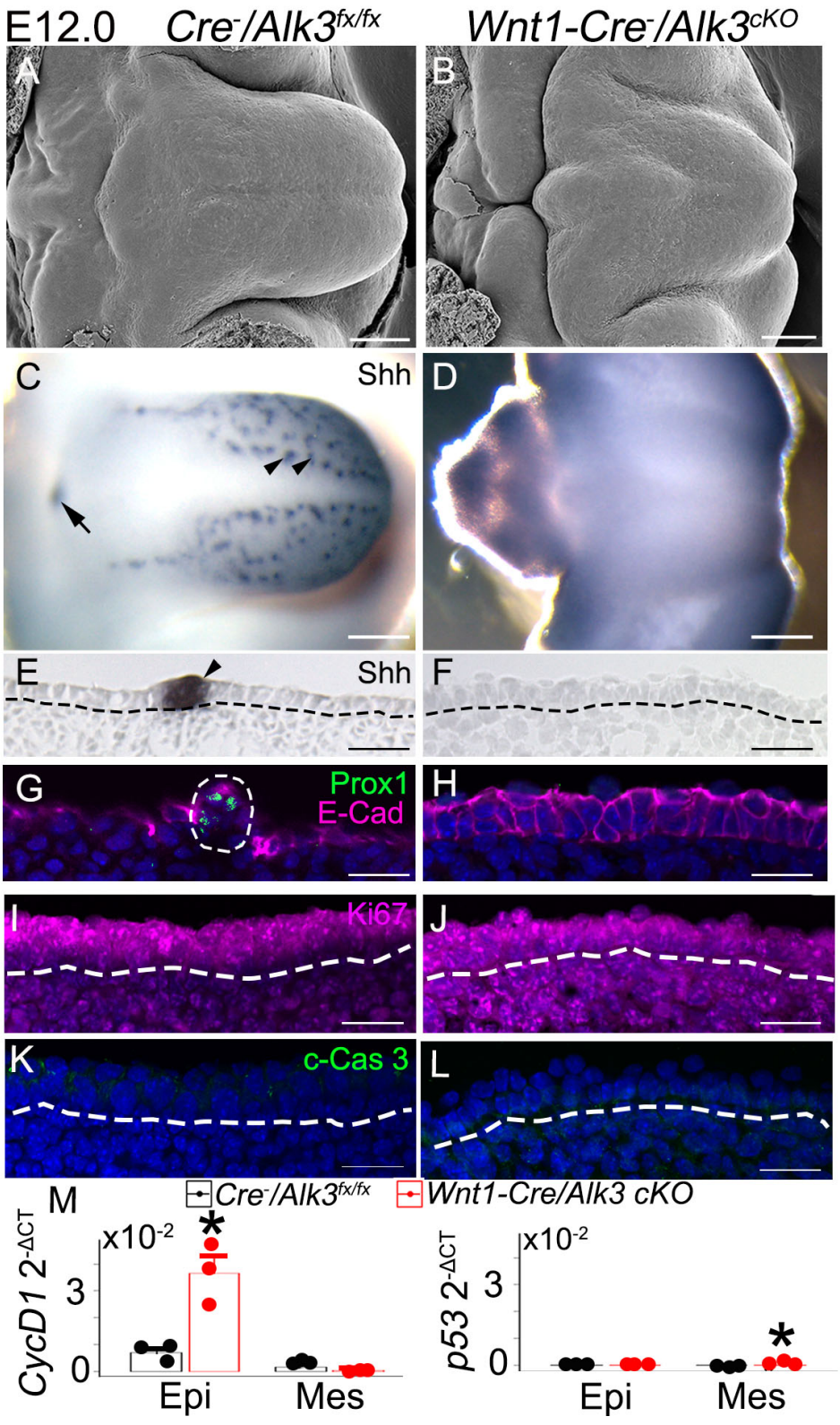
E12.0
Cre-/Alk3fx/fx
Wnt1-Cre-/Alk3cKO
A
B
C
Shh
D
E
Shh
F
G
Prox1
E-Cad
H
I
Ki67
J
K
c-Cas 3
L
M
Cre-/Alk3fx/fx
Wnt1-Cre/Alk3 cKO
CycD1 2-ΔCT
x10-2
3
0
Epi
Mes
p53 2-ΔCT
x10-2
3
0
Epi
Mes

Figure 3.3. Representative photomicrographs of E12.0 *Cre^{-}/Alk3$^{fx/fx}$* littermate control and *Wnt1-Cre/Alk3^{cKO}* tongues. **A-D:** Scanning electron microscopy (A, B) and whole mount Shh immunostained (C, D) images of *Cre^{-}/Alk3$^{fx/fx}$* littermate control (A, C) and *Wnt1-Cre/Alk3^{cKO}* mutant (B, D) tongues. Scale bars: 200 µm in A-D. **E-F:** High magnification images of the Shh immunostained sagittal tongue sections of *Cre^{-}/Alk3$^{fx/fx}$* littermate control (E) and *Wnt1-Cre/Alk3^{cKO}* mutant (F) tongues. Arrowheads in C and E point to the Shh^{+} fungiform taste papilla placode. The arrow in C points to the Shh^{+} circumvallate papilla (CV) placode. **G-L**: Single-plane laser scanning confocal high magnification images of sagittal tongue sections immunostained with taste papilla placode marker Prox1 (green in G), epithelial marker E-Cadherin (magenta in G, H), cell proliferation marker Ki67 (magenta in I, J), and apoptosis marker cleaved (c) caspase 3 (c-Cas 3, green in K, L) in *Cre^{-}/Alk3$^{fx/fx}$* littermate control (G, I, K) and, *Wnt1-Cre/Alk3^{cKO}* mutant (H, J, L) tongues. Dashed lines in E, F, and, I-L separate the epithelium from the mesenchyme. Dashed ring in G encircles the taste papilla. Scale bars: 25 µm in E-L. **M:** Histograms (X±SD; n=3) represent the $2^{-\Delta CT}$ values of cell proliferation marker gene *Cyclin-D1* (*CycD1*) and apoptosis marker gene *p53* mRNA transcripts from quantitative RT-PCR analyses. *$p \leq 0.05$, **$p \leq 0.01$ compared to the *Cre^{-}/Alk3$^{fx/fx}$* littermate control using two-way ANOVA followed by Fisher's LSD analyses.

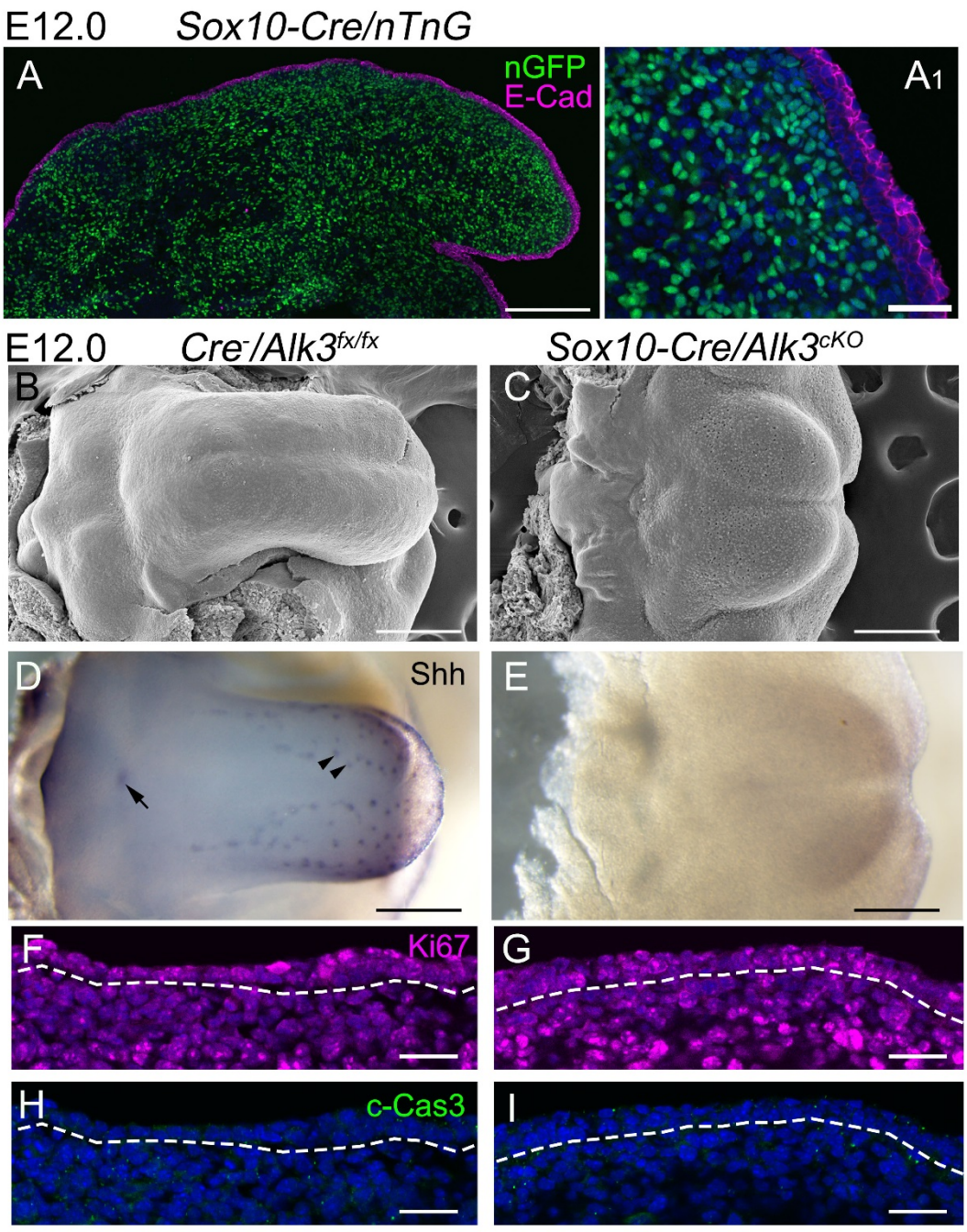
E12.0 Sox10-Cre/nTnG
A
nGFP
E-Cad
A1
E12.0 Cre-/Alk3fx/fx
Sox10-Cre/Alk3cKO
B
C
D
Shh
E
F
Ki67
G
H
c-Cas3
I

Figure 3.4. Representative photomicrographs of E12.0 *Sox10-Cre/nTnG*, *Cre^{-}/Alk3$^{fx/fx}$* littermate control and *Sox10-Cre/Alk3^{cKO}* tongues. **A:** Single-plane laser scanning confocal images of sagittal tongue sections immunostained with E-Cadherin in *Sox10-Cre/nTnG* tongues. A_1 is the high magnification image of the anterior tongue tip of *Sox10-Cre/nTnG* mice. **B-E:** Scanning electron microscopy (B, C) and whole mount Shh immunostained (D, E) images of *Cre^{-}/Alk3$^{fx/fx}$* littermate control (B, D) and *Wnt1-Cre/Alk3^{cKO}* mutant (C, E) tongues. Arrowheads in D point to the Shh^{+} fungiform papilla placode. The arrow in D points to the Shh^{+} CV papilla placode. **F-I:** Single-plane laser scanning confocal high magnification images of sagittal tongue sections immunostained with Ki67 (magenta in F, G) and c-Cas 3 (green in H, I) in *Cre^{-}/Alk3$^{fx/fx}$* littermate control (F, H) and *Wnt1-Cre/Alk3^{cKO}* mutant (G, I) tongues. Dashed lines in F-I separate the epithelium from the mesenchyme. Scale bars: 200 μm in A, B-D; 25 μm in A1, F-I.

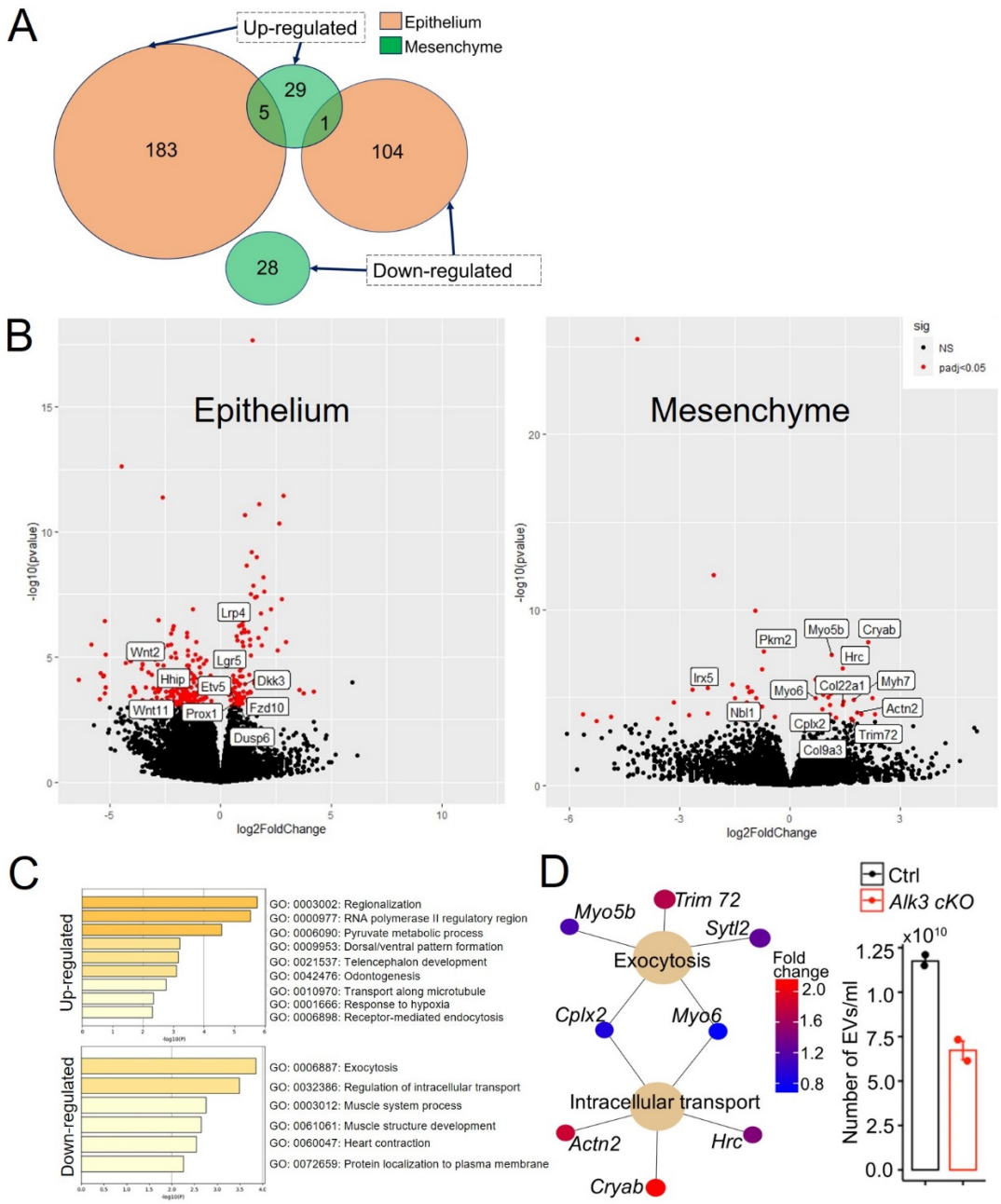
A
Up-regulated
Epithelium
Mesenchyme
183
29
5
1
104
28
Down-regulated
B
Epithelium
Mesenchyme
sig
NS
padj<0.05
-log10(pvalue)
log2FoldChange
Lrp4
Wnt2
Lgr5
Hhip
Etv5
Dkk3
Wnt11
Prox1
Fzd10
Dusp6
Pkm2
Myo5b
Cryab
Hrc
Irx5
Myo6
Col22a1
Myh7
Nbl1
Actn2
Cplx2
Trim72
Col9a3
C
Up-regulated
GO: 0003002: Regionalization
GO: 0000977: RNA polymerase II regulatory region
GO: 0006090: Pyruvate metabolic process
GO: 0009953: Dorsal/ventral pattern formation
GO: 0021537: Telencephalon development
GO: 0042476: Odontogenesis
GO: 0010970: Transport along microtubule
GO: 0001666: Response to hypoxia
GO: 0006898: Receptor-mediated endocytosis
Down-regulated
GO: 0006887: Exocytosis
GO: 0032386: Regulation of intracellular transport
GO: 0003012: Muscle system process
GO: 0061061: Muscle structure development
GO: 0060047: Heart contraction
GO: 0072659: Protein localization to plasma membrane
D
Myo5b
Trim 72
Sytl2
Exocytosis
Cplx2
Myo6
Intracellular transport
Actn2
Hrc
Cryab
Fold change
2.0
1.6
1.2
0.8
Ctrl
Alk3 cKO
x10^10
Number of EVs/ml

Figure 3.5. Transcriptomic analyses of E12.0 *Cre^{-}/Alk3$^{fx/fx}$* littermate control and *Wnt1-Cre/Alk3^{cKO}* mutant tongue epithelium and mesenchyme. **A:** Venn diagram to show number and percentage of differentially expressed genes (DEGs) in the epithelium and mesenchyme of *Wnt1-Cre/Alk3^{cKO}* mutant tongue compared *Cre^{-}/Alk3$^{fx/fx}$* littermate control tongue. **B:** Volcano plots to exhibit DEGs in *Wnt1-Cre/Alk3^{cKO}* mutant and *Cre^{-}/Alk3$^{fx/fx}$* littermate control epithelium and mesenchyme. The Y-axis shows the mean expression value of -log10 (p-Value) and the X-axis displays the log2 (Fold_Change). Significantly ($p \leq 0.05$) up- and down-regulated genes are presented with red dots. Black dots indicate the expression of genes with no significant differences. **C:** Gene ontology (GO) terms to represent the major cellular activities associated with the up- and down-regulated DEGs identified from the *Wnt1-Cre/Alk3^{cKO}* mutant tongue mesenchyme compared to *Cre^{-}/Alk3$^{fx/fx}$* littermate control tongue mesenchyme. **D:** A map to illustrate the down-regulated DEGs associated with exocytosis and intracellular transport in *Wnt1-Cre/Alk3^{cKO}* mutant tongue mesenchyme compared to *Cre^{-}/Alk3$^{fx/fx}$* littermate control tongue mesenchyme. Histogram represents the concentration of extracted extracellular vesicles (EVs) from the *Cre^{-}/Alk3$^{fx/fx}$* littermate control (Ctrl) and *Wnt1-Cre/Alk3^{cKO}* mutant (*Alk3 cKO*) tongue mesenchymal cells-derived conditioned media.

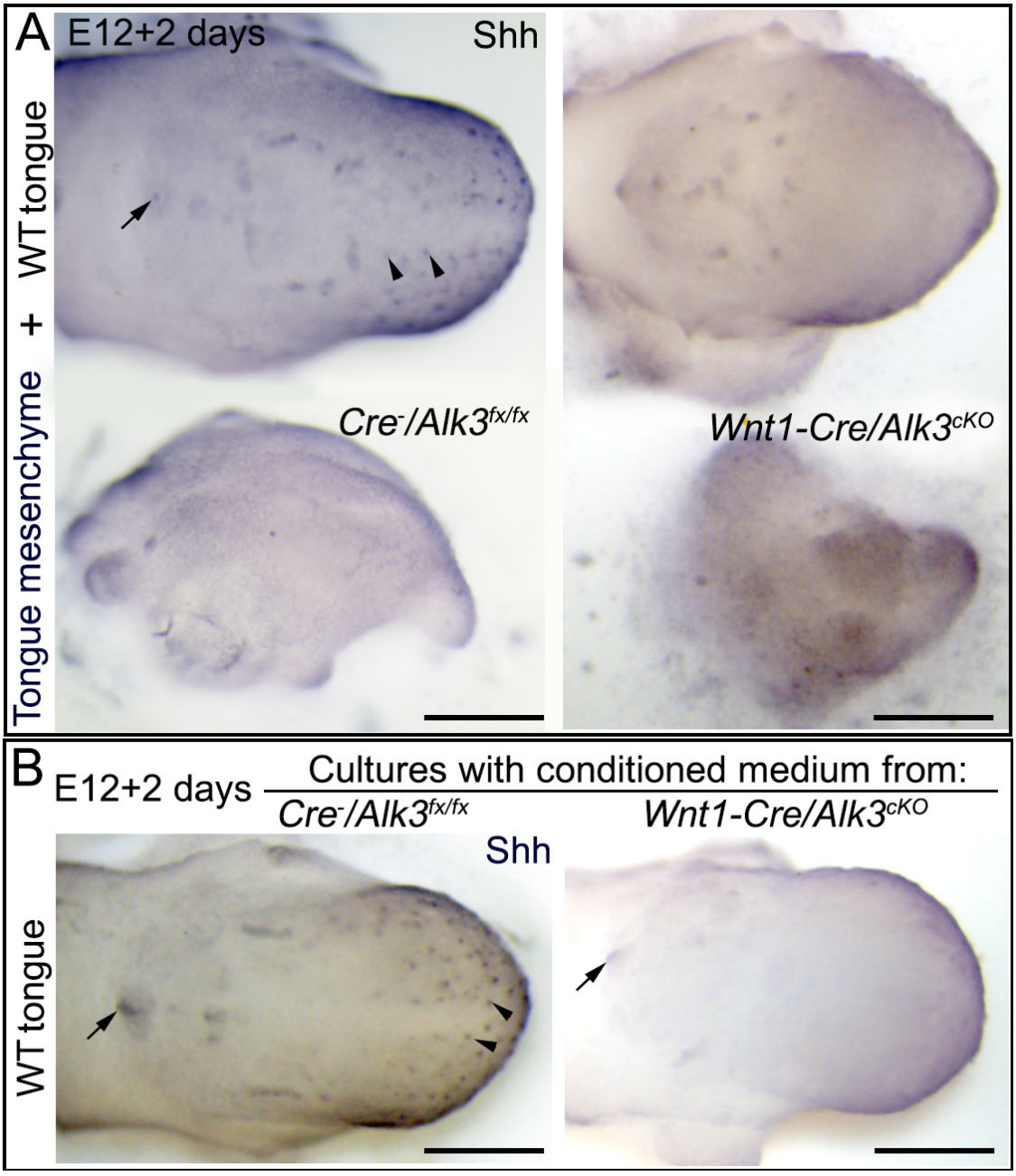
A
E12+2 days
Shh
Tongue mesenchyme + WT tongue
Cre-/Alk3fx/fx
Wnt1-Cre/Alk3cKO
B
E12+2 days
Cultures with conditioned medium from:
Cre-/Alk3fx/fx
Wnt1-Cre/Alk3cKO
Shh
WT tongue

Figure 3.6. Effects on taste papilla development when cultured with *Cre^{-}/Alk3$^{fx/fx}$* littermate control and *Wnt1-Cre/Alk3^{cKO}* mutant tongue mesenchyme or conditioned media. A: Representative light microscopy images of the Shh immunostained E12.0+2 day wild type (WT) tongues co-cultured with *Cre^{-}/Alk3$^{fx/fx}$* littermate control (left) and *Wnt1-Cre/Alk3^{cKO}* mutant (right) mesenchyme. **B:** Representative light microscopy images of the Shh immunostained E12.0+2 day WT tongues cultured with *Cre^{-}/Alk3$^{fx/fx}$* littermate control (left) and *Wnt1-Cre/Alk3^{cKO}* mutant (right) mesenchyme-derived conditioned media. Arrowheads point to the Shh^{+} fungiform papillae. Arrows point to the Shh^{+} CV papilla. Scale bars: 200 μm.

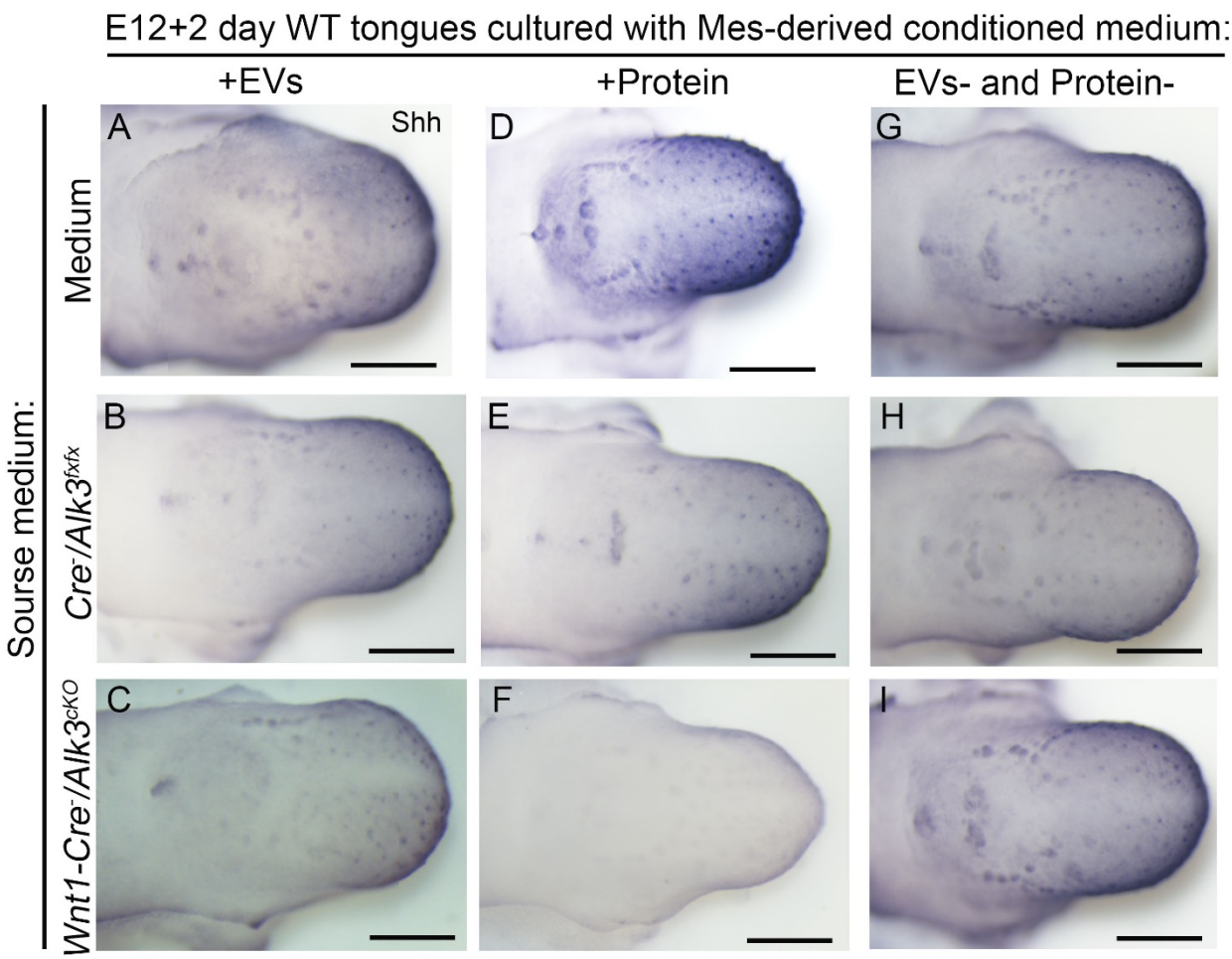
E12+2 day WT tongues cultured with Mes-derived conditioned medium:
+EVs
+Protein
EVs- and Protein-
Sourse medium:
Medium
Cre-/Alk3fxfx
Wnt1-Cre-/Alk3cKO
A
Shh
B
C
D
E
F
G
H
I

Figure 3.7. Effects on taste papilla development when cultured with components isolated from *Cre^{-}/Alk3$^{fx/fx}$* littermate control and *Wnt1-Cre/Alk3^{cKO}* mutant tongue mesenchyme-derived conditioned media. **A-I:** Representative light microscopy images of the Shh immunostained E12.0+2 day WT tongues, cultured with Extracellular vesicles (EVs)-enriched (A-C), protein-enriched (D-F) and, EVs and protein depleted media (G-I) isolated from the culture media (A, D, E); E11.5 *Cre^{-}/Alk3$^{fx/fx}$* littermate control (B, E, H) and, *Wnt1-Cre/Alk3^{cKO}* mutant (C, F, I) mesenchymal cells-derived conditioned media. Scale bars: 200 μm.

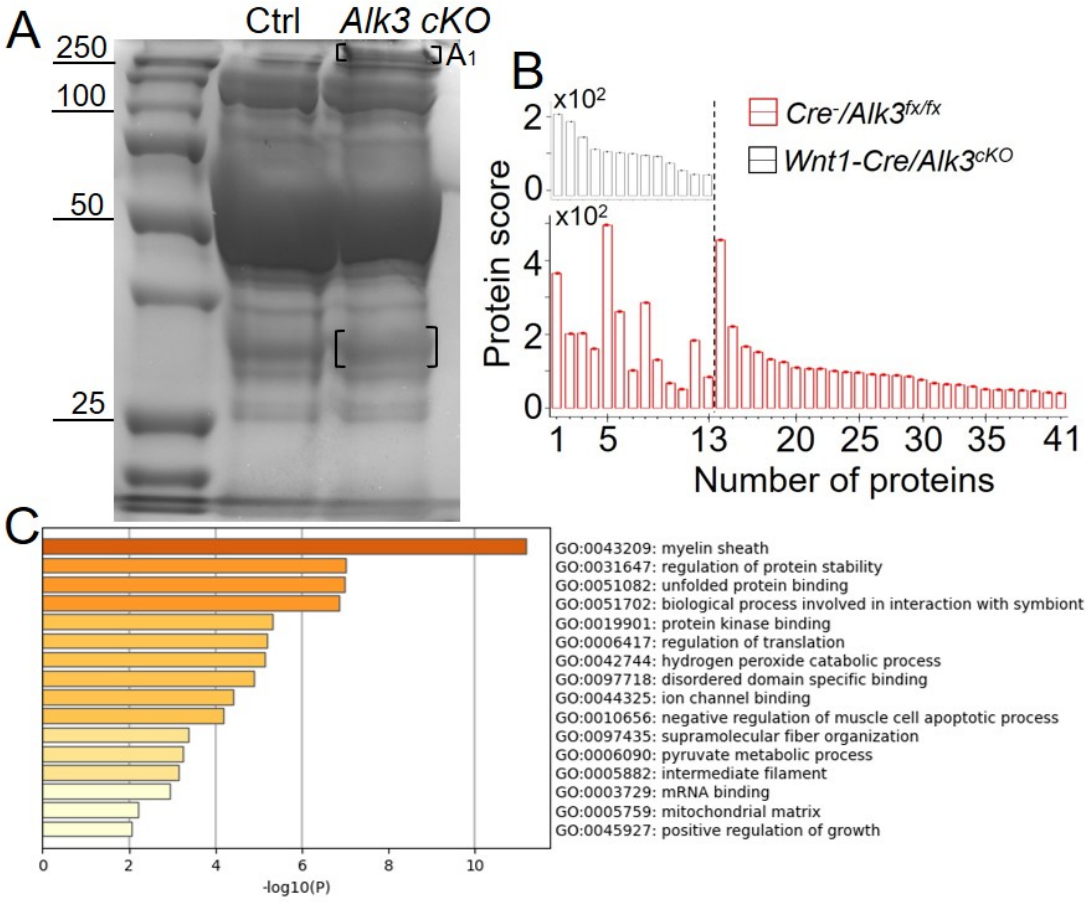
A
Ctrl
Alk3 cKO
A1
250
100
50
25
B
x10²
2
0
x10²
4
2
0
Protein score
Cre-/Alk3fx/fx
Wnt1-Cre/Alk3cKO
1
5
13
20
25
30
35
41
Number of proteins
C
GO:0043209: myelin sheath
GO:0031647: regulation of protein stability
GO:0051082: unfolded protein binding
GO:0051702: biological process involved in interaction with symbiont
GO:0019901: protein kinase binding
GO:0006417: regulation of translation
GO:0042744: hydrogen peroxide catabolic process
GO:0097718: disordered domain specific binding
GO:0044325: ion channel binding
GO:0010656: negative regulation of muscle cell apoptotic process
GO:0097435: supramolecular fiber organization
GO:0006090: pyruvate metabolic process
GO:0005882: intermediate filament
GO:0003729: mRNA binding
GO:0005759: mitochondrial matrix
GO:0045927: positive regulation of growth
0
2
4
6
8
10
-log10(P)

Figure 3.8. Liquid chromatography–mass spectrometry (LC-MS) analyses on the conditioned media isolated from the *Cre^{-}/Alk3$^{fx/fx}$* littermate control and *Wnt1-Cre/Alk3^{cKO}* mutant tongue mesenchymal cell cultures. **A:** Coomassie blue stained sodium dodecyl sulphate–polyacrylamide gel to show the proteins detected from the conditioned media isolated from the E11.5 *Cre^{-}/Alk3$^{fx/fx}$* littermate control (Ctrl) and *Wnt1-Cre/Alk3^{cKO}* mutant (*Alk3 cKO*) tongue mesenchymal cell cultures. Brackets A_1 and A_2 mark the regions where *Wnt1-Cre/Alk3^{cKO}* mutant had differentially expressed protein bands **B:** Histograms represent the protein score and the number of proteins identified from the LC-MS analyses on *Cre^{-}/Alk3$^{fx/fx}$* littermate control and *Wnt1-Cre/Alk3^{cKO}* mutant tongue mesenchymal cells-derived conditioned media. Dashed line separate the proteins detected in both *Cre^{-}/Alk3$^{fx/fx}$* littermate controls and *Wnt1-Cre/Alk3^{cKO}* mutants from the proteins only detected in *Wnt1-Cre/Alk3^{cKO}* mutants. **C:** GO terms to represent the major cellular activities associated with the proteins identified from the *Wnt1-Cre/Alk3^{cKO}* mutant mesenchymal cells-derived conditioned media compared to *Cre^{-}/Alk3$^{fx/fx}$* littermate control mesenchymal cells-derived conditioned media.

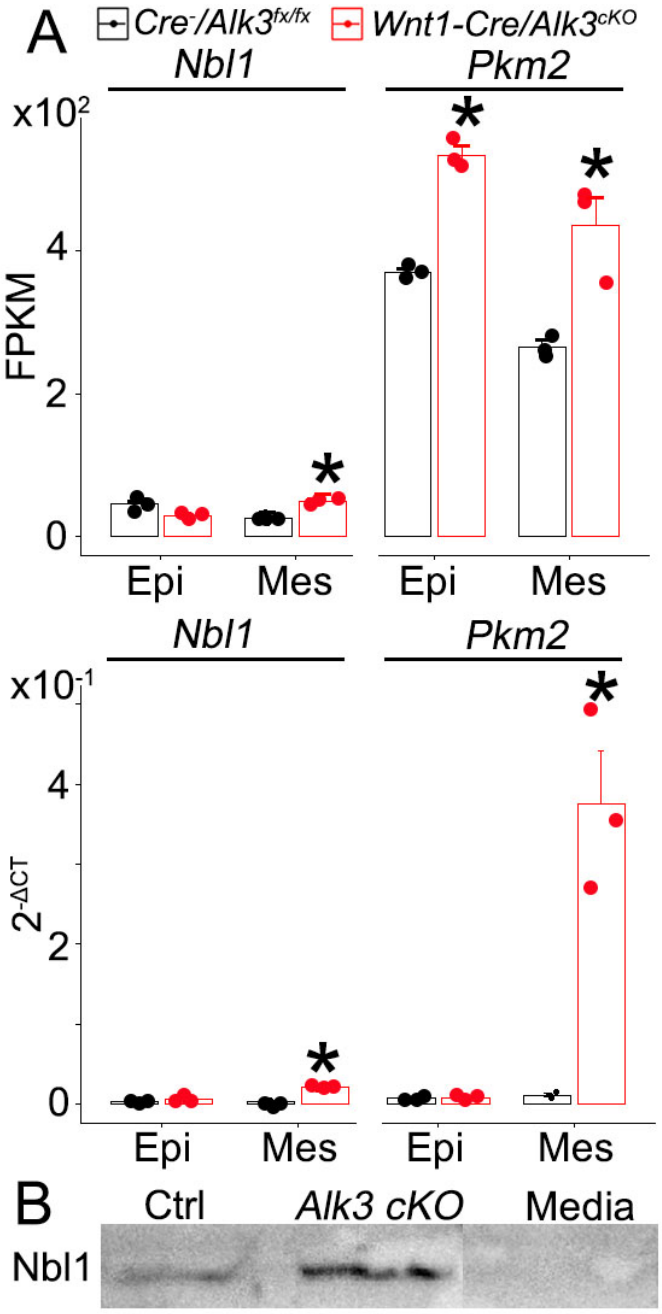
A
Cre-/Alk3fx/fx
Wnt1-Cre/Alk3cKO
Nbl1
Pkm2
x10^2
FPKM
4
2
0
Epi
Mes
Epi
Mes
Nbl1
Pkm2
x10^-1
2^-ΔCT
4
2
0
Epi
Mes
Epi
Mes
B
Ctrl
Alk3 cKO
Media
Nbl1

Figure 3.9. Secretory protein candidates identified from the *Wnt1-Cre/Alk3^{cKO}* mutant tongue mesenchyme. A: Histograms (X±SD; n=3) represent the FPKM and $2^{-\Delta CT}$ values of *Nbl1, Pkm2* mRNA transcripts. *$p \leq 0.05$, **$p \leq 0.01$ compared to the *Cre^{-}/Alk3$^{fx/fx}$* littermate control using two-way ANOVA followed by Fisher's LSD analyses. **B:** Western blot bands of Nbl1 in the conditioned media isolated from the E11.5 *Cre^{-}/Alk3$^{fx/fx}$* littermate control (Ctrl), *Wnt1-Cre/Alk3^{cKO}* mutant (*Alk3 cKO*) mesenchymal cell cultures.

CHAPTER 4

DELETION OF NF2 IN NEURAL CREST-DERIVED TONGUE MESENCHYME ALTERS TONGUE SHAPE AND SIZE THROUGH REGULATION OF HIPPO SIGNALING AND CELL PROLIFERATION IN A REGION- AND STAGE-SPECIFIC MANNER[1]

[1]Mohamed Ishan, Guiqian Chen, Wenxin Yu, Zhonghou Wang, Marco Giovannini, Xinwei Cao, Hong-Xiang Liu. Submitted to *Cell proliferation*, 07/04/2021.

4.1 Abstract

The mammalian tongue develops from the branchial arches (1-4) and is comprised of highly organized tissues compartmentalized by mesenchyme/connective tissue that is largely derived from neural crest (NC). Here, we report the important roles of tumor suppressor Neurofibromin 2 (Nf2) in regulating the development of tongue shape and size. The Hippo pathway activity typically restrains growth and cell proliferation and as a result, loss of Nf2 decreases Hippo pathway activity and promotes an enlarged organ development. However, Nf2 deletion in NC-derived tongue mesenchyme resulted in distinct alterations of Hippo signaling activity and cell proliferation in different tongue regions in a stage-specific manner, i.e., low Yap level with decreased cell proliferation anteriorly and high Yap level with increased cell proliferation posteriorly, which lead to a tip-pointed and posteriorly widened tongue at the early stages of tongue development. At later stages, loss of Nf2 in the NC lineage significantly decreased cell proliferation with a low level of Yap throughout the entire tongue organ suggesting a stage-specific role of Nf2 in regulating cell proliferation. Our data show a distinct role of Nf2 in NC-derived tongue mesenchyme in regulating Hippo signaling and cell proliferation.

Key Words: Neurofibromin 2, Hippo signaling, neural crest, tongue, mesenchyme, cell proliferation

4.2 Introduction

The tongue development requires a proper regulation of its molecular mechanisms to attain its stereotypical shape, while developmental defects including microglossia, macroglossia, and aglossia (Chandrashekar et al., 2014) can hamper the normal function of the tongue, e.g., taste sensing, speaking, and food processing. It has been shown that molecular signaling pathways and their interactions play important roles in the proper formation of the tongue (Ishan et al., 2020; Iwata et al., 2013; Liu et al., 2009; Liu et al., 2012a; Liu et al., 2004; Liu et al., 2012b; Millington et al., 2017). However, our current understanding of tongue development in relation to molecular signaling pathways is far from complete.

In mice, the tongue forms from four branchial arches (BAs) 1-4, i.e., tongue primordia. Among these four BAs, BAs 1-2 give rise to the anterior two-thirds of the tongue - the oral tongue, and BAs 3-4 give rise to the posterior third of the tongue - the pharyngeal tongue (Cobourne et al., 2019). The tongue emerges as three lingual swellings, two lateral and one posterior (tubercula impar) on the floor of the mandible at embryonic day (E) 11.5 (Kaufman, 1992). These swellings fuse and grow into a spatulate tongue at E12.5. Thereafter, the tongue organ continues to grow, various types of cells are differentiated and highly organized, including formed appendages such as taste papillae and taste buds.

Neurofibromin 2 (Nf2), the product of the gene responsible for the disease neurofibromatosis type 2 (Xiao et al., 2003), is pivotal for embryo development, including the development of neural crest (Akhmametyeva et al., 2006; Serinagaoglu et al., 2015) and oral structures (Geist et al., 1992). Nf2 is well known as cell proliferation and tumor suppressor (Cooper and Giancotti, 2014; Hovens and Kaye, 2001; Moon et al., 2018). In many cases, Nf2 activates Hippo signaling, an evolutionarily conserved potent regulator of cell proliferation and organ size (Hamaratoglu et al., 2006; Kim and Jho, 2018). The Hippo pathway is driven by a core kinase cascade that includes Mst1/2 and Lats1/2, which in turn phosphorylate and inactivate Yes-associated protein 1 (YAP) and TAZ transcriptional coactivators (Kim and Jho,

2018). Deficiencies in Nf2 function and Hippo signaling activity lead to excess cell proliferation, organ overgrowth, tumorigenesis (Petrilli et al., 2017; Schulz et al., 2013) and metastasis (Lallemand et al., 2003) which are often promoted by the nuclear translocation of Hippo signaling repressor form, Yap protein (Camargo et al., 2007a; Pan, 2010; Panciera et al., 2016).

In the present study, we report the important role of Nf2 in the NC and NC-derived tongue mesenchymal cells in regulating tongue shape and size that is paradoxically distinct from that in other organs. *Wnt1-Cre* driven conditional knockout of *Nf2* alters Hippo signaling activities and cell proliferation in a tongue region- and stage-specific manner. In combination with previously reported data in the literature, our results indicate tissue context-specific roles of Nf2 in regulating Hippo signaling, cell proliferation, and shape and size of organs.

4.3 Materials and Methods

4.3.1 Animals use and tissue collection

The use of animals was approved by the Institutional Animal Care and Use Committee at the University of Georgia and St Jude Children's Research Hospital. The study was performed in compliance with the National Institutes of Health Guidelines for the care and use of animals in research. The animals were maintained in the animal facilities in the Department of Animal and Dairy Science at the University of Georgia.

C57BL/6 wild type (WT) mice were purchased from The Jackson Laboratory (Stock No: 000664). The *Nf2* floxed allele (fx) was provided by Inserm (Giovannini et al., 2000) . *Wnt1-Cre* (Stock No: 007807, Jackson Laboratory) transgene and *Nf2* fx are both located in Chromosome 11. The recombined allele of *Wnt1-Cre/ Nf2*$^{fx/+}$ was generated in Dr. Xinwei Cao's lab in St Jude Children's Research Hospital (Serinagaoglu et al., 2015). The conditional (or tissue-specific) knockout (cKO) of *Nf2* was generated by breeding *Wnt1-Cre/ Nf2*$^{fx/+}$ mice with *Nf2*$^{fx/fx}$. Cre negative littermates served as controls.

Pregnant mice were euthanized with CO_2 followed by cervical dislocation. Embryos (E10.5-E18.5) were dissected from the uterus under a dissection microscope. E0.5 was designated as

noon of the day on which the dam was positive for the vaginal plug. The stages of embryos were confirmed by the development of multiple organs. E10.5 branchial arches and various stages of tongues were collected and processed for different analyses.

The following primers were used for genotyping: 5'-CTTCCCAGACAAGCAGGGTTC-3' and 5'-GAAGGCAGCTTCCTTAAGTC-3' for *Nf2* fx (~442 bp) and WT (~305 bp) fragments; 5'-GAAGGCAGCTTCCTTAAGTC-3' and 5'-CTCTATTTGAGTGCGTGCCATG-3' for the deleted allele (338 bp) driven by *Wnt1-Cre*; 5′-TCCAATTTACTGACCGTACACC-3′ and 5'-CGTTTTCTTTTCGGATCC-3' for the *Cre* gene product (~372 bp).

4.3.2 Immunohistochemistry on sections

Tongue tissues were carefully dissected from the mandible and fixed in 4% paraformaldehyde (PFA) in 0.1 M phosphate-buffered saline (PBS) at 4°C for 2 hr. PFA-fixed tissues were cryoprotected in 30% sucrose in 0.1 M PBS at 4°C for at least 24 hr, embedded in O.C.T. compound (#23730571; Fisher Scientific, Waltham, MA), and rapidly frozen for cryostat sectioning at 10 μm in thickness for immunohistochemistry.

Tongue sections were air-dried at room temperature for 1 hr and rehydrated in 0.1 M PBS. Blocking of nonspecific staining was carried out by incubation with 10% normal donkey serum in 0.1 M PBS containing 0.3% Triton X-100 (X100, Sigma, St. Louis, MO) at room temperature for 30 min. Then the sections were incubated with primary antibodies (Table 4.1) in the carrier solution (1% normal donkey serum, 0.3% Triton X-100 in 0.1 M PBS) at 4°C for overnight. Sections without a primary antibody treatment were used as the negative control. Following three rinses in 0.1 M PBS, sections were incubated with Alexa Fluor® 488 or 647-conjugated secondary antibody (1:500, Invitrogen, Eugene, OR) in carrier solution at room temperature for 1 hr. Following rinses with 0.1 M PBS sections were counterstained with DAPI (200 ng/ml in PBS, D1306; Life Technologies, Carlsbad, CA) at room temperature for 10 min. After thorough rinsing in 0.1 M PBS, sections were air-dried and coverslipped with Prolong® Diamond antifade mounting medium (P36970; Fisher Scientific, Waltham, MA). The sections were examined

under a fluorescent light microscope (EVOS FL, Life Technologies, Carlsbad, CA) and then photographed using a laser scanning confocal microscope (Zeiss LSM 710, Biomedical Microscopy Core at the University of Georgia).

4.3.3 Scanning electron microscopy (SEM)

E11.5-E18.5 tongues from *Wnt1-Cre/Nf2*^{cKO} mutants and *Cre*$^{-}$*/Nf2*$^{fx/fx}$ littermate controls were fixed in 2.5% glutaraldehyde (#75520; Electron Microscopy Science, Hatfield, PA) and 4% PFA in 0.1 M PBS (pH 7.3) at 4°C for 24 hr. After rinsing in 0.1 M PBS for three times, tissues were post-fixed in a sequence of 1% O_SO_4 (#19150, Electron Microscopy Science, Hatfield, PA) in 0.1 M PBS, 1% tannic acid (#16201, Sigma Aldrich, St. Louis, MO) in MQ-H_2O, 1% O_SO_4 in MQ-H_2O, on ice for 1 hr each. Dehydration was performed in an ascending series of ethanol (35, 50, 70, 90, 100%), and hexamethyldisilazane (HMDS, #440191; Sigma Aldrich, St. Louis, MO) at room temperature (three changes in each solution, 1 hr each). Tongue tissues were slowly air-dried in a fume hood and mounted on specimen stubs, sputter-coated with gold/palladium (Leica Gold/Carbon coater; Georgia Electron Microscope Core Facility, University of Georgia) and imaged using a scanning electron microscope (FEI Teneo FE-SEM; Georgia Electron Microscope Core Facility, University of Georgia).

4.3.4 Quantification and measurements

SEM images of E12.5-E18.5 tongues from *Wnt1-Cre/Nf2*^{cKO} mutants and *Cre*$^{-}$*/Nf2*$^{fx/fx}$ littermate controls were used to measure the width of anterior and posterior tongue, length of the oral tongue using NIH Image-J software (n=3, each group). The width of the anterior 1/3 of the oral tongue was considered as the anterior tongue width. The width of the widest region where oral tongue connects to the mandible was considered as the width of the posterior oral tongue (posterior width). The distance between the anterior tongue tip and the posterior edge of the circumvallate papilla was considered as the length of the oral tongue (oral length).

Quantitative analyses were made to obtain the number of $BrdU^+$ cells per unit area (mm^2) on E10.5 branchial arches (BAs) and E12.5, E15.5, E18.5 *Wnt1-Cre/Nf2*^{cKO}, and *Cre*$^{-}$*/Nf2*$^{fx/fx}$

littermate control tongues. BrdU immunoreacted serial sections of BAs/tongues from *Wnt1-Cre/Nf2*^{cKO} mutants (n=3 per each stage) and *Cre*$^{-}$*/Nf2*$^{fx/fx}$ littermate controls (n=3 per each stage) were thoroughly analyzed under a fluorescent light microscope (EVOS FL, Life Technologies). Single-plane laser scanning confocal photomicrographs were taken from every other section using a scanning confocal microscope (Zeiss LSM 710, Biomedical Microscopy Core at the University of Georgia). BrdU^{+} cells were counted in a unit area (mm^2) of BAs or the E12.5, E15.5, E18.5 tongues (n=3).

4.3.5 *In situ* hybridization

Tongues and BAs of *Wnt1-Cre/Nf2*^{cKO} mutants and *Cre*$^{-}$*/Nf2*$^{fx/fx}$ littermate controls were dissected in 0.1 M PBS, fixed with 4% PFA at 4°C for 24 hr. PFA-fixed tissues were washed three times 0.1 M PBS and dehydrated through ascending series of methanol (35, 50, 70, 90, 100%) and stored in 100% methanol at -20°C. Tissues were rehydrated using 0.1 M PBS and *in situ* hybridization was performed as previously described (Lauter et al., 2011) . Riboprobes for Nf2 was generated by *in vitro* transcription using primers 5'-GAGGCAATTAACCCTCACTAAAGGTTGGCTGAAAAGGCTCAGAT-3', 5'-GAGTAATACGACTCACTATAGGGCCCGCTCTTTGAGTTTCAAG-3' and a dig-UTP labeling mix (Roche, Basel, Switzerland) following the manufacturer's specifications.

4.3.6 RNA extraction and quantitative reverse transcriptase PCR (qRT-PCR)

Epithelium and mesenchyme were separated from the E12.0 *Cre*$^{-}$*/Nf2*$^{fx/fx}$ littermate control and *Wnt1-Cre/Nf2*^{cKO} mutant tongues as described in (Liu et al., 2008). Briefly, dissected E12.0 *Cre*$^{-}$*/Nf2*$^{fx/fx}$ littermate control and *Wnt1-Cre/Nf2*^{cKO} mutant tongue were incubated in a mixture of 1 mg/ml Collagenase A (#10103578001; Roche Diagnostics, Basal, Switzerland) and 2.5 mg/ml Dispase II (# 10374300; Roche Diagnostics, Basal, Switzerland) enzymes at 37°C for 30 min. After a thorough rinse in 0.1 M PBS, epithelia were removed from the mesenchyme. Separated mesenchyme was then transferred to Trizol (#15596018; Life technologies, Carlsbad, CA) solution for RNA extraction. RNA extraction was performed using an RNA extraction kit

(#74136; Qiagen, Hilden, Germany) following the manufacturer's specifications. A total of nine mesenchymal tissues (pooled three tissues x three replicates) from each tongue were used for RNA extraction. RNA concentrations were measured using Nanodrop 8000 spectrophotometer (Nanodrop, Thermo Scientific, Waltham, MA). Complementary DNA (cDNA) synthesized from the extracted RNA using SuperScript™ First-Strand Synthesis System (#11902018; Fisher scientific, Waltham, MA).

4.3.7 Western blot

Proteins in BAs and tongues of *Wnt1-Cre/Nf2*^{cKO} mutants and *Cre*$^{-}$*/Nf2*$^{fx/fx}$ littermate controls were extracted using radioimmunoprecipitation assay (RIPA) buffer (1% NP-40, 150 mmol/L NaCl, 50 mmol/L Tris-HCl, 0.5% sodium deoxycholate, 0.1% SDS, 1 mmol/L EDTA, pH 7.4). The concentration of extracted proteins was determined using Pierce™ BCA protein assay kit (#23225; Thermo Fisher Scientific, Waltham, MA) and Synergy™ 4 microplate reader (#7161000; BioTek Instruments, Winooski, VT). Sodium dodecyl sulfate–polyacrylamide gel electrophoresis (SDS-PAGE) was used to resolve the protein bands and transferred to the nitrocellulose membrane. Non-specific binding was blocked using blocking buffer containing 3% bovine serum albumin (A-420-100; Gold Biotechnology, St Louis, MO) in tris-buffered saline and Tween-20 buffer (TBST) buffer (20 mM Tris pH 7.5, 150 mM NaCl, 0.1% Tween 20) at room temperature for 1 hr. The membranes were incubated with primary antibodies (Yap, p-Yap, Gapdh and β-actin; table 4.1) in blocking buffer at 4^{o}C for 24 hr. Following three rinses in TBST (10 min each), membranes were incubated with Alexa Fluor 647-conjugated secondary antibodies in blocking buffer at room temperature for 2 hr. ChemiDocMP Imaging System (Bio-Rad ChemiDoc, Hercules, CA) was used to image the Western blot bands.

4.3.8 Statistical analysis

Student's *t*-test was used to analyze the statistical significance of differences between *Wnt1-Cre/Nf2*^{cKO} mutants and *Cre*$^{-}$*/Nf2*$^{fx/fx}$ littermate controls for the indices below: the oral tongue length, anterior and posterior tongue width, Western blot band intensities of Yap, p-Yap, and

Gapdh. Two-way analyses of variance (ANOVA) followed by Fisher's LSD analyses were used to compare $BrdU^+$ cells per unit area (mm^2) in individual BAs and tongues between *Wnt1-Cre/Nf2*^{cKO} mutants and *Cre*$^-$*/Nf2*$^{fx/fx}$ littermate controls. A *p*-value less than 0.05 was taken as statistically significant.

For the quantitative RT-PCR, changes of Nf2 gene expression levels in epithelium and mesenchyme of *Wnt1-Cre/Nf2*^{cKO} mutant and *Cre*$^-$*/Nf2*$^{fx/fx}$ littermate control groups were presented as means ± standard deviation (X ± SD; n = 3) of $2^{-\Delta CT}$ values.

4.4 Results

4.4.1 The expression of Neurofibromin 2 is abundant in the developing tongue

Neurofibromin 2 (Nf2) is expressed in migrating neural crest cells (Akhmametyeva et al., 2006) that give rise to a large population, if not all, of the lingual mesenchyme (Liu et al., 2012a; Thirumangalathu et al., 2009). To understand where *Nf2* is expressed during tongue development, E12.5, E15.5, and E18.5 tongues were analyzed (Fig. 4.1). *Nf2* in situ hybridization analyses revealed that mRNA transcripts were abundantly distributed in both epithelium and mesenchyme of *Cre*$^-$*/Nf2*$^{fx/fx}$ littermate control tongues at all three stages (E12.5, E15.5, and E18.5) tested (Fig. 4.1A, B). In addition, our RNA sequencing data also showed that *Nf2* mRNA transcripts were present in both epithelium and mesenchyme in E12.5, E14.5, and postnatal day 1 (P0) tongues with the exception at E12.5, where mesenchyme had more *Nf2* mRNA transcripts compared to the epithelium ($p<0.05$ in Fig. 4.1C). In contrast, *Nf2* transcripts were significantly reduced in both epithelium and mesenchyme of *Wnt1-Cre/Nf2*^{cKO} mutants at all three stages tested (Fig. 4.1A, B). Quantitative RT-PCR analyses confirmed the significantly low *Nf2* expression in both epithelium and mesenchyme of E12.5 *Wnt1-Cre/Nf2*^{cKO} mutant tongues compared to the epithelium and mesenchyme of the *Cre*$^-$*/Nf2*$^{fx/fx}$ littermate control tongues ($p<0.05$ in Fig. 4.1D).

4.4.2 *Nf2 cKO* in neural crest and neural crest-derived tongue mesenchyme leads to a disproportioned tongue during the early stages of tongue development.

To understand the roles of Nf2 in the tongue development, phenotypic analyses were performed in *Cre^{-}/Nf2$^{fx/fx}$* littermate control and *Wnt1-Cre/Nf2^{cKO}* mutant tongues at multiple embryonic stages. At E11.5 when tongue swellings emerged from the branchial arches, tongue swellings were clearly seen in *Cre^{-}/Nf2$^{fx/fx}$* littermate controls (Fig. 4.2A). In *Wnt1-Cre/Nf2^{cKO}* mutants, tongue swellings were not obvious compared to the *Cre^{-}/Nf2$^{fx/fx}$* littermates (Fig. 4.2A).

At later stages (E12.5 and E13.5, Fig. 4.2A), tongue shape and size in *Wnt1-Cre/Nf2^{cKO}* mutants were altered significantly compared to *Cre^{-}/Nf2$^{fx/fx}$* littermate controls (Fig. 4.2A). The width of *Wnt1-Cre/Nf2^{cKO}* mutant tongues was significantly narrower in the anterior oral tongue region (Fig. 4.2A; $p<0.05$ in Fig. 4.2B) and significantly wider towards the posterior oral tongue region (Fig. 4.2A; $p<0.05$ in Fig. 4.2B) compared to that of *Cre^{-}/Nf2$^{fx/fx}$* littermate control tongues (Fig. 4.2). Even though the length of the oral tongue was not significantly altered in the *Wnt1-Cre/Nf2^{cKO}* mutants (Fig. 4.2A; $p>0.05$ in Fig. 4.2B), overall changes in the tongue width resulted in an enlarged tongue (i.e., macroglossia) in *Wnt1-Cre/Nf2^{cKO}* mutants compared to *Cre^{-}/Nf2$^{fx/fx}$* littermate control (Fig. 4.2).

At E15.5-E16.5, *Wnt1-Cre/Nf2^{cKO}* mutants continued to develop a significantly wider posterior oral tongue (Fig. 4.2A; $p<0.05$ in Fig. 4.2B) compared to that of *Cre^{-}/Nf2$^{fx/fx}$* littermates (Fig. 4.2). In contrast to the early stages (i.e., E12.5 and E13.5), the E15.5-E16.5 oral tongues of *Wnt1-Cre/Nf2^{cKO}* mutants were significantly shorter (Fig. 4.2A; $p<0.05$ in Fig. 4.2B) than those of *Cre^{-}/Nf2$^{fx/fx}$* littermates (Fig. 4.2). No significant differences in anterior oral tongue were noticed between *Wnt1-Cre/Nf2^{cKO}* mutants (Fig. 4.2A; $p>0.05$ in Fig. 4.2B) and *Cre^{-}/Nf2$^{fx/fx}$* littermates (Fig. 4.2). As a result of the collective changes in the tongue length and width, E15.5-E16.5 *Wnt1-Cre/Nf2^{cKO}* mutants had a relatively smaller tongue (i.e., microglossia, Fig. 4.2) compared to the *Cre^{-}/Nf2$^{fx/fx}$* littermates (Fig. 4.2).

At E18.5, microglossia phenotype in the *Wnt1-Cre/Nf2*^{cKO} mutants was evident compared to the *Cre*$^{-}$*/Nf2*$^{fx/fx}$ littermates (Fig. 4.2). *Wnt1-Cre/Nf2*^{cKO} mutant mice had a significantly wider but shorter anterior oral tongue compared to those of *Cre*$^{-}$*/Nf2*$^{fx/fx}$ littermate controls (Fig. 4.2A; $p<0.05$ in Fig. 4.2B). Unlike the early stages (E12.5-E16.5), no significant changes in the width of posterior oral tongue were observed in the *Wnt1-Cre/Nf2*^{cKO} mutants (Fig. 4.2A; $p>0.05$ in Fig. 4.2B) compared to *Cre*$^{-}$*/Nf2*$^{fx/fx}$ littermates (Fig. 4.2).

4.4.3 *Wnt1-Cre/Nf2 cKO* leads to alterations of Yap activity and cell proliferation in a tongue region- and stage-specific manner

Nf2 is a known cell proliferation suppressor and often acts via Hippo-YAP signaling to regulate organ size (Hamaratoglu et al., 2006; Kim and Jho, 2018). To understand the potential cause of the alteration of tongue shape and size, we examined the Hippo signaling activity in BAs 1-4 of *Wnt1-Cre/Nf2*^{cKO} mutants and *Cre*$^{-}$*/Nf2*$^{fx/fx}$ littermate controls.

Western blot analyses on downstream signaling components of Hippo pathway revealed that the deactivated form of transcriptional regulator p-Yap was at a significantly lower level in the anterior (Fig. 4.3A; $p<0.05$, Fig. 4.3D), but not posterior (Fig. 4.3A; $p<0.05$, Fig. 4.3D), oral tongue mesenchyme of E12.5 *Wnt1-Cre/Nf2*^{cKO} mutants compared to the corresponding regions of the *Cre*$^{-}$*/Nf2*$^{fx/fx}$ littermate control mesenchyme (Fig. 4.3A, D). In contrast to the p-Yap, Yap, the transcriptional activator for cell proliferation, was at significantly higher level in the posterior, however significantly lower in the anterior, oral tongue mesenchyme in *Wnt1-Cre/Nf2*^{cKO} mutant (Fig. 4.3A; $p<0.05$ in Fig. 4.3D) compared to the corresponding tongue regions of the *Cre*$^{-}$*/Nf2*$^{fx/fx}$ littermates (Fig. 4.3A, D).

At E15.5, the anterior oral tongue mesenchyme of the *Wnt1-Cre/Nf2*^{cKO} mutant had a significantly lower level of p-Yap (Fig. 4.3B; $p<0.05$ in Fig. 4.3E) than the corresponding region of the *Cre*$^{-}$*/Nf2*$^{fx/fx}$ littermates (Fig. 4.3B, E). However, no significant changes of p-Yap level were detected in the posterior oral tongue mesenchyme of E15.5 *Wnt1-Cre/Nf2*^{cKO} mutants (Fig. 4.3B; $p>0.05$ in Fig. 4.3E) compared to *Cre*$^{-}$*/Nf2*$^{fx/fx}$ littermates. In contrast to p-Yap, Yap was

detected at a significantly low level in both posterior and anterior oral tongue mesenchyme of E15.5 *Wnt1-Cre/Nf2*^{cKO} mutants (Fig. 4.3B; p<0.01 in Fig. 4.3E) compared to the respective regions of *Cre*$^{-}$*/Nf2*$^{fx/fx}$ littermates. At E18.5, no significant changes in p-Yap or Yap level were detected in the tongue mesenchyme of *Wnt1-Cre/Nf2*^{cKO} mutants (Fig. 4.3C; p>0.05 in Fig. 4.3F) compared to the *Cre*$^{-}$*/Nf2*$^{fx/fx}$ littermates.

To understand the effects of altered Hippo signaling activity in the *Wnt1-Cre/Nf2*^{cKO} mutant mesenchyme, cell proliferation was analyzed in *Wnt1-Cre/Nf2*^{cKO} mutants at multiple stages. We found distinct alterations in different tongue regions at different stages. At E12.5, more BrdU^{+} cells were observed in the posterior (Fig. 4.4B$_1$; p<0.05 in Fig. 4.4C), however fewer in the anterior (Fig. 4.4B$_2$; p<0.05 in Fig. 4.4C), oral tongue mesenchyme of the *Wnt1-Cre/Nf2*^{cKO} mutants (p<0.05, Fig. 4.4B) compared to the *Cre*$^{-}$*/Nf2*$^{fx/fx}$ littermate control (Fig. 4.4A). No obvious changes in the number of BrdU^{+} cells were seen in the tongue epithelium of E12.5 *Wnt1-Cre/Nf2*^{cKO} mutants (Fig. 4.4B; p>0.05 in Fig. 4.4C) compared to the *Cre*$^{-}$*/Nf2*$^{fx/fx}$ littermates (Fig. 4.4A)

At E15.5, a significantly higher amount of BrdU^{+} cells were detected in the epithelium (Epi in Fig. 4.5B; Fig. 4.5B$_2$, B$_4$; p<0.05 in Fig. 4.5C) and mesenchyme just beneath the epithelium (Mes1 in Fig. 4.5B; Fig. 4.5B$_2$, B$_4$; p<0.05 in Fig. 4.5C) of the posterior (Fig. 4.5B$_2$) and anterior (Fig. 4.5B$_4$) oral tongue as compared to the corresponding regions of the *Cre*$^{-}$*/Nf2*$^{fx/fx}$ littermates (Epi and Mes1 in Fig. 4.5A; Fig. 4.5A$_2$, A$_4$). In contrast, a significantly lower amount of BrdU^{+} cells were detected in the deeper layers of the posterior (Fig. 4.5B$_1$; p<0.05 in Fig. 4.5C) and anterior (Fig. 4.5B$_3$; p<0.05 in Fig. 4.5C) oral tongue mesenchyme of the *Wnt1-Cre/Nf2*^{cKO} mutants (Mes2 in Fig. 4.5B) compared to the corresponding deeper layers of the posterior (Fig. 4.5A$_1$) and anterior (Fig. 4.5A$_3$) *Cre*$^{-}$*/Nf2*$^{fx/fx}$ littermate control oral tongue mesenchyme (Mes2 in Fig. 4.5A).

At E18.5, a significantly lower number of BrdU^{+} cells was detected in both posterior (Fig. 4.6B$_1$) and anterior (Fig. 4.6B$_2$) oral tongue regions in the *Wnt1-Cre/Nf2*^{cKO} mutants (Fig. 4.6B)

compared to the *Cre*$^{-}$*/Nf2*$^{fx/fx}$ littermate controls (Fig. 4.6A, A_1, and A_2). Unlike E15.5, all three layers (i.e., Epi, Mes1, and Mes2) of E18.5 *Wnt1-Cre/Nf2*^{cKO} mutants had a significantly lower number of BrdU^{+} cells (Fig. 4.6B; p<0.01 in Fig. 4.6C) compared to those of *Cre*$^{-}$*/Nf2*$^{fx/fx}$ littermate tongues (Epi, Mes1, and Mes2 in Fig. 4.6A). Collectively E18.5 *Wnt1-Cre/Nf2*^{cKO} mutants had significantly low BrdU^{+} cells in the oral tongue mesenchyme compared to the *Cre*$^{-}$*/Nf2*$^{fx/fx}$ littermate control tongue (p<0.01 in Fig. 4.6C).

4.4.4 Mesenchymal *Nf2 cKO* results in alterations of tongue primordium (branchial arches)

To understand where *Nf2* is expressed in the tongue primordia (i.e., branchial arches 1-4/ BAs 1-4), *Nf2* in situ hybridization was performed in E10.5 BAs. Our results revealed that in *Cre*$^{-}$*/Nf2*$^{fx/fx}$ littermate controls *Nf2* mRNA transcripts were abundantly distributed in all four BAs that eventually give rise to the developing tongue (Fig. 4.7A). In contrast, *Nf2* transcripts were absent in the corresponding regions of all four BAs in *Wnt1-Cre/Nf2*^{cKO} mutants (Fig. 4.7B). Similar to *Cre*$^{-}$*/Nf2*$^{fx/fx}$ littermate controls (Fig. 4.7C), all four BAs (n = 3) were developed in the *Wnt1-Cre/Nf2*^{cKO} mutants (Fig. 4.7D). However, the distance between the lateral edges of the each of BAs was significantly narrower in *Wnt1-Cre/Nf2*^{cKO} mutants (Fig. 4.7D, p<0.05 in Fig. 4.7E) compared to those of *Cre*$^{-}$*/Nf2*$^{fx/fx}$ littermate controls (Fig. 4.7C).

To understand the potential cause of the alteration of tongue shape and size, we examined the Hippo signaling activity in BAs 1-4 of *Wnt1-Cre/Nf2*^{cKO} mutants and *Cre*$^{-}$*/Nf2*$^{fx/fx}$ littermate controls. The downstream transcriptional regulators of Hippo signaling, i.e., Yap and p-Yap, were both detected in the *Wnt1-Cre/Nf2*^{cKO} mutants and *Cre*$^{-}$*/Nf2*$^{fx/fx}$ littermate control BAs (Fig. 4.7F). No significant differences in Western blot band intensities of p-Yap and Yap were detected in the BAs between *Cre*$^{-}$*/Nf2*$^{fx/fx}$ littermate control and *Wnt1-Cre/Nf2*^{cKO} mutants (Fig. 4.7F; p>0.05 in Fig. 4.7G).

To understand the relevance of cell proliferation with the Hippo signaling activity, changes in cell proliferation (Fig. 4.7H) were analyzed in all four BAs of E10.5 *Wnt1-Cre/Nf2*^{cKO} mutants

and *Cre⁻/Nf2$^{fx/fx}$* littermate controls. Distinct alterations of cell proliferation were seen in different BAs. The BA1 and BA2 of *Wnt1-Cre/Nf2^{cKO}* mutants had a significantly lower number of BrdU^{+} cells (Fig. 4.7H$_5$, H$_6$; p<0.01 in Fig. 4.7I) than that of *Cre⁻/Nf2$^{fx/fx}$* littermate controls (Fig. 4.7H$_1$, H$_2$). However, in the BA3 and BA4 *Wnt1-Cre/Nf2^{cKO}* mutants had a significantly higher number of BrdU^{+} cells (Fig. 4.7H$_7$, H$_8$; p<0.01 in Fig. 4.7I) compared to the *Cre⁻/Nf2$^{fx/fx}$* littermate controls (Fig. 4.7H$_3$, H$_4$).

4.5 Discussion

Our present study demonstrated that the absence of Neurofibromin 2 (Nf2)/Merlin in the neural crest derived-mesenchyme leads to macroglossia at early (E12.5-E13.5) and microglossia at later (E15.5-E18.5) stages of embryonic tongue development. The tongue deformity (i.e., pointed anterior oral tongue and wider posterior oral tongue) along the anteroposterior axis and distinct changes in the Nf2/Hippo signaling activity accompanied by changes in cell proliferation in different regions of the *Wnt1-Cre/Nf2^{cKO}* mutant tongue indicate that neural crest-derived mesenchymal cells in developing tongue respond to the absence of Nf2/Hippo singling in a region- and stage-specific manner. Overall, our results indicated that Nf2/Hippo signaling activity in neural crest-derived mesenchyme plays an essential role in regulating cell proliferation for the proper development of tongue shape and size.

4.5.1 Nf2/Hippo signaling activity in the neural crest-derived mesenchyme regulates tongue organogenesis in a stage-specific manner

Neural crest cells migrate into the tongue primordium (i.e., branchial arches) at early embryonic stages (Chen et al., 2017; Cobourne et al., 2019) and fully occupy the mesenchyme of the tongue bud (Han et al., 2012). Structural and molecular integrity of the neural crest (NC) and NC-derived cells in the tongue primordium is critical for proper tongue organ development. As an example, the absence of primary cilia in NC cells causes aglossia (Millington et al., 2017). Deficient molecular signaling such as BMP (Ishan et al., 2020), TGF-β (Han et al., 2012; Hosokawa et al., 2010; Iwata et al., 2013) and Wnt (Liu et al., 2009; Liu et al., 2012b; Zhong et

al., 2015; Zhu et al., 2017) result in microglossia due to defects in structural organization and cell migration in the developing tongue. In the present study, we report the importance of Nf2/Hippo signaling in NC and NC-derived tongue mesenchymal cells for proper tongue organogenesis.

Neurofibromin 2 (Nf2) is considered a tumor suppressor gene that activates the Hippo signaling pathway through its gene product known as merlin (Sourbier et al., 2018). In the normal cellular conditions, merlin recruits mammalian sterile 20-like protein kinase (Mst1/2), a large tumor suppressor (Lats1/2), and adaptor protein Salvador (Salv) to activate the Hippo signaling pathway by phosphorylating the transcriptional activator Yes-associated protein (Yap) (Boopathy and Hong, 2019; Kim and Jho, 2018). Phosphorylation causes Yap to remain in the cytoplasm and prevents the transcription of proliferation and apoptotic genes (Mia et al., 2016). On the other hand, the absence of *Nf2* results in the lack of merlin, hence prevents Yap from phosphorylation and promotes the nuclear translocation of Yap to transcribe cell proliferation specific genes (Mia et al., 2016).

In most organs, the absence of Nf2/Hippo signaling causes an enhanced organ growth (Yu et al., 2015a; Yu and Guan, 2013). i.e., liver-specific genetic knockout of *Mst1/2*, *Sav1*, *Nf2* or over-expression of *Yap* resulted in an enlarged liver (Camargo et al., 2007b; Dong et al., 2007; Yin et al., 2013; Zhang et al., 2010), deletion of *Sav1*, *Mst1/2*, or *Lats1/2* caused a hyperproliferation and enlarged heart (Del Re et al., 2013; Heallen et al., 2011; Lin et al., 2014; von Gise et al., 2012; Xin et al., 2013; Xin et al., 2011). However, our data indicate that Nf2/Hippo signaling regulates tongue organogenesis in a stage-specific manner. The primordia (BAs) of the tongue organ were narrower at E10.5 and lingual swellings were less profound in *Wnt1-Cre/Nf2*^{cKO} mutants. At E12.5-E13.5, deletions of *Nf2* in NC lineage driven by *Wnt1-Cre* lead to a non-proportionally enlarged tongue, i.e., macroglossia, with a widened posterior region and pointed tip at E12.5-E16.5. At E18.5, in contrast to many other organs, we observed a

smaller tongue (microglossia) suggesting that the effects of altered Nf2/Hippo signaling activity are distinct in different organs.

4.5.2 Mesenchymal Nf2/Hippo signaling regulates cell proliferation in a stage- and tongue region-specific manner.

As aforementioned, Nf2/Hippo signaling serve as a cell proliferation suppressor (Xiao et al., 2005). To understand the stage-specific alterations of tongue shape and size in *Wnt1-Cre/Nf2*^{cKO} mice, we analyzed the levels of Yap and p-Yap, and cell proliferation in different tongue region and tissue types at various stages. We detected regional and dynamic changes of Yap and p-Yap level over the developmental course, and found that cell proliferation was altered corresponding to the Yap level as the Yap typically promotes cell proliferation (Camargo et al., 2007a; Pan, 2010; Panciera et al., 2016). For examples, in the E12.5 *Wnt1-Cre/Nf2*^{cKO} mutants, a high Yap level was concurrent with more proliferative cells in the posterior oral tongue where the tongue is wider, and low Yap level with less proliferative cells in the anterior oral tongue where the tongue is smaller and more pointed.

Notably, at later stages of tongue development (E15.5-E18.5) the loss of *Nf2* in the NC lineage paradoxically resulted in decreased cell proliferation (reduced Yap level) thus resulting in a smaller tongue (i.e., microglossia) in *Wnt1-Cre/Nf2*^{cKO} mutants compared to the *Cre*$^{-}$*/Nf2*$^{fx/fx}$ littermates. Even though cell proliferation was reduced as a whole in the E15.5 *Wnt1-Cre/Nf2*^{cKO} mutants, different tissue compartments had significantly different numbers of BrdU^{+} cells in the *Wnt1-Cre/Nf2*^{cKO} mutants, for example, the increased vs decreased cell proliferation in the shallow and deep layer of mesenchyme respectively. Increase cell proliferation noticed in the mesenchyme layer subjacent to the epithelium is self-explanatory as the majority of the cells populated in this region retain their NC linage and as a result, Hippo signaling might have been inactivated hence promoting the cell proliferation.

To understand the cause for the tongue deformity along the anterior-posterior axis, we analyzed BrdU^{+} proliferative cells in E10.5 BAs of *Wnt1-Cre/Nf2*^{cKO} mutant and *Cre*$^{-}$*/Nf2*$^{fx/fx}$

littermate control mice, since inactivation of Hippo signaling leads to increased cell proliferation. Even though individual BAs of *Wnt1-Cre/Nf2*^{cKO} mutant mice had no significant changes of levels of Hippo signaling downstream transcriptional regulator Yap and deactivated form p-Yap, significantly different amounts of BrdU^{+} cells suggest that cell proliferation is very sensitive and responded to subtle yet undetectable changes of Yap and p-Yap levels in individual BAs of *Wnt1-Cre/Nf2*^{cKO} mutant. Consequently, a low number of proliferative cells in BAs 1-2 and more proliferative cells in BAs 3-4 might be the reason to have a pointed anterior tongue and widened posterior tongue since BA 1-2 give rise to the anterior tongue and BA 3-4 give rise to the posterior tongue (Cobourne et al., 2019) respectively. It is also possible that the initial formation of lingual swellings at E11.5 was deficient on the *Wnt1-Cre/Nf2*^{cKO} mutant as a result of low amount proliferative cells in BA1-2. It is important to note that E10.5 *Wnt1-Cre/Nf2*^{cKO} mutant BAs are smaller compared to the corresponding BAs of *Cre*$^{-}$*/Nf2*$^{fx/fx}$ littermates. Smaller BAs at E10.5 and deficient tongue swellings at E11.5 indicate that deficient Nf2/Hippo signaling affects the initial tongue formation due to the reduced cell proliferation.

It is possible that the effects of *Nf2* deletion on other signaling pathways oppose or reverse the effects of diminished Hippo signaling in the tongue compared to those in other organs that caused an enlarged organ. For instance, Wnt5a/non-canonical Wnt signaling has been reported to be important for tongue outgrowth (Liu et al., 2012b) and is likely to be involved in the regulatory role of Nf2/Hippo signaling in tongue mesenchyme in promoting tongue formation. Moreover, tongue mesenchyme acts as a scaffold for the organization of migrating myoblasts into the myogenic cord and operates as a niche that releases molecular instructions (e.g., TGF-β2) to direct survival, proliferation, and differentiation of myogenic progenitors, as well as patterning of muscle fibers (Parada and Chai, 2015; Parada et al., 2012). Thus, disrupted myogenesis might be another cause of microglossia observed in *Wnt1-Cre/Nf2*^{cKO} mutants at E15.5-E18.5.

4.5.3 Mesenchymal deletion of *Nf2* alters the development of overlying tongue epithelium.

It is intriguing that although the genetic deletion of *Nf2* driven by *Wnt1-Cre* is supposed to be largely tongue mesenchyme-specific (Liu et al., 2012a; Thirumangalathu et al., 2009), however, a lack of *Nf2* expression in the tongue epithelium was noticed in *Wnt1-Cre/Nf2*^{cKO} mice. Consistently to the reduced *Nf2* level, a higher number of proliferative cells was found in the epithelium of the E15.5 *Wnt1-Cre/Nf2*^{cKO} mutant tongue compared to the *Cre*$^{-}$*/Nf2*$^{fx/fx}$ littermates. Our data suggest that Nf2/Hippo signaling in the mesenchyme plays an important role in the mesenchymal-epithelial interactions. Further studies are important to address whether and how the development of tongue epithelial appendages including taste papillae and taste buds is affected in the mesenchymal *Nf2 cKO*.

Overall, we provide evidence that Nf2/Hippo signaling in the NC and NC-derived mesenchyme plays an essential role in tongue organogenesis. Further, our results suggest that mesenchymal Nf2 regulates Hippo signaling and cell proliferation in a stage- and tongue region-specific manner, and that continuous expression of *Nf2* NC-derived mesenchymal cells is required for the proper tongue formation in shape and size.

4.6 Acknowledgements

This study was supported by the National Institute on Deafness and other Communication Disorders (NIDCD), National Institutes of Health, grant number R01DC012308 and R21DC018089 to HXL. The authors acknowledge the assistance of the Biomedical Microscopy Core at the University of Georgia with imaging using a Zeiss LSM 710 confocal microscope.

Table 4.1 Primary antibodies used for immunohistochemistry or western blot.

Primary antibody	Source (catalog number, company)	Dilution
Rabbit anti p-Yap	#4911, Cell Signaling Technology, Danvers, M	1:5000
Rabbit anti Yap	#4912S, Cell Signaling Technology, Danvers, MA	1:5000
Mouse anti Gapdh	G8795, Sigma Aldrich, St Louis, MO	1:10,000
Goat anti β-actin	Ab8229, Abcam, Cambridge, United Kingdom	1:10,000
Rat anti BrdU	MCA2060, Bio Rad, Hercules, CA	1:500
Goat anti E-cadherin	AF748, R&D systems, Minneapolis, MN	1:1000
Rabbit anti Krt5	PVB-160P, Covance, Emeryville CA	1:5000

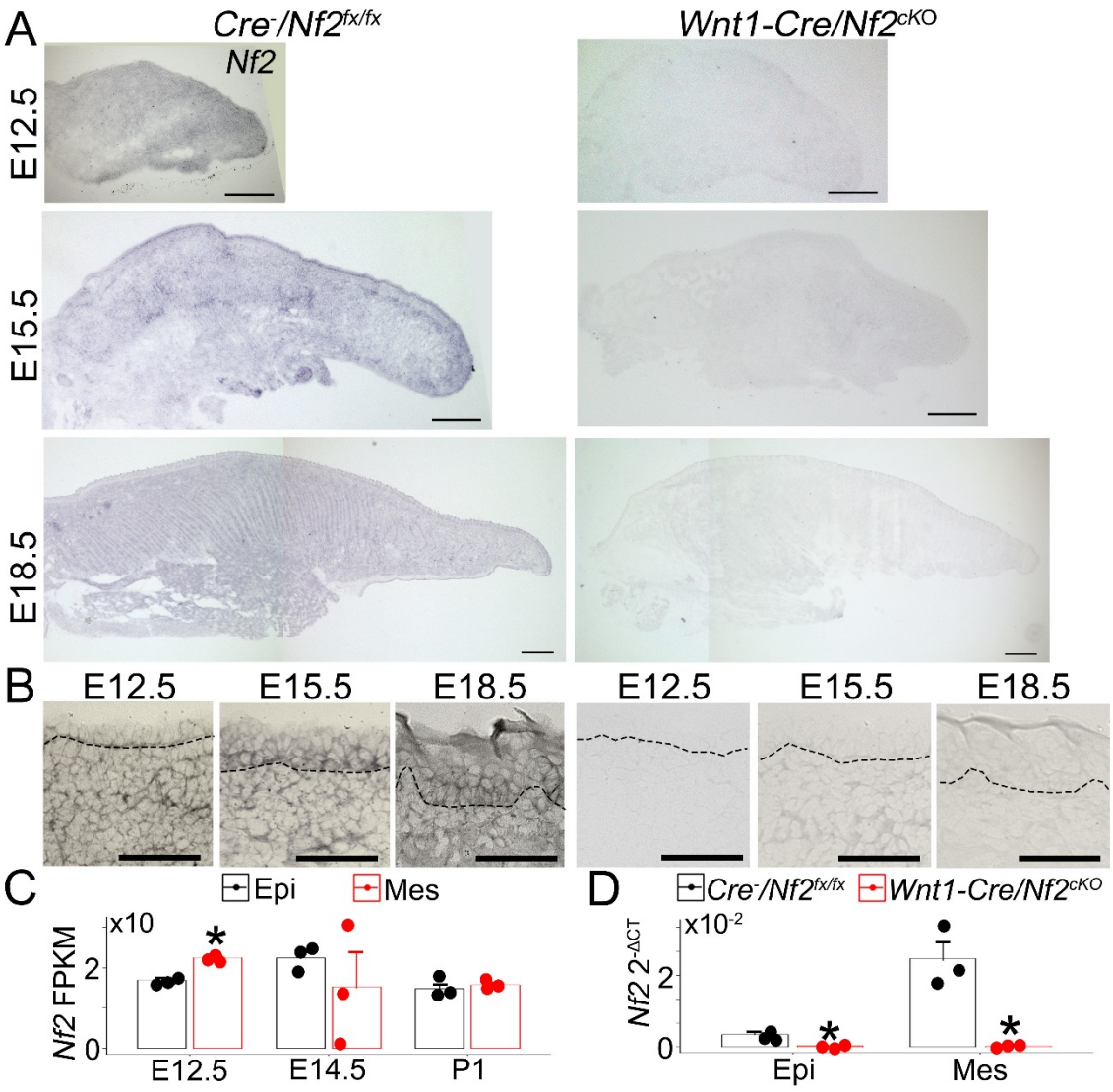
A
Cre-/Nf2fx/fx
Wnt1-Cre/Nf2cKO
Nf2
E12.5
E15.5
E18.5
B
E12.5
E15.5
E18.5
E12.5
E15.5
E18.5
C
Epi
Mes
x10
Nf2 FPKM
2
0
E12.5
E14.5
P1
D
Cre-/Nf2fx/fx
Wnt1-Cre/Nf2cKO
x10-2
Nf2 2-ΔCT
2
0
Epi
Mes

Figure 4.1. A-B: Representative low (A) and high (B) magnification light microscopy images of E12.5, E15.5, and E18.5 tongue sections from *Cre^{-}/Nf2$^{fx/fx}$* littermate control and *Wnt1-Cre/Nf2^{cKO}* mutants. *In situ* hybridization was performed using an antisense probe for Nf2. Dashed lines in B separate the epithelium form the mesenchyme. Scale bars: 100 μm in A; 25 μm in B. **C-D**: Histograms (X±SD; n=3) to represent the Fragments Per Kilobase of transcripts per Million mapped reads(FPKM) in wild type (C) or $2^{-\Delta CT}$ values of *Nf2* gene transcripts (D) in *Cre^{-}/Nf2$^{fx/fx}$* littermate control, and *Wnt1-Cre/Nf2^{cKO}* mutant tongue epithelium (Epi) and mesenchyme (Mes). *$p \leq 0.05$, **$p \leq 0.01$ compared to the corresponding tissues of *Cre^{-}/Nf2$^{fx/fx}$* littermate control using two-way ANOVA followed by Fisher's least significant difference (LSD) analyses.

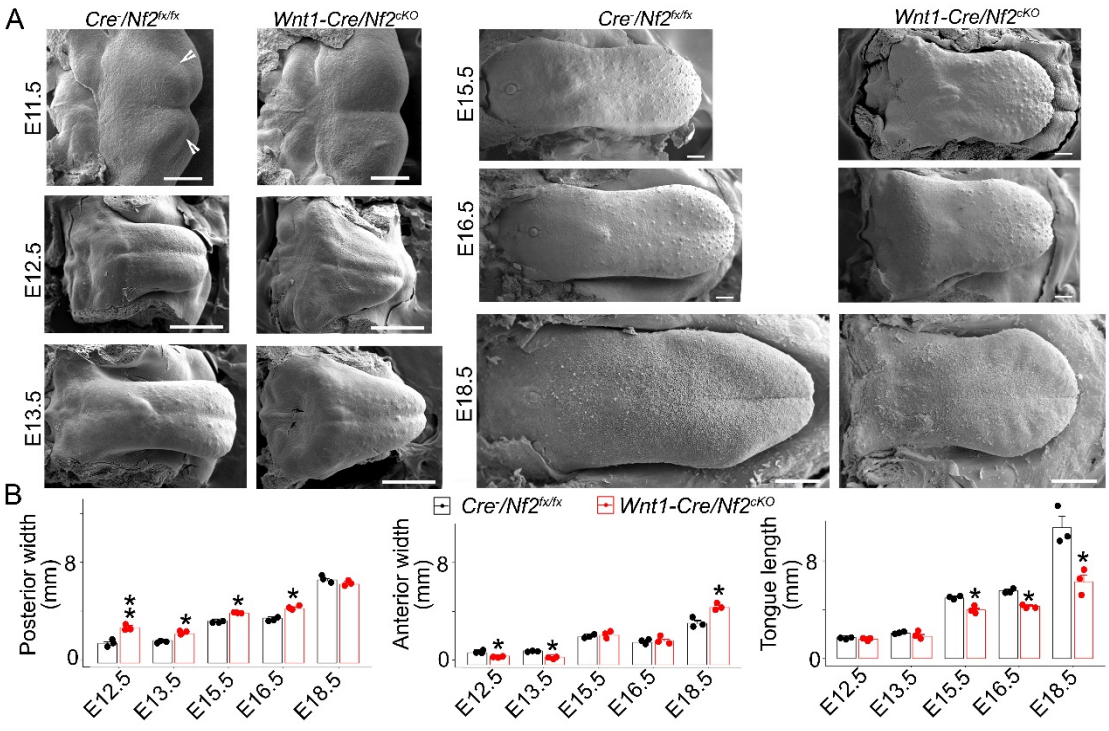
A
Cre-/Nf2fx/fx
Wnt1-Cre/Nf2cKO
Cre-/Nf2fx/fx
Wnt1-Cre/Nf2cKO
E11.5
E12.5
E13.5
E15.5
E16.5
E18.5
B
Cre-/Nf2fx/fx
Wnt1-Cre/Nf2cKO
Posterior width (mm)
Anterior width (mm)
Tongue length (mm)
0
8
E12.5
E13.5
E15.5
E16.5
E18.5

Figure 4.2. A: Representative Scanning electron microscopy (SEM) images of tongues on mandible in *Cre^{-}/Nf2$^{fx/fx}$* littermate control and *Wnt1-Cre/Nf2^{cKO}* embryos at E11.5, E12.5, E13.5, E15.5, E16.5, and E18.5. Open arrowheads point to tongue swellings. Scale bars: 200 µm. **B**: Histograms (X±SD; n=3) to present the width of the anterior and posterior oral tongue and length of the oral tongue in *Cre^{-}/Nf2$^{fx/fx}$* littermate controls and *Wnt1-Cre/Nf2^{cKO}* mutants. **p*≤0.05, ***p*≤0.01 Student's *t*-test compared to *Cre^{-}/Nf2$^{fx/fx}$* littermate control group.

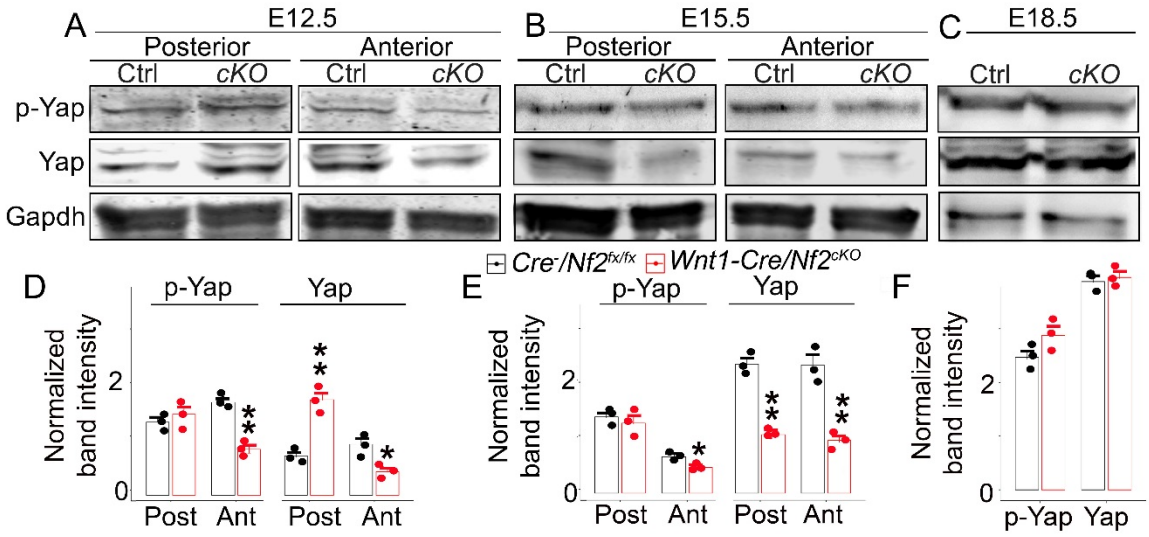
A
E12.5
Posterior
Anterior
Ctrl
cKO
Ctrl
cKO
p-Yap
Yap
Gapdh
B
E15.5
Posterior
Anterior
Ctrl
cKO
Ctrl
cKO
C
E18.5
Ctrl
cKO
Cre-/Nf2fx/fx
Wnt1-Cre/Nf2cKO
D
p-Yap
Yap
Normalized band intensity
2
0
Post
Ant
Post
Ant
E
p-Yap
Yap
Normalized band intensity
2
0
Post
Ant
Post
Ant
F
Normalized band intensity
2
0
p-Yap
Yap

Figure 4.3. A-C: Western blot bands of p-Yap, Yap, and Gapdh in the E12.5 (A), E15.5 (B), and E18.5 (C) tongue mesenchyme from the anterior (Ant) and posterior (Post) oral tongue (E12.5 and E15.5) or entire tongue (E18.5) of *Cre^{-}/Nf2$^{fx/fx}$* littermate controls (Ctrl) and *Wnt1-Cre/Nf2^{cKO}* mutants (*cKO*). D-F: Histograms (X±SD; n=3) to present the normalized band intensities of p-Yap and Yap with respect to the Gapdh in the E12.5 (D), E15.5 (E), and E18.5 (F) tongue mesenchyme. *p≤0.05, **p≤0.01 Student's t-test compared to *Cre^{-}/Nf2$^{fx/fx}$* littermate control group.

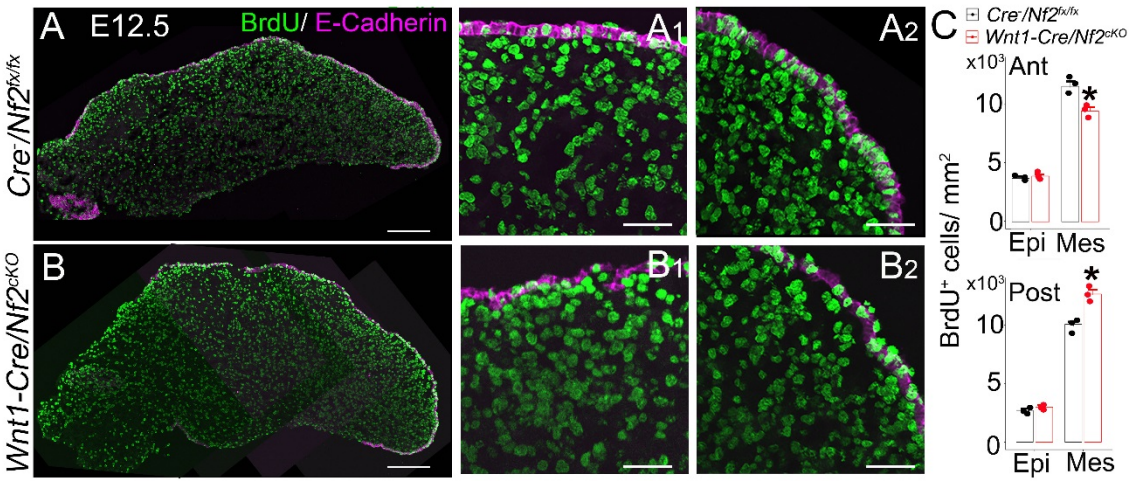
A E12.5
BrdU/ E-Cadherin
A1
A2
Cre-/Nf2fx/fx
B
B1
B2
Wnt1-Cre/Nf2cKO
C
Cre-/Nf2fx/fx
Wnt1-Cre/Nf2cKO
x10³
Ant
10
5
0
Epi Mes
BrdU⁺ cells/ mm²
x10³
Post
10
5
0
Epi Mes

Figure 4.4. A-B: Single-plane laser scanning confocal images of tongue sections in E12.5 *Cre^{-}/Nf2$^{fx/fx}$* littermate control (A) and *Wnt1-Cre/Nf2^{cKO}* (B) mutants. Sections were immunoreacted with cell proliferation marker BrdU (green) and, epithelial cell marker E-cadherin (magenta). $A_{1\text{-}2}$ and $B_{1\text{-}2}$ are high magnification images of the posterior (A_1, B_1) and anterior (A_2, B_2) oral tongue regions. Scale bars: 200 µm in A-B; 50 µm in $A_{1\text{-}2}$, $B_{1\text{-}2}$. **C**: Histograms (X±SD; n=3) to represent the number of $BrdU^+$ cells per mm^2 in the anterior (Ant) and posterior (Post) oral tongues of *Cre^{-}/Nf2$^{fx/fx}$* littermate control and *Wnt1-Cre/Nf2^{cKO}* mutants. **p*≤0.05, ***p*≤0.01 compared to the corresponding regions of *Cre^{-}/Nf2$^{fx/fx}$* littermate control using two-way ANOVA followed by Fisher's LSD analyses.

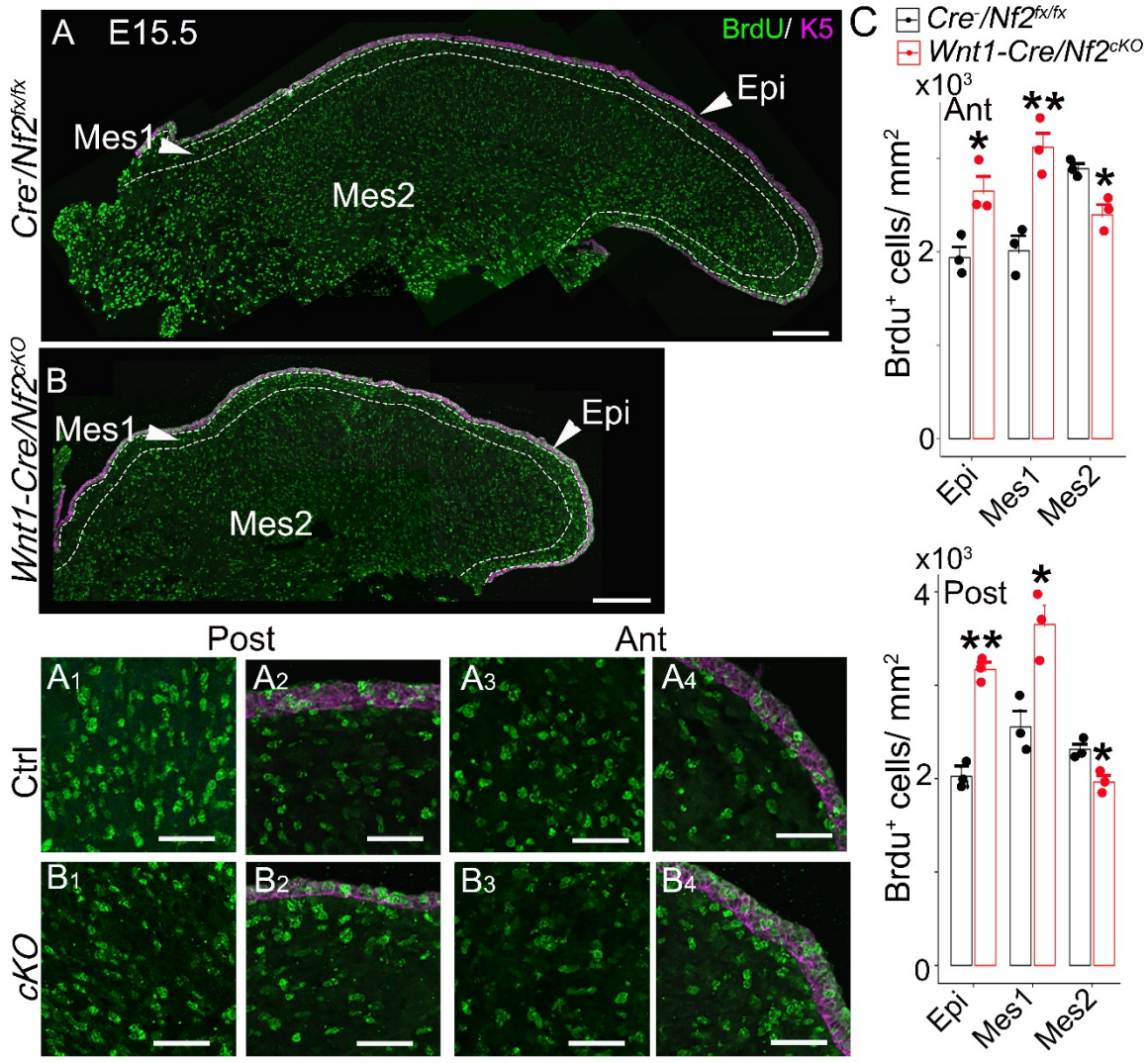
A E15.5
BrdU/ K5
Epi
Mes1
Mes2
Cre-/Nf2fx/fx
B
Mes1
Epi
Mes2
Wnt1-Cre/Nf2cKO
Post
Ant
A1
A2
A3
A4
Ctrl
B1
B2
B3
B4
cKO
C
Cre-/Nf2fx/fx
Wnt1-Cre/Nf2cKO
x10³
Ant
Brdu⁺ cells/ mm²
0
2
Epi
Mes1
Mes2
x10³
4
Post
Brdu⁺ cells/ mm²
0
2
Epi
Mes1
Mes2

Figure 4.5. A-B: Single-plane laser scanning confocal images of tongue sections in E15.5 *Cre^{-}/Nf2$^{fx/fx}$* littermate control (Ctrl, A) and *Wnt1-Cre/Nf2^{cKO}* (*cKO*, B) mutants. Sections were immunoreacted with cell proliferation marker BrdU (green) and, basal epithelial cell marker K5 (magenta). $A_{1\text{-}4}$ and, $B_{1\text{-}4}$ are high magnification images of the posterior ($A_{1\text{-}2}$, $B_{1\text{-}2}$) and anterior ($A_{3\text{-}4}$, $B_{3\text{-}4}$) oral tongue regions. Epi: epithelium (A_2, B_2, and, A_4, B_4), Mes1: mesenchyme layer just beneath the epithelium (A_2, B_2, and A_4, B_4), Mes2: deeper mesenchymal layers (A_1, B_1 and, A_3, B_3) of the posterior (A_1, B_1) and anterior (A_3, B_3) oral tongue. Scale bars: 200 µm in A-B; 50 µm in $A_{1\text{-}4}$ and, $B_{1\text{-}4}$. **C**: Histograms (X±SD; n=3) to represent the number of BrdU^{+} cells per mm^2 in the anterior (Ant) and posterior (Post) oral tongue epithelium and mesenchyme of *Cre^{-}/Nf2$^{fx/fx}$* littermate control and *Wnt1-Cre/Nf2^{cKO}* mutants. *$p \leq 0.05$, **$p \leq 0.01$ compared to the corresponding regions of *Cre^{-}/Nf2$^{fx/fx}$* littermate control using two-way ANOVA followed by Fisher's LSD analyses.

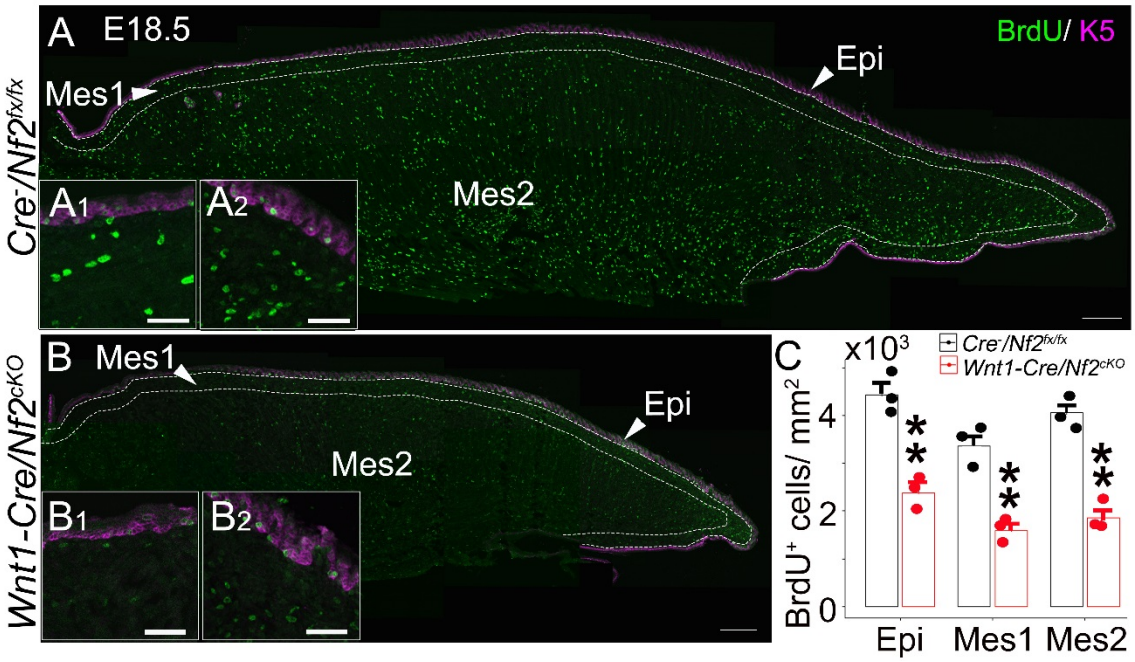
A E18.5
BrdU/ K5
Epi
Mes1
Mes2
A1
A2
Cre-/Nf2fx/fx
B Mes1
Epi
Mes2
B1
B2
Wnt1-Cre/Nf2cKO
C
x10^3
Cre-/Nf2fx/fx
Wnt1-Cre/Nf2cKO
BrdU+ cells/ mm2
0
2
4
Epi
Mes1
Mes2

Figure 4.6. A-B: Single-plane laser scanning confocal images of tongue sections in E18.5 *Cre^{-}/Nf2$^{fx/fx}$* littermate control (A) and *Wnt1-Cre/Nf2^{cKO}* (B) mutants. Sections were immunoreacted with cell proliferation marker BrdU (green) and, basal epithelial cell marker K5 (magenta). Insets $A_{1\text{-}2}$ and, $B_{1\text{-}2}$ are high magnification images of the posterior (A_1, B_1) and anterior (A_2, B_2) oral tongue regions. Epi: epithelium, Mes1: mesenchyme layer just beneath the epithelium, Mes2: deeper mesenchymal layers. Scale bars: 200 µm in A-B; 50 µm in $A_{1\text{-}4}$ and, $B_{1\text{-}4}$. **C**: Histogram (X±SD; n=3) to represent the number of BrdU^{+} cells per mm^2 in the tongue epithelium and mesenchyme of *Cre^{-}/Nf2$^{fx/fx}$* littermate control and *Wnt1-Cre/Nf2^{cKO}* mutants. **p*≤0.05, ***p*≤0.01 compared to the corresponding regions of *Cre^{-}/Nf2$^{fx/fx}$* littermate control using two-way ANOVA followed by Fisher's LSD analyses.

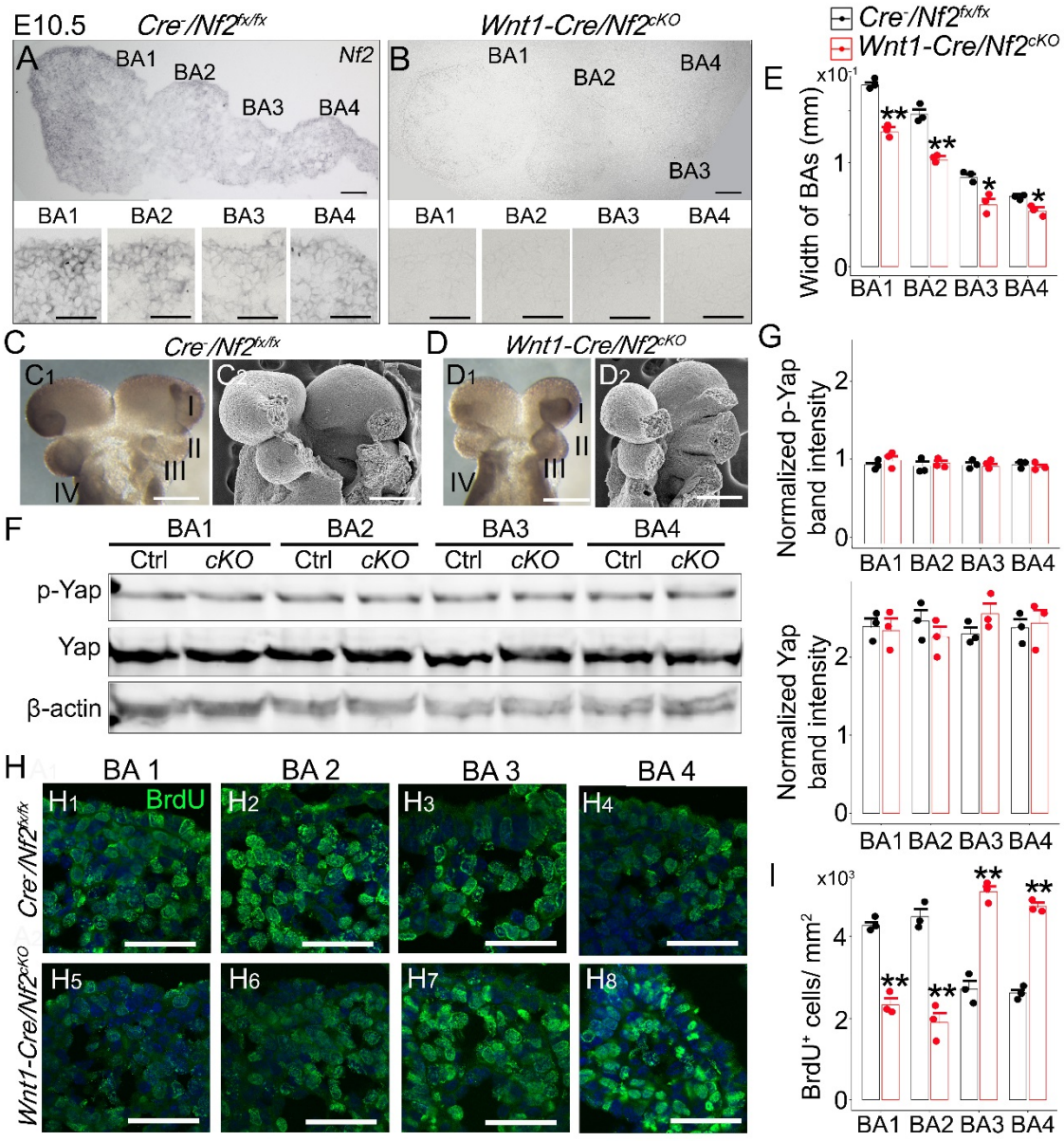
E10.5
Cre-/Nf2fx/fx
Wnt1-Cre/Nf2cKO
A
BA1
BA2
BA3
BA4
Nf2
B
BA1
BA2
BA4
BA3
BA1 BA2 BA3 BA4
BA1 BA2 BA3 BA4
E
Cre-/Nf2fx/fx
Wnt1-Cre/Nf2cKO
x10-1
Width of BAs (mm)
1
0
BA1 BA2 BA3 BA4
C
Cre-/Nf2fx/fx
D
Wnt1-Cre/Nf2cKO
C1
C2
D1
D2
I
II
III
IV
G
Normalized p-Yap band intensity
2
1
0
BA1 BA2 BA3 BA4
F
BA1
BA2
BA3
BA4
Ctrl
cKO
Ctrl
cKO
Ctrl
cKO
Ctrl
cKO
p-Yap
Yap
β-actin
Normalized Yap band intensity
2
1
0
BA1 BA2 BA3 BA4
H
BA 1
BA 2
BA 3
BA 4
Cre-/Nf2fx/fx
Wnt1-Cre/Nf2cKO
H1
BrdU
H2
H3
H4
H5
H6
H7
H8
I
x103
BrdU+ cells/ mm2
4
2
0
BA1 BA2 BA3 BA4

Figure 4.7. A-B: Light microscopy images of sections of E10.5 branchial arches (BAs) from a *Cre^{-}/Nf2$^{fx/fx}$* littermate control (A) and *Wnt1-Cre/Nf2^{cKO}* mutant (B). *In situ* hybridization was performed using an antisense probe for *Nf2*. In the bottom panel in A and B are high magnification images of the individual BAs. Scale bars: 25 µm. **C-D:** Whole-mount images (sonic hedgehog (Shh) immunostained light microscopy in C_1, D_1, and SEM in C_2, D_2) of the *Cre^{-}/Nf2$^{fx/fx}$* littermate control (C) and *Wnt1-Cre/Nf2^{cKO}* (D) BAs. Roman numerals I-IV in C_1 and D_1 represent BAs 1-4. Scale bar: 200 µm. **E:** Histogram (X±SD; n=3) to represent the distance between the lateral edges of the each of BAs in *Cre^{-}/Nf2$^{fx/fx}$* littermate controls and *Wnt1-Cre/Nf2^{cKO}* mutants. *$p \leq 0.05$, **$p \leq 0.01$ Student's *t*-test compared to *Cre^{-}/Nf2$^{fx/fx}$* littermate control group. **F**: Western blot bands of p-Yap, Yap, and β-actin in the mesenchyme of individual BAs from *Cre^{-}/Nf2$^{fx/fx}$* littermate controls and *Wnt1-Cre/Nf2^{cKO}* mutants. **G**: Histograms (X±SD; n=3) represent the normalized band intensities of p-Yap and Yap with respect to the β-actin. *$p \leq 0.05$, **$p \leq 0.01$ Student's *t*-test compared to *Cre^{-}/Nf2$^{fx/fx}$* littermate control group. **H**: Single-plane laser scanning confocal images of sagittal BA sections immunostained with cell proliferation marker BrdU (green) in *Cre^{-}/Nf2$^{fx/fx}$* littermate control (H_{1-4}) and *Wnt1-Cre/Nf2^{cKO}* mice (H_{5-8}). Scale bars: 50 µm. **I**: Histogram (X±SD; n=3) represents the number of $BrdU^{+}$ cells per mm^2 in individual BAs of *Cre^{-}/Nf2$^{fx/fx}$* littermate controls and *Wnt1-Cre/Nf2^{cKO}* mutants. *$p \leq 0.05$, **$p \leq 0.01$ compared to the corresponding BA of *Cre^{-}/Nf2$^{fx/fx}$* littermate control using two-way ANOVA followed by Fisher's LSD analyses.

CHAPTER 5

CONCLUSIONS AND FUTURE DIRECTIONS

Molecular signaling pathways play essential roles in regulating mesenchymal-epithelial interaction for the proper development of the tongue and taste papillae. In rodents, when initial tongue swellings emerge from the tongue primordium (i.e., the branchial arches), almost all the cells in the mesenchyme are populated by the neural crest (NC) or NC-derived cells. The NC and NC-derived cells will then be replaced by other progenitor cells, such as muscle progenitors, which will then begin to differentiate and form the stereotypical tongue. When the tongue attains its spatulated shape, taste papilla placodes emerge on the epithelium of the tongue. Multiple fungiform papillae form in the anterior oral tongue and a single circumvallate papilla forms in the border between the oral and pharyngeal tongue. From tongue to taste papillae, the entire developmental process is fine-tuned and tightly regulated by multiple molecular signaling pathways. However, our understanding of these molecular signaling pathways and their specific roles is far from complete, particularly of the specific roles played by the underlying mesenchyme in regulating tongue and taste papilla development. In this PhD dissertation, we attempted to explore the specific roles and mechanisms of Type I BMP receptors ALK2 and ALK3 and Neurofibromin 2-mediated Hippo signaling in the mesenchyme in regulating tongue and taste papilla development.

5.1 ALK2-mediated BMP signaling activity in the tongue mesenchyme regulates tongue organogenesis.

In chapter 2, using *Wnt1-Cre*, a transgenic mouse model to constitutively activate Type I BMP receptor *Alk2* (*caAlk2*) in a mesenchyme-specific manner, we found a dramatically smaller (microglossia) and misshapen tongue with a progressively severe reduction in size along the anteroposterior axis. Moreover, the absence of a pharyngeal tongue region and apparent

changes in lingual tissues, including the epithelium, muscle and nerve fibers, were also observed in *Wnt1-Cre/caAlk2* mutants. Based on the results we identified, we can state the following:

1) Appropriate levels of ALK2-BMP signaling activity in the NC and the derived lingual mesenchyme is required for proper tongue organogenesis;
2) ALK2-BMP signaling in NC-derived mesenchyme regulates mesenchymal interactions with other lingual tissues, including the epithelium, muscles, and nerves, governing their development and organization.

5.2 ALK3-mediated BMP signaling activity in the tongue mesenchyme suppresses the secretion of inhibitory secretory proteins and promotes the development of taste papillae.

In chapter 3, to understand the importance of mesenchymal ALK3-mediated BMP (ALK3-BMP) signaling activity in the development of taste papillae, we conditionally knocked out the *Alk3* receptor in the mesenchyme using *Wnt1-Cre* and *Sox10-Cre* mouse models. Both *Wnt1-Cre/Alk3*^{cKO} and *Sox10-Cre/Alk3*^{cKO} mutants had smaller tongues with truncated anterior tips compared to *Cre*$^{-}$*/Alk3*$^{fx/fx}$ littermate controls. Strikingly, in both groups of mutants, an absolute absence of Sonic hedgehog (Shh)$^{+}$ taste papilla placodes was seen at E12.0, the stage in which taste papilla placodes emerge. To explore the underlying mechanisms by which ALK3-BMP signaling in the tongue mesenchyme regulates the development of taste papillae, bulk RNA-Seq analysis was performed on *Wnt1-Cre/Alk3*^{cKO} mutants and *Cre*$^{-}$*/Alk3*$^{fx/fx}$ littermate controls. Our data demonstrated that many more differentially expressed genes (DEGs) were detected in the E12.0 *Wnt1-Cre/Alk3*^{cKO} mutant tongue epithelium than in the tongue mesenchyme, suggesting that ALK3-BMP signaling in the mesenchyme regulates mesenchymal-epithelial interactions for the development of taste papillae. The inhibition of Shh^{+} taste papillae in E12.0 wild-type tongues co-cultured with the *Wnt1-Cre/Alk3*^{cKO} mutant tongue mesenchyme or cultured with mesenchyme-derived conditioned media from *Wnt1-Cre/Alk3*^{cKO} mutant mesenchymal cell

cultures collectively revealed an enhanced secretion of inhibitory factors from the *Wnt1-Cre/Alk3*^{cKO} mutant tongue mesenchyme compared to the *Cre*$^{-}$*/Alk3*$^{fx/fx}$ littermate controls. Furthermore, the absence of Shh^{+} taste papillae in the E12+2D cultures with proteins, but not those with extracellular vesicles or the remainder of the culture constituents that were isolated from the mesenchyme-derived conditioned media isolated from the *Wnt1-Cre/Alk3*^{cKO} mutant mesenchymal cell cultures, confirms that the proteins secreted from the *Wnt1-Cre/Alk3*^{cKO} mutant tongue mesenchyme act as inhibitors of taste papilla development. To identify potential secretory proteins, liquid chromatography-mass spectrometry (LC-MS) analysis was performed on the mesenchyme-derived conditioned media isolated from the *Wnt1-Cre/Alk3*^{cKO} mutants and *Cre*$^{-}$*/Alk3*$^{fx/fx}$ littermate controls. We found Pkm2, a known secretory protein that promotes the breakdown of β-catenin. The Wnt/β-catenin signaling pathway in the epithelium is a known regulator of the development of taste papillae. Next, western blot analyses were performed on the mesenchyme-derived conditioned media isolated from the *Wnt1-Cre/Alk3*^{cKO} mutants and *Cre*$^{-}$*/Alk3*$^{fx/fx}$ littermate controls. We detected Nbl1, a known secretory protein that inhibits the Wnt/β-catenin signaling pathway, at a significantly higher level in *Wnt1-Cre/Alk3*^{cKO} mutant tongue mesenchyme-derived conditioned media than in the *Cre*$^{-}$*/Alk3*$^{fx/fx}$ littermate control group. *Pkm2* and *Nbl1* were also detected in our bulk RNA-Seq analyses as mesenchymal DEGs in the *Wnt1-Cre/Alk3*^{cKO} mutants. Together, our data suggest that ALK3-BMP signaling in the tongue mesenchyme controls and suppresses the secretion of inhibitory secretory proteins, potentially Nbl1 and/or Pkm2, and promotes the development of taste papillae. Furthermore, it is possible that, in the absence of mesenchymal ALK3-BMP signaling activity, these secreted proteins (Nbl1, Pkm2, etc.) either directly or indirectly inhibit the epithelial Wnt/β-catenin signaling pathway and suppress the development of taste papillae.

5.3 Neurofibromatosis 2-mediated Hippo signaling activity in the mesenchyme regulates cell proliferation in a stage- and region-specific manner during tongue organogenesis.

In chapter 4, we conditionally knocked out Neurofibromatosis 2 (NF2) in the tongue mesenchyme using *Wnt1-Cre* and found a larger, misshapen tongue with a wider posterior oral tongue region and pointed anterior tongue tip in the early stages of tongue development (E12.5-E13.5). In contrast, from E15.5 through E18.5, a smaller tongue was observed in the *Wnt1-Cre/Nf2*^{cKO} mutants compared to the *Cre*$^{-}$*/Nf2*$^{fx/fx}$ littermate controls. Hippo signaling activity is a known regulator in organogenesis, which typically restrains cell growth and proliferation through phosphorylating and inhibiting Yap, a transcriptional activator of the Hippo signaling pathway. Interestingly, in the *Wnt1-Cre/Nf2*^{cKO} mutants, we found increased Yap level and increased cell proliferation in the stages and regions where the tongue is larger and wider (i.e., E12.5, posterior oral tongue), indicating that such increased Yap level promotes cell proliferation and, consequently, an enlarged and wider posterior oral tongue. In contrast, we detected decreased Yap level and decreased cell proliferation in the stages and regions where the tongue is smaller and thinner (i.e., E12.5 pointed tongue tip, E15.5-E18.5 tongue), suggesting that decreased Yap level causes decreased cell proliferation. However, no apparent changes in Yap levels were detected in the E10.5 branchial arches (tongue primordium), demonstrating that Nf2 mediated Hippo signaling likely plays a crucial role in tongue shape determination. Collectively, our data indicate that Nf2-mediated Hippo signaling activity in the tongue mesenchyme regulates the cell proliferation in a stage- and region-specific manner and thereby controls tongue size and shape during tongue organogenesis.

5.4 Future directions

Mesenchymal-epithelial interactions are highly context-specific in multiple ways, including direct contact or secreted factors (e.g., soluble proteins/peptides, extracellular vesicles [EVs]). Based on the findings in this dissertation, several important questions arise that future studies should address: (i) What are the mesenchyme-secreted factors (EVs, soluble proteins) under

the control of the ALK3-BMP pathway that regulate epithelial cell differentiation? (ii) What are the specific roles of mesenchymal factors in regulating epithelial cell differentiation? (iii) What are the direct target genes of the ALK3-BMP pathway in tongue mesenchymal cells? (Fig. 5.1)

A comprehensive examination of extracellular vesicles, their carrier substances and dose responses is needed to enhance our understanding of the specific roles and mechanisms by which mesenchymal ALK3-BMP mediates EVs in regulating mesenchymal-epithelial interactions.

Multiple molecular signaling pathways, including Wnt/β-catenin, are known to be involved in the differentiation of tongue epithelial cells and the formation of taste papillae. Among the DEGs in the tongue epithelium of *Wnt1-Cre/Alk3*^{cKO}, we found downregulated genes (*Lrp4*, *Fzd10*, *Lgr5*, *Prox1*) related to Wnt/β-catenin signaling and upregulated Wnt/β-catenin signaling inhibitor Sostdc1. We also identified promising mesenchymal secretory proteins Nbl1 and Pkm2, which are known inhibitors of β-catenin mediated signaling, suggesting that ALK3-BMP signaling in the mesenchyme possibly interacts with epithelial Wnt/β-catenin signaling during taste papilla development. The specific mechanism by which ALK3-BMP signaling mediates Nbl1 and Pkm2 in taste papilla development is yet to be discovered. To demonstrate the specific role of secretory proteins such as Nbl1 and Pkm2 in tongue epithelial cell differentiation and taste papilla formation, functional analyses using Nbl1 and/or Pkm2 recombinant proteins, Pkm2 inhibitors and/or Nbl1-neutralizing antibodies can be used in a tongue organ culture system.

ChIP-Seq is a high-throughput technique that enables us to identify the binding sites of a transcription factor using its specific antibody, thus allowing us to distinguish direct from indirect target genes. Using phosphorylated (p) Smad1/5/8, a well-known transcription factor that mediates BMP signaling, we can identify the genomic distribution of p-Smad1/5/8 binding sites in p-Smad1/5/8+ tongue mesenchymal cells. Together with the list of DEGs from our bulk RNA-Seq analyses and of genes encoding LC-MS detected proteins, we will be able to distinguish

target genes between those directly and indirectly regulated by p-Smad1/5/8. In addition, there is a great potential for finding previously unrecognized target genes of p-Smad1/5/8.

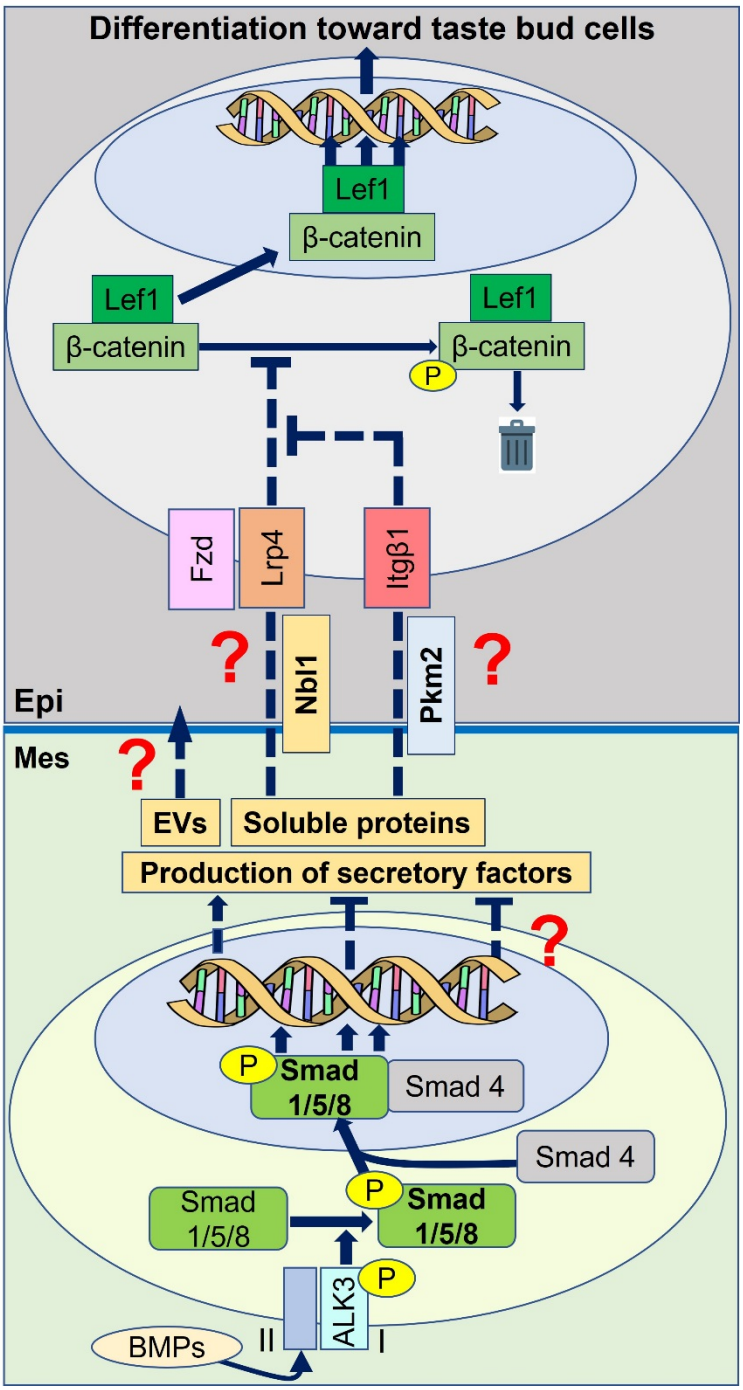
Differentiation toward taste bud cells
Lef1
β-catenin
Lef1
β-catenin
Lef1
β-catenin
P
Fzd
Lrp4
Itgβ1
?
Nbl1
Pkm2
?
Epi
Mes
?
EVs
Soluble proteins
Production of secretory factors
?
P
Smad 1/5/8
Smad 4
Smad 4
P
Smad 1/5/8
Smad 1/5/8
P
ALK3
BMPs
II
I

Figure 5.1. Schematic diagram to represent the future directions from the dissertation. Lef1: Lymphoid enhancer-binding factor-1; Fzd: frizzled; Lrp4: low-density lipoprotein receptor-related protein 4; Itgβ1: integrin beta-1; Nbl1: neuroblastoma suppressor of tumorigenicity-1, Pkm2: Pyruvate kinase isozymes M1/M2; EVs: Extracellular vesicles; ALK3: activin like kinase 3; BMP: bone morphogenetic protein. Question marks indicate the future directions.

REFERENCES

Abu-Abed, S., MacLean, G., Fraulob, V., Chambon, P., Petkovich, M., Dollé, P., 2002. Differential expression of the retinoic acid-metabolizing enzymes CYP26A1 and CYP26B1 during murine organogenesis. Mechanisms of development 110, 173-177.

Ahn, Y., Sanderson, B.W., Klein, O.D., Krumlauf, R., 2010. Inhibition of Wnt signaling by Wise (Sostdc1) and negative feedback from Shh controls tooth number and patterning. Development 137, 3221-3231.

Akhmametyeva, E.M., Mihaylova, M.M., Luo, H., Kharzai, S., Welling, D.B., Chang, L.-S., 2006. Regulation of the neurofibromatosis 2 gene promoter expression during embryonic development. Dev Dyn 235, 2771-2785.

Balemans, W., Van Hul, W., 2002. Extracellular Regulation of BMP Signaling in Vertebrates: A Cocktail of Modulators. Developmental biology 250, 231-250.

Barembaum, M., Bronner-Fraser, M., 2005. Early steps in neural crest specification. Semin Cell Dev Biol 16, 642-646.

Barlow, L.A., 2015. Progress and renewal in gustation: new insights into taste bud development. Development 142, 3620-3629.

Barlow, L.A., Klein, O.D., 2015. Developing and regenerating a sense of taste. Current topics in developmental biology 111, 401-419.

Barron, F., Woods, C., Kuhn, K., Bishop, J., Howard, M.J., Clouthier, D.E., 2011. Downregulation of Dlx5 and Dlx6 expression by Hand2 is essential for initiation of tongue morphogenesis. Development 138, 2249-2259.

Beites, C.L., Hollenbeck, P.L.W., Kim, J., Lovell-Badge, R., Lander, A.D., Calof, A.L., 2009. Follistatin modulates a BMP autoregulatory loop to control the size and patterning of sensory domains in the developing tongue. Development 136, 2187.

Berkes, C.A., Tapscott, S.J., 2005. MyoD and the transcriptional control of myogenesis. Seminars in Cell & Developmental Biology 16, 585-595.

Bernier, G., Brown, A., Dalpé, G., De Repentigny, Y., Mathieu, M., Kothary, R., 1995. Dystonin Expression in the Developing Nervous System Predominates in the Neurons That Degenerate indystonia musculorumMutant Mice. Molecular and Cellular Neuroscience 6, 509-520.

Bitgood, M.J., McMahon, A.P., 1995. Hedgehog and Bmp genes are coexpressed at many diverse sites of cell-cell interaction in the mouse embryo. Developmental biology 172, 126-138.

Boggs, K., Venkatesan, N., Mederacke, I., Komatsu, Y., Stice, S., Schwabe, R.F., Mistretta, C.M., Mishina, Y., Liu, H.-X., 2016. Contribution of Underlying Connective Tissue Cells to Taste Buds in Mouse Tongue and Soft Palate. PLoS One 11, e0146475-e0146475.

Boopathy, G.T.K., Hong, W., 2019. Role of Hippo Pathway-YAP/TAZ Signaling in Angiogenesis. Frontiers in Cell and Developmental Biology 7.

Böse, J., Grotewold, L., Rüther, U., 2002. Pallister–Hall syndrome phenotype in mice mutant for Gli3. Human Molecular Genetics 11, 1129-1135.

Botchkarev, V.A., Kishimoto, J., 2003. Molecular Control of Epithelial–Mesenchymal Interactions During Hair Follicle Cycling. Journal of Investigative Dermatology Symposium Proceedings 8, 46-55.

Botchkarev, V.A., Sharov, A.A., 2004. BMP signaling in the control of skin development and hair follicle growth. Differentiation; research in biological diversity 72, 512-526.

Bradley, R.M., Stern, I.B., 1967. The development of the human taste bud during the foetal period. J Anat 101, 743-752.

Bragdon, B., Moseychuk, O., Saldanha, S., King, D., Julian, J., Nohe, A., 2011. Bone morphogenetic proteins: a critical review. Cell Signal 23, 609-620.

Briscoe, J., Thérond, P.P., 2013. The mechanisms of Hedgehog signalling and its roles in development and disease. Nature reviews. Molecular cell biology 14, 416-429.

Camargo, F.D., Gokhale, S., Johnnidis, J.B., Fu, D., Bell, G.W., Jaenisch, R., Brummelkamp, T.R., 2007a. YAP1 Increases Organ Size and Expands Undifferentiated Progenitor Cells. Current Biology 17, 2054-2060.

Camargo, F.D., Gokhale, S., Johnnidis, J.B., Fu, D., Bell, G.W., Jaenisch, R., Brummelkamp, T.R., 2007b. YAP1 increases organ size and expands undifferentiated progenitor cells. Current biology : CB 17, 2054-2060.

Caplan, H., Olson, S.D., Kumar, A., George, M., Prabhakara, K.S., Wenzel, P., Bedi, S., Toledano-Furman, N.E., Triolo, F., Kamhieh-Milz, J., Moll, G., Cox, C.S., Jr., 2019. Mesenchymal Stromal Cell Therapeutic Delivery: Translational Challenges to Clinical Application. Frontiers in immunology 10, 1645-1645.

Carballo, G.B., Honorato, J.R., de Lopes, G.P.F., Spohr, T.C.L.d.S.E., 2018. A highlight on Sonic hedgehog pathway. Cell Commun Signal 16, 11-11.

Castillo-Azofeifa, D., Losacco, J.T., Salcedo, E., Golden, E.J., Finger, T.E., Barlow, L.A., 2017. Sonic hedgehog from both nerves and epithelium is a key trophic factor for taste bud maintenance. Development 144, 3054.

Castillo, D., Seidel, K., Salcedo, E., Ahn, C., de Sauvage, F.J., Klein, O.D., Barlow, L.A., 2014. Induction of ectopic taste buds by SHH reveals the competency and plasticity of adult lingual epithelium. Development 141, 2993-3002.

Cervantes, S., Yamaguchi, T.P., Hebrok, M., 2009. Wnt5a is essential for intestinal elongation in mice. Developmental biology 326, 285-294.

Chai, Y., Maxson, R.E., Jr., 2006. Recent advances in craniofacial morphogenesis. Dev Dyn 235, 2353-2375.

Chandrashekar, L., Kashinath, K.R., Suhas, S., 2014. Labial ankyloglossia associated with oligodontia: a case report. Journal of dentistry (Tehran, Iran) 11, 481-484.

Charité, J., McFadden, D.G., Merlo, G., Levi, G., Clouthier, D.E., Yanagisawa, M., Richardson, J.A., Olson, E.N., 2001. Role of Dlx6 in regulation of an endothelin-1-dependent, dHAND branchial arch enhancer. Genes & development 15, 3039-3049.

Chaudhari, N., Roper, S.D., 2010. The cell biology of taste. Journal of Cell Biology 190, 285-296.

Chen, D., Zhao, M., Mundy, G.R., 2004. Bone morphogenetic proteins. Growth factors (Chur, Switzerland) 22, 233-241.

Chen, G., Ishan, M., Yang, J., Kishigami, S., Fukuda, T., Scott, G., Ray, M.K., Sun, C., Chen, S.-Y., Komatsu, Y., Mishina, Y., Liu, H.-X., 2017. Specific and spatial labeling of P0-Cre versus Wnt1-Cre in cranial neural crest in early mouse embryos. Genesis (New York, N.Y. : 2000) 55, e23034.

Chen, J.K., Taipale, J., Young, K.E., Maiti, T., Beachy, P.A., 2002. Small molecule modulation of Smoothened activity. Proceedings of the National Academy of Sciences of the United States of America 99, 14071-14076.

Choi, S.-C., Han, J.-K., 2002. Xenopus Cdc42 Regulates Convergent Extension Movements during Gastrulation through Wnt/Ca2+ Signaling Pathway. Developmental biology 244, 342-357.

Clausen, K.A., Blish, K.R., Birse, C.E., Triplette, M.A., Kute, T.E., Russell, G.B., D'Agostino, R.B., Jr., Miller, L.D., Torti, F.M., Torti, S.V., 2011. SOSTDC1 differentially modulates Smad and beta-catenin activation and is down-regulated in breast cancer. Breast Cancer Res Treat 129, 737-746.

Cobourne, M.T., Iseki, S., Birjandi, A.A., Adel Al-Lami, H., Thauvin-Robinet, C., Xavier, G.M., Liu, K.J., 2019. How to make a tongue: Cellular and molecular regulation of muscle and connective tissue formation during mammalian tongue development. Semin Cell Dev Biol 91, 45-54.

Cooper, J., Giancotti, F.G., 2014. Molecular insights into NF2/Merlin tumor suppressor function. FEBS letters 588, 2743-2752.

Cordero, D.R., Brugmann, S., Chu, Y., Bajpai, R., Jame, M., Helms, J.A., 2011. Cranial neural crest cells on the move: their roles in craniofacial development. American journal of medical genetics. Part A 155A, 270-279.

D'Agostino, M., Lemma, V., Chesi, G., Stornaiuolo, M., Cannata Serio, M., D'Ambrosio, C., Scaloni, A., Polishchuk, R., Bonatti, S., 2013. The cytosolic chaperone α-crystallin B rescues folding and compartmentalization of misfolded multispan transmembrane proteins. Journal of cell science 126, 4160-4172.

Dalpé, G., Leclerc, N., Vallée, A., Messer, A., Mathieu, M., De Repentigny, Y., Kothary, R., 1998. Dystonin Is Essential for Maintaining Neuronal Cytoskeleton Organization. Molecular and Cellular Neuroscience 10, 243-257.

Davis, J.R., Tapon, N., 2019. Hippo signalling during development. Development 146.

de Roos, K., Sonneveld, E., Compaan, B., ten Berge, D., Durston, A.J., van der Saag, P.T., 1999. Expression of retinoic acid 4-hydroxylase (CYP26) during mouse and Xenopus laevis embryogenesis. Mechanisms of development 82, 205-211.

Del Re, D.P., Yang, Y., Nakano, N., Cho, J., Zhai, P., Yamamoto, T., Zhang, N., Yabuta, N., Nojima, H., Pan, D., Sadoshima, J., 2013. Yes-associated protein isoform 1 (Yap1) promotes cardiomyocyte survival and growth to protect against myocardial ischemic injury. The Journal of biological chemistry 288, 3977-3988.

Dollé, P., Fraulob, V., Kastner, P., Chambon, P., 1994. Developmental expression of murine retinoid X receptor (RXR) genes. Mechanisms of development 45, 91-104.

Dollé, P., Ruberte, E., Leroy, P., Morriss-Kay, G., Chambon, P., 1990. Retinoic acid receptors and cellular retinoid binding proteins. I. A systematic study of their differential pattern of transcription during mouse organogenesis. Development 110, 1133-1151.

Dong, J., Feldmann, G., Huang, J., Wu, S., Zhang, N., Comerford, S.A., Gayyed, M.F., Anders, R.A., Maitra, A., Pan, D., 2007. Elucidation of a universal size-control mechanism in Drosophila and mammals. Cell 130, 1120-1133.

Du, W., Prochazka, J., Prochazkova, M., Klein, O.D., 2016. Expression of FGFs during early mouse tongue development. Gene expression patterns : GEP 20, 81-87.

Ducy, P., Zhang, R., Geoffroy, V., Ridall, A.L., Karsenty, G., 1997. Osf2/Cbfa1: a transcriptional activator of osteoblast differentiation. Cell 89, 747-754.

El-Sharaby, A., Ueda, K., Kurisu, K., Wakisaka, S., 2001a. Development and maturation of taste buds of the palatal epithelium of the rat: Histological and immunohistochemical study. The Anatomical record 263, 260-268.

El-Sharaby, A., Ueda, K., Wakisaka, S., 2001b. Differentiation of the lingual and palatal gustatory epithelium of the rat as revealed by immunohistochemistry of alpha-gustducin. Archives of histology and cytology 64, 401-409.

El Shahawy, M., Reibring, C.G., Neben, C.L., Hallberg, K., Marangoni, P., Harfe, B.D., Klein, O.D., Linde, A., Gritli-Linde, A., 2017. Cell fate specification in the lingual epithelium is controlled by antagonistic activities of Sonic hedgehog and retinoic acid. PLoS genetics 13, e1006914.

Farbman, A.I., Mbiene, J.P., 1991. Early development and innervation of taste bud-bearing papillae on the rat tongue. The Journal of comparative neurology 304, 172-186.

Ferguson, C.A., Tucker, A.S., Christensen, L., Lau, A.L., Matzuk, M.M., Sharpe, P.T., 1998. Activin is an essential early mesenchymal signal in tooth development that is required for patterning of the murine dentition. Genes & development 12, 2636-2649.

Fritzsch, B., Sarai, P.A., Barbacid, M., Silos-Santiago, I., 1997. Mice with a targeted disruption of the neurotrophin receptor trkB lose their gustatory ganglion cells early but do develop taste buds. International Journal of Developmental Neuroscience 15, 563-576.

Fujimoto, S., Yamamoto, K., Yoshizuka, M., Yokoyama, M., 1993. Pre- and postnatal development of rabbit foliate papillae with special reference to foliate gutter formation and taste bud and serous gland differentiation. Microscopy research and technique 26, 120-132.

Fukuda, T., Scott, G., Komatsu, Y., Araya, R., Kawano, M., Ray, M.K., Yamada, M., Mishina, Y., 2006. Generation of a mouse with conditionally activated signaling through the BMP receptor, ALK2. Genesis (New York, N.Y. : 2000) 44, 159-167.

Gaillard, D., Barlow, L.A., 2011. Taste bud cells of adult mice are responsive to Wnt/β-catenin signaling: implications for the renewal of mature taste cells. Genesis (New York, N.Y. : 2000) 49, 295-306.

Gaillard, D., Bowles, S.G., Salcedo, E., Xu, M., Millar, S.E., Barlow, L.A., 2017. β-catenin is required for taste bud cell renewal and behavioral taste perception in adult mice. PLoS genetics 13, e1006990-e1006990.

Gaillard, D., Xu, M., Liu, F., Millar, S.E., Barlow, L.A., 2015. β-Catenin Signaling Biases Multipotent Lingual Epithelial Progenitors to Differentiate and Acquire Specific Taste Cell Fates. PLoS genetics 11, e1005208.

Gao, B., Song, H., Bishop, K., Elliot, G., Garrett, L., English, M.A., Andre, P., Robinson, J., Sood, R., Minami, Y., Economides, A.N., Yang, Y., 2011. Wnt signaling gradients establish planar cell polarity by inducing Vangl2 phosphorylation through Ror2. Dev Cell 20, 163-176.

Gao, Y., Toska, E., Denmon, D., Roberts, S.G., Medler, K.F., 2014. WT1 regulates the development of the posterior taste field. Development 141, 2271-2278.

Geist, J.R., Gander, D.L., Stefanac, S.J., 1992. Oral manifestations of neurofibromatosis types I and II. Oral surgery, oral medicine, and oral pathology 73, 376-382.

Giovannini, M., Robanus-Maandag, E., van der Valk, M., Niwa-Kawakita, M., Abramowski, V., Goutebroze, L., Woodruff, J.M., Berns, A., Thomas, G., 2000. Conditional biallelic Nf2

mutation in the mouse promotes manifestations of human neurofibromatosis type 2. Genes & development 14, 1617-1630.

Goodrich, L.V., Johnson, R.L., Milenkovic, L., McMahon, J.A., Scott, M.P., 1996. Conservation of the hedgehog/patched signaling pathway from flies to mice: induction of a mouse patched gene by Hedgehog. Genes & development 10, 301-312.

Grönroos, E., Kingston, I.J., Ramachandran, A., Randall, R.A., Vizán, P., Hill, C.S., 2012. Transforming growth factor β inhibits bone morphogenetic protein-induced transcription through novel phosphorylated Smad1/5-Smad3 complexes. Mol Cell Biol 32, 2904-2916.

Habas, R., Dawid, I.B., He, X., 2003. Coactivation of Rac and Rho by Wnt/Frizzled signaling is required for vertebrate gastrulation. Genes & development 17, 295-309.

Hall, J.M., Hooper, J.E., Finger, T.E., 1999. Expression of Sonic hedgehog, Patched, and Gli1 in developing taste papillae of the mouse. Journal of Comparative Neurology 406, 143-155.

Hall, J.M.H., Bell, M.L., Finger, T.E., 2003. Disruption of sonic hedgehog signaling alters growth and patterning of lingual taste papillae. Developmental biology 255, 263-277.

Hamaratoglu, F., Willecke, M., Kango-Singh, M., Nolo, R., Hyun, E., Tao, C., Jafar-Nejad, H., Halder, G., 2006. The tumour-suppressor genes NF2/Merlin and Expanded act through Hippo signalling to regulate cell proliferation and apoptosis. Nat Cell Biol 8, 27-36.

Han, D., Zhao, H., Parada, C., Hacia, J.G., Bringas, P., Jr., Chai, Y., 2012. A TGFβ-Smad4-Fgf6 signaling cascade controls myogenic differentiation and myoblast fusion during tongue development. Development 139, 1640-1650.

Hansen, C.G., Moroishi, T., Guan, K.L., 2015. YAP and TAZ: a nexus for Hippo signaling and beyond. Trends in cell biology 25, 499-513.

Harada, S., Yamaguchi, K., Kanemaru, N., Kasahara, Y., 2000. Maturation of taste buds on the soft palate of the postnatal rat. Physiology & behavior 68, 333-339.

Hartwig, S., Ho, J., Pandey, P., Macisaac, K., Taglienti, M., Xiang, M., Alterovitz, G., Ramoni, M., Fraenkel, E., Kreidberg, J.A., 2010. Genomic characterization of Wilms' tumor

suppressor 1 targets in nephron progenitor cells during kidney development. Development 137, 1189-1203.

He, F., Xiong, W., Yu, X., Espinoza-Lewis, R., Liu, C., Gu, S., Nishita, M., Suzuki, K., Yamada, G., Minami, Y., Chen, Y., 2008. Wnt5a regulates directional cell migration and cell proliferation via Ror2-mediated noncanonical pathway in mammalian palate development. Development 135, 3871-3879.

Heallen, T., Zhang, M., Wang, J., Bonilla-Claudio, M., Klysik, E., Johnson, R.L., Martin, J.F., 2011. Hippo pathway inhibits Wnt signaling to restrain cardiomyocyte proliferation and heart size. Science (New York, N.Y.) 332, 458-461.

Henkin, R.I., Larson, A.L., Powell, R.D., 1975. Hypogeusia, dysgeusia, hyposmia, and dysosmia following influenza-like infection. The Annals of otology, rhinology, and laryngology 84, 672-682.

Holleville, N., Matéos, S., Bontoux, M., Bollerot, K., Monsoro-Burq, A.H., 2007. Dlx5 drives Runx2 expression and osteogenic differentiation in developing cranial suture mesenchyme. Developmental biology 304, 860-874.

Hosokawa, R., Oka, K., Yamaza, T., Iwata, J., Urata, M., Xu, X., Bringas, P., Jr., Nonaka, K., Chai, Y., 2010. TGF-beta mediated FGF10 signaling in cranial neural crest cells controls development of myogenic progenitor cells through tissue-tissue interactions during tongue morphogenesis. Developmental biology 341, 186-195.

Hovens, C.M., Kaye, A.H., 2001. The tumour suppressor protein NF2/merlin: the puzzle continues. Journal of clinical neuroscience : official journal of the Neurosurgical Society of Australasia 8, 4-7.

Hui, C.C., Slusarski, D., Platt, K.A., Holmgren, R., Joyner, A.L., 1994. Expression of three mouse homologs of the Drosophila segment polarity gene cubitus interruptus, Gli, Gli-2, and Gli-3, in ectoderm- and mesoderm-derived tissues suggests multiple roles during postimplantation development. Developmental biology 162, 402-413.

Ichikawa, H., De Repentigny, Y., Kothary, R., Sugimoto, T., 2006. The survival of vagal and glossopharyngeal sensory neurons is dependent upon dystonin. Neuroscience 137, 531-536.

Imajo, M., Ebisuya, M., Nishida, E., 2015. Dual role of YAP and TAZ in renewal of the intestinal epithelium. Nat Cell Biol 17, 7-19.

Irmer, D., Funk, J.O., Blaukat, A., 2007. EGFR kinase domain mutations - functional impact and relevance for lung cancer therapy. Oncogene 26, 5693-5701.

Ishan, M., Chen, G., Sun, C., Chen, S.-Y., Komatsu, Y., Mishina, Y., Liu, H.-X., 2020. Increased activity of mesenchymal ALK2-BMP signaling causes posteriorly truncated microglossia and disorganization of lingual tissues. Genesis (New York, N.Y. : 2000) 58, e23337.

Ito, A., Nosrat, I.V., Nosrat, C.A., 2010. Taste cell formation does not require gustatory and somatosensory innervation. Neuroscience letters 471, 189-194.

Iwata, J., Hacia, J.G., Suzuki, A., Sanchez-Lara, P.A., Urata, M., Chai, Y., 2012. Modulation of noncanonical TGF-β signaling prevents cleft palate in Tgfbr2 mutant mice. The Journal of clinical investigation 122, 873-885.

Iwata, J., Suzuki, A., Pelikan, R.C., Ho, T.V., Chai, Y., 2013. Noncanonical transforming growth factor β (TGFβ) signaling in cranial neural crest cells causes tongue muscle developmental defects. The Journal of biological chemistry 288, 29760-29770.

Iwatsuki, K., Liu, H.-X., Grónder, A., Singer, M.A., Lane, T.F., Grosschedl, R., Mistretta, C.M., Margolskee, R.F., 2007. Wnt signaling interacts with Shh to regulate taste papilla development. Proceedings of the National Academy of Sciences of the United States of America 104, 2253-2258.

Jabbour, E., El Ahdab, S., Cortes, J., Kantarjian, H., 2008. Nilotinib: a novel Bcr-Abl tyrosine kinase inhibitor for the treatment of leukemias. Expert opinion on investigational drugs 17, 1127-1136.

Jain, P., Rathee, M., 2021. Embryology, Tongue, StatPearls. StatPearls Publishing Copyright © 2021, StatPearls Publishing LLC., Treasure Island (FL).

Jeong, J., Mao, J., Tenzen, T., Kottmann, A.H., McMahon, A.P., 2004. Hedgehog signaling in the neural crest cells regulates the patterning and growth of facial primordia. Genes & development 18, 937-951.

Jorissen, R.N., Walker, F., Pouliot, N., Garrett, T.P.J., Ward, C.W., Burgess, A.W., 2003. Epidermal growth factor receptor: mechanisms of activation and signalling. Exp Cell Res 284, 31-53.

Jung, H.-S., Oropeza, V., Thesleff, I., 1999. Shh, Bmp-2, Bmp-4 and Fgf-8 are associated with initiation and patterning of mouse tongue papillae. Mechanisms of development 81, 179-182.

Jussila, M., Thesleff, I., 2012. Signaling networks regulating tooth organogenesis and regeneration, and the specification of dental mesenchymal and epithelial cell lineages. Cold Spring Harbor perspectives in biology 4, a008425.

Kaufman, M.H., 1992. The Atlas of Mouse Development 1st Edition. 512.

Kawasaki, K., Porntaveetus, T., Oommen, S., Ghafoor, S., Kawasaki, M., Otsuka-Tanaka, Y., Blackburn, J., Kessler, J.A., Sharpe, P.T., Ohazama, A., 2012. Bmp signalling in filiform tongue papilla development. Arch Oral Biol 57, 805-813.

Keller, H., Rentsch, P., Hagmann, J., 2002. Differences in cortical actin structure and dynamics document that different types of blebs are formed by distinct mechanisms. Exp Cell Res 277, 161-172.

Kim, J.-Y., Kim, T.-Y., Lee, E.-S., Aryal, Y.P., Pokharel, E., Sung, S., Sohn, W.-J., Kim, J.-Y., Jung, J.-K., 2021. Implications of the specific localization of YAP signaling on the epithelial patterning of circumvallate papilla. Journal of molecular histology 52, 313-320.

Kim, J.Y., Lee, M.J., Cho, K.W., Lee, J.M., Kim, Y.J., Kim, J.Y., Jung, H.I., Cho, J.Y., Cho, S.W., Jung, H.S., 2009. Shh and ROCK1 modulate the dynamic epithelial morphogenesis in circumvallate papilla development. Developmental biology 325, 273-280.

Kim, M., Jho, E.H., 2014. Cross-talk between Wnt/β-catenin and Hippo signaling pathways: a brief review. BMB reports 47, 540-545.

Kim, S., Jho, E.-H., 2016. Merlin, a regulator of Hippo signaling, regulates Wnt/β-catenin signaling. BMB reports 49, 357-358.

Kim, W., Jho, E.H., 2018. The history and regulatory mechanism of the Hippo pathway. BMB reports 51, 106-118.

Kist, R., Watson, M., Crosier, M., Robinson, M., Fuchs, J., Reichelt, J., Peters, H., 2014. The Formation of Endoderm-Derived Taste Sensory Organs Requires a Pax9-Dependent Expansion of Embryonic Taste Bud Progenitor Cells. PLoS genetics 10, e1004709.

Komiya, Y., Habas, R., 2008. Wnt signal transduction pathways. Organogenesis 4, 68-75.

Komori, T., Yagi, H., Nomura, S., Yamaguchi, A., Sasaki, K., Deguchi, K., Shimizu, Y., Bronson, R.T., Gao, Y.H., Inada, M., Sato, M., Okamoto, R., Kitamura, Y., Yoshiki, S., Kishimoto, T., 1997. Targeted disruption of Cbfa1 results in a complete lack of bone formation owing to maturational arrest of osteoblasts. Cell 89, 755-764.

Kramer, N., Chen, G., Ishan, M., Cui, X., Liu, H.-X., 2019. Early taste buds are from Shh+ epithelial cells of tongue primordium in distinction from mature taste bud cells which arise from surrounding tissue compartments. Biochemical and Biophysical Research Communications 515, 149-155.

Krimm, R.F., 2007. Factors that regulate embryonic gustatory development. BMC neuroscience 8 Suppl 3, S4.

Krimm, R.F., Thirumangalathu, S., Barlow, L.A., 2015. Development of the taste system. Handbook of Olfaction and Gustation, 727-748.

Lalakea, M.L., Messner, A.H., 2003. Ankyloglossia: does it matter? Pediatric clinics of North America 50, 381-397.

Lallemand, D., Curto, M., Saotome, I., Giovannini, M., McClatchey, A.I., 2003. NF2 deficiency promotes tumorigenesis and metastasis by destabilizing adherens junctions. Genes & development 17, 1090-1100.

Lauter, G., Söll, I., Hauptmann, G., 2011. Two-color fluorescent in situ hybridization in the embryonic zebrafish brain using differential detection systems. BMC Developmental Biology 11, 43.

Leal, L.F., Bueno, A.C., Gomes, D.C., Abduch, R., de Castro, M., Antonini, S.R., 2015. Inhibition of the Tcf/beta-catenin complex increases apoptosis and impairs adrenocortical tumor cell proliferation and adrenal steroidogenesis. Oncotarget 6, 43016-43032.

Leikola, A., 1976. The neural crest: migrating cells in embryonic development. Folia morphologica 24, 155-172.

Leung, C.L., Sun, D., Liem, R.K., 1999. The intermediate filament protein peripherin is the specific interaction partner of mouse BPAG1-n (dystonin) in neurons. J Cell Biol 144, 435-446.

Li, L., Wang, Y., Lin, M., Yuan, G., Yang, G., Zheng, Y., Chen, Y., 2013. Augmented BMPRIA-mediated BMP signaling in cranial neural crest lineage leads to cleft palate formation and delayed tooth differentiation. PLoS One 8, e66107.

Lin, Z., von Gise, A., Zhou, P., Gu, F., Ma, Q., Jiang, J., Yau, A.L., Buck, J.N., Gouin, K.A., van Gorp, P.R., Zhou, B., Chen, J., Seidman, J.G., Wang, D.Z., Pu, W.T., 2014. Cardiac-specific YAP activation improves cardiac function and survival in an experimental murine MI model. Circulation research 115, 354-363.

Liu, F., Thirumangalathu, S., Gallant, N.M., Yang, S.H., Stoick-Cooper, C.L., Reddy, S.T., Andl, T., Taketo, M.M., Dlugosz, A.A., Moon, R.T., Barlow, L.A., Millar, S.E., 2007. Wnt-β-catenin signaling initiates taste papilla development. Nature genetics 39, 106-112.

Liu, H.-X., Grosse, A.M.S., Walton, K.D., Saims, D.A., Gumucio, D.L., Mistretta, C.M., 2009. WNT5a in tongue and fungiform Papilla development. Ann N Y Acad Sci 1170, 11-17.

Liu, H.-X., Henson, B.S., Zhou, Y., D'Silva, N.J., Mistretta, C.M., 2008. Fungiform papilla pattern: EGF regulates inter-papilla lingual epithelium and decreases papilla number by means of PI3K/Akt, MEK/ERK, and p38 MAPK signaling. Dev Dyn 237, 2378-2393.

Liu, H.-X., Komatsu, Y., Mishina, Y., Mistretta, C.M., 2012a. Neural crest contribution to lingual mesenchyme, epithelium and developing taste papillae and taste buds. Developmental biology 368, 294-303.

Liu, H.-X., MacCallum, D.K., Edwards, C., Gaffield, W., Mistretta, C.M., 2004. Sonic hedgehog exerts distinct, stage-specific effects on tongue and taste papilla development. Developmental biology 276, 280-300.

Liu, H.X., Ermilov, A., Grachtchouk, M., Li, L., Gumucio, D.L., Dlugosz, A.A., Mistretta, C.M., 2013. Multiple Shh signaling centers participate in fungiform papilla and taste bud formation and maintenance. Developmental biology 382, 82-97.

Liu, H.X., Grosse, A.S., Iwatsuki, K., Mishina, Y., Gumucio, D.L., Mistretta, C.M., 2012b. Separate and distinctive roles for Wnt5a in tongue, lingual tissue and taste papilla development. Developmental biology 361, 39-56.

Mak, K.K., Chan, S.Y., 2003. Epidermal growth factor as a biologic switch in hair growth cycle. The Journal of biological chemistry 278, 26120-26126.

Marigo, V., Johnson, R.L., Vortkamp, A., Tabin, C.J., 1996a. Sonic hedgehog Differentially Regulates Expression ofGLIandGLI3during Limb Development. Developmental biology 180, 273-283.

Marigo, V., Scott, M.P., Johnson, R.L., Goodrich, L.V., Tabin, C.J., 1996b. Conservation in hedgehog signaling: induction of a chicken patched homolog by Sonic hedgehog in the developing limb. Development 122, 1225-1233.

Massagué, J., 1998. TGF-beta signal transduction. Annual review of biochemistry 67, 753-791.

Massagué, J., Gomis, R.R., 2006. The logic of TGFbeta signaling. FEBS letters 580, 2811-2820.

Matise, M.P., Epstein, D.J., Park, H.L., Platt, K.A., Joyner, A.L., 1998. Gli2 is required for induction of floor plate and adjacent cells, but not most ventral neurons in the mouse central nervous system. Development 125, 2759-2770.

Mayor, R., Theveneau, E., 2013. The neural crest. Development 140, 2247-2251.

Mbiene, J.-P., Maccallum, D.K., Mistretta, C.M., 1997. Organ cultures of embryonic rat tongue support tongue and gustatory papilla morphogenesis in vitro without intact sensory ganglia. Journal of Comparative Neurology 377, 324-340.

McDermott, A., Gustafsson, M., Elsam, T., Hui, C.C., Emerson, C.P., Jr., Borycki, A.G., 2005. Gli2 and Gli3 have redundant and context-dependent function in skeletal muscle formation. Development 132, 345-357.

Merrill, A.E., Eames, B.F., Weston, S.J., Heath, T., Schneider, R.A., 2008. Mesenchyme-dependent BMP signaling directs the timing of mandibular osteogenesis. Development 135, 1223-1234.

Mia, M.M., Chelakkot-Govindalayathil, A.L., Singh, M.K., 2016. Targeting NF2-Hippo/Yap signaling pathway for cardioprotection after ischemia/reperfusion injury. Ann Transl Med 4, 545-545.

Mill, P., Mo, R., Fu, H., Grachtchouk, M., Kim, P.C.W., Dlugosz, A.A., Hui, C.-c., 2003. Sonic hedgehog-dependent activation of Gli2 is essential for embryonic hair follicle development. Genes & development 17, 282-294.

Millington, G., Elliott, K.H., Chang, Y.-T., Chang, C.-F., Dlugosz, A., Brugmann, S.A., 2017. Cilia-dependent GLI processing in neural crest cells is required for tongue development. Developmental biology 424, 124-137.

Mishina, Y., Suzuki, A., Ueno, N., Behringer, R.R., 1995. Bmpr encodes a type I bone morphogenetic protein receptor that is essential for gastrulation during mouse embryogenesis. Genes & development 9, 3027-3037.

Mistretta, C.M., 1972. Topographical and histological study of the developing rat tongue, palate and taste buds. J.F. Bosma (Ed.), Oral Sensation and Perception: The Mouth of the Infant , Thomas, Springfield, IL, 163-187

Mistretta, C.M., 1991. Smell and taste in health and disease. New York: Raven Press XXI

Mistretta, C.M., 1998. The role of innervation in induction and differentiation of taste organs: introduction and background. Ann N Y Acad Sci 855, 1-13.

Mistretta, C.M., Goosens, K.A., Farinas, I., Reichardt, L.F., 1999. Alterations in size, number, and morphology of gustatory papillae and taste buds in BDNF null mutant mice demonstrate neural dependence of developing taste organs. The Journal of comparative neurology 409, 13-24.

Mistretta, C.M., Grigaliunas, A., Liu, H.-X., 2005. Development of Gustatory Organs and Innervating Sensory Ganglia. Chemical Senses 30, i52-i53.

Mistretta, C.M., Liu, H.-X., Gaffield, W., MacCallum, D.K., 2003. Cyclopamine and jervine in embryonic rat tongue cultures demonstrate a role for Shh signaling in taste papilla development and patterning: fungiform papillae double in number and form in novel locations in dorsal lingual epithelium. Developmental biology 254, 1-18.

Miura, H., Barlow, L.A., 2010. Taste bud regeneration and the search for taste progenitor cells. Arch Ital Biol 148, 107-118.

Mo, R., Freer, A.M., Zinyk, D.L., Crackower, M.A., Michaud, J., Heng, H.H., Chik, K.W., Shi, X.M., Tsui, L.C., Cheng, S.H., Joyner, A.L., Hui, C., 1997. Specific and redundant functions of Gli2 and Gli3 zinc finger genes in skeletal patterning and development. Development 124, 113-123.

Mohammadi, M., McMahon, G., Sun, L., Tang, C., Hirth, P., Yeh, B.K., Hubbard, S.R., Schlessinger, J., 1997. Structures of the tyrosine kinase domain of fibroblast growth factor receptor in complex with inhibitors. Science (New York, N.Y.) 276, 955-960.

Moon, S., Yeon Park, S., Woo Park, H., 2018. Regulation of the Hippo pathway in cancer biology. Cellular and molecular life sciences : CMLS 75, 2303-2319.

Morita, H., Mazerbourg, S., Bouley, D.M., Luo, C.-W., Kawamura, K., Kuwabara, Y., Baribault, H., Tian, H., Hsueh, A.J.W., 2004. Neonatal lethality of LGR5 null mice is associated with ankyloglossia and gastrointestinal distension. Mol Cell Biol 24, 9736-9743.

Nie, X., 2005. Apoptosis, proliferation and gene expression patterns in mouse developing tongue. Anatomy and embryology 210, 125-132.

Niederreither, K., Fraulob, V., Garnier, J.M., Chambon, P., Dollé, P., 2002. Differential expression of retinoic acid-synthesizing (RALDH) enzymes during fetal development and organ differentiation in the mouse. Mechanisms of development 110, 165-171.

Niederreither, K., McCaffery, P., Dräger, U.C., Chambon, P., Dollé, P., 1997. Restricted expression and retinoic acid-induced downregulation of the retinaldehyde dehydrogenase type 2 (RALDH-2) gene during mouse development. Mechanisms of development 62, 67-78.

Nishita, M., Yoo, S.K., Nomachi, A., Kani, S., Sougawa, N., Ohta, Y., Takada, S., Kikuchi, A., Minami, Y., 2006. Filopodia formation mediated by receptor tyrosine kinase Ror2 is required for Wnt5a-induced cell migration. J Cell Biol 175, 555-562.

Nolan, K., Kattamuri, C., Luedeke, D.M., Angerman, E.B., Rankin, S.A., Stevens, M.L., Zorn, A.M., Thompson, T.B., 2015. Structure of neuroblastoma suppressor of tumorigenicity 1 (NBL1): insights for the functional variability across bone morphogenetic protein (BMP) antagonists. The Journal of biological chemistry 290, 4759-4771.

Nolan, K., Thompson, T.B., 2014. The DAN family: modulators of TGF-β signaling and beyond. Protein science : a publication of the Protein Society 23, 999-1012.

Okubo, T., Clark, C., Hogan, B.L., 2009. Cell lineage mapping of taste bud cells and keratinocytes in the mouse tongue and soft palate. Stem cells (Dayton, Ohio) 27, 442-450.

Okubo, T., Pevny, L.H., Hogan, B.L., 2006. Sox2 is required for development of taste bud sensory cells. Genes & development 20, 2654-2659.

Orriols, M., Gomez-Puerto, M.C., Ten Dijke, P., 2017. BMP type II receptor as a therapeutic target in pulmonary arterial hypertension. Cellular and molecular life sciences : CMLS 74, 2979-2995.

Otto, F., Thornell, A.P., Crompton, T., Denzel, A., Gilmour, K.C., Rosewell, I.R., Stamp, G.W., Beddington, R.S., Mundlos, S., Olsen, B.R., Selby, P.B., Owen, M.J., 1997. Cbfa1, a candidate gene for cleidocranial dysplasia syndrome, is essential for osteoblast differentiation and bone development. Cell 89, 765-771.

Pan, D., 2010. The Hippo Signaling Pathway in Development and Cancer. Developmental Cell 19, 491-505.

Panciera, T., Azzolin, L., Fujimura, A., Di Biagio, D., Frasson, C., Bresolin, S., Soligo, S., Basso, G., Bicciato, S., Rosato, A., Cordenonsi, M., Piccolo, S., 2016. Induction of Expandable Tissue-Specific Stem/Progenitor Cells through Transient Expression of YAP/TAZ. Cell stem cell 19, 725-737.

Parada, C., Chai, Y., 2015. Mandible and Tongue Development. Current topics in developmental biology 115, 31-58.

Parada, C., Han, D., Chai, Y., 2012. Molecular and cellular regulatory mechanisms of tongue myogenesis. Journal of dental research 91, 528-535.

Paulson, R.B., Sucheston, M.E., Hayes, T.G., Paulson, G.W., 1985. Teratogenic effects of valproate in the CD-1 mouse fetus. Archives of neurology 42, 980-983.

Pennimpede, T., Cameron, D.A., MacLean, G.A., Li, H., Abu-Abed, S., Petkovich, M., 2010. The role of CYP26 enzymes in defining appropriate retinoic acid exposure during

embryogenesis. Birth defects research. Part A, Clinical and molecular teratology 88, 883-894.

Petersen, C.I., Jheon, A.H., Mostowfi, P., Charles, C., Ching, S., Thirumangalathu, S., Barlow, L.A., Klein, O.D., 2011. FGF signaling regulates the number of posterior taste papillae by controlling progenitor field size. PLoS genetics 7, e1002098-e1002098.

Petrilli, A.M., Garcia, J., Bott, M., Klingeman Plati, S., Dinh, C.T., Bracho, O.R., Yan, D., Zou, B., Mittal, R., Telischi, F.F., Liu, X.-Z., Chang, L.-S., Welling, D.B., Copik, A.J., Fernández-Valle, C., 2017. Ponatinib promotes a G1 cell-cycle arrest of merlin/NF2-deficient human schwann cells. Oncotarget 8, 31666-31681.

Pietsch, E.C., Sykes, S.M., McMahon, S.B., Murphy, M.E., 2008. The p53 family and programmed cell death. Oncogene 27, 6507-6521.

Poulsen, E.T., Iannuzzi, F., Rasmussen, H.F., Maier, T.J., Enghild, J.J., Jørgensen, A.L., Matrone, C., 2017. An Aberrant Phosphorylation of Amyloid Precursor Protein Tyrosine Regulates Its Trafficking and the Binding to the Clathrin Endocytic Complex in Neural Stem Cells of Alzheimer's Disease Patients. Front Mol Neurosci 10, 59.

Prochazkova, M., Häkkinen, T.J., Prochazka, J., Spoutil, F., Jheon, A.H., Ahn, Y., Krumlauf, R., Jernvall, J., Klein, O.D., 2017. FGF signaling refines Wnt gradients to regulate the patterning of taste papillae. Development 144, 2212.

Puthiyaveetil, J.S.V., Kota, K., Chakkarayan, R., Chakkarayan, J., Thodiyil, A.K.P., 2016. Epithelial - Mesenchymal Interactions in Tooth Development and the Significant Role of Growth Factors and Genes with Emphasis on Mesenchyme - A Review. J Clin Diagn Res 10, ZE05-ZE09.

Qian, D., Jones, C., Rzadzinska, A., Mark, S., Zhang, X., Steel, K.P., Dai, X., Chen, P., 2007. Wnt5a functions in planar cell polarity regulation in mice. Developmental biology 306, 121-133.

Ren, W., Aihara, E., Lei, W., Gheewala, N., Uchiyama, H., Margolskee, R.F., Iwatsuki, K., Jiang, P., 2017. Transcriptome analyses of taste organoids reveal multiple pathways involved in taste cell generation. Scientific Reports 7, 4004.

Ribatti, D., Santoiemma, M., 2014. Epithelial-mesenchymal interactions: a fundamental Developmental Biology mechanism. The International journal of developmental biology 58, 303-306.

Rinon, A., Lazar, S., Marshall, H., Büchmann-Møller, S., Neufeld, A., Elhanany-Tamir, H., Taketo, M.M., Sommer, L., Krumlauf, R., Tzahor, E., 2007. Cranial neural crest cells regulate head muscle patterning and differentiation during vertebrate embryogenesis. Development 134, 3065-3075.

Roehl, H., Nüsslein-Volhard, C., 2001. Zebrafish pea3 and erm are general targets of FGF8 signaling. Current biology : CB 11, 503-507.

Roper, S.D., Chaudhari, N., 2017. Taste buds: cells, signals and synapses. Nat Rev Neurosci 18, 485-497.

Ruberte, E., Friederich, V., Morriss-Kay, G., Chambon, P., 1992. Differential distribution patterns of CRABP I and CRABP II transcripts during mouse embryogenesis. Development 115, 973-987.

Sangkhathat, S., Kanngurn, S., Chaiyapan, W., Gridist, P., Maneechay, W., 2010. Wilms' tumor 1 gene (WT1) is overexpressed and provides an oncogenic function in pediatric nephroblastomas harboring the wild-type WT1. Oncol Lett 1, 615-619.

Sasai, N., Briscoe, J., 2012. Primary cilia and graded Sonic Hedgehog signaling. WIREs Developmental Biology 1, 753-772.

Sasaki, H., Hui, C., Nakafuku, M., Kondoh, H., 1997. A binding site for Gli proteins is essential for HNF-3beta floor plate enhancer activity in transgenics and can respond to Shh in vitro. Development 124, 1313-1322.

Schlessinger, K., McManus, E.J., Hall, A., 2007. Cdc42 and noncanonical Wnt signal transduction pathways cooperate to promote cell polarity. Journal of Cell Biology 178, 355-361.

Schulz, A., Baader, S.L., Niwa-Kawakita, M., Jung, M.J., Bauer, R., Garcia, C., Zoch, A., Schacke, S., Hagel, C., Mautner, V.F., Hanemann, C.O., Dun, X.P., Parkinson, D.B., Weis, J., Schröder, J.M., Gutmann, D.H., Giovannini, M., Morrison, H., 2013. Merlin isoform 2 in neurofibromatosis type 2-associated polyneuropathy. Nature neuroscience 16, 426-433.

Serbedzija, G.N., Bronner-Fraser, M., Fraser, S.E., 1992. Vital dye analysis of cranial neural crest cell migration in the mouse embryo. Development 116, 297-307.

Serinagaoglu, Y., Paré, J., Giovannini, M., Cao, X., 2015. Nf2-Yap signaling controls the expansion of DRG progenitors and glia during DRG development. Developmental biology 398, 97-109.

Sourbier, C., Liao, P.-J., Ricketts, C.J., Wei, D., Yang, Y., Baranes, S.M., Gibbs, B.K., Ohanjanian, L., Spencer Krane, L., Scroggins, B.T., Keith Killian, J., Wei, M.-H., Kijima, T., Meltzer, P.S., Citrin, D.E., Neckers, L., Vocke, C.D., Marston Linehan, W., 2018. Targeting loss of the Hippo signaling pathway in NF2-deficient papillary kidney cancers. Oncotarget 9, 10723-10733.

Southard-Smith, E.M., Kos, L., Pavan, W.J., 1998. Sox10 mutation disrupts neural crest development in Dom Hirschsprung mouse model. Nature genetics 18, 60-64.

Stone, L.M., Finger, T.E., Tam, P.P., Tan, S.S., 1995. Taste receptor cells arise from local epithelium, not neurogenic ectoderm. Proceedings of the National Academy of Sciences of the United States of America 92, 1916-1920.

Stottmann, R.W., Choi, M., Mishina, Y., Meyers, E.N., Klingensmith, J., 2004. BMP receptor IA is required in mammalian neural crest cells for development of the cardiac outflow tract and ventricular myocardium. Development 131, 2205-2218.

Suga, T., Fukui, T., Shinohara, A., Luan, X., Diekwisch, T.G., Morito, M., Yamane, A., 2007. BMP2, BMP4, and their receptors are expressed in the differentiating muscle tissues of mouse embryonic tongue. Cell and tissue research 329, 103-117.

Suzuki, Y., Ikeda, K., Kawakami, K., 2010a. Expression of Six1 and Six4 in mouse taste buds. Journal of molecular histology 41, 205-214.

Suzuki, Y., Ikeda, K., Kawakami, K., 2010b. Regulatory role of Six1 in the development of taste papillae. Cell and tissue research 339, 513-525.

Suzuki, Y., Ikeda, K., Kawakami, K., 2011. Development of gustatory papillae in the absence of Six1 and Six4. J Anat 219, 710-721.

Tabata, T., Takei, Y., 2004. Morphogens, their identification and regulation. Development 131, 703-712.

Thesleff, I., 2003. Epithelial-mesenchymal signalling regulating tooth morphogenesis. Journal of cell science 116, 1647-1648.

Thesleff, I., Jalkanen, M., Vainio, S., Bernfield, M., 1988. Cell surface proteoglycan expression correlates with epithelial-mesenchymal interaction during tooth morphogenesis. Developmental biology 129, 565-572.

Thesleff, I., Vaahtokari, A., Vainio, S., Jowett, A., 1996. Molecular mechanisms of cell and tissue interactions during early tooth development. The Anatomical record 245, 151-161.

Thirumangalathu, S., Barlow, L.A., 2015. β-Catenin signaling regulates temporally discrete phases of anterior taste bud development. Development 142, 4309-4317.

Thirumangalathu, S., Harlow, D.E., Driskell, A.L., Krimm, R.F., Barlow, L.A., 2009. Fate mapping of mammalian embryonic taste bud progenitors. Development 136, 1519-1528.

Trainor, P.A., 2005. Specification and patterning of neural crest cells during craniofacial development. Brain, behavior and evolution 66, 266-280.

Trainor, P.A., 2015. Preface, in: Trainor, P.A. (Ed.), Current Topics in Developmental Biology. Academic Press, pp. xv-xvi.

Tzavlaki, K., Moustakas, A., 2020. TGF-β Signaling. Biomolecules 10, 487.

Urban, S., Brown, G., Freeman, M., 2004. EGF receptor signalling protects smooth-cuticle cells from apoptosis during Drosophila ventral epidermis development. Development 131, 1835-1845.

Venkatesan, N., Boggs, K., Liu, H.X., 2016. Taste Bud Labeling in Whole Tongue Epithelial Sheet in Adult Mice. Tissue engineering. Part C, Methods 22, 332-337.

von Gise, A., Lin, Z., Schlegelmilch, K., Honor, L.B., Pan, G.M., Buck, J.N., Ma, Q., Ishiwata, T., Zhou, B., Camargo, F.D., Pu, W.T., 2012. YAP1, the nuclear target of Hippo signaling, stimulates heart growth through cardiomyocyte proliferation but not hypertrophy. Proceedings of the National Academy of Sciences of the United States of America 109, 2394-2399.

Wang, R.N., Green, J., Wang, Z., Deng, Y., Qiao, M., Peabody, M., Zhang, Q., Ye, J., Yan, Z., Denduluri, S., Idowu, O., Li, M., Shen, C., Hu, A., Haydon, R.C., Kang, R., Mok, J., Lee, M.J., Luu, H.L., Shi, L.L., 2014. Bone Morphogenetic Protein (BMP) signaling in development and human diseases. Genes & Diseases 1, 87-105.

Wang, Y., Yu, A., Yu, F.X., 2017. The Hippo pathway in tissue homeostasis and regeneration. Protein & cell 8, 349-359.

White, R.J., Schilling, T.F., 2008. How degrading: Cyp26s in hindbrain development. Dev Dyn 237, 2775-2790.

Whitehead, M.C., Kachele, D.L., 1994. Development of fungiform papillae, taste buds, and their innervation in the hamster. Journal of Comparative Neurology 340, 515-530.

Whittaker, T.E., Nagelkerke, A., Nele, V., Kauscher, U., Stevens, M.M., 2020. Experimental artefacts can lead to misattribution of bioactivity from soluble mesenchymal stem cell paracrine factors to extracellular vesicles. Journal of Extracellular Vesicles 9, 1807674.

Winklbauer, R., Medina, A., Swain, R.K., Steinbeisser, H., 2001. Frizzled-7 signalling controls tissue separation during Xenopus gastrulation. Nature 413, 856-860.

Witze, E.S., Litman, E.S., Argast, G.M., Moon, R.T., Ahn, N.G., 2008. Wnt5a Control of Cell Polarity and Directional Movement by Polarized Redistribution of Adhesion Receptors. Science (New York, N.Y.) 320, 365.

Xiao, G.-H., Chernoff, J., Testa, J.R., 2003. NF2: The wizardry of merlin. Genes, Chromosomes and Cancer 38, 389-399.

Xiao, G.-H., Gallagher, R., Shetler, J., Skele, K., Altomare, D.A., Pestell, R.G., Jhanwar, S., Testa, J.R., 2005. The NF2 tumor suppressor gene product, merlin, inhibits cell proliferation and cell cycle progression by repressing cyclin D1 expression. Mol Cell Biol 25, 2384-2394.

Xin, M., Kim, Y., Sutherland, L.B., Murakami, M., Qi, X., McAnally, J., Porrello, E.R., Mahmoud, A.I., Tan, W., Shelton, J.M., Richardson, J.A., Sadek, H.A., Bassel-Duby, R., Olson, E.N., 2013. Hippo pathway effector Yap promotes cardiac regeneration. Proceedings of the National Academy of Sciences of the United States of America 110, 13839-13844.

Xin, M., Kim, Y., Sutherland, L.B., Qi, X., McAnally, J., Schwartz, R.J., Richardson, J.A., Bassel-Duby, R., Olson, E.N., 2011. Regulation of insulin-like growth factor signaling by Yap governs cardiomyocyte proliferation and embryonic heart size. Science signaling 4, ra70.

Yamaguchi, T.P., Bradley, A., McMahon, A.P., Jones, S., 1999. A Wnt5a pathway underlies outgrowth of multiple structures in the vertebrate embryo. Development 126, 1211-1223.

Yamamoto, H., Yoo, S.K., Nishita, M., Kikuchi, A., Minami, Y., 2007. Wnt5a modulates glycogen synthase kinase 3 to induce phosphorylation of receptor tyrosine kinase Ror2. Genes to cells : devoted to molecular & cellular mechanisms 12, 1215-1223.

Yang, K., Hitomi, M., Stacey, D.W., 2006. Variations in cyclin D1 levels through the cell cycle determine the proliferative fate of a cell. Cell Division 1, 32.

Yin, F., Yu, J., Zheng, Y., Chen, Q., Zhang, N., Pan, D., 2013. Spatial organization of Hippo signaling at the plasma membrane mediated by the tumor suppressor Merlin/NF2. Cell 154, 1342-1355.

Yu, F.-X., Zhao, B., Guan, K.-L., 2015a. Hippo Pathway in Organ Size Control, Tissue Homeostasis, and Cancer. Cell 163, 811-828.

Yu, F.X., Guan, K.L., 2013. The Hippo pathway: regulators and regulations. Genes & development 27, 355-371.

Yu, F.X., Meng, Z., Plouffe, S.W., Guan, K.L., 2015b. Hippo pathway regulation of gastrointestinal tissues. Annual review of physiology 77, 201-227.

Zhang, C., Oakley, B., 1996. The distribution and origin of keratin 20-containing taste buds in rat and human. Differentiation; research in biological diversity 61, 121-127.

Zhang, J., Li, L., 2005. BMP signaling and stem cell regulation. Developmental biology 284, 1-11.

Zhang, N., Bai, H., David, K.K., Dong, J., Zheng, Y., Cai, J., Giovannini, M., Liu, P., Anders, R.A., Pan, D., 2010. The Merlin/NF2 tumor suppressor functions through the YAP oncoprotein to regulate tissue homeostasis in mammals. Dev Cell 19, 27-38.

Zhong, Z., Zhao, H., Mayo, J., Chai, Y., 2015. Different Requirements for Wnt Signaling in Tongue Myogenic Subpopulations. Journal of Dental Research 94, 421-429.

Zhou, Y., Liu, H.-X., Mistretta, C.M., 2006. Bone morphogenetic proteins and noggin: Inhibiting and inducing fungiform taste papilla development. Developmental biology 297, 198-213.

Zhu, X.-J., Yuan, X., Wang, M., Fang, Y., Liu, Y., Zhang, X., Yang, X., Li, Y., Li, J., Li, F., Dai, Z.-M., Qiu, M., Zhang, Z., Zhang, Z., 2017. A Wnt/Notch/Pax7 signaling network supports tissue integrity in tongue development. The Journal of biological chemistry 292, 9409-9419.

Zhu, X., Liu, Y., Zhao, P., Dai, Z., Yang, X., Li, Y., Qiu, M., Zhang, Z., 2014. Gpr177-mediated Wnt Signaling is Required for Fungiform Placode Initiation. J Dent Res 93, 582-588.

Zorn, A.M., 2001. Wnt signalling: antagonistic Dickkopfs. Current biology : CB 11, R592-595.